CES 541–652

ISSN 0003–2654

ROYAL SOCIETY
OF
CHEMISTRY

The Analyst

A monthly international journal dealing with all branches of the theory and practice of analytical chemistry, including instrumentation and sensors, and physical, biochemical, clinical, pharmaceutical, biological, environmental, automatic and computer-based methods

Vol. 114 No. 5 May 1989

The Analyst

The Analytical Journal of The Royal Society of Chemistry

Editorial Office: The Royal Society of Chemistry, Thomas Graham House, Science Park, Milton Road, Cambridge CB4 4WF. Telephone 0223 420066. Telex No. 818293 ROYAL. Fax 0223 423623.

Advertisements: Advertisement Department, The Royal Society of Chemistry, Burlington House, Piccadilly, London, W1V 0BN. Telephone 01-437 8656. Telex No. 268001.

The Analyst (ISSN 0003–2654) is published monthly by The Royal Society of Chemistry, Burlington House, London W1V 0BN, England. All orders accompanied with payment should be sent directly to The Royal Society of Chemistry, The Distribution Centre, Blackhorse Road, Letchworth, Herts. SG6 1HN, England. 1989 Annual subscription rate UK £200.00, Rest of World £230.00, USA $460.00. Purchased with *Analytical Abstracts* UK £432.50, Rest of World £490.00, USA $963.00. Purchased with *Analytical Abstracts* plus *Analytical Proceedings* UK £510.00, Rest of World £580.00, USA $1142.00. Purchased with *Analytical Proceedings* UK £254.00, Rest of World £292.00, USA $584.00. Air freight and mailing in the USA by Publications Expediting Inc., 200 Meacham Avenue, Elmont, NY 11003.
USA Postmaster: Send address changes to: *The Analyst*, Publications Expediting Inc., 200 Meacham Avenue, Elmont, NY 11003. Second class postage paid at Jamaica, NY 11431. All other despatches outside the UK by Bulk Airmail within Europe, Accelerated Surface Post outside Europe. PRINTED IN THE UK.

Information for Authors

Full details of how to submit material for publication in *The Analyst* are given in the Instructions to Authors in the January issue. Separate copies are available on request.

The Analyst publishes papers on all aspects of the theory and practice of analytical chemistry, fundamental and applied, inorganic and organic, including chemical, physical, biochemical, clinical, pharmaceutical, biological, environmental, automatic and computer-based methods. Papers on new approaches to existing methods, new techniques and instrumentation, detectors and sensors, and new areas of application with due attention to overcoming limitations and to underlying principles are all equally welcome. There is no page charge.

The following types of papers will be considered:

Full papers, describing original work.

Short papers: the criteria regarding originality are the same as for full papers, but short papers generally report less extensive investigations or are of limited breadth of subject matter

Communications, which must be on an urgent matter and be of obvious scientific importance. Rapidity of publication is enhanced if diagrams are omitted, but tables and formulae can be included. Communications receive priority and are usually published within 5–8 weeks of receipt. They are intended for brief descriptions of work that has progressed to a stage at which it is likely to be valuable to workers faced with similar problems. A fuller paper may be offered subsequently, if justified by later work.

Reviews, which must be a critical evaluation of the existing state of knowledge on a particular facet of analytical chemistry.

Every paper (except Communications) will be submitted to at least two referees, by whose advice the Editorial Board of *The Analyst* will be guided as to its acceptance or rejection. Papers that are accepted must not be published elsewhere except by permission. Submission of a manuscript will be regarded as an undertaking that the same material is not being considered for publication by another journal.

Regional Advisory Editors. For the benefit of potential contributors outside the United Kingdom, a Panel of Regional Advisory Editors exists. Requests for help or advice on any matter related to the preparation of papers and their submission for publication in *The Analyst* can be sent to the nearest member of the Panel. Currently serving Regional Advisory Editors are listed in each issue of *The Analyst.*

Manuscripts (three copies typed in double spacing) should be addressed to:
The Editor, *The Analyst,*
Royal Society of Chemistry,
Thomas Graham House,
Science Park,
Milton Road,
CAMBRIDGE CB4 4WF, UK

Particular attention should be paid to the use of standard methods of literature citation, including the journal abbreviations defined in Chemical Abstracts Service Source Index. Wherever possible, the nomenclature employed should follow IUPAC recommendations, and units and symbols should be those associated with SI.

All queries relating to the presentation and submission of papers, and any correspondence regarding accepted papers and proofs, should be directed to the Editor, *The Analyst* (address as above). Members of the Analytical Editorial Board (who may be contacted directly or via the Editorial Office) would welcome comments, suggestions and advice on general policy matters concerning *The Analyst.*

Fifty reprints of each published contribution are supplied free of charge, and further copies can be purchased.

Dual-beam Thermal Lens Spectrophotometry in Flowing Samples With Chopped Continuous Wave Laser Excitation

Joseph Georges and Jean-Michel Mermet
Laboratoire des Sciences Analytiques, Batiment 308, Université Claude Bernard-Lyon 1, 69622 Villeurbanne Cedex, France

The thermal lens response for flowing samples following chopped continuous wave laser excitation has been studied with respect to the chopping frequency and flow-rate. The use of two types of flow cell and distinct configurations of flow direction with respect to beam propagation enabled the main ways by which the flow may disturb the thermal lens signal to be considered. With a cell in which the flow is perpendicular to the beam axis, the signal was mainly degraded by the bulk flow the effect of which was related to the chopping period and the residence time of the sample in the probe region as defined by the beam spot size. When the flow was parallel to the beam propagation and the optical path length not sufficiently long the decrease in signal amplitude was found to no longer depend on the bulk flow, but rather to originate from turbulence and mixing in the channel cell. With a chopping frequency of 10 Hz and flow-rate of 1 ml min^{-1}, the signal was degraded by a factor of 2 by the bulk flow and by less than a factor of 1.2 by mixing compared with a static sample signal. At 80 Hz, the signal for continuously flowing samples was nearly independent of flow for flow-rates as high as 1.2 and 2 ml min^{-1} in the transverse and axial configurations, respectively. However, for flow-injected samples the signal was found to depend on the time response of the detection system.

Keywords: *Thermal lensing; chopped continuous wave excitation; flowing samples; detection configuration*

Various thermo-optical spectrophotometric methods are currently being developed for the analysis of weakly absorbing samples.[1-3] Basically, excitation by a pump laser followed by thermal relaxation produces a temperature rise within the sample. Because the refractive index of a material changes with temperature, the heated part of the sample behaves as an optical element, lens, prism or grating and as such is probed by a second laser.

Among the different techniques used to probe the optical element, thermal lens spectrophotometry is the most developed for liquid samples. This method involves co-linear or crossed-beam thermal lensing according to the experimental configuration. In the former,[4-7] the probe and pump beams are made co-linear or nearly co-linear before crossing the sample and the optical element behaves as a spherical lens. In crossed-beam thermal lensing,[8,9] also referred to as photothermal refraction, the pump and probe beams are co-planar but cross the sample at right angles, and the heated sample acts as a cylindrical lens. In both instances, the excitation beam may be a modulated continuous wave (CW) laser or a pulsed laser that produces a time-dependent thermal lens which defocuses the probe beam. The resulting modulated probe-beam intensity is measured with a power-sensitive detector and demodulated with a lock-in amplifier or a boxcar averager.

In thermal lensing, the signal may be integrated over the entire optical path of the cell allowing low-concentration samples and relatively large sample volumes. In contrast, with crossed-beam geometry, the probe volume is defined as the interaction region of the two beams; the signal is integrated over the pump beam diameter and is independent of the cell length. This configuration, which allows very small probe volumes ($\approx 10^{-12}$ l), is well suited to small-volume analysis and especially to detection in microbore liquid chromatography.[10]

When thermal lensing is intended for liquid chromatography, flow injection or automated analysis the effect of the flow on the thermal lens behaviour must be considered. Indeed, in chopped CW laser excitation, the thermal lens signal increases with time following the onset of illumination in a chopper cycle and a steady state is achieved only when the rate of heat input from the pump laser is just balanced by the rate of heat conduction out of the illuminated region. The response depends on a characteristic signal rise time constant t_c (typically in the order of milliseconds) and the steady state is approached after a time $t > 10t_c$. If the solution is flowing at a linear velocity sufficiently high to remove the heated volume from the probe beam region on the time scale of t_c, the thermal lens signal will be substantially decreased.[11-14] On the other hand, with pulsed excitation, the signal rise time should be much faster than the heat-transfer effects caused by conduction; this time is limited by the rate of thermalisation and lies approximately in the microsecond range.[15,16] As a result, the signal is nearly independent of the flow because the maximum temperature rise induced by absorbance is attained before the heated sample can be removed from the monitored region of the detection cell by the flowing liquid.

According to Dovichi and Harris,[14] the effects of flow may be divided into two components: bulk flow and mixing. Bulk flow includes axial flow, which is parallel to the cell axis, and transverse flow for which both sample introduction and removal are perpendicular to the cell axis. Bulk flow results in a movement of heated material in the flow direction, from the entrance to the exit of the cell. Mixing, due to turbulence within the cell, has the effect of mixing the heated material with the surrounding material in a section of the flow, independently of the bulk flow.[15] A kinetic model, based on time-resolved thermal lens spectrophotometry has been constructed to improve signal to noise ratios and detection limits in flowing samples.[13]

The aim of this work was to study the thermal lens response of flowing samples using chopped CW laser excitation. In order to evaluate the contributions to the signal amplitude of bulk flow and mixing, the thermal lens behaviour was studied with two types of flow cell: a square-duct cell with flow perpendicular to the laser propagation and a cylindrical channel cell with flow parallel to the beam axis. In both instances, the thermal lens response was studied with respect to the chopping frequency and for flow-rates ranging from tens of microlitres to several millilitres per minute. The use of these cells under the flow injection conditions is examined in terms of the peak amplitude with respect to the flow-rate and injected sample volume.

Experimental

The single-laser - dual-beam thermal lens experimental set-up used was the same as that described previously.[17] An He - Ne

laser that produces a 7.5-mW linearly polarised TEM_{00} beam at 632.8 nm was used. The laser beam was separated by a polarising beam splitter into two linearly polarised beams that emerged from the cube at exactly 90° to each other. The transmitted beam was used as the probe beam and the reflected one as the pump beam. The pump beam was then modulated before being re-combined with the probe beam via a polarisation-sensitive beam splitter in order to minimise energy losses. A lens focused both beams through the flow cell, which was located at about $\sqrt{3}$ times the confocal distance beyond the beam waist and tilted slightly with respect to the normal incidence beam to avoid interference effects due to back-reflection. The pump beam was then stopped with a Glan prism. The intensity of the centre portion of the probe beam was sampled by a 0.4 mm i.d. aperture and detected using a reversed-biased PIN photodiode. The signal from the photodiode was observed on an oscilloscope and sent to a lock-in amplifier or a boxcar averager. The entire optical system was mounted on a 0.8 × 1.6 m granite optical table.

The choice of focusing lens ($f = 100$ mm) and the distance from the lens to the detector (0.5 m) were optimised in previous work.[17] Indeed, the use of a lens having a short focal length presented several advantages. As t_c varies as the square of the spot size (beam radius) in the cell, the steady state is approached more rapidly and the sensitivity of the thermal response to the sample flow should be reduced. From another point of view, the probe beam diverges more rapidly when focused more tightly, hence the detector can be placed closer to the sample cell. The detection stage is, therefore, less sensitive to laser stability and alignment drift and it allows the experimental set-up to be more compact.

Two flow cells were used successively. The first was a 1.5 × 1.5 mm square-channel cell (Hellma, 176.352-QS) with a quartz window 11 mm high. The cell was positioned with the sample flowing up vertically through the laser beams. The laser propagated at about 5 mm from the cell entrance so the effective dead volume was about 11 µl. The second cell was a 12-µl, 1.4 mm i.d. tubular cell with a path length of 8 mm (Kratos, 2900-0146). In the latter, the cell axis and therefore the sample stream were parallel to the laser beam.

In order to reduce the noise originating from optical interferences between the probe and pump beams, the two beams were slightly crossed in the sample cell (crossing angle, *ca.* 0.9°). In this condition, the pump - probe interaction length, l_i, could be approximated by the equation[18]

$$l_i = 2w_i/\sin\phi$$

where w_i is the spot size in the cell and ϕ the angle at which the beams cross. The spot size could be evaluated from the equation[4,7]

$$w_i^2 = w_0^2[1 + (Z/Z_c)^2]$$

where Z is the distance of the cell centre from the beam waist (12 mm), Z_c the confocal distance (7.9 mm) and w_0 the spot size at the waist (40 µm).[17] In this instance $w_i = 72$ µm, which corresponds to an interaction length of about 9 mm. As this value is not much greater than the path length of the tubular cell, the effective interaction length was calculated by comparing the signals given by the same sample in the two cells and assuming that, in the square-channel cell, the effective interaction length equals the 1.5-m path length; an effective interaction length of 6.5 mm was calculated for the tubular cell.

The samples or the solvent alone were pumped through the flow cell using a precision micropump fitted with a pulse-damping system and connected to an injection valve equipped with an interchangeable sample loop. The injection valve was connected to the flow cell with 0.25 mm i.d. Teflon tubing. Samples of copper(II) - EDTA in water were prepared from stock solutions of known absorbance. These were then either pumped continuously through the flow cell or injected with the injection valve into a water stream, as required by the experiment.

Results and Discussion

Thermal Lens Behaviour For a Continuously Flowing Sample

Initially it was of interest to study the shape of the periodic signal seen on the oscilloscope. The time-resolved periodic signals for a solution of copper(II) - EDTA in water, corresponding to the "on" portion of the chopper and monitored with a boxcar averager, are shown in Figs. 1 and 2. For a static non-flowing sample, the probe beam intensity decreases as the thermal lens forms and the signal, expressed as $I_0 - I(t)$, reaches a steady-state value when $t > t_c$. The temporal response of the thermal lens signal for CW laser excitation is given by the equation[19]

$$S(t) = S(t = \infty)(1 + t_c/t)^{-1}$$

Hence the graph may be used to calculate t_c, the time at which the signal is half its steady-state value. The values obtained, 11.6 and 11.9 ms, are in good agreement with the theoretical value of 9 ms calculated from the following equation:

$$t_c = w_i^2\rho C_p/4k$$

where w_i is the beam radius in the sample cell (72 µm), ρ the density (1 g cm^{-3}), C_p the heat capacity (4.19 J g^{-1} K^{-1}) and k the thermal conductivity (6 × 10^{-3} J s^{-1} cm^{-1} K^{-1}).

The effects of flow-rate on the signal intensity using each flow cell are also shown in Figs. 1 and 2. For both cells, the signal amplitude was dependent on the flow-rate; the higher the flow-rate, the faster was the rise time and the smaller the signal amplitude. Nevertheless, the flow disturbance was much greater when the flow was perpendicular to the laser propagation. Moreover, as the flow-rate was increased, the shape of the time-dependent signal changed; the flow-rate had no effect on the initial intensity because the refractive index of the medium was constant, but with increasing time and during the "on" phase of the chopper, the signal reached a maximum value and then decreased. According to Dovichi and Harris,[14] the thermal lens signal would change as a result of two effects. Firstly, mixing would result in a decrease in the effective

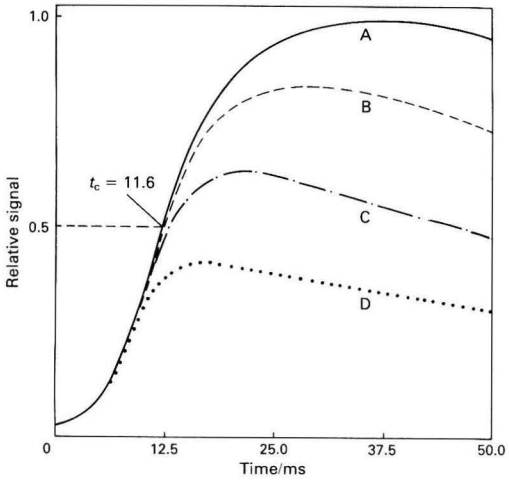

Fig. 1. Time-resolved thermal lens signal obtained with the square-duct cell (Hellma) and transverse configuration during the "on" phase of the chopper cycle. Chopper frequency = 10 Hz (data from 10^4 chopper cycles were averaged using a boxcar). Flow-rate: A, 0; B, 0.34; C, 0.75; and D, 1.5 ml min^{-1}

characteristic time constant t_c and a more rapid approach towards the steady state. Secondly, the bulk flow or cooling would lead to a decrease in the temperature gradient and hence reduce the thermal lens effect. In fact, the two effects cannot be distinguished by comparison of the graphs obtained with the different cells (Figs. 1 and 2) if it is assumed that the steady-state signal is influenced more when the flow direction is perpendicular to the beam axis (Fig. 1). With the second configuration, for which mixing is the most important factor, the rising part of the curves is not affected by the flow (Fig. 2). With pulsed excitation,[15] the influence of the flow-rate on signal decay provides further evidence that the signal evolves as a result of competition between the signal rise due to heat input from laser excitation and heat removal originating from mass transfer. At times that are long compared with the thermal time constant t_c, the signal decreases because the probe laser no longer interacts with the centre of the refractive index gradient and the steady state is not achieved.

The frequency dependence of the lock-in amplifier signal for both static and flowing samples is shown in Fig. 3. For a static sample, the signal increases as the chopping frequency decreases; however, there is some discrepancy between these graphs and those representing the periodic signal. In fact, when measurements were performed at 10 Hz, the periodic signal reached a steady-state value well before the end of the "on" phase of the chopper. In contrast, the output of the lock-in amplifier increased continuously even below 10 Hz. The frequency dependence of the demodulated signal is more consistent with t_c because for $t_c = 10$ ms, the signal obtained at 10 Hz is theoretically 83% of the maximum signal. With sample flowing through the cell, the maximum signal is approached more quickly when the chopping period is increased, as for the periodic time-dependent signal; however, the amplitude of the former decreases as the flow-rate increases. As already stated, the bulk flow acts as a thermal transport mechanism contributing to thermal diffusion. Nevertheless, the observed frequency dependence of the signal is different for each of the two cells; at 10 Hz, a steady-state signal is obtained at flow-rates >0.5 ml min^{-1} with the square-duct cell [transverse configuration, Fig. 3(*a*)] and >3 ml min^{-1} with the tubular cell [axial configuration, Fig. 3(*b*)]. At higher frequencies (≥80 Hz), the chopping period is comparable to or lower than t_c and the signal is nearly independent of the flow-rate.

Figs. 4 and 5 show the variation of the thermal lens signal with flow-rate when operating at a constant chopping frequency. At low flow-rates, and up to a critical value that depends on the chopping frequency, the signal remains constant. The maximum flow-rate, d_m, giving a constant signal is given in Table 1. In order to compare the two types of flow cell, these values must be expressed in terms of the linear velocity, v_1, which is used to determine the residence time of the sample in the laser beam. According to Dovichi and Harris,[14] the time scale necessary for axial bulk flow (tubular cell, flow parallel to the beam axis) to influence the thermal lens behaviour is given by the residence time of the sample in the cell. In the present context, we prefer to define the residence time as that time for which the sample is in the active part of the beam, *i.e.*, the effective path length divided by the linear velocity. In contrast, for the square-duct cell, the bulk flow is perpendicular to the beam axis and the residence time of the sample is equal to the beam diameter divided by the linear velocity. According to Nickolaisen and Bialkowski,[15] the signal would be substantially degraded if the solution were flowing at a sufficiently high linear rate to remove the heated sample from the laser beam on a time scale of t_c and hence the limiting flow-rate could be calculated by dividing the beam radius by t_c. In fact, the limiting residence time, t_r, calculated from the graphs shown in Fig. 4(*a*), depends on the chopping frequency and is in good agreement with the chopping period (Table 1); as long as t_r is greater than the chopping period, the thermal lens will have the same amount of time to evolve and the signal will not be affected by the flow. In order to corroborate this result, the same measurements were carried out with a beam, twice as large, obtained using a focusing lens with a focal length $f = 200$ mm. With this lens the spot size in the sample was calculated to be about 120 μm, and the calculated values of t_r corresponding to d_m [Fig. 4(*b*) and Table 1] were also found to be in the same range as the chopping period. As t_c varies with w^2, a dependence of t_r on w/t_c would give a value of d_m twice as low as that obtained with the smaller spot size. It is interesting to note that t_r corresponds to the chopping period and not to half the time of formation of the thermal lens. Indeed, with a continuously chopped heating source, if the durations of the "on" and "off" phases of the chopper are not sufficiently long with respect to t_c, the thermal lens will not reach equilibrium during the "on" phase and will not relax completely during the "off" phase. Hence, the temperature rise in the sample is caused not only by the action of the excitation beam during the current chopper cycle but also by a contribution from the previous chopper cycles. Because in our experiment the "on" and "off" phases of a chopper cycle are equal, the cumulative effect would depend only on the period of the chopper cycle, which determines the equilibrium between repetitive formation and relaxation of the thermal lens. The agreement of t_r with the chopping period would indicate that, for a flow perpendicular to the beam axis, bulk flow represents the major contribution to signal disturbance.

In contrast, with the tubular cell where the flow is parallel to the beam axis, t_r is much greater than the chopping period (Fig. 5 and Table 2) and the axial bulk flow is not the limiting

Table 1. Dependence of the limiting flow-rate and corresponding residence time on the chopping frequency and beam spot size in the square-duct cell (Hellma) with flow perpendicular to the beam axis. Sectional area of the flux = 0.0225 cm^2; d_m = maximum flow-rate giving an unchanged signal (from Fig. 4); and $t_r = 2w_i/v_1$

Frequency/ Hz	Chopping period/ms	d_m/ ml min^{-1}	v_1/cm s^{-1}	t_r/ms
10	100	0.16*	0.12	120
		0.32†	0.24	100
20	50	0.34*	0.25	56
		0.70†	0.52	46
80	12.5	1.20*	0.89	16

* $w_i = 72$ μm [data from Fig. 4(*a*)].
† $w_i = 119$ μm [data from Fig. 4(*b*)].

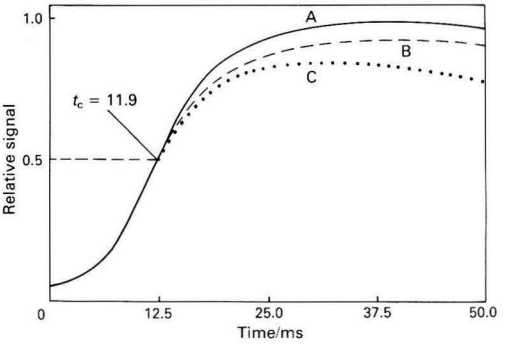

Fig. 2. Time-resolved thermal lens signal obtained with the tubular cell (Kratos) and axial configuration during the "on" phase of the chopper cycle. Chopper frequency = 10 Hz (data from 10^4 chopper cycles were averaged with a boxcar). Flow-rate: A, 0; B, 0.34; and C, 1.5 ml min^{-1}

Table 2. Dependence of the limiting flow-rate and corresponding residence time on the chopping frequency for the tubular cell (Kratos) with flow parallel to the beam axis. Sectional area of the flux = 0.0154 cm^2; d_m = maximum flow-rate giving an unchanged signal (from Fig. 5); and t_r = effective path length (0.65 cm) divided by v_1

Frequency/Hz	d_m/ml min^{-1}	v_1/cm s^{-1}	t_r/s
10	0.37	0.4	1.62
	5.5*	5.95	0.11
20	0.77	0.83	0.78
80	2	2.16	0.30

* Value corresponding to X on curve A, Fig. 5.

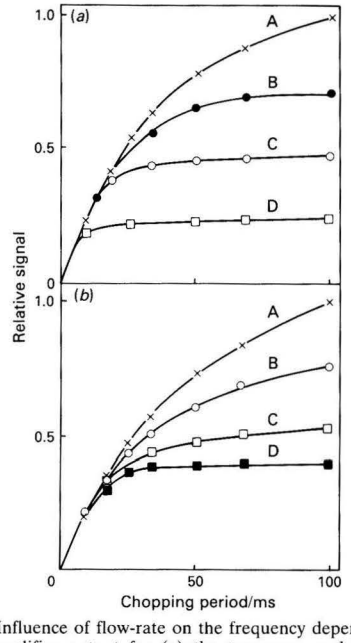

Fig. 3. Influence of flow-rate on the frequency dependence of the lock-in amplifier output for (*a*) the transverse and (*b*) the axial configuration. (*a*) Flow-rate: A, 0; B, 0.5; C, 1.4; and D, 2.3 ml min^{-1}. (*b*) Flow-rate: A, 0; B, 1.5; C, 3; and D, 4 ml min^{-1}

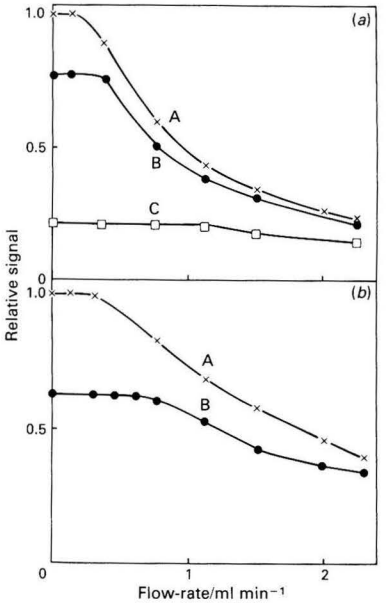

Fig. 4. Dependence of the thermal lens signal (lock-in output) on the flow-rate at constant frequency (Hellma cell, transverse configuration). Focal length of the focusing lens: (*a*) 100 and (*b*) 200 mm. Chopping frequency: A, 10; B, 20; and C, 80 Hz

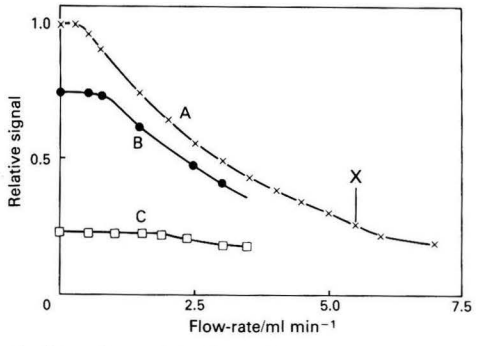

Fig. 5. Dependence of the thermal lens signal on the flow-rate at constant frequency (Kratos cell, axial configuration). Chopping frequency: A, 10; B, 20; and C, 80 Hz. Focal length of the focusing lens, 100 mm. X corresponds to the limiting axial bulk flow

factor. Previously, a dependence on the transverse bulk flow was ruled out on the basis that no beam deflection was observed.[14] The decrease in signal intensity was thought to be caused by turbulence within the cylindrical channel, which has the effect of mixing the heated material with the surrounding material in a section of the bulk flow. Also, as shown in Figs. 1–3, the effect of mixing in the tubular cell is less important than the effect of bulk flow in the square-duct cell. At a flow-rate of 1 ml min^{-1}, and operating at 10 Hz, the signal was about 85% and less than 50% of that for a static sample with the tubular cell (axial configuration) and the square-duct cell (transverse configuration), respectively. At higher flow-rates, the plot of signal intensity *versus* flow-rate, with the tubular cell, shows a small inflection centred at about 5.5 ml min^{-1} (Fig. 5); this corresponds to $v_1 \approx 6$ cm s^{-1} and $t_r = 108$ ms. This latter value is close to the chopping period (100 ms) and characterises the limiting axial bulk flow for such a configuration.

Thermal Lens Response for Flow-injected Samples

In order to minimise the effect of flow and to reduce degradation of the thermal lens signal, the chopper was operated at 80 Hz. The signals obtained (expressed as peak height) with various flow-rates and injected sample volumes in the range 7–200 μl are shown in Fig. 6. As expected, the peak height increased with the injected sample volume and, at moderate flow-rates, reached a steady-state value corresponding to the signal obtained for an undiluted sample (H_0). The upper curves in Fig. 6(*a*) and (*b*), corresponding to a flow-rate of 0.12 ml min^{-1}, may be used to characterise the dispersion of the system. In flow injection techniques, the dispersion, D, is defined as the ratio of the concentrations before and after the dispersion process has taken place in the segment of sample that yields the signal, *i.e.*, the ratio of signal height H_0 obtained when the undiluted sample flows continuously through the cell to peak height, H, in the flow injection mode[20] ($D = H_0/H$). The minimum dispersion is unity, and a dispersion of two was obtained for both cells with an injected volume of about 10–12 μl. By injecting a sample volume equal to the dead volume of the cell, a signal readout of about half the steady-state signal was obtained giving a good compromise between sample volume and peak intensity.

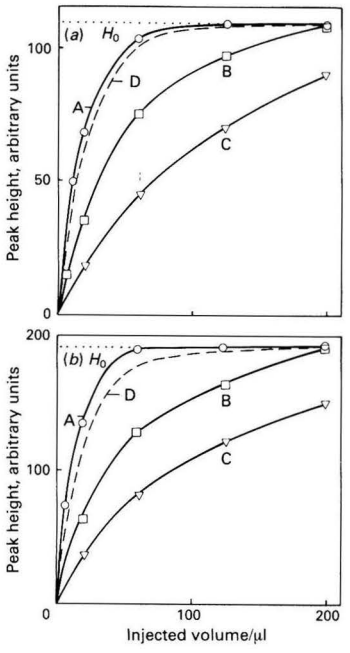

Fig. 6. Dependence of peak height on the injected sample volume and flow-rate. (*a*) Square-duct cell and transverse configuration; and (*b*) tubular cell and axial configuration. Chopping frequency, 80 Hz. Flow-rate: A, 0.12; B, 0.75; and C, 1.5 ml min^{-1} (lock-in operating with a 3-s time constant); and D, 0.75 ml min^{-1} (lock-in operating with a 1-s time constant). H_0 = steady-state signal for an undiluted sample

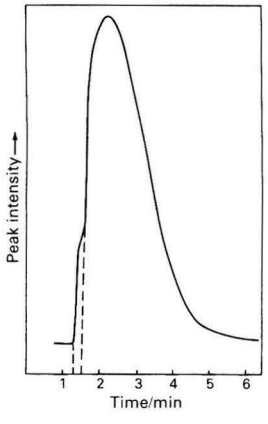

Fig. 7. Distortion of the rising part of the peak of a flow-injected sample (tubular cell, axial configuration). Chopping frequency = 80 Hz; flow-rate = 50 μl min^{-1}; and injected volume = 60 μl

When the flow-rate was increased to a range where the thermal lens response for a continuously flowing sample was independent of flow, the result was a loss of sensitivity. This may have originated partly from an increase in the dispersion and mainly from the response time of the detection system. As the photodiode had a rise time of 1 ns, the large decrease in the peak intensity arose from the response of the lock-in amplifier, which operated at a 3-s time constant. As is also shown in Fig. 6, operation at a 1-s response time cancels the

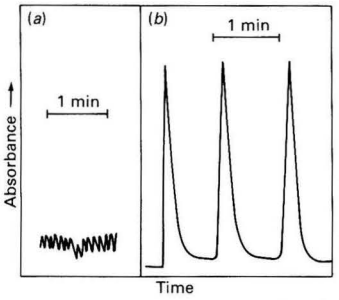

Fig. 8. Typical recording of flow-injected sample peaks (square-duct cell, transverse configuration). Chopping frequency, 80 Hz; flow-rate, 0.34 ml min^{-1}; and solvent, water. (*a*) Base-line noise with a 1-mV lock-in scale. (*b*) Flow-injected sample peaks in triplicate with a 5-mV lock-in scale. Copper(II) - EDTA in water; A = 0.024; cell path length, 1.5 mm; and injection loop volume, 7 μl

sensitivity loss almost completely, at least at moderate flow-rates. Nevertheless, if the 1-s time response is convenient at low flow-rates, allowing satisfactory spatial resolution of the peaks, it leads to a greater band pass of the fluctuations and spikes on the recording and, consequently, to less reproducible peak heights at higher flow-rates. Considering that, for a continuously flowing sample, the effect of flow is less with the tubular cell (Kratos), the sensitivity loss with this configuration is, by comparison, more important in the flow injection mode.

This result can be discussed with respect either to the volume or the length of the probed element, which is different for each configuration. In the transverse configuration (Hellma), the probed length is equal to the beam diameter (about 0.14 mm), whereas in the axial configuration (Kratos), it equals the effective path length (about 6.5 mm), a path length ratio of 45 : 1. This may be a serious drawback at low flow-rates and for small injection volumes, as can be seen in Fig. 7 in which the rising portion of the peak obtained at a low flow-rate in the axial configuration has a shoulder the width of which is exactly equal to the time necessary for the front of the sample zone to cross the path length of the cell (6.5 mm). In this part of the curve, which actually corresponds to the dead volume of the cell (10 μl), the intensity increases with both the sample concentration and the effective path length. Although both cells have the same dead volume, the transverse configuration enabled smaller volumes to be probed and this should result in a better spatial resolution of the peaks for small sample volumes and low flow-rates. On the other hand the axial configuration provided greater sensitivity.

Systematic comparison of cell performance with respect to flow-rate and injected sample volume would have been tedious and was not the aim of this work. As an example of such a comparison, the flow injection response of the thermal lens at a moderate flow-rate and with an injected sample volume approximately equal to the dead volume of the cell is shown in Fig. 8. The blank response was fairly constant and was not significantly affected by the flow for flow-rates <1 ml min^{-1}. The peak to peak base-line noise corresponded to an absorbance of 7.2×10^{-5}, which, with a peak signal to peak to peak blank noise ratio of 2 (*i.e.*, 10σ), gave a minimum measurable absorbance of 1.5×10^{-4}.

In conclusion, the effects of axial bulk flow and mixing, which arise from the flow cell geometry and beam propagation with respect to the flow direction, may significantly affect the thermal lens signal. Nevertheless, with an appropriate configuration and at flow-rates compatible with most applications of flowing sample detection, the signal is reduced only to a small extent. The small volume probed with the transverse configuration is more convenient for low flow-rate and small

injection volume applications such as liquid chromatography; the axial configuration is well suited to high flow-rate and large injection volume applications, such as high-speed titrations by flow injection or automated analysis. The performance of the transverse configuration (Hellma) can be improved by increasing the optical path length and reducing the channel width to obtain a higher sensitivity without increasing the dead volume of the cell. However, the combination of high sensitivity and very low detection volume is not compatible with co-linear thermal lensing because of the dependence of Beer's law on the path length and because of optical constraints. Finally, the development of a very small volume detector for microbore liquid chromatography requires the use of the crossed-beam geometry implemented in photothermal refraction.[21,22]

References

1. Morris, M. D., and Peck, K., *Anal. Chem.*, 1986, **58**, 811A.
2. Dovichi, N. J., *Crit. Rev. Anal. Chem.*, 1987, **17**, 357.
3. Harris, T. D., *Anal. Chem.*, 1982, **54**, 741A.
4. Harris, J. M., and Dovichi, N. J., *Anal. Chem.*, 1980, **52**, 695A.
5. Fang, H. L., and Swofford, R. L., *in* Kliger, D. S., *Editor*, "Ultrasensitive Laser Spectroscopy," Academic Press, New York, 1983, p. 176.
6. Harris, J. M., *in* Piepmeier, E. H., *Editor*, "Analytical Applications of Lasers," Volume 87, Wiley-Interscience, New York, 1986, p. 451.
7. Georges, J., and Mermet, J.-M., *Analusis*, 1988, **16**, 203.
8. Dovichi, N. J., *Prog. Anal. Spectrosc.*, 1988, **11**, 179.
9. Dovichi, N. J., Nolan, T. G., and Weimer, W. A., *Anal. Chem.*, 1984, **56**, 1700.
10. Nolan, T. G., and Dovichi, N. J., *Anal. Chem.*, 1987, **59**, 2803.
11. Weimer, W. A., and Dovichi, N. J., *Appl. Opt.*, 1985, **24**, 2981.
12. Weimer, W. A., and Dovichi, N. J., *Appl. Spectrosc.*, 1985, **39**, 1009.
13. Weimer, W. A., and Dovichi, N. J., *Anal. Chem.*, 1985, **57**, 2436.
14. Dovichi, N. J., and Harris, J. M., *Anal. Chem.*, 1981, **53**, 689.
15. Nickolaisen, S. L., and Bialkowski, S. E., *Anal. Chem.*, 1986, **58**, 215.
16. Nickolaisen, S. L., and Bialkowski, S. E., *Anal. Chem.*, 1985, **57**, 758.
17. Georges, J., and Mermet, J.-M., *Analyst*, 1988, **113**, 1113.
18. Jackson, W. B., Amer, N. M., Boccara, A. C., and Fournier, D., *Appl. Opt.*, 1981, **20**, 1333.
19. Carter, C. A., and Harris, J. M., *Appl. Opt.*, 1984, **23**, 476.
20. Růžička, J., and Hansen, E. H., "Flow Injection Analysis," Wiley, New York, 1981
21. Kettler, C. N., and Sepaniak, M. J., *Anal. Chem.*, 1987, **59**, 1733.
22. Nolan, T. G., Hart, B. K., and Dovichi, N. J., *Anal. Chem.*, 1985, **57**, 2703.

Paper 8/03383H
Received August 22nd, 1988
Accepted January 4th, 1989

Study of Dynamic Processes by Impulse Response Photoacoustic Spectroscopy

Richard M. Miller
Unilever Research, Port Sunlight Laboratory, Quarry Road East, Bebington, Wirral, Merseyside L63 3JW, UK

Graham R. Surtees and Christopher T. Tye
Department of Instrumentation and Analytical Science, University of Manchester Institute of Science and Technology, P.O. Box 88, Manchester M60 1QD, UK

Impulse response photoacoustic spectroscopy has been used to study variations in chromophore distribution with time in a dynamic system. A system in which a dye diffuses through a polymer film has been examined, and it is shown that it is possible to monitor the diffusion process *in situ* and non-destructively. Comparison of the experimental results with a theoretical model demonstrates that the results are consistent with classical diffusion processes.

Keywords: *Photoacoustic spectroscopy; impulse response measurements; diffusion; polymers*

Alexander Graham Bell discovered that when an absorbing solid mounted in a closed container was illuminated by an amplitude modulated light source, an acoustic signal was produced at the same frequency as the modulation of the light.[1] This phenomenon became known as the optoacoustic or photoacoustic effect, and has subsequently found application in the analysis of gases,[2] the measurement of vibrational relaxation times of gases,[3,4] the spectroscopy of opaque and light-scattering solids[5–7] and the imaging of sub-surface details in thin films.[8,9]

The mechanisms behind the photoacoustic effect are well documented,[7,10] and of its many applications the spectroscopic characterisation of solids is the most widespread. Besides its obvious advantages in the analysis of difficult samples, photoacoustic spectroscopy (PAS) offers a unique, non-destructive method of obtaining depth related information in solids.[7,11] When a sample is illuminated by a modulated radiation source of a wavelength absorbed by the sample, a modulated heat source will be produced by internal conversion of excited molecular states. The spatial distribution of the heat source will be a function of the optical absorption of the sample. A sample of high absorbance will produce a localised heat source close to the illuminated face of the sample. A weaker absorber will produce a more distributed heat source in the sample. A sample with strong sub-surface absorption will produce a localised sub-surface heat source, and so on. As the heat released by radiation absorption must diffuse through the sample to the surface before detection, different initial heat source distributions produce variations in the evolution of the photoacoustic signal with time. Analysis of the photoacoustic signal in the time domain provides information on the absorption coefficient, distribution of the chromophore and thermal properties of the sample.

Attention has focused on the measurement of the photoacoustic impulse response of a sample as a means of gaining the necessary time domain information. Studies have included the measurement of film thickness,[12] dye distribution in coloured films[13–15] and the examination of chromophore distributions in intact leaves and petals.[13,16] It has been shown that the shape of the photoacoustic impulse response depends on the chromophore distribution and that by measuring the impulse response at a series of wavelengths, a response surface can be constructed which gives information about variations in the photoacoustic signal with both wavelength and depth. This technique is usually called impulse response photoacoustic spectroscopy (IMPAS) or correlation photoacoustic spectroscopy (CPAS).

Impulse response photoacoustic spectroscopic measurements can be performed by illuminating a sample in a photoacoustic cell with a brief pulse of light and recording the resulting photoacoustic transient. However, the duty cycle of such a measurement system is very low and time-consuming signal averaging is required to produce usable results.[17] A more convenient method of making impulse response measurements is to use multi-frequency modulation of the incident radiation and to recover the system impulse response by cross-correlation of the modulation with the detected photoacoustic signal. This technique is used widely in engineering and telecommunications[18,19] and has proved very successful in recovering impulse responses in noisy environments. It can be shown that the cross-correlation between the input and output of a system is the convolution of the auto-correlation of the input to the system with the system weighting function.[19] If the input signal has the same auto-correlation function as an impulse, then the cross-correlation function will be a good estimate of the system impulse response. A suitable multi-frequency test signal for this application is the pseudo-random binary sequence (PRBS). This has the same auto-correlation function as a single pulse, but has a 50% duty cycle. As the strength of the photoacoustic signal is a function of the total amount of energy released in the sample per unit time, the use of PRBS modulation with cross-correlation signal recovery provides a dramatic improvement in signal to noise ratio over single pulse methods.[12] It has been the basis of most of the IMPAS studies.[12–16] An alternative approach has been demonstrated successfully by Mandelis and co-workers,[20,21] who used a swept frequency sine wave modulation coupled with a correlation signal recovery process to obtain the system transfer function and impulse response.

As the photoacoustic impulse response can be measured in a short time using the cross-correlation technique, it is logical to apply the method to systems where the chromophore distribution is a function of time. Hence dynamic physico-chemical systems can be studied. In a preliminary paper,[22] we have reported the observation of dynamic changes in the impulse response as a result of varying chromophore distribution. In this paper we extend the work to a study of dye diffusion in a polymer matrix.

Experimental

Apparatus

A block diagram of the experimental apparatus used is shown in Fig. 1. The radiation source was a krypton ion laser (Innova

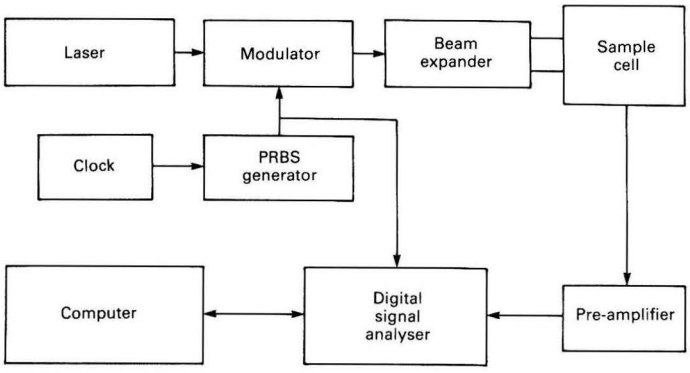

Fig. 1. Block diagram of the experimental apparatus

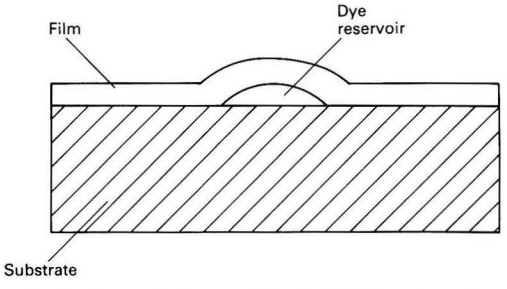

Fig. 2. Schematic diagram of the dye diffusion test sample

90-K, Coherent UK, UK). Measurements were made using the 647-nm laser line, at an output power of 40 mW. Amplitude modulation was carried out using an acousto-optic modulator (Model 304, Coherent UK). The PRBS modulation signal was generated using a PSI A108 correlator (Prosser Scientific Instruments, UK). A 127-bit PRBS was used for all experiments. The clock frequency of the PRBS was determined by a variable frequency square wave generator (Model TG 310, Levell, UK). A clock frequency of 333 Hz was used for all experiments, giving a PRBS equivalent to a 3×10^{-3} s impulse excitation.

The modulated source was directed via a beam expander on to samples contained in a gas-microphone photoacoustic cell (Model OAS 401, EDT Research, UK). The sample chamber of this cell had a usable area of 15 × 5 mm and was *ca.* 1 mm deep.

The photoacoustic signal from the cell was amplified by a low noise pre-amplifier (Model 450S, EG & G Brookdeal, UK) and passed into a digital signal analyser (Solatron 1200, Solatron, UK), where it was cross-correlated with a reference PRBS from the generator. Data acquisition and the storage of impulse responses were controlled by an HP 9816 microcomputer [Hewlett-Packard (UK), UK] connected to the Solatron 1200 analyser through an IEEE-488 interface bus.

Software which allowed the remote control of the signal analyser, the acquisition and storage of data and its subsequent manipulation and display was written in HP BASIC 2.0. Impulse responses were plotted on a digital plotter [Model HP7470A, Hewlett-Packard (UK)] connected to the IEEE-488 interface bus.

Sample Preparation

Small amounts of a blue, solvent-based ink were placed on to the underside of pieces of a waterproof sealing film (Parafilm, Gallenkamp, UK). The Parafilm was then mounted on to a piece of double-sided adhesive foam strip, providing a thermally thick substrate. The ink drop was sandwiched between the film and substrate (Fig. 2). As soon as the ink made contact with the film, it began to diffuse through the film to the upper surface. The samples were placed in the photoacoustic cell, film uppermost, and illuminated through the film. Light would be absorbed by the dye and heat released.

Method

At specified time intervals, the microcomputer initiated the impulse response measurement by the signal analyser. Each impulse response was the result of averaging 50 measurement cycles, typically taking 35 s in total. At the end of each measurement the impulse response was transferred to the microcomputer. Each experiment consisted of 20 individual impulse responses. The time between impulse response measurements could be varied at the beginning of each experiment to take account of varying diffusion rates. At the end of each experiment the 20 impulse responses were stored on disk for later analysis.

Digital Simulation

In order to be able to compare the results with theoretical predictions, a digital simulation model was used. A numerical method of solution was chosen rather than an analytical solution, because of the difficulties in handling complex distributed heat sources in the currently available closed form solutions. The numerical method of solution permits flexible definition of the problem conditions and rapid modification of the underlying assumptions. It is therefore a more appropriate approach for the type of problem being considered here.

The model used was a one-dimensional simulation of the optically induced heat flux in the sample under pulse excitation, using the finite difference method of solution. The finite difference simulation involves iteratively calculating the temperature distribution throughout the model system for successive small increments in time. The changes in temperature distribution are calculated by allowing for heat transfer between adjacent discrete elements in the model, taking into account any known heat sources or sinks within the model.

To simulate a system where the chromophore distribution through the thickness of the film was varying with time due to diffusion, a separate diffusion model was constructed in which the rear surface of the sample was assumed to be in contact with an infinite reservoir of diffusing species. Using similar methods of calculation, the fractional concentration of the diffusing species in each of the thickness elements of the sample was calculated for a series of time intervals after the start of the diffusion experiment. The results of these calculations were then fed to the main finite difference model

where the concentration distribution at a particular instant in time was used, together with the specified optical absorption coefficient of the chromophore, to generate the initial heat source distribution which would give rise to the photoacoustic impulse response. The modified impulse response was calculated for each time increment and the resulting series of impulse responses were compared with the experimental results.

By varying the parameters and assumptions used in the dye diffusion calculations, various possible interpretations of the experimental data could be assessed.

The simulation model was written in FORTRAN 77 on a VAX 11/785B (Digital Equipment, USA). Double precision arithmetic was used to avoid the accumulation of truncation rounding errors in the iterative calculation of heat diffusion. Graphical output was obtained using the FREELANCE + graphics package (Lotus Development, USA). Full details of the model and the simulations carried out have been published elsewhere.[23,24]

Results and Discussion

Fig. 3 shows the sample impulse response at the beginning of a diffusion experiment and Fig. 4 shows the response after diffusion for 30 min. Significant differences between the impulse responses are evident. In Fig. 3 there is a small sharp peak at a short delay, followed by a much broader, flatter peak with a much greater peak delay.

The first feature is probably due to residual surface absorption. This phenomenon has also been observed in other systems.[14,15] Most samples have a residual broad band optical absorption at the sample/gas interface. This residual absorption produces a small sharp peak in the response at a very small delay. Improved sample handling can reduce the size of this surface feature, but cannot eliminate it. However, this surface feature can be useful in providing a reference time marker in the system, which is relatively constant between impulse responses.

The second feature is typical of the impulse response obtained from a sub-surface chromophore.[14] It is broadened by diffusion and of relatively low amplitude due to energy dissipation within the sample as the heat propagates.

In Fig. 4, the diffusion of the dye has brought the chromophore much closer to the surface of the sample. As a result, the peak of the impulse response has moved to much shorter delays and the peak height is much greater. The width of the impulse response peak is also significantly reduced. All these changes are consistent with a shift in the chromophore position from deep within the sample to much closer to the surface.[14] The surface feature is still present, but has been obscured by the much bigger response from the chromophore.

This interpretation is supported by the results shown in Fig. 5. Three impulse response curves are shown for static systems. Curve A shows the impulse response obtained from a sample of film applied directly to the standard adhesive foam strip. For this sample there is no strong sub-surface absorption and the impulse response shows only the residual surface absorption. The total signal intensity is very low for this sample. Curve B shows the impulse response obtained for a sample in which carbon black was trapped between the foam substrate and the film. As a non-diffusing material, the carbon black gives an indication of the type of impulse response which would be observed at diffusion time zero if it were possible to perform this experiment. The expected broad sub-surface signal is seen. Curve C shows the result of applying a high concentration of a strongly absorbing dye directly to the surface of sample A. A very strong surface signal is obtained which grows in during the 3×10^{-3} s period equivalent to the pulse width of the excitation and which then decays exponentially. This result should be equivalent in form to the result obtained from the diffusion experiment after infinite diffusion time.

The surface features obtained from these static samples are sharper than those seen in the diffusion experiments. This is attributed to a different batch of film being used for the diffusion studies that had a small residual absorption throughout the film thickness giving a more distributed surface feature.

Fig. 6 shows curves A and C from Fig. 5 normalised with respect to each other and overplotted. Despite the large difference in signal amplitude, the signal form is very similar for the two curves. Both are surface signals and exhibit virtually identical time courses. This is further evidence that the system is linear over a large range of signal amplitudes.[12] The response from the dye-coated sample shows a slight

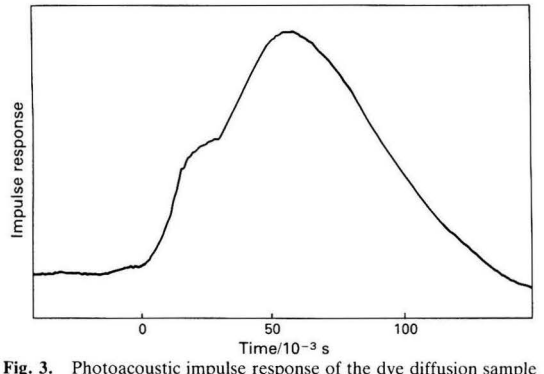

Fig. 3. Photoacoustic impulse response of the dye diffusion sample at time zero

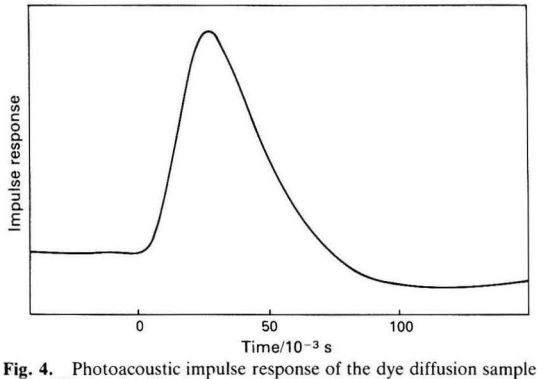

Fig. 4. Photoacoustic impulse response of the dye diffusion sample after diffusion for 30 min

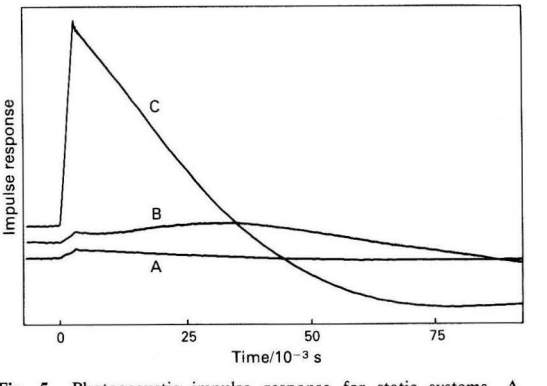

Fig. 5. Photoacoustic impulse response for static systems. A, Untreated film; B, untreated film backed with carbon black; and C, film surface coated with a strongly absorbing dye

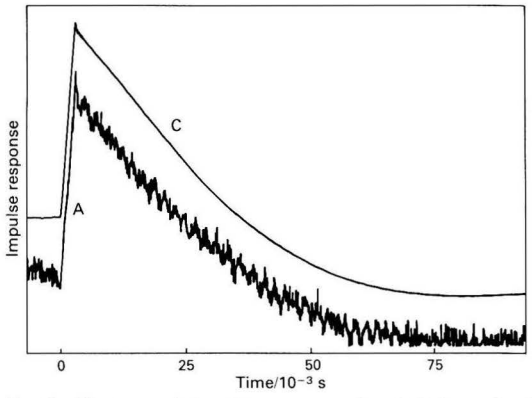

Fig. 6. Photoacoustic impulse responses A and C from Fig. 5 normalised to the same amplitude

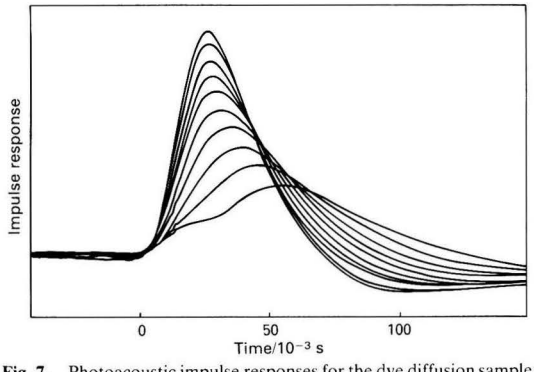

Fig. 7. Photoacoustic impulse responses for the dye diffusion sample recorded at 3-min intervals over a period of 30 min

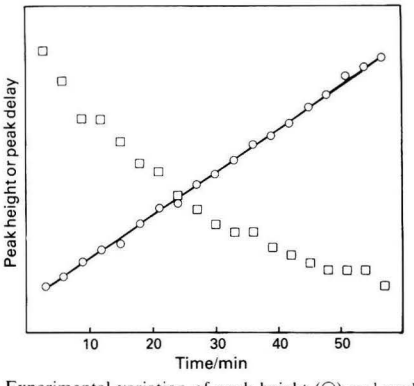

Fig. 8. Experimental variation of peak height (○) and peak delay (□) with time for the dye diffusion sample. The linear regression line for the peak height data is indicated

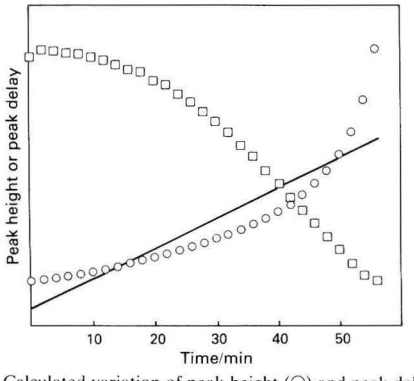

Fig. 9. Calculated variation of peak height (○) and peak delay (□) with time assuming a moving boundary transport mechanism. The linear regression line for the peak height data is indicated

positive deviation from the typical exponential decay in the region just after the peak of the response. This may be due to penetration of the dye into the matrix or an absorption coefficient for the dye at the laser wavelength which allows some penetration of the incident radiation below the sample surface. The response is consistent with a resulting surface-weighted distributed heat source.[23] Because of the higher noise level on the uncoated sample, the two responses are not significantly different.

Fig. 7 summarises results from a complete experiment. It consists of ten overlaid impulse response measurements taken at 3-min intervals over a period of 30 min. At the start of the run the impulse response appears as in Fig. 3, with two distinct peaks, one arising from a surface feature and the other from a sub-surface chromophore. During the course of the experiment there is a gradual movement of the sub-surface peak to shorter time delays. This is due to dye diffusing towards the surface of the film.

The changes in peak delay and peak height with time are illustrated in Fig. 8. The peak delay shows a decaying trend with increasing diffusion time as the chromophore diffuses towards the surface of the sample. The peak height shows an approximately linear increase with time. A linear regression line has been plotted for the changes in peak height. These results are typical of a number of experiments which were carried out and which show influences due to the experimental conditions. For example, the apparent linear increase in peak height with time was observed for all experiments, although the slope varied. This variation was associated with the amount of dye solution used and may indicate variations in the rate of diffusion.

Although there is a clear empirical relationship between the changes in the impulse response and changes in the chromophore distribution with time, we needed to determine if the experimental results were consistent with a reasonable physical model of the processes involved. To attempt to resolve this question, the experimental results were compared with the results obtained from the digital simulation model.

Initially, we wished to determine whether the experimental results were consistent with the assumption that the dye was being transported through the membrane in accordance with Fick's law.[25] Two alternative hypotheses were evaluated; that the chromophore was diffusing according to Fick's law or that the chromophore formed a sharply defined boundary which progressed through the thickness of the polymer membrane at a constant velocity. The second hypothesis is not physically realistic, but represented a test of whether we could distinguish between two very different assumptions about the transport mechanisms using the experimental data available.

Fig. 9 summarises the predicted responses assuming the moving boundary hypothesis. The peak delay shows a positive deviation from a straight line rather than the negative deviations seen experimentally and the peak height shows a strong negative deviation from the approximately linear dependence observed in the experimental data. It is clear that the form of the curves are completely different to those shown in Fig. 8. Variation of the absorption coefficient for the chromophore and the boundary velocity did not change the shape of the curves substantially and it is therefore clear that the experimental data cannot be accounted for by postulating a moving boundary transport mechanism.

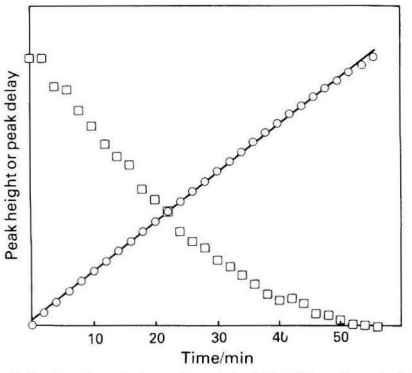

Fig. 10. Calculated variation of peak height (○) and peak delay (□) with time assuming a diffusion according to Fick's law. The linear regression line for the peak height data is indicated

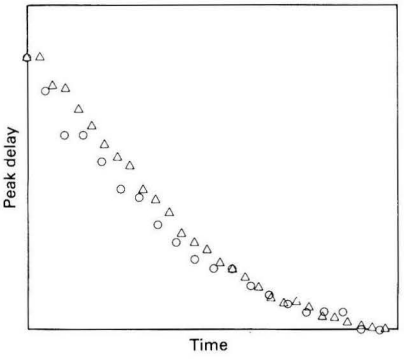

Fig. 11. Comparison of experimental (○) and simulated (△) data for the variation of peak delay with diffusion time

Fig. 10 summarises the theoretical predictions based on the assumption of classical diffusion in accordance with Fick's law. The linear relationship between peak height and diffusion time observed in the experimental data is also found in the simulated data and the curve representing the variation of peak delay with diffusion time is of the same general form in both experimental and simulated data. The linear relationship between peak height and diffusion time is preserved over a range of diffusion coefficients and the slope varies in a manner analogous to that observed in the experimental data.

Fig. 11 illustrates the variation in peak delay with diffusion time for the experimental data and a simulation experiment where the variation in peak height with time agrees closely with the experimental data. It is important to note that the simulation results are expressed in arbitrary units. It is therefore easy to scale the simulation results so that the end points of the curve agree with the experimental data. In assessing the fit between the simulation and experimental data, the criterion of agreement must be the deviations of the simulation and experiment between these two points. It is clear that the simulated curve is not inconsistent with the experimental one, although the deviations are still greater than can be accounted for by the scatter in the experimental points. In addition, because of the way in which the simulation has been carried out it is not possible to specify the diffusion coefficient in physically meaningful units. Further work will be required on a range of samples to quantify the transfer function of the cell and to complete the mapping between the model and sample. At present, the technique can be used on a comparative basis, but not on an absolute basis.

Conclusions

Impulse response photoacoustic spectroscopy has been used successfully to monitor chromophore distribution in a dynamic physico-chemical system. The results have been shown to be consistent with simulations based on physically realistic assumptions. The method is non-destructive and offers considerable advantages over alternative approaches to characterising dynamic systems. It is anticipated that the technique will find application in a wide range of systems, including the uptake of dye by films and fibres, the dynamics of controlled release drug formulations and the study of transport mechanisms in biological and clinical systems.

Future developments of the technique should include a better theoretical understanding of the relationship between the chromophore distribution and the resulting impulse response, its use with tunable light sources for time dependent IMPAS and the application of non-contacting detection systems to allow a wider range of sample types to be studied.

We thank Simon Johnson and Ed Staples of Unilever Research, Port Sunlight Laboratory, for their assistance in the studies carried out on the static systems.

References

1. Bell, A. G., *Philos. Mag.*, 1881, **11**, 510.
2. Pfund, A. H., *Science*, 1939, **90**, 326.
3. Read, A. W., *Adv. Mol. Relaxation Processes*, 1967, **1**, 257.
4. Cottrell, T. L., Macfarlane, I. M., Read, A. W., and Young, A. H., *Trans. Faraday Soc.*, 1966, 62.
5. Adams, M. J., King, A. A., and Kirkbright, G. F., *Analyst*, 1976, **101**, 119.
6. Rosencwaig, A., *in* Pao, Y.-H., *Editor*, "Optoacoustic Spectroscopy and Detection," Academic Press, New York, London, 1977, Chapter 8.
7. Rosencwaig, A., "Photoacoustics and Photoacoustic Spectroscopy," Wiley-Interscience, New York, 1980.
8. Kirkbright, G. F., and Miller, R. M., *Analyst*, 1982, **107**, 798.
9. Kirkbright, G. F., Liezers, M., Miller, R. M., and Sugitani, Y., *Analyst*, 1984, **109**, 465.
10. McDonald, F. A., *Am. J. Phys.*, 1980, **48**, 41.
11. Adams, M. J., Beadle, B. C., King, A. A., and Kirkbright, G. F., *Analyst*, 1976, **101**, 553.
12. Kirkbright, G. F., and Miller, R. M., *Anal. Chem.*, 1983, **55**, 502.
13. Sugitani, Y., Uejima, A., and Kato, K., *J. Photoacoustics*, 1982, **1**, 217.
14. Kirkbright, G. F., Miller, R. M., Spillane, D. E. M., and Sugitani, Y., *Anal. Chem.*, 1984, **56**, 2043.
15. Uejima, A., Sugitani, Y., and Nagashima, K., *Anal. Sci.*, 1985, **1**, 5.
16. Kirkbright, G. F., Miller, R. M., Spillane, D. E. M., and Vickery, I. P., *Analyst*, 1984, **109**, 1443.
17. Cox, M. F., and Coleman, G. N., *Anal. Chem.*, 1981, **53**, 2034.
18. Davies, W. D. T., "System Identification for Self Adaptive Control," Wiley, London, 1970.
19. Lynn, P. A., "An Introduction to the Analysis & Processing of Signals," Second Edition, Macmillan, London, 1984.
20. Mandelis, A., *Rev. Sci. Instrum.*, 1986, **57**, 622.
21. Mandelis, A., and Sin, E. K. M., *Phys. Rev. B*, 1986, **34**, 7209.
22. Miller, R. M., Surtees, G. R., Tye, C. T., and Vickery, I. P., *Can. J. Phys.*, 1986, **64**, 1146.
23. Miller, R. M., *Can. J. Phys.*, 1986, **64**, 1049.
24. Miller, R. M., *Spectrochim. Acta, Part B*, 1988, **43**, 687.
25. Crank, J., "The Mathematics of Diffusion," Second Edition, Oxford University Press, London, 1975.

Paper 8/03998D
Received November 15th, 1985
Accepted January 6th, 1989

Production and Certification of Ten High-purity Polychlorinated Biphenyls as Reference Materials

Alan S. Lindsey and Peter J. Wagstaffe
Community Bureau of Reference, BCR, Commission of the European Communities, Rue de la Loi 200, B-1049 Brussels, Belgium

The development by the Community Bureau of Reference of ten polychlorinated biphenyl reference materials of certified purity is reported. The identity of the specially synthesised compounds was mostly confirmed by either nuclear magnetic resonance spectroscopy or X-ray crystallography. Measurements to establish the purity of the ten compounds were carried out in a collaborative certification campaign by 11 European Laboratories. The purity was based on the determination of individual impurities in each compound by applying various well-established measurement techniques. A statistical analysis of the results obtained provided the basis of the certified purity values, which also take account of the presence of trace inorganic impurities.

Keywords: *Polychlorinated biphenyls; reference materials; high-purity; certification*

The contamination of the biosphere by polychlorinated biphenyls (PCBs) has been long established,[1–4] and their potential health hazards have been well documented.[5–8] The European Economic Community and many other countries have promulgated various regulatory controls on the manufacture of PCBs and acceptable PCB levels.[9–11] The regulation of acceptable levels of these compounds in environmental samples and foodstuffs, where the levels can be very low, rests on the accuracy and reliability of their identification and quantitative analytical measurement. In turn the analytical techniques which are applied for this purpose, based mainly on gas - liquid chromatography (GC) and high-performance liquid chromatography (HPLC) with various detection systems, are essentially dependent on the availability of very pure reference samples of prominent PCBs which can serve as calibration materials for the measurement of specific PCB compounds. A comprehensive review of the analytical chemistry of PCBs has been published recently.[12]

This paper describes the production and certification of ten PCBs which possess purities of between 0.986 and 0.999 g g^{-1}. The choice of this series of compounds was based on the following considerations: key representatives of PCBs found in the environment; desirability of the availability of at least one high-purity isomer representing each of the six isomeric groups of dichloro- to heptachloro-biphenyls; toxicological aspects; non-availability from commercial sources; and requirements of legislative control within the European Community.

In the experimental work associated with the production of the series of PCB reference materials (RMs) used here, the following quality criteria were adopted: the materials should possess a purity of preferably at least 0.990 g g^{-1}; the purity analysis should be carried out by at least three different analytical methods in each participating laboratory; and impurities detected at mass fractions of 0.001 g g^{-1} or higher should be identified, if possible, and determined quantitatively.

The general aim of the method was to certify the purity of the reference material with a total uncertainty of less than 0.01 g g^{-1}, by subtracting the impurities from unity. The certified PCB reference materials are intended mainly for the qualitative and quantitative calibration of analytical apparatus and methods (*e.g.*, determination of retention times, response factors and reference spectra in chromatographic and spectroscopic analyses) and for the study of biological activity.

As the individual PCB compounds have been systematically numbered based on the IUPAC rules of substitution for biphenyl,[13,14] for convenience of reference in this paper, these systematic numbers are indicated in addition to the chemical nomenclature and are given in the form PCB-*n* where *n* represents the position number in the sequential series.

Experimental

Syntheses of Polychlorinated Biphenyls

One PCB isomer (PCB-28) was prepared by Sandmeyer's method in which the diazonium group was replaced with chlorine using copper(I) chloride. Two of the symmetrically substituted PCBs (PCB-52 and PCB-153) were prepared from an appropriate, specially synthesised, iodo-derivative by an Ullmann-type condensation reaction. The other seven compounds were prepared from suitable chloroanilines, which were diazotised and reacted with an appropriate chlorobenzene to provide the required compound. In some instances the product was admixed with one or more isomeric compounds. The methods of synthesis and the identification techniques used are given in Table 1 (see also reference 22).

Purification of Polychlorinated Biphenyls

After removal of the reaction solvent by steam distillation and an initial crystallisation of the crude product (for PCB-20 and PCB-35 after separation by vacuum distillation), the materials were purified by column chromatography (on either silica gel or alumina) and then recrystallised.

A contaminating by-product which is formed during the synthesis of PCB-153 is 2,3,7,8-tetrachlorodibenzofuran (TCDF). After purification of PCB-153 TCDF was found to be present at a concentration of about 400 μg g^{-1}, which, in view of its potential toxicity, was considered to be too high. Therefore, an additional chromatographic purification was carried out, and a GC and mass spectrometric (MS) examination of the final purified sample indicated that TCDF, if present, was at concentrations below 1 μg g^{-1}.

Characterisation of the Polychlorinated Biphenyls

Proton nuclear magnetic resonance (NMR) spectra were recorded using a Varian Model XL-100 FT instrument; tetramethylsilane was used as the internal reference and $CDCl_3$ as solvent. The X-ray analyses were carried out using an Enraf-Nonius CAD-4 diffractometer (ω,θ scan, Mo K or Cu K radiation monochromated by pyrolytic graphite).[23,25] Mass spectra recording the relative isotopic molecular ion intensities, shown in Fig. 1, were measured using a Finnigan Model 4510 quadrupole mass spectrometer equipped with an

Table 1. Synthesis and identification of polychlorinated biphenyl RMs

RM	Biphenyl compound	Synthesis reference	M.p./°C	Identity confirmed by	Reference
289	PCB-8 2,4′-Dichloro-	15–17	40.5	M.p., IR, X-ray crystallography	22
290	PCB-20 2,3,3′-Trichloro-	17	42.0	X-ray crystallography	23
291	PCB-28 2,4,4′-Trichloro-	15	56.0	M.p., IR, mass spectrometry	15, 24
292	PCB-35 3,3′,4-Trichloro-	17	62.0	X-ray crystallography	23
293	PCB-52 2,2′,5,5′-Tetrachloro-	15, 18	88.0	M.p., IR, relative molecular mass, NMR	19, 24
294	PCB-101 2,2′,4,5,5′-Pentachloro-	19	76.5	NMR, IR	19
295	PCB-118 2,3′,4,4′,5-Pentachloro-	20	111.5	NMR, IR	19
296	PCB-138 2,2′,3,4,4′,5′-Hexachloro-	*cf.* 19	81.0	NMR, IR, mass spectrometry	24
297	PCB-153 2,2′,4,4′,5,5′-Hexachloro-	21	102.0	X-ray crystallography	25
298	PCB-180 2,2′,3,4,4′,5,5′-Heptachloro-	19	114.5	NMR, IR	19

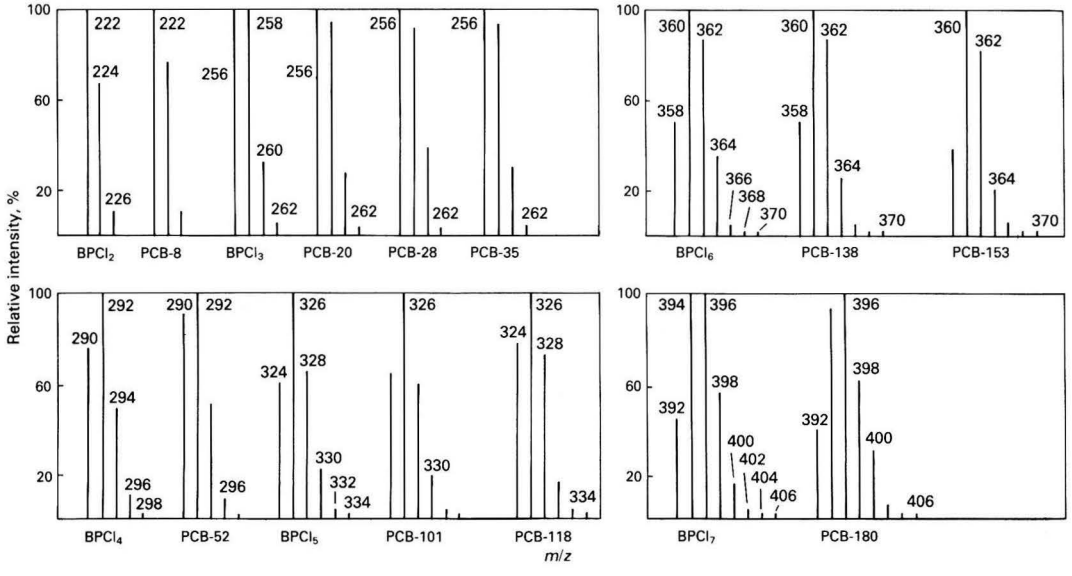

Fig. 1. Mass spectra: comparison of theoretical and measured relative intensities of isotopic parent ions. [$BPCl_n$ = theoretical relative ion intensities for biphenyls substituted with n chlorine atoms (n = 2–7). Corresponding measured intensities shown against each PCB number.]

Incos data system. Electron impact mass spectra were recorded at an electron energy of 70 eV.

Methods of Quantification of Impurities

Gas - liquid chromatography was carried out using both packed and capillary columns under various conditions. Commercially available products such as the silicone-based OV-101, CP-Sil-5CB, SE-54, BP-5, DB-5 and other similar types, in addition to Apiezon L, were utilised as stationary phases. Both isothermal and temperature programmed (in the range 60–300 °C) conditions were applied. A solution of the PCB in a suitable solvent such as hexane, isooctane, dichloromethane, toluene and cyclohexane at mass concentrations of between 0.5 and 20 mg g^{-1}, was applied either as a cold on-column injection or as a split or splitless injection. The

eluted peaks were detected by flame ionisation or by coupling to a mass spectrometer.

For HPLC, carried out at room temperature, columns of 15 to 25 cm in length and 4–5 mm internal diameter were used. A variety of both normal and reversed-phase type packings were employed which included (normal type): LiChrosorb Si-60 (5 μm), Silica A (8 μm), CP Spher Si (10 μm) and Zorbax S91 (5 μm); and (reversed-phase type): LiChrosorb RP18 (5 μm), Hypersil-ODS (5 μm), Supelcosil LC-PAH (10 μm) and Zorbax ODS (5 μm). The peaks were measured by ultraviolet detection. Prior measurements of the UV spectra of isooctane solutions of PCBs were made at the Biochemisches Institut für Umweltcarcinogene, through the courtesy of Professor J. Jacob.

Organic Impurities Detected by GC - MS

The *m/z* values of trace organic impurities present in each of the reference materials were recorded by GC - MS and showed that the impurities consisted mainly of isomeric and higher PCBs, *e.g.*, for RM 293 hexachloroterphenyl was found to be present. A list of these trace impurities and the amounts detected have been given elsewhere.[22]

Homogeneity Study of the Candidate Reference Materials

All materials were homogenised in solution followed by single batch recrystallisation, or evaporation to dryness and subsequent thorough mixing, to promote uniform distribution of possible impurities. The materials were dispensed as 25-mg units into glass vials, and the between-bottle homogeneity of each series was then investigated in a laboratory employing a method which had been shown in preliminary studies to give reliable results. Analysis by HPLC with reversed-phase adsorbent columns (HPLC-RP) was used for RMs 289, 291, 293, 296, 297 and 298, and with normal phase adsorbent columns (HPLC-Ad), for RMs 290, 294 and 295. Capillary GC (GC-Cap) was used to analyse RM 292.

The between-bottle homogeneity was assessed using six vials taken at random from each series. Typically, 0.1-mg test portions were dissolved in a suitable solvent (acetonitrile - water or acetonitrile for HPLC-RP; hexane for HPLC-Ad and GC-Cap) and two sub-samples from each of the six vials were analysed by the method indicated above. The purity of each test portion was obtained by quantifying the impurities. In each instance the standard deviation of the results obtained for six different vials was not significantly different from that of the replicate analyses of a single solution. Detailed results have been reported elsewhere.[22]

Stability of the Candidate Reference Materials

The analyses carried out over a period of 1 year, in conjunction with the initial purity and homogeneity controls carried out in two laboratories, together with the certification analyses showed no evidence of instability of the ten compounds in the solid form.

Certification Procedure

The certification procedure adopted for the PCB compounds was similar to that utilised for the polycyclic aromatic compound (PAC) series (see reference 26) which involved dividing the reference materials and the 11 participating laboratories into two groups. Each group consisted of five or six laboratories of which two were common to both, each laboratory in each group analysing at least five materials. All laboratories reported triplicate results obtained by three or more methods. This procedure permitted the number of results available for technical and statistical evaluation to be of adequate size and comparable to similar PAC certification rounds.

Results and Discussion

Confirmation of Identity of the PCB Compounds

The synthetic routes utilised generally gave one main product, but in some instances an appreciable amount of a secondary product was formed. Hence, although PCB-20 and PCB-35 were synthesised together they were purified separately. For all compounds a comparison of their melting-points and infrared spectra with those recorded in the literature (where these data were available) gave little reason to doubt the identity of the isolated compound, although the data cannot be taken as providing an absolute confirmation. The structures of PCB-8 (RM 289), PCB-28 (RM 291) and PCB-52 (RM 293) are well established; however, as many of the PCB isomers are similar, the other synthesised products were subjected to additional physical measurements to provide further confirmation.

Examination of the individual mass spectra of the isomers confirmed that the *m/z* value of the parent molecular ions of the all ^{35}Cl compounds corresponded to the expected relative molecular mass of the isomer. If the natural abundance ratio $^{35}Cl : ^{37}Cl$, which is close to 3 : 1, is assumed to hold true for the PCB compounds then the binomial distribution of the isotopic molecular ions, and hence their theoretical relative intensities can be calculated by expansion of the binomial $(a + b)^n$ where $a = 3$, $b = 1$ and n = number of chlorine atoms present in the biphenyl. Although in practice the relative intensities may suffer distortion through the presence of adventitious ions, or the asymmetry of the molecule, a good agreement was observed when the theoretical and measured relative intensities were compared (Fig. 1).

The structures of PCB-101, PCB-118, PCB-138 and PCB-180 (RMs 294, 295, 296 and 298, respectively) were confirmed by examination of their proton NMR spectra. The proton NMR spectra of these compounds revealed chemical shifts relative to tetramethylsilane (TMS) (δ p.p.m.) as follows (interpretation in brackets): PCB-101 (RM 294): 7.24 (H-6′), 7.35 (H-4′), 7.36 (H-6), 7.42 (H-3′) and 7.60 (H-3); PCB-118 (RM 295): 7.24 (H-6′), 7.41 (H-6), 7.49 (H-2′), 7.52 (H-5′) and 7.59 (H-3); PCB-138 (RM 296): 7.09 (H-6), 7.34 (H-6′), 7.46 (H-5) and 7.60 (H-3′); PCB-180 (RM 298): 7.28 (H-6), 7.33 (H-6′) and 7.62 (H-3′). These data provide good evidence for the accepted structures (*cf.*, references 19 and 27).

X-ray diffraction data were obtained for the prepared PCB-8 (RM 289), PCB-20 (RM 290), PCB-35 (RM 292) and PCB-153 (RM 297) compounds. These were identified unequivocally as 2,4′-dichlorobiphenyl, 2,3,3′-trichlorobiphenyl, 3,3′,4-trichlorobiphenyl and 2,2′,4,4′,5,5′-hexachlorobiphenyl, respectively.[23,25]

All the measured data, together, provide a sufficient basis for the conclusion that the synthesised products have the expected structures.

Methods of Determining Purity

An indirect method for determining the purity of the PCBs for certification was used. The mass fractions of the observed impurities were determined and the purity of the material was then established by subtraction from unity of the total mass fraction of all detected impurities. The implications of this procedure on the accuracy of the purity determination are discussed below.

Each laboratory received a sample, taken at random, of 25 mg of each material to be analysed. Three analytical methods, in which the laboratory had particular experience selected from the following techniques, were then applied. Gas - liquid chromatography with capillary or packed columns and quantification of resolved impurities by means of a flame ionisation detector (FID) or a mass spectrometer. High-performance liquid chromatography on normal- or reversed-phase adsorbents with ultraviolet (UV) detection at a suitable wavelength and quantification of each resolved impurity by measurement

of its peak parameters. At least three replicate measurements by each method applied were carried out to demonstrate that the instrumental technique provided repeatable results. Only two laboratories provided GC measurements using an electron capture (EC) detector. These measurements were not accepted for inclusion in the final certification due to their doubtful quantitative reliability in view of the unknown nature of the impurities present and the large and unpredictable differences in detector response which may occur with such impurities. Large differences in detector response are known to occur between PCB congeners of similar chemical composition and structure.[27]

Laboratories were asked to guard against the possibility of cross-contamination of samples by using a new syringe for each PCB isomer and to obviate errors due to "memory effects" from the chromatographic column by running solvent blanks between samples. Where HPLC was utilised for quantification, the UV wavelength used to determine the absorbance of the solution was selected, where possible, to provide the maximum sensitivity from the instrument used. Laboratories were also asked to run each compound at least once on each analytical system for an extended period of time to ensure that errors did not arise through non-detection of late-eluting peaks.

Where flame ionisation detection (FID) was utilised to obtain measurements, the response factors of the impurities and of the principal component were assumed to be the same; subsequent to the present work Zoller *et al.*[28] have examined the effect of hydrogen flow-rate on the relative molar response factors of the PCBs described in this paper. Where a mass spectrometer coupled to a gas chromatograph was employed, quantification of impurities was based on the total ion current chromatogram. In some instances selected ion recording (SIR) allowed the detection of impurities present at very low levels.

Sources of Error

Although a systematic examination of the analytical errors which can occur in the purity determination of PCB materials is not feasible because of the differences in equipment (instruments, chromatographic columns) and experimental conditions used by the participating laboratories, some of the potential errors can be discussed.

A fundamental source of error arises from the method used for the determination of purity by the subtraction of mass fractions of impurities from unity. It is clear that those impurities that remain undetected because they are not separated from the main component or are not detected in its presence, or are retained on the column, will lead directly to an over-estimation of the purity. The certification procedure was therefore designed to minimise the risk of non-detection of impurities by the use of a wide range of separation systems. Hence, the HPLC methods covered the possibility of detecting organic non-volatile impurities which might not otherwise be detected by the GC measurements.

A second, general, source of error in the evaluation of analytical results obtained by the chromatographic techniques is linked with the various methods of peak-area quantification and with the difficulty in assigning correct response factors to minute impurity components.

A third source of error lies in the possible presence of trace amounts of inorganic impurities in the candidate reference materials. The determination of inorganic impurities after ashing samples of the PCB isomers at a moderate temperature led to the detection of their presence only in PCB-8 (RM 289) at a mass fraction of 0.0003 g g^{-1}, in PCB-35 (RM 292) at 0.002 g g^{-1} and in PCB-52 (RM 293) at 0.0004 g g^{-1}. In the other compounds inorganic impurities were present at levels of less than 0.0002 g g^{-1} which was the detection limit of the method used.

Results and Their Evaluation

All the results received were grouped according to the method used. The statistical means of the individual measurements supplied by each laboratory for each analytical method (hereafter referred to as the set means) were used for the evaluation.

The results obtained were subjected to an evaluation at a meeting of the participants and, as far as possible, technical reasons were sought before any result or set of results was eliminated by following the general principles adopted for the certification of Community Bureau of Reference (BCR) (Brussels, Belgium) reference materials.[29] Results rejected during the evaluation were in accordance with the following criteria: results showing a substantial divergence from the means of results by similar methods applied in other laboratories and technically judged to be incorrect values. Reasons for these discrepancies could not be established in every instance however; those results where no impurities were detected by the method and the given value was the laboratory's lower estimate of purity based on the detection limits for impurities of their methods and equipment. Results obtained with similar methods applied in another laboratory indicated the presence of impurities, such results were eliminated on the grounds of a failure of the application of the technique by the laboratory rather than because of an inherent weakness in the method itself; in several instances, it was apparent that measurements made by certain methods systematically gave the wrong results, all results by these methods were rejected.

Only the accepted results (P) were used for the purity calculation. The organic impurity values, the values of P, the estimated inorganic impurities present and the certified purity values of the ten reference materials are given in Table 2.

Table 2. Certified purity values

RM	PCB No.	Biphenyl compound	Organic impurities/g g^{-1}	P*	Inorganic impurities/g g^{-1}	Certified purity/g g^{-1}
289	8	2,4′-Dichloro-	$0.0034^{+0.0024}_{-0.0009}$	23	0.0003 ± 0.0003	$0.9963^{+0.0012}_{-0.0027}$
290	20	2,3,3′-Trichloro-	0.0014 ± 0.0006	18	0.0002 ± 0.0002	0.9984 ± 0.0008
291	28	2,4,4′-Trichloro-	0.0020 ± 0.0006	22	0.0002 ± 0.0002	0.9978 ± 0.0008
292	35	3,3′,4-Trichloro-	0.0119 ± 0.0012	9	0.0020 ± 0.0020	0.9861 ± 0.0032
293	52	2,2′,5,5′-Tetrachloro-	0.0037 ± 0.0012	22	0.0004 ± 0.0004	0.9959 ± 0.0016
294	101	2,2′,4,5,5′-Pentachloro-	0.0059 ± 0.0008	19	0.0002 ± 0.0002	0.9939 ± 0.0010
295	118	2,3′,4,4′,5-Pentachloro-	0.0038 ± 0.0012	19	0.0002 ± 0.0002	0.9960 ± 0.0014
296	138	2,2′,3,4,4′,5′-Hexachloro-	0.0007 ± 0.0003	12	0.0002 ± 0.0002	0.9991 ± 0.0005
297	153	2,2′,4,4′,5,5′-Hexachloro-	$0.0005^{+0.0004}_{-0.0002}$	12	0.0002 ± 0.0002	$0.9993^{+0.0004}_{-0.0006}$
298	180	2,2′,3,4,4′,5,5′-Heptachloro-	0.0042 ± 0.0007	19	0.0002 ± 0.0002	0.9956 ± 0.0009

* P = number of accepted sets of results for organic impurities.

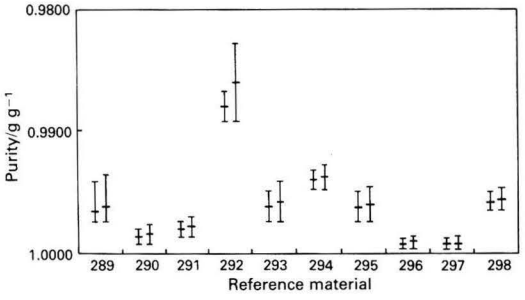

Fig. 2. Range bar graphs of certified purity of the reference materials. (For each reference material the first bar represents the uncertainty limits for the organic purity when inorganic impurities are disregarded and the second bar represents the uncertainty limits when these are included. The mean purity value is indicated by a cross-stroke.)

Statistical Treatment of the Results for Organic Impurities

The statistical evaluation of the accepted results of the purity measurements made on the PCB reference materials was essentially the same as that adopted in the earlier PAC series.[26] The results were expressed as follows: the certified organic impurity was derived from the mean of the individual set means, each set mean representing a given method in a given laboratory; the uncertainty was expressed in terms of the 95% confidence limits of the mean organic purity; in addition to the calculated mean organic purity, a certified over-all purity was calculated which took account of both the organic and inorganic impurities present.

In the initial phase of the statistical evaluation, the distribution of the accepted set means was tested for normality for each of the materials. Inspection of the data suggested that, especially for those compounds of very high purity, the skewed distribution would be more consistent with a logarithmic-normal distribution. Hence, the set means, expressed as mass fractions of the impurities, and, in a separate calculation, their logarithms, were tested for conformity to a normal distribution using the Kolmogorov - Lilliefors test. It was found generally that the accepted results for the majority of the compounds conformed to a normal distribution. The results for two of the compounds (RMs 289 and 297) however were found to conform more satisfactorily to a logarithmic-normal distribution. The 95% confidence limits were established by standard procedures.

Table 2 gives a summary of these final values together with results for the determination of inorganic impurities. The mean values of the purities of the ten PCB isomers with their associated uncertainties with and without taking account of the presence of trace inorganic impurities are shown in Fig. 2.

The members of the following laboratories are thanked for their participation: J. Jacob, Biochemisches Institut für Umweltcarcinogene, Ahrensburg, FRG*,§; Tin Win, Bundesanstalt für Materialprüfung, Berlin, FRG§; P. Payen, Centre d'Etudes et Recherches des Charbonnages de France, Verneuil, France§; A. Liberti, CNR Istituto Inquinamento Atmosferico, Rome, Italy§; J. Gielen, Instituut voor Toegepaste Chemie (Hoofdgroep Maatschappelijke Technologie), TNO, Delft, The Netherlands§; E. Gevers, Instituut voor Toegepaste Chemie (Hoofdgroep Maatschappelijke Technologie), TNO, Zeist, The Netherlands*,†,§; M. Henderson, Inveresk Research International, Musselburgh, Scotland, UK*; L. Boniforti, Istituto Superiore di Sanità, Rome, Italy§; A. Head, National Physical Laboratory, Teddington, UK§; H. Kienhuis, Prins Maurits Laboratory, TNO, Rijswijk, The Netherlands*,‡; T. Rymen, Studiecentrum voor Kernenergie/Centre d'Etudes Nucléaires, Mol, Belgium§; K. Ballschmiter, University of Ulm, Ulm/Donau, FRG*; and M. Metzler, University of Würzburg, Würzburg, FRG.§

* Laboratories where compounds were synthesised.
† Laboratories where homogeneity was evaluated.
‡ Laboratories where structural studies were carried out.
§ Laboratories that contributed measurement data for use in the certification programme.

References

1. Jensen, S., PCB Conference, National Swedish Environmental Protection Board, Research Secretariat, Solna, Sweden, 1970.
2. Anon., *New Sci.*, 1966, **32**, 612.
3. Jensen, S., Johnels, A. G., Olsen, M., and Olterlind, G., *Nature (London)*, 1969, **224**, 247.
4. Fishbein, L., *J. Chromatogr.*, 1972, **68**, 345.
5. Haley, T. J., "Dangerous Properties of Industrial Materials Report," 1984, 4, No. 6, p. 2.
6. *IARC Monographs*, "Some Antithyroid and Related Substances, Nitrofurans and Industrial Chemicals," International Agency for Research on Cancer, Lyon, 1974, Volume 7, p. 261.
7. *IARC Monographs*, "Polychlorinated and Polybrominated Biphenyls," International Agency for Research on Cancer, Lyon, 1978, Volume 18.
8. *IARC Supplement* 4 *to Monographs Volumes* 1–29, "Chemicals, Industrial Processes and Industries Associated With Cancer in Humans," International Agency for Research on Cancer, Lyon, 1982, p. 217.
9. Official Journal of the European Communities: 1976, L108, 41, Directive 76/403; 1976, L262, 201, Directive 76/769; 1985, L269. 56, Directive 85/467.
10. Regulation No. 81735 of Permitted Maximum Content of PCB-components in Food Products (September, 1985). Published in the Netherlands Staatscourant 200, 1985.
11. Official Journal of the European Communities: 1980, L229, 11, Directive 80/778.
12. Erikson, M. D., "Analytical Chemistry of PCBs," Butterworth, London, 1986.
13. Hutzinger, O., Safe, S., and Zitko, V., "The Chemistry of PCBs," CRC Press, Cleveland, OH, 1974.
14. Ballschmiter, K., and Zell, M., *Fresenius Z. Anal. Chem.*, 1980, **302**, 20.
15. Hutzinger, O., Safe, S., and Zitko, V., *Bull. Environ. Contam. Toxicol.*, 1971, **6**, 209.
16. Willis, D. E., and Addison, R. V., *J. Fish. Res. Board Can.*, 1972, **29**, 592.
17. Cadogan, J. I. G., *J. Chem. Soc.*, 1962, 4257.
18. Hutzinger, O., and Safe, S., *Bull. Environ. Contam. Toxicol.*, 1972, **7**, 374.
19. Erb, F., Pommery, J., van Aerde, C., and Vermeersch, J., *Bull. Soc. Chim. Fr.*, 1976, 964.
20. Sundstrom, G., *Acta Chem. Scand.*, 1973, **27**, 600.
21. Moron, M., Sundstrom, G., and Wachtmeister, C. A., *Acta Chem. Scand.*, 1973, **27**, 3121.
22. Jacob, J., Lindsey, A. S., and Wagstaffe, P. J., "The Certification of the Purity of Polychlorinated Biphenyl Isomers. BCR Reference Materials Nos. 289–298. EUR 10998 En-1987," Commission of the European Communities, Luxembourg, 1987.
23. Moes, G. W. H., and Lenstra, A. T. H., *Toxicol. Environ. Chem.*, 1986, **12**, 255.
24. Safe, S., and Hutzinger, O., *J. Chem. Soc., Perkin Trans. 1*, 1972, 686.
25. Geise, H. J., Lenstra, A. T. H., de Borst, C., and Moes, G. W. H., *Acta Crystallogr., Sect. C*, 1986, **42**, 1176.
26. Jacob, J., Belliardo, J. J., and Wagstaffe, P. J., "The Certification of Polycyclic Aromatic Compounds. Part VI: CRM Nos. 152, 265–272. EUR 10295 En-1985," Commission of the European Communities, Luxembourg, 1985.
27. Mullin, M. D., Pochini, C. M., McCrindle, S., Romkes, M., Safe, S. H., and Safe, L. M., *Environ. Sci. Technol.*, 1984, **18**, 468.
28. Zoller, W., Schäfer, W., Class, T., and Ballschmiter, K., *Fresenius Z. Anal. Chem.*, 1985, **321**, 247.
29. Marchandise, H., and Colinet, E., *Fresenius Z. Anal. Chem.*, 1983, **316**, 669.

Paper 8/03539C
Received September 19th, 1988
Accepted January 4th, 1989

Direct Determination of Zinc, Lead, Iron and Total Sulphur in Zinc Ore Concentrates by X-ray Fluorescence Spectrometry

Josefina de Gyves
Departamento de Química Analítica, Facultad de Química, Universidad Nacional Autónoma de México, Mexico

Montserrat Baucells*
Servei d'Espectroscopía, Universitat de Barcelona, 080028 Barcelona, Spain

E. Cardellach and J. L. Briansó
Departamento de Geologia, Universidad Autónoma de Barcelona, Barcelona, Spain

A direct X-ray fluorescence (XRF) method has been developed for the rapid determination of zinc, lead, iron and total sulphur present in zinc ore concentrates. The concentrations of the elements present, mainly as sphalerite, galena, pyrite and pyrrhotite, vary widely: Zn, 40–65; Pb, 0.1–10; Fe, 0.5–11; and S, 25–33% *m/m*. Using a wavelength-dispersive X-ray spectrometer and samples prepared as briquettes, Zn and Pb may be determined directly using the Kβ and $L\gamma_1$ lines, respectively. For Zn, a mathematical model (concentration-based correction equation) was applied to correct for inter-element effects. For the determination of Fe the ratio of the fluorescence intensities of the Fe Kα and Zn Kβ lines was used and, for the determination of total S, the intensity of the S Kα line was corrected with the Rayleigh scatter tube line, Rh Lα. For both iron and total sulphur, subsequent application of the mathematical model helped to correct for the residual inter-element effects. Good agreement was obtained between experimental and certified values for two international reference materials.

Keywords: *Zinc; lead; iron; zinc sulphide matrix; X-ray fluorescence spectrometry*

The accurate analysis of geological samples with complex matrices by X-ray fluorescence (XRF) spectrometry requires the use of a correction method. Such samples include zinc ore concentrates, for which the large variation in the composition of several major elements (Zn, 40–65; Pb, 0.1–10; Fe, 0.5–11; and total S, 25–33% *m/m*) gives rise to severe absorption and enhancement effects. The many approaches proposed for the solution of inter-element effects may be divided into two main groups[1]: (a) mathematical methods, in which inter-element effects are calculated (*e.g.*, fundamental parameters and influence coefficients) and (b) comparative methods (internal standard, standard additions or spiking, simple or double dilution, scatter intensity, etc.) in which such effects are compensated for.

Mathematical correction methods based on the calculation of influence coefficients can be classified further into two categories: intensity-based (*e.g.*, Lucas Tooth - Pyne model[2]) and concentration-based (*e.g.*, Lachance - Traill model[3]) correction methods. The latter offers the advantages of requiring relatively small computer facilities and of being applicable over relatively wide concentration ranges. The X-ray spectrometer used in this work has built-in software for the concentration-based correction equation proposed by de Jongh,[4] namely

$$c_i = (D_i + E_i R_i)(1 + \alpha_{ij} c_j) \quad . . \quad . . \quad . . \quad (1)$$

where c_i is the concentration to be determined of element i, D_i and E_i are element/instrument dependent parameters, R_i is the intensity ratio, α_{ij} is the influence coefficient for the effect of element j on i and C_j is the concentration of j. Alpha constants are calculated by regression analysis of data obtained from a relatively large number of calibration standards or from fundamental constants. To apply equation (1) the concentrations of all elements in the mid to high concentration range that could give rise to inter-element effects must be known. These concentrations can be calculated from intensity data by regression analysis. The concentration of the unknown is then estimated by an iterative calculation.

For the work described here, as insufficient, well characterised standards for zinc ore concentrates were available, synthetic pelleted standards were prepared. Because the chosen calibration procedure involves matching the matrix composition of standards and samples, standards were prepared to contain all major elements which could significantly modify the matrix mass absorption coefficient (μ_{matrix}) at the analytical working wavelengths. Account was also taken of the elements that could give rise to enhancement effects. Matrix mass absorption coefficients of all the specimens used as standards calculated at the wavelengths of the XRF emission lines of Pb $L\gamma_1$ (λ, 0.84 Å) and Zn Kβ (λ, 1.295 Å) show that this parameter does not vary significantly: $\bar{\mu}_{matrix,\ Pb\ L\gamma_1} = 61.65 \pm 1.59$ and $\bar{\mu}_{matrix,\ Zn\ K\beta} = 111.63 \pm 3.21$, in spite of the wide concentration variations (Table 1). Further, no enhancement effects might be expected for these lines from any of the elements present in the standards and samples. Consequently, Zn and Pb could be determined directly with good precision and accuracy. Alpha coefficients for Fe can be used in the determination of Zn to improve the accuracy even more, as they correct the weak inter-element effects in the analysed specimens. The analogous calculations of μ_{matrix} at the emission lines of Fe Kα (λ, 1.936 Å) and S Kα (λ, 5.375 Å) showed a more important variation in this parameter: $\bar{\mu}_{matrix,\ Fe\ K\alpha} = 124.1 \pm 4.9$ and $\bar{\mu}_{matrix,\ S\ K\alpha} = 1544 \pm 113$. An enhancement effect of Zn over Fe might be expected because of the lower atomic number of Fe and the very high Zn concentration; however, a direct analysis for these two elements did not give satisfactory results. Accuracy was improved with empirical application of the alpha correction method together with alternative approaches such as the use of the Zn Kβ line to correct the Fe Kα line and the Rh Lα Rayleigh scatter line to correct the S Kα line; such procedures compensate for inter-element effects to a great extent and decrease the divergence from the calibration line. Heterogeneity effects due to particle size were overcome by carefully grinding the specimens to obtain a particle size of less than 10 μm. A study using optical microscopy was carried out in order

* To whom correspondence should be addressed.

Table 1. Analysis of synthetic standards (specimens 1–13) and reference materials

	Fe, % *m/m*		Total S, % *m/m*		Zn, % *m/m*		Pb, % *m/m*	
Specimen	A*	B†	A*	B†	A*	B†	A*	B†
1	12.50	12.42	20.3	20.0	39.0	39.0	7.50	7.47
2	10.00	9.98	24.1	24.2	48.7	48.0	4.95	5.04
3	5.00	4.84	28.4	28.4	57.4	56.7	2.50	2.42
4	2.50	2.39	30.6	30.3	62.2	61.7	1.25	1.18
5	1.25	1.22	32.5	32.6	64.6	64.7	0.59	0.56
6	0.60	0.60	32.7	32.5	65.8	66.2	0.30	0.28
7	0.30	0.32	32.6	32.3	66.6	66.8	0.098	0.085
8	11.00	11.18	25.0	25.4	49.1	49.4	6.25	6.03
9	7.50	7.45	27.6	27.6	55.3	55.2	3.75	3.58
10	4.00	4.12	25.6	25.8	56.2	56.9	0.48	0.53
11	4.00	4.07	28.9	29.3	58.4	58.0	0.48	0.52
12	4.00	3.97	30.2	30.5	61.2	61.0	0.48	0.49
13	4.00	3.90	30.7	30.6	63.0	62.4	0.48	0.50
BCR 108 . .	7.21	7.41	31.0	30.9	54.0	54.5	0.90	0.89
CZN-1	10.93	10.85	30.2	30.0	44.7	44.7	7.45	7.50

* Calculated or certified concentrations.
† Concentrations found.

Table 2. Measuring conditions for Zn, Pb, Fe and total S

Element (line)	Collimator	Detector	Crystal	Voltage/ kV	Current/ mA	2θ/°	Time/s
Zn(Kβ)	F*	FS†	LiF 200	50	50	37.53	20
Pb($L\gamma_1$)	F	S‡	LiF 200	50	50	24.07	40
Background Pb ($L\gamma_1$) . .	F	S	LiF 200	50	50	25.27	40
Background Pb ($L\gamma_1$) . .	F	S	LiF 200	50	50	22.87	40
Fe(Kβ)	F	FS	LiF 200	55	45	51.73	40
Background Fe(Kβ) . .	F	FS	LiF 200	55	45	49.73	40
Fe (Kα)	F	FS	LiF 200	55	45	57.52	20
S (Kα)	C§	Flow	Ge 111	40	75	110.86	20
Background S(Kα) . .	C	Flow	Ge 111	40	75	113.86	20
Rh (Lα)	C	Flow	Ge 111	40	75	89.605	40
Background Rh(Lα) . .	C	Flow	Ge 111	40	75	87.605	40

* F = Fine.
† FS = Flow - scintillation.
‡ S = Scintillation.
§ C = Coarse.

to define the grinding process and to control strictly the average particle size.

Experimental

Apparatus

X-ray fluorescence intensities were measured with a Philips PW 1400 computer-controlled wavelength-dispersive X-ray spectrometer equipped with an Rh source. The operating conditions used are specified in Table 2.

Calibration Standards

Analytical-reagent and spectroscopic grade chemicals were used to prepare synthetic pelleted standards of "infinite" thickness for calibration. The ZnS used was 99.99% pure and PbS was obtained by precipitation with H_2S from $Pb(NO_3)_2$. For the pellet formation, commercially available Albacite 2044 (butyl methacrylate resin), prepared as a 20% *m/V* acetone solution, was used as a binder.

In order to simulate the composition of the unknown as closely as possible, 13 standards were prepared to contain the major elements found in such minerals: Zn^{II}, Fe^{III}, Pb^{II}, S and O. Also, minor gangue elements such as Al^{III}, Si^{IV}, Ca^{II} and Ba^{II} were added in amounts usually found in zinc ore concentrates (Al_2O_3, 0.025–0.25%; SiO_2, 0.1–3.0; BaO, 0.005–0.5; and CaO, 0.005–0.3% *m/m*). Gangue elements were added as oxides (Al and Si) and carbonates (Ba and Ca), Zn^{II} and Pb^{II} as sulphides and Fe^{III} as the oxide.

Calibration standards (5.0 g) were prepared from accurately weighed portions of the metal compounds which were mixed together for 20 min in a Spex Mixer-Mill (Model 8000). The particle size of the specimens was determined to be <10 μm. The 5.0-g specimens were mixed with 2 ml of Albacite - acetone solution in an agate mortar. Pellets of 40-mm diameter were prepared at pressures of 200 kN applied for 60 s. The precision of pellet formation (RSD), obtained by measuring the Pb $L\gamma_1$, Zn Kβ, Fe Kα and S Kα lines for eight pellets of the same specimen, is given in Table 3.

Procedure

Zinc and Pb are determined directly using the operating conditions specified in Table 2. The alpha coefficients for Fe to be used in the determination of Zn are calculated by regression analysis from the concentration data of standards.

For the determination of Fe, the intensity of the Kα line is corrected using the intensity of the Zn Kβ line. In addition, the alpha coefficients of Zn are calculated by regression analysis of data obtained from synthetic standards.

In the determination of total S, the intensity of the S Kα line is corrected using the Rayleigh dispersion Rh Lα line. Both Zn and Pb alpha coefficients are calculated as described previously.

Table 3. Precision of pellet formation (n = 5)

Element	Mean concentration, % *m/m*	SD/ counts s^{-1}	RSD, %
Zn	54.10	0.21	0.39
S	26.40	0.34	1.28
Fe	3.77	0.037	0.98
Pb	0.324	0.0074	2.28

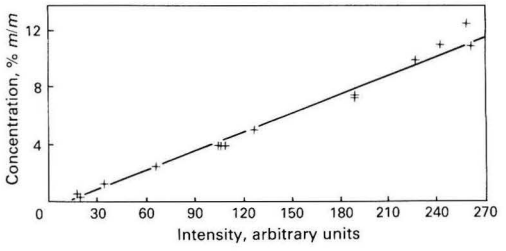

Fig. 1. Calibration graph for Fe obtained using the Kα line

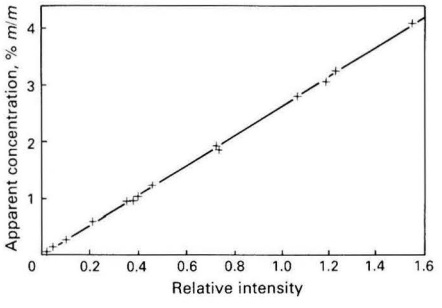

Fig. 2. Calibration graph for Fe obtained after correcting the Kα line with the Zn Kβ line (and using the alpha coefficients of Zn)

Results and Discussion

Iron Determination

The presence of high concentrations of heavy elements such as Zn and Pb gives rise to important absorption effects at the XRF emission wavelength of Fe. Also, as Zn has a higher atomic number than Fe, its XRF radiation is sufficiently energetic to excite Fe atoms and a specific enhancement effect might be observed on the XRF emission lines (Kα and Kβ) of Fe (Fig. 1). When the mass absorption coefficient of a sample differs from the average mass absorption coefficient of the standards by about ±5% use of the de Jongh mathematical model,[4] which involves calculating the alpha coefficients for Zn and Pb to correct for inter-element effects, gives results of acceptable accuracy. However, for the application of this correction procedure, the use of a considerable number of standards is recommended. The presence of an inter-element effect means that an extra degree of freedom must be determined in the analysis. As a guide, each degree of freedom determined requires at least three standards in order for it to be statistically significant.[5] The combination of a compensation method, using the intensity of the Zn Kβ line to correct the intensity of the Fe Kα line, and the de Jongh mathematical model, to calculate the alpha coefficients of Zn, reduces the dispersion of the calibration points and improves the accuracy of the Fe determination (Fig. 2). As only one alpha coefficient is calculated in this procedure, the number of standards required is reduced by three.

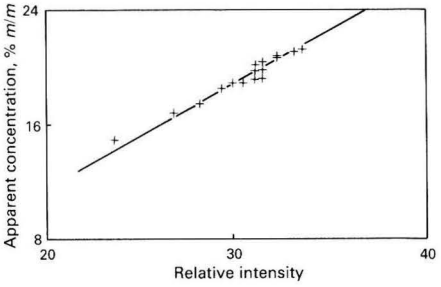

Fig. 3. Calibration graph for total S obtained after correcting the Kα line with the coherently dispersed Rh Lα line (and using the alpha coefficients of Zn and Pb)

Similar results are achieved in the determination of Fe using the Fe Kβ line. The Zn Kβ line is also used as the internal standard in this instance.

Total Sulphur Determination

Sulphur is particularly well suited to determination by XRF spectrometry because of the magnitude of its atomic number.[6,7] However, the presence of elements that will change the mass absorption coefficient of the sample by more than ±5% from the average mass absorption coefficients of the standards will introduce errors into the determination of S owing to changes in the absorption behaviour of the S Kα line. Enhancement effects due to the presence mainly of Zn, Fe and Pb and of the tube element, Rh, might also be expected. The use of only one correction procedure, either the de Jongh mathematical model (to correct for inter-element effects by calculating the alpha coefficients for Zn and Pb) or the compensation method (using the Rayleigh scatter dispersion tube line, Rh Lα, to correct the measured intensity of the S Kα line), gives values of moderate accuracy. By combining the two procedures dispersion about the calibration graph is reduced and the accuracy is significantly improved (Fig. 3).

The moderately accurate concentrations obtained in the determination of total S by the single-correction method might be explained as follows. Use of the Rayleigh scatter dispersion procedure does not correct the enhancement effect due to the very high concentrations of Zn present (the use of the scatter radiation method is applicable, in principle, only to elements with an atomic number higher than those of all major constituents of the matrix, as the method does not compensate for enhancement effects).[1] The mathematical procedure corrects enhancement effects due to the major elements present in the matrix; however, it does not correct for enhancement effects due to the tube element. By combining both procedures all inter-element effects can be corrected as indicated by the good agreement between the results obtained by the proposed method and the certified values for two international reference materials (Table 1).

The presence of an absorption edge of S between the two selected radiations apparently has no important consequences due to the fact that, although $\mu_{\text{matrix, S K}\alpha} > \mu_{\text{matrix, Rh L}\alpha}$ for all the standards used, $\mu_{\text{matrix, S K}\alpha}/\mu_{\text{matrix, Rh L}\alpha}$ does not vary significantly.

Zinc Determination

In zinc ore concentrates it is possible to determine Zn using either Kα or Kβ radiation. In this work Kβ was used because the count rates measured for the Kα line were so high that a direct procedure could not be used. The calibration graph for Zn was linear for concentrations in the range 39–67% *m/m* and could be applied to specimens with a mass absorption coefficient no greater than ±5% with respect to the average

mass absorption coefficient of the standards. The use of Fe alpha coefficients corrected for dispersion about the calibration graph and improved the accuracy. For the determination of 0–30% *m/m* Zn in Zn - Pb minerals Mahapatra[8] has suggested the use of the Cu Kα line as the internal standard.

Lead Determination

In principle, for the determination of Pb in zinc sulphide minerals it is possible to use the Lβ and $L\gamma_1$ lines; the most useful Pb Lα line suffers from spectral interference due to the close proximity of the As Kα line. For this work the Pb $L\gamma_1$ line was selected because the mass absorption coefficient of the specimens used as standards is less influenced by the Zn concentration at this wavelength than at the Pb Lβ wavelength. It was subsequently observed that the determination of Pb in specimens with a relatively low Zn content and a high content of Pb was more satisfactory when the $L\gamma_1$ line was used. In addition, to improve the accuracy of the Pb determination we recommend that PbS is used for the preparation of standards; when PbO is used differences are obtained in the measured XRF intensities.[9]

Accuracy and Precision

The accuracy of the recommended procedures was assessed by analysing the standard reference materials BCR 108 (Commission of the European Communities) and CZN-1 (Canada Centre for Mineral and Energy Technology). As can be seen from Table 1, the Zn, Pb, Fe and total S concentrations obtained are in agreement with the certified values.

The RSDs of the four elements, based on eight replicate analyses of each sample, were as follows: Zn, 0.136% (52.66 ± 0.071% *m/m*); Pb, 0.72% (0.555 ± 0.004% *m/m*); Fe, 0.304% (3.75 ± 0.011% *m/m*); and total S, 0.313% (25.95 ± 0.08% *m/m*).

References

1. Tertian, R., and Claisse, F., *in* "Principles of Quantitative X-ray Fluorescence Analysis," Heyden, London, 1982, p. 118.
2. Lucas Tooth, H. J., and Pyne, C., *Adv. X-Ray Anal.*, 1964, **7**, 523.
3. Lachance, G. R., and Traill, R. J., *Can. Spectrosc.*, 1966, **11**, 43.
4. de Jongh, W. K., *X-Ray Spectrom.*, 1973, **2**, 151.
5. Jenkins, R., "An Introduction to X-ray Spectrometry," Heyden, London, 1974, Chapter 7.
6. Fabbi, B. P., and Moore, W. J., *Appl. Spectrosc.*, 1970, **24**, 426.
7. Weber, H. T., van Willigen, J. H. H. G., and van der Linden, E., *Anal. Chim. Acta*, 1984, **160**, 271.
8. Mahapatra, N. S., *X-Ray Spectrom.*, 1987, **16**, 171.
9. Baucells, M., Lacort, G., Roura, M., and de Gyves, J., *Analyst*, 1988, **113**, 1325.

Paper 8/04296I
Received October 28th, 1988
Accepted January 4th, 1989

Determination of Ammonium-, Nitrite- and Nitrate-nitrogen by Molecular Emission Cavity Analysis Using a Cavity Containing an Entire Flame

Ali Çelik and Emur Henden
Department of Chemistry, Faculty of Science, University of Ege, Bornova, Izmir, Turkey

Ammonium-, nitrite- and nitrate-nitrogen were determined by molecular emission cavity analysis using a cavity containing an entire flame. Ammonium-nitrogen was converted to ammonia by injection on to solid sodium hydroxide. The calibration graph was linear for 5–100 μg ml^{-1} of nitrogen when the ammonia generated was swept directly into the cavity and for 0.05–1.0 μg ml^{-1} of nitrogen when it was collected in a liquid nitrogen cold-trap. Concentrations of 1.5 and 0.01 μg ml^{-1} of nitrogen could be detected using the direct and cold-trap methods, respectively. Nitrite was determined after conversion to nitrogen monoxide by iodide. Nitrate was reduced to nitrite using a copperised cadmium column and then determined as nitrite. The calibration graphs for both anions were linear up to 7 μg ml^{-1} of nitrogen and 0.1 μg ml^{-1} of nitrogen could be detected. The methods were applied successfully to the determination of nitrite and nitrate in meat products, and nitrate-nitrogen in drinking water samples.

Keywords: *Molecular emission cavity analysis; ammonium-nitrogen; nitrite-nitrogen; nitrate-nitrogen*

Although most spectrophotometric methods for the determination of ammonium, nitrite and nitrate ions are highly sensitive, special precautions are required when applying them to samples of coloured solutions or suspensions.[1] In contrast, the flame emission methods, which produce spectral bands for molecules containing nitrogen,[2,3] are fast and are not affected by the colour of the solutions; however, they are generally not highly sensitive.

The determination of ammoniacal nitrogen in effluents and fertilisers by molecular emission cavity analysis (MECA) with an oxy-cavity has been described by Belcher *et al.*[4,5] Ammonium ion was converted to ammonia and swept by nitrogen into the cavity. By monitoring the NO–O continuum, 10–200 μg ml^{-1} of nitrogen could be determined with a detection limit of 1 μg ml^{-1}. Al-Zamil and Townshend[6] also applied MECA with an oxy-cavity to the determination of nitrite and nitrate after their reduction to nitrogen monoxide by iodide or zinc; 5–300 μg ml^{-1} of nitrogen could be determined with a detection limit of 0.5 μg ml^{-1} of nitrite-nitrogen and 2 μg ml^{-1} of nitrate-nitrogen.

The use of MECA with an oxy-cavity for producing oxide-based emissions of various elements involves the introduction of a small amount of oxygen into the cavity held in a hydrogen - nitrogen diffusion flame.[7] It has been shown that oxide-based emissions of boron, selenium, arsenic and antimony can also be obtained using another cavity containing an entire flame within the oxy-cavity.[8] This cavity eliminates the need for the burner system required by the oxy-cavity and consumes much smaller amounts of gases. In this paper, the application of a cavity containing an entire flame to the determination of ammonium-nitrogen, with and without cold-trap collection, and of nitrite and nitrate after their reduction to nitrogen monoxide using a copperised cadmium column is described. Significant improvements in the detection limits compared with previous MECA studies were obtained.

Experimental

Apparatus

A modified Pye Unicam SP 90A flame spectrometer, with a 1.4-mm slit (band width at 400 nm = 45 nm) was used to measure the emissions as described previously.[9] The emission intensity was recorded on a Varian G-2500 chart recorder (response time, 0.5 s for full-scale deflection). The stainless-steel cavity used (4 mm in diameter, 10 mm deep) was as described previously,[9] but was cooled by passing a small flow of water through the copper tube at the rear of the cavity (Fig. 1).

The volatilisation system[10] was modified as shown in Fig. 2. It consisted of a bent glass reaction vessel (5.5 cm long, 1.7 cm in diameter) with an injection hole 3 cm from its closed end. A silicone-rubber septum in an O-ring was placed over the injection hole and tightened with a clip. The reaction vessel was connected by means of PTFE tubing to a stainless-steel tube (0.8 mm i.d.) in one of the rear openings of the cavity through a drying tube and a three-way valve. When the cold-trap was required, a coiled PTFE tube (2 mm i.d., 70 cm long) was connected between the three-way valve and the cavity and immersed in liquid nitrogen in a Dewar flask. The drying tube was packed with calcium chloride powder for the determination of nitrite- and nitrate-nitrogen and with sodium hydroxide pellets for the determination of ammonium-nitrogen. When the cold-trap was not in use, the reaction vessel was heated at 85–90 °C by placing it in a small heating mantle constructed in a 25-ml beaker using a heating coil. The tubes between the reaction vessel and the cavity were also wrapped in the heating coil and kept at 85–90 °C. A small plug of glass-wool (5 cm long) was placed in the PTFE tube before the cavity. The three-way valve was connected after the drying tube so that the carrier gas could be supplied to the cavity while waiting for the reactions to go to completion.

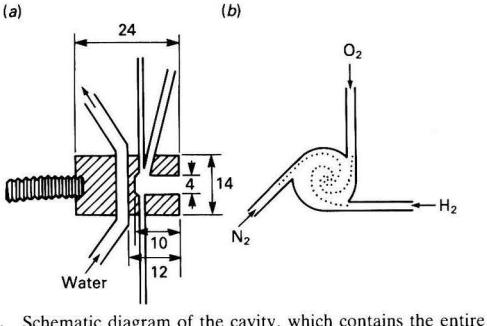

Fig. 1. Schematic diagram of the cavity, which contains the entire flame. (*a*) Cross-section; and (*b*) front view (all dimensions in millimetres)

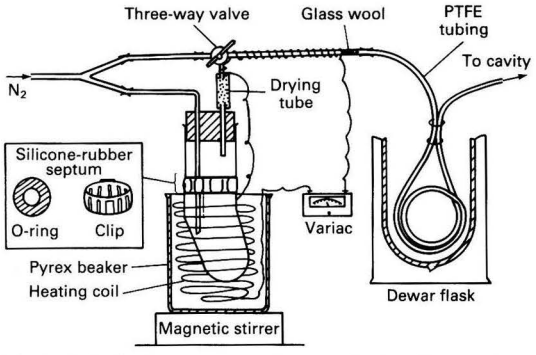

Fig. 2. Volatilisation system for the determination of ammonium-, nitrite- and nitrate-nitrogen (not to scale)

Reagents

All chemicals used were of analytical-reagent grade. Stock solutions of ammonium, nitrite and nitrate ions (1000 μg ml^{-1} of nitrogen) were prepared by dissolving ammonium chloride, sodium nitrite and sodium nitrate, respectively, in distilled water. The nitrite solutions, the low-concentration solutions of ammonium and nitrate and the iodide solution were prepared fresh.

Procedure for the Determination of Ammonium-nitrogen

Procedure without cold-trap collection

Transfer 0.5–0.6 g (about three pellets) of solid sodium hydroxide into the reaction vessel and close the volatilisation system. De-aerate the system for 20 s with nitrogen carrier gas and turn the three-way valve to direct the nitrogen into the cavity without it passing through the reaction vessel. Inject 0.2 ml of the sample solution into the reaction vessel and wait for 2 min. Sweep the ammonia generated into the cavity by turning the three-way valve to the direction of the reaction vessel. Record the emission intensity at 640 nm and use the peak height for the determination.

Procedure using cold-trap collection

Transfer ten pellets of sodium hydroxide into the reaction vessel and close the system. Purge the system for 15–20 s with nitrogen carrier gas and immerse the trap in liquid nitrogen in a Dewar flask. Inject 5 ml of the sample solution and collect the ammonia generated for 4 min. Remove the cold-trap from the liquid nitrogen and immerse it in a water-bath at 90–95 °C. Record the emission at 640 nm and measure the peak height.

Procedure for the Determination of Nitrite-nitrogen

Introduce 0.5 ml of a reducing solution containing 0.5 M potassium iodide in 0.5 M hydrochloric acid into the reaction vessel containing a magnetic bar. Purge the system with nitrogen and turn the three-way valve so that the nitrogen carrier gas by-passes the reaction vessel. Turn on the magnetic stirrer and inject 0.5 ml of the sample solution. One minute after injection turn the three-way valve so that the nitrogen monoxide produced is swept with the nitrogen carrier gas into the cavity. Record the emission as above and use the peak height for measurements.

Procedure for the Determination of Nitrate-nitrogen

Reduce nitrate to nitrite using a copperised cadmium column[1,11] and then proceed as described above for nitrite-nitrogen.

Results and Discussion

The spectrum of the white emission obtained by presenting ammonia vapour or nitrogen monoxide at a constant speed to the flame in the cavity was similar to that reported previously,[6] but with maximum intensity at 640 nm. The emission is probably due to the NO–O continuum.[6] The spectrum appeared to have been shifted to longer wavelengths when compared with the reported spectrum.[4–6] This shift may be attributed to an increase in the spectral band width of the prism monochromator used as the wavelength increased and/or to the differences in the composition and temperature of the flame used in this work. Similar shifts have also been observed in the spectrum of arsenic.[7,9]

The gas flow-rates were optimised in order to obtain the highest signal to noise ratio. Flow-rates of 115, 45 and 75 ml min^{-1} for hydrogen, oxygen and nitrogen, respectively, were found to be optimum for all the determinations.

Determination of Ammonium-nitrogen

Injection of an aqueous solution on to solid sodium hydroxide caused a sudden increase in the temperature of the solution, which in turn caused sputtering of the solution into the gas phase in the reaction vessel and carry-over of a sodium-containing mist into the flame. A very noisy flame with a strong and unstable sodium emission was obtained after each injection. This problem was overcome by placing a small glass-wool plug in the PTFE tubing before the nitrogen inlet into the cavity.

Because ammonia is highly water soluble, it is difficult to de-gas the solution. Therefore, when the volume of the sample solution was increased the peaks became lower and broader. The optimum sample volume was 0.2 ml, as reported by Belcher *et al.*,[4,5] and this volume was used in the determination of ammonium-nitrogen without the cold-trap.

When the cold-trap was used to collect ammonia before measurements were made, the volatilisation system could not be heated and so the condensation of water vapour in the tubing could not be prevented. It was, however, found to be necessary to prevent the condensation of water in the tubing, otherwise erratic results were obtained, probably due to the dissolution of ammonia in the condensed water. Various drying agents were used to dry the ammonia vapour; sodium hydroxide pellets did not reduce the emission intensity and were, therefore, used in the following experiments.

A linear calibration graph (Fig. 3) was obtained for 5.0–100 μg ml^{-1} of ammonium-nitrogen by sweeping the ammonia directly into the cavity. The relative standard deviations (seven experiments) for the determination of 20 and 40 μg ml^{-1} of ammonium-nitrogen were 5.9 and 4.9%, respectively. The limit of detection (signal equal to twice the background noise) was 1.5 μg ml^{-1} of nitrogen. The limit of detection could be improved by collecting the ammonia generated; this was achieved by injecting much larger sample volumes into the liquid nitrogen cold-trap and introducing the ammonia collected into the flame for a short period of time. Hence, sharp emission peaks were obtained and 0.01 μg ml^{-1} of nitrogen could be detected. The calibration graph obtained with the cold-trap method was linear for 0.05–1.0 μg ml^{-1} of nitrogen, whereas for 2 μg ml^{-1} of nitrogen an apparent self-absorption was observed (Fig. 3). The relative standard deviation for the determination of 0.5 μg ml^{-1} of ammonium-nitrogen with the cold-trap system (seven experiments) was 4.1%.

Determination of Nitrite- and Nitrate-nitrogen

Nitrite was reduced by iodide to nitrogen monoxide which was then swept into the flame by the nitrogen carrier gas and the emission was monitored. When the nitrogen monoxide, generated by injecting 0.5 ml of a sample solution into 0.5 ml

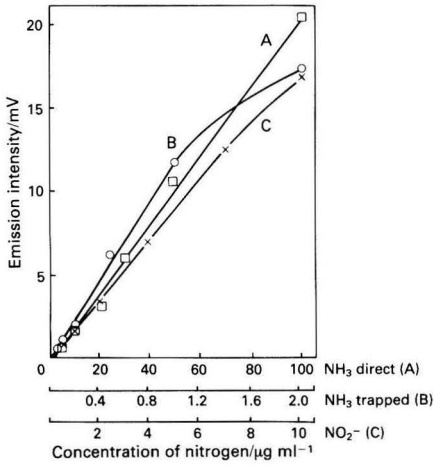

Fig. 3. Calibration graphs: A, 5–100 μg ml^{-1} of ammonium-nitrogen by direct sweeping; B, 0.05–2.0 μg ml^{-1} of ammonium-nitrogen by the cold-trap method; and C, 0.5–10 μg ml^{-1} of nitrite-nitrogen

of the iodide solution, was swept directly into the flame, a broad peak with pronounced tailing was obtained. This could be due to the slowness of the reaction and/or the slowness of the diffusion of the nitrogen monoxide out of the solution. The reaction was complete in 1 min and a sharp peak with a base of 12-s duration was obtained when a 1-min reaction time was allowed before the measurements were made. The volumes of the sample and iodide solutions were chosen so as to obtain the highest sensitivity and reproducibility. A 0.5-ml volume of each solution was used in the following experiments.

The calibration graph was linear up to 7 μg ml^{-1} of nitrite-nitrogen (Fig. 3). The relative standard deviation for the determination of 5 μg ml^{-1} of nitrite-nitrogen (seven experiments) was 3.9% and 0.1 μg ml^{-1} of nitrite-nitrogen could be detected.

Nitrate was determined by the iodide method after its reduction to nitrite by means of a copperised cadmium column (17 cm long, 8 mm in diameter) as described elsewhere.[1,11] The pH of the nitrate solution was adjusted using boric acid - borax buffer instead of ammonia solution to avoid any spectral interferences from the latter. A change in the pH of the buffer within the range 5.3–9.6 did not affect the reduction of nitrate to nitrite. The efficiency of the conversion of nitrate to nitrite for a sample containing 0.5–10 μg ml^{-1} of nitrogen was 95–100%. The calibration graph and the limit of detection were the same as that obtained for nitrite-nitrogen. The relative standard deviation for the determination of 5 μg ml^{-1} of nitrate-nitrogen was 4.3%.

Interferences

Various cations and anions have been reported to have no effect on the generation of nitrogen monoxide from nitrite by iodide[6] (apart from oxidising nitrite to nitrate) nor on the reduction of nitrate to nitrite by the copperised cadmium column.[11] However, in this work carbon dioxide and an excess of hydrogen sulphide gave emissions within the cavity and produced spectral interferences. These two interferents were eliminated by placing a trap between the reaction vessel and the cavity. The trap was packed in series with cotton-wool moistened with lead acetate solution, potassium hydroxide pellets and barium hydroxide powder. Using this trap, the effect of 0.01 M sodium carbonate solution on the determination of 0.5–10 μg ml^{-1} of nitrite-nitrogen was eliminated.

Table 1. Determination of nitrite in meat products

Sample	Amount of nitrite per 10 g of sample/mg Found	Added	Recovered
Soudjik I*	0.085	0.33	0.31
Soudjik II*	0.21	4.11	4.03
Soudjik II†	0.21	4.11	3.90
Soudjik III*	‡	2.05	2.14
Soudjik III†	‡	0.82	0.79
Salami*	‡	2.05	1.95
Salami†	‡	2.05	1.99
Salami II*	‡	0.82	0.81
Salami III*	‡	0.82	0.81
Sausage I*	0.20	0.82	0.83
Sausage II*	0.12	2.05	1.94
Sausage II†	0.12	2.05	1.88

* Proteins precipitated before the measurements were made.
† Measurements made without separating the proteins.
‡ Not detectable.

Table 2. Concentration of nitrate in meat products

Sample	Concentration of nitrate/mg kg^{-1}
Soudjik I	17
Soudjik II	11
Salami I	45
Salami II	53
Sausage I	62

Table 3. Determination of nitrate-nitrogen in drinking water. All values in mg l^{-1}

Sample	MECA technique	Spectrophotometric method
1	1.40	1.30
2	1.52	1.48
3	6.80	6.80
4	5.20	5.20
5	1.72	1.68

Determination of Nitrite and Nitrate in Meat Products

The proposed MECA method was applied to the determination of nitrite and nitrate in soudjiks, salami and sausage. The samples were taken randomly from the supermarket.

The samples were prepared for analysis according to a standard procedure.[12] A 10-g amount of the minced samples was extracted with hot water at 75–80 °C. The proteins in the extracts were separated by precipitation with potassium hexacyanoferrate(II) and zinc acetate. Nitrite was determined directly in the extract. For the recovery studies, known amounts of sodium nitrite were added to 10 g of the minced samples. The results obtained (Table 1) indicate that the recovery of added nitrite is satisfactory when the standard sample preparation procedure is coupled with MECA.

The nitrate in the extracts was also determined without separating the proteins. The results were similar to those obtained after separation of the proteins (Table 1).

The nitrate in the extracts was reduced with the copperised cadmium column[12] and the total nitrite and nitrate was then determined. The nitrate concentration was calculated as the difference between the total nitrite and nitrate, and nitrite concentrations (Table 2). The column did not affect the results of the nitrite determination. Proteins in the extract blocked the reductor column and, therefore, had to be separated prior to the determination of nitrate.

Determination of Nitrate-nitrogen in Drinking Water

The water samples were taken from various sources in İzmir. No detectable levels of nitrite- and ammonium-nitrogen were

found in the samples. The nitrate in the samples was reduced to nitrite using the reductor column and then determined by both the MECA and a standard spectrophotometric method[1] [diazotisation of nitrite ion with sulphanilamide and coupling with *N*-(1-naphthyl)ethylenediamine dihydrochloride to form an azo dye which is then measured spectrophotometrically]. Table 3 shows that the results given by both methods are comparable.

Conclusion

The MECA technique using a cavity containing an entire flame and coupled with a volatilisation system constitutes a simple, fast and highly sensitive method for the determination of ammonium-, nitrite- and nitrate-nitrogen; the limits of detection are 100, 5 and 20 times better, respectively, than those reported previously using MECA with an oxy-cavity.[4–6]

The proposed method was applied successfully to the determination of nitrate-nitrogen in drinking water and nitrite and nitrate in meat products.

References

1. "Annual Book of ASTM Standards," American Society for Testing and Materials, Easton, Philadelphia, PA, 1982, Part 31, Nos. D 1426, D 992 and D 3867.
2. Honma, M., and Smith, C. L., *Anal. Chem.*, 1954, **26**, 458.
3. Butcher, J. M. S., and Kirkbright, G. F., *Analyst*, 1978, **103**, 1104.
4. Belcher, R., Bogdanski, S. L., Calokerinos, A. C., and Townshend, A., *Analyst*, 1977, **102**, 220.
5. Belcher, R., Bogdanski, S. L., Calokerinos, A. C., and Townshend, A., *Analyst*, 1981, **106**, 625.
6. Al-Zamil, I. Z., and Townshend, A., *Anal. Chim. Acta*, 1982, **142**, 151.
7. Belcher, R., Bogdanski, S. L., Ghonaim, S. L., and Townshend, A., *Anal. Chim. Acta*, 1974, **72**, 183.
8. Bogdanski, S. L., Henden, E., and Townshend, A., *Anal. Chim. Acta*, 1980, **116**, 93.
9. Henden, E., *Anal. Chim. Acta*, 1985, **173**, 89.
10. Belcher, R., Bogdanski, S. L., Henden, E., and Townshend, A., *Anal. Chim. Acta*, 1977, **92**, 33.
11. Henriksen, A., and Selmer-Olsen, A. R., *Analyst*, 1970, **95**, 514.
12. International Standards Organization, Standard Nos. ISO 2918 (1975) and ISO 3091 (1974), International Organization for Standardization, Geneva, Switzerland.

Paper 8/03688H
Received September 21st, 1988
Accepted December 14th, 1988

Gas Chromatographic Determination of Ethyl 2-Cyanoacrylate in the Workplace Environment

Virindar S. Gaind and Kazik Jedrzejczak
Occupational Health Laboratory, Ontario Ministry of Labour, 101 Resources Road, Weston, Ontario M9P 3T1, Canada

Low levels of airborne ethyl 2-cyanoacrylate (ECA) were monitored by drawing air through sampling tubes containing Tenax GC. After desorption with acetone, ECA was quantified by gas chromatography using a thermionic specific detector in the nitrogen mode. Polymerised ECA was shown to yield ECA monomer under the conditions of gas chromatographic analysis.

Keywords: *Gas chromatography; airborne ethyl 2-cyanoacrylate; glue*

Ethyl 2-cyanoacrylate (ECA) and other alkyl 2-cyanoacrylates such as methyl 2-cyanoacrylate (MCA) are highly reactive monomers that undergo rapid anionic polymerisation when a small amount of the monomer is pressed between two surfaces. The polymerisation is catalysed even by the small amount of water vapour normally present in the atmosphere. Alkyl cyanoacrylates set rapidly resulting in their widespread use as adhesives in a variety of industrial, household and medical applications. Krazy Glue adhesive is reported to contain 99.9% ECA.

Both ECA and MCA are moderate eye irritants and can cause transient blurred vision at levels of 2 p.p.m.[1] Further, ECA has toxic effects if ingested or absorbed through the skin. The American Conference of Governmental Industrial Hygienists[2] has adopted a threshold limit value for an 8-h time-weighted average of 8 mg m^{-3} (2 p.p.m.) for MCA and the Ontario Ministry of Labour[3] has recommended a working exposure guideline of 2 p.p.m. of ECA measured over 15 min. The gas chromatographic and infrared analytical procedures used for the determination of ECA and MCA in manufacturing processes are not sufficiently sensitive for monitoring the low concentrations of these monomers likely to be present in the workplace atmosphere. Leonard *et al.*[4] developed a more sensitive procedure in which MCA was determined by measuring the amount of formaldehyde released by polymerised MCA on its reaction with 4,5-dihydroxynaphthalene-2,7-disulphonic acid (chromotropic acid). However, this method is not specific.

This paper describes a highly sensitive and specific procedure for the determination of airborne ECA based on the collection of ECA on a Teflon (polytetrafluoroethylene bonded to polypropylene) filter and a tube containing Tenax adsorbent. The quantification of ECA or MCA is carried out by gas chromatography using a thermionic specific detector in the nitrogen mode.

Experimental

Reagents

Ethyl 2-cyanoacrylate and methyl 2-cyanoacrylate were received as a gift from 3M (London, Ontario, Canada). Acetone (analytical-reagent grade) was obtained from Caledon Laboratories (Georgetown, Ontario, Canada).

Apparatus

The portable air sampling pump was a Bendix Model 44. The air sampling tubes (Catalogue No. 226-35-03) and Teflon filters (Catalogue No. 225-17-01) were obtained from SKC (Eighty Four, PA, USA). A Varian Vista Model 44 gas chromatograph equipped with a thermionic specific detector (TSD) and a Model 401 data system, and a Hewlett-Packard Model 5985 gas chromatograph - mass spectrometer with an HP 7920 data system were used.

Sample Collection

Air was drawn at 1 l min^{-1}, for 30 min, through a Teflon filter and then through a sorbent tube containing two sections of Tenax. The filter and Tenax from both sections of the tube were extracted separately using acetone and the extracts of ECA and MCA were quantified by gas chromatography (GC).

Gas Chromatographic Analyses

Column. Glass, 1.8 m × 6 mm o.d. and 2 mm i.d., packed with Tenax GC, 50/80 mesh.

Temperatures. Oven, 200; injector, 220; and detector, 230 °C.

Carrier gas. Nitrogen, 30 ml min^{-1}.

Under these chromatographic conditions, the peak for ECA was well resolved from both that of the solvent and MCA, as shown in Fig. 1. Further experiments on stability and recovery were conducted on ECA only.

Preparation of Polymeric ECA

Approximately 0.5 ml of liquid monomeric ECA was spread thinly on a watch-glass and left overnight in a fume cupboard.

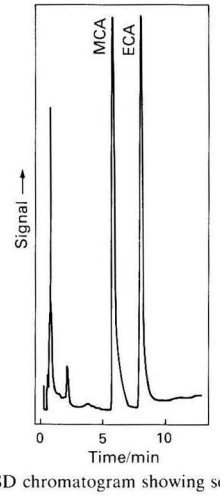

Fig. 1. GC - TSD chromatogram showing separation of MCA and ECA

Table 1. Precision data obtained by measurement of peak areas (arbitrary units)

Concentration of ECA/μg ml^{-1}		
5	10	20
49 718	108 887	205 586
49 749	103 339	197 332
50 266	98 080	201 111
50 321	96 153	206 840
48 186	106 595	196 053
49 214	110 023	204 213
49 204	99 235	192 983
47 717	104 575	204 245
$\bar{X}$: 49 297	$\bar{X}$: 103 361	$\bar{X}$: 201 045
SD: 935	SD: 5123	SD: 5045
CV: 0.019	CV: 0.049	CV: 0.025

Table 2. Recovery of ECA from spiked Tenax tubes

ECA added/μg	ECA found/μg	Average recovery, %
5.0	4.4	
	4.8	93
	4.8	
10.0	10.1	
	10.2	100
	9.6	
20.0	19.8	
	19.3	97
	19.2	
		$\bar{X}$: 97%
		SD: 3.5%
		CV: 0.036

Table 3. Stability of ECA on Tenax tubes under various storage conditions

Day sample was analysed	ECA added/μg	ECA found/μg	Average recovery, %
Ambient temperature (20–23 °C)—			
0	5.0	4.6	
0	10.0	9.5	94
0	20.0	19.2	
3	5.0	4.7	
3	10.0	9.4	95
3	20.0	19.3	
7	5.0	4.8	
7	10.0	10.2	99
7	20.0	19.8	
14	5.0	4.4	
14	10.0	9.1	92
14	20.0	19.5	
Refrigerated at 4 °C—			
0	5.0	4.8	
0	10.0	10.2	98
0	20.0	19.3	
3	5.0	4.2	
3	10.0	9.8	95
3	20.0	20.4	
7	5.0	4.7	
7	10.0	9.6	96
7	20.0	19.8	
14	5.0	4.5	
14	10.0	9.2	93
14	20.0	19.7	

The brittle solid that formed was weighed and dissolved in acetone to prepare standard solutions of polymeric ECA.

Results

Precision and Linearity

The detector response to ECA showed excellent precision and linearity when replicate injections (2 μl) were made of three standard solutions (5, 10 and 20 μg ml^{-1}). The results are given in Table 1.

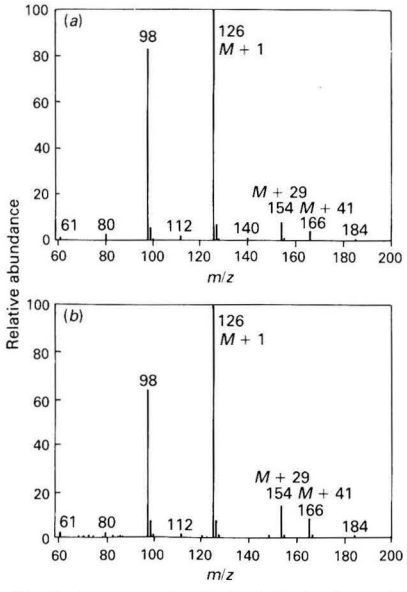

Fig. 2. Identical mass spectra obtained in the chemical ionisation mode for both (*a*) a monomeric ECA and (*b*) a polymeric ECA

Recovery of ECA Spiked on Tenax

The front sections of several tubes packed with Tenax were spiked with 5, 10 or 20 μg of ECA using a syringe and air (30 l) was drawn through the spiked tubes at 1 l min^{-1}. Each section of Tenax was placed in a separate vial, which was then crimp-sealed, and extracted with 1.0 ml of acetone. The acetone extracts were analysed for ECA and the percentage recovery was calculated by comparison with standard solutions of ECA. The results given in Table 2 indicate near quantitative recoveries at all levels of spiking.

Stability of ECA Spiked on Tenax

Replicate Tenax tubes were spiked with known amounts of ECA and then stored at 4 °C and at ambient temperature (20–23 °C) for various periods of time. The ECA was determined after storing the tubes for 0, 3, 7 and 14 d. The amount of ECA recovered is given in Table 3. It was found that samples collected on Tenax remained stable for at least 14 d with recoveries in the range 93–100% at different levels of spiking.

Mass Spectra of ECA

The electron impact mass spectrum of ECA obtained at 70 eV yielded a negligible molecular ion peak at *m/z* 125 (1%) and a base peak at *m/z* 98 that was of little value for identification or quantification purposes. However, the chemical ionisation spectrum obtained with methane as the reagent gas yielded the molecular ion peak at *m/z* 126 (*M* + 1) as the base peak. Other characteristic peaks at *m/z* 154 (*M* + 29) and *m/z* 166 (*M* + 41) were also discernible (Fig. 2). The presence of a molecular ion peak in the chemical ionisation mode provides an alternative procedure for confirming the presence of and quantifying ECA in samples. Adams[5] studied the chemical ionisation pyrolysis mass spectra of a number of polymers other than polycyanoacrylates and found that polystyrene, polybutadiene, polymethylmethacrylate, etc., yielded characteristic

Table 4. Relationship between the injector temperature and the depolymerisation level. Sample mass, 10 μg

Injector temperature/°C	Peak area, arbitrary units	Depolymerisation level, %
Polymeric ECA—		
90	70 958	8
100	296 571	35
120	429 854	51
140	641 113	77
160	718 878	86
200	830 222	99
220	831 420	99
Monomeric ECA—		
220	836 460	100

molecular ions, especially (M + 1), corresponding to the respective monomer on pyrolysis. Our work, however, shows the reproducible and quantitative nature of the polymerisation - depolymerisation process for ECA when it occurs at temperatures above 220 °C and in an inert atmosphere in the gas chromatograph. The mass spectra obtained for solutions of monomeric and polymeric ECA, injected through the heated injection port (220 °C), were identical in all respects, confirming that the polymer depolymerises to the monomer under these conditions.

Discussion

The quantitative recovery of ECA spiked on Tenax tubes, achieved even after passing air through the tubes or keeping the tubes for 2 weeks, was intriguing in view of the known high reactivity of the monomer. One plausible explanation was that monomeric ECA collected on Tenax polymerised at some stage. However, on dissolution in acetone and subsequent injection into the gas chromatograph the polymer depolymerised completely in the heated injection port.

In order to validate the above hypothesis, 500 mg of monomeric ECA were spread as a thin film on a watch-glass and allowed to solidify. After 16 h, the brittle solid formed was dissolved in acetone (50 ml) to yield a standard solution (10.0 mg ml^{-1}). After further dilution, a standard solution prepared from polymeric ECA (10 μg ml^{-1}) was compared against a standard solution of the same concentration freshly prepared from monomeric ECA. The peak areas and retention times obtained for both solutions were essentially similar. The chemical ionisation mass spectrometric profiles of both solutions were indistinguishable. Further support for our hypothesis that polymerised ECA depolymerised to monomeric ECA as a result of heating in the gas chromatograph injection port was obtained when it was found that the peak area obtained by injecting 10 μg of polymerised ECA increased progressively with an increase in the injection temperature up to 200 °C, after which it became constant and almost equal to that obtained on injection of 10 μg of monomeric ECA. The peak area obtained by injecting monomeric ECA did not change significantly with injection temperature (Table 4).

Rooney[6] studied the effect of heating cyanoacrylate oligomers using thermogravimetric techniques on a qualitative level and showed using NMR spectra of ECA oligomers that during pyrolysis there were no structural alterations other than a gradual decrease in the relative molecular mass. The work described in this paper shows that the process of depolymerisation, under the controlled conditions of GC analysis, is highly reproducible and quantitative.

From the preceding discussion it is apparent that the GC determination of ECA collected on sampling tubes containing Tenax would include both the monomer and polymerised ECA as the analytical procedure is unable to distinguish between the two. However, completely polymerised ECA is unlikely to have sufficient vapour pressure to allow its collection on the Tenax tubes during sampling. Any particulate ECA (arising from polymeric ECA) can be distinguished from the monomer vapours by placing a Teflon filter between the sampling pump and the Tenax tube. To validate this, the following experiment was conducted to simulate the actual sampling process.

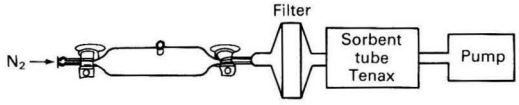

Fig. 3. Configuration of apparatus for ECA sampling

A sampling glass bulb with a rubber septum and two Teflon stopcocks was connected to a cassette containing a Teflon filter followed by a Tenax tube (Fig. 3). Dry nitrogen was passed through the system at 1 l min^{-1}. The ECA monomer (100 μg) in acetone was injected through the rubber septum and the flow of nitrogen maintained for 30 min (30 l). At the end of this period, the Teflon filter and two sections of Tenax from the sampling tube were extracted with acetone and ECA was quantified in each extract. For three replicate determinations at ambient temperature (20–23 °C) the recoveries of ECA from the Tenax tubes were 87, 94 and 95% with a standard deviation (SD) of 4.3% and a coefficient of variation (CV) of 0.48. No ECA was found on the Teflon filter and the major portion of ECA added to the sampling bulb was found on the Tenax tube. The experiment was repeated with the injection of 100 μg of polymerised ECA. Analysis of the filter and Tenax tubes indicated no detectable amount of ECA on either of the sampling media. This shows that polymerised ECA does not have sufficient vapour pressure at ambient temperature to be carried even in a stream of inert gas, in contrast to monomeric ECA, most of which is retained by Tenax under similar conditions.

Conclusions

Airborne ECA and MCA can be monitored by drawing air through tubes containing Tenax followed by desorption with acetone and quantification of cyanoacrylate by GC with thermionic specific detection or selected ion monitoring using chemical ionisation mass spectrometry. If particulate material is suspected to be present in the atmosphere, a Teflon filter placed before the Tenax tube can be used to distinguish between polymeric and monomeric ECA or MCA. This method is capable of monitoring concentrations of ECA well below 0.01 mg m^{-3}.

The authors thank M. A. Nazar, Chief Scientist, Occupational Health Laboratory of Ontario Ministry of Labour for helpful suggestions during preparation of the manuscript.

References

1. McGee, W. A., Oglesby, F. L., Raleigh, R. L., and Fassett, D. W., *Am. Ind. Hyg. Assoc. J.*, 1968, November/December, 558.
2. "Threshold Limit Values and Biological Exposure Indices for 1988–1989," American Conference of Governmental Industrial Hygienists, Cincinnati, OH, p. 26.
3. "Regulation Respecting Control of Exposure to Biological or Chemical Agents," O. REG. 654/86, Ontario Ministry of Labour, Ontario, p. 60.
4. Leonard, F., Kulkarni, R. K., Brander, G., Nelson, J., and Cameron, J. J., *J. Appl. Polym. Sci.*, 1966, **10**, 259.
5. Adams, R. E., *Anal. Chem.*, 1983, **55**, 414.
6. Rooney, J. M., *Br. Polym. J.*, 1981, December, 160.

Paper 8/04453H
Received November 9th, 1988
Accepted January 11th, 1989

Chemically Bonded Cyclodextrin Stationary Phase for the High-performance Liquid Chromatographic Separation and Determination of Sulphonamides

Abd-El Hamid N. Ahmed and Samia M. El-Gizawy
College of Pharmacy, Department of Pharmaceutical Chemistry, Assiut University, Assiut, Egypt

Mixtures of seven sulphonamides have been separated successfully on a β-cyclodextrin stationary phase by high-performance liquid chromatography (HPLC) using phosphate buffer (pH 7.0) - methanol (85 + 15). The HPLC determination of trisulphapyrimidines and Polysulpha in dosage forms is described. That the proposed method is accurate was established from the percentage recoveries of standard sulphonamide solutions.

Keywords: *High-performance liquid chromatography; β-cyclodextrin-bonded stationary phase; trisulphapyrimidines; Polysulpha and sulphonamides*

Methods for the quantification of sulphonamides were performed traditionally by sodium nitrite titration or thin-layer chromatography - ultraviolet spectrophotometry and were generally not specific, slow and tedious.[1] Sulphonamides have been separated by ion-exchange chromatography on a cation-exchange resin,[2] ion-pair partition chromatography[3] and adsorption chromatography on silica.[4] These methods have been applied to the determination of these drugs in pharmaceutical dosage forms, body fluids and tissues.[5]

Recently, reversed-phase high-performance liquid chromatography has been developed for the quantification of sulphonamides in various combinations.[6,7]

There has also been considerable interest in the utilisation of cyclodextrins as a stationary or mobile phase in chromatography because of their ability to form inclusion complexes with a variety of organic molecules or ions both in the solid state and in aqueous solution.[8–14]

The interaction of β-cyclodextrin (β-CyD) with some sulphonamides in aqueous solution has been investigated by circular dichroism (CD), ultraviolet (UV) absorption, solubility techniques and by high-performance liquid chromatography (HPLC).[15,16]

In this paper, we describe the use of a β-CyD-bonded stationary phase in HPLC for the successful separation of sulphonamides and for the quantification of certain sulphonamides in dosage forms.

Experimental

Apparatus

For HPLC a Du Pont 8800 pump module, equipped with a stainless-steel column (100 × 4.6 mm i.d.) packed with β-CyD chemically bonded to a high-purity silica gel (Cyclobond I, Advanced Separation Technologies, USA), was used. Detection was effected spectrophotometrically at 257 nm using a Du Pont variable-wavelength UV spectrophotometer. A Servogor 310 recorder combined with an SP 4100 computing integrator was used to monitor the chromatographic characteristics.

A PW 9418 pH meter (Pye Unicam, Cambridge, UK) was used to adjust the pH.

Chemicals and Reagents

All chemicals and reagents used were either US Pharmacopeia (USP) - National Formulary or ACS grade.

Dosage Forms

Trisulphapyrimidine tablets (*USP*) (*Triple Sulpha*). Each tablet (501 mg) contained equal parts of sulphadiazine, sulphadimidine and sulphamerazine (167 mg of each).

Polysulpha tablets (*CID Laboratories, Egypt*). Each tablet contained sulphadiazine (0.133 g), sulphathiazole (0.133 g), sulphadimidine (0.134 g) and sulphamerazine (0.100 g).

Solutions

Sodium orthophosphate (0.05 M) solution was prepared using distilled water and its pH adjusted to 7 with 0.1 M NaOH.

Stock solutions (1 mg ml^{-1}) of sulphathiazole, sulphaguanidine, sulphadiazine, sulphamerazine, sulphadimidine, sulphaphenazole and sulphacetamide were prepared in methanol and diluted serially with phosphate buffer (0.05 M NaH_2PO_4, pH 7) so as to give final concentrations of 10–30, 5–20, 10–30, 5–20, 5–20, 10–30 and 10–30 μg ml^{-1} of each sulphonamide, respectively, for the construction of calibration graphs.

Chromatographic Conditions

The mobile phase was phosphate buffer (pH 7.0) - methanol prepared in the ratios of 50 + 50, 55 + 45, 60 + 40, 65 + 35, 70 + 30, 75 + 25, 80 + 20, 85 + 15 and 90 + 10. The mobile phase was degassed directly before use. The flow-rate was varied from 1.5 to 0.5 ml min^{-1} and the temperature adjusted to 35 °C. The chart speed was 0.25 cm min^{-1} and the attenuation unit for full-scale deflection was set at 1 mV.

Preparation of Assay Solutions

For trisulphapyrimidine tablets (*Triple Sulpha*)

One tablet was placed in each of ten 100-ml calibrated flasks and 50 ml of methanol were added. The sample was sonicated (15 min) and the solution made up to the mark with methanol. A portion of the solution was centrifuged (15 min), then 0.1 ml of the clear supernatant solution was transferred quantitatively into a 10-ml calibrated flask and made up to the mark with phosphate buffer (pH 7.0) - methanol (85 + 15).

The final concentrations were equivalent to 16.7 μg ml^{-1} of sulphadiazine, 16.7 μg ml^{-1} of sulphadimidine and 16.7 μg ml^{-1} of sulphamerazine.

For Polysulpha tablets

The procedure was identical with that described above for trisulphapyrimidine tablets.

The final concentrations were equivalent to 13.3 μg ml^{-1} of sulphadiazine, 13.3 μg ml^{-1} of sulphathiazole, 13.4 μg ml^{-1} of sulphadimidine and 10.0 μg ml^{-1} of sulphamerazine.

Assay

The standard and prepared solutions (50 ml of each) were injected into the chromatograph and the peak areas were determined. The amount of active components was determined by comparing the peak area of the sample with the representative peak area of the standard of known concentration.

Results and Discussion

The β-CyD-bonded stationary phase (Cyclobond I) retains a wide variety of compounds via the formation of inclusion complexes. Consequently, compounds that were previously thought to be difficult to separate by conventional liquid chromatography can be resolved easily.

To form the inclusion complexes, the guest sulphonamide molecules approach and penetrate the hydrophobic cavity of the cyclodextrin from the more open and accessible secondary hydroxyl group of the glucose unit. As a result, some of the physico-chemical properties of the guest sulphonamide molecule can be modified.[15]

The stability of the inclusion complexes varies with the size of both the guest sulphonamide molecule and the host β-CyD. The basis of the separation and resolution of some of the sulphonamides studied was observed from the selectivity in binding towards the CyD cavity.[16,17] Knowing the stability of the β-CyD inclusion complexes formed, an accurate prediction could be made concerning the expected elution behaviour on the column of the seven sulphonamides studied. The sulphonamides could be detected easily and monitored using HPLC.

Sulphathiazole interacts strongly with β-CyD and is retained longer; therefore it exhibits a relatively longer retention time than all the other sulphonamides studied. Sulphacetamide interacts weakly with β-CyD and is eluted rapidly with a consequent short retention time.

The elution order of the seven sulphonamides was dependent on the amount of methanol in the mobile phase. The composition of the mobile phase [phosphate buffer (pH 7.0) - methanol (55 + 45, 60 + 40, 65 + 35, 70 + 30, 75 + 25, 80 + 20, 85 + 15 and 90 + 10] was varied to investigate its effect on the resolution and retention times. The presence of the phosphate buffer at the expense of methanol was essential for complete separation. The effect of the flow-rate (1.5, 1.0 and 0.5 ml min^{-1}) of the mobile phase on the resolution of the seven sulphonamides was also studied. Efficient separation of the seven sulphonamides was achieved using phosphate buffer (pH 7.0) - methanol (85 + 15) at a flow-rate of 0.5 ml min^{-1} (Fig. 1).

The proposed HPLC method was applied to the analysis of trisulphapyrimidine (Triple Sulpha) and Polysulpha tablets using phosphate buffer (pH 7.0) - methanol (85 + 15) as the mobile phase at a flow-rate of 0.5 ml min^{-1}. The results for the synthetic mixtures were quantitative and showed complete recovery, Table 1.

A linear regression was obtained by plotting the standard concentrations of sulphamerazine, sulphadiazine, sulphadimidine and sulphathiazole *versus* peak area. Table 2 gives the slope, correlation coefficient and intercept for each sulphonamide.

Figs. 2 and 3 illustrate the utility of the Cyclobond I column for the separation of sulphonamides in trisulphapyrimidine and Polysulpha tablets. There was no indication that the tablet excipients interfered with the separated peaks.

It is apparent that the effect of the accumulation and competition of seven sulphonamides in the standard mixture (Fig. 1) on the resolution from the β-CyD cavity is different from the competition of three or four sulphonamides (Figs. 2 and 3) so that minor differences in the retention times were obtained. Also the differences in the composition of the mobile phase from day to day should also be taken into consideration.

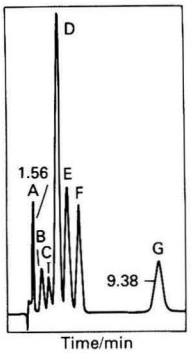

Fig. 1. Separation of sulphonamides using phosphate buffer (pH 7) - methanol (85 + 15) at a flow-rate of 0.5 ml min^{-1}. A, Sulphacetamide; B, sulphadiazine; C, sulphamerazine; D, sulphaphenazole; E, sulphaguanidine; F, sulphadimidine; and G, sulphathiazole

Table 1. Determination of sulphonamides in known synthetic mixtures

No.	Prepared mixture	Added/ mg	Found ± SD*/ mg	Recovery, %
1	Sulphadiazine	133	133.0 ± 0.25	100.00
	Sulphathiazole	133	132.7 ± 0.61	99.77
	Sulphadimidine	134	134.2 ± 1.03	100.15
2	Sulphadiazine	185	185.5 ± 0.49	100.27
	Sulphamerazine	185	185.0 ± 1.27	100.00
	Sulphathiazole	185	184.8 ± 1.07	99.89
3	Sulphadiazine	167	166.6 ± 0.16	99.76
	Sulphamerazine	167	167.2 ± 0.35	100.12
	Sulphadimidine	167	167.5 ± 1.31	100.30

* Based on five replicate analyses of known mixtures.

Table 2. Calibration data for standard drug solutions

Compound	Concentration/ μg ml^{-1}	Correlation coefficient, r (SD)*	Slope	Intercept
Sulphadiazine . .	10–30	0.998 (0.015)	0.893	0.046
Sulphamerazine . .	5–20	0.999 (0.001)	0.151	0.001
Sulphadimidine . .	5–20	0.998 (0.027)	0.275	0.176
Sulphathiazole . .	10–30	0.997 (0.012)	0.623	0.117

* Average of five determinations.

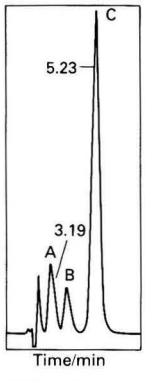

Fig. 2. Chromatogram of 50 μl of a solution of trisulphapyrimidine tablets containing: A, sulphadiazine; B, sulphamerazine; and C, sulphadimidine

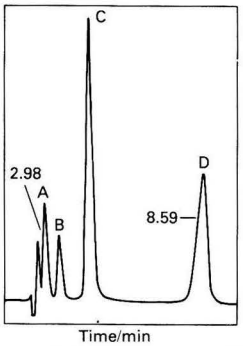

Fig. 3. Chromatogram of 50 µl of a solution of Polysulpha tablets containing: A, sulphadiazine; B, sulphamerazine; C, sulphadimidine; and D, sulphathiazole

Table 3. Analysis of dosage forms

Preparation	Label claim	Assay results	Recovery, %	SD	CV,* %
	mg per tablet				
Trisulphapyrimidine tablets—					
Sulphadiazine . .	167	166.1	99.46	0.51	0.31
Sulphamerazine . .	167	165.7	99.22	1.29	0.77
Sulphadimidine . .	167	167.8	100.48	1.03	0.61
Polysulpha tablets—					
Sulphadiazine . .	133	134.0	100.75	1.04	0.78
Sulphamerazine . .	100	101.1	101.1	1.30	1.03
Sulphadimidine . .	134	132.9	99.18	1.27	0.95
Sulphathiazole . .	133	134.0	100.75	1.09	0.81

* Standard deviation of the mean of five determinations divided by the mean expressed as a percentage.

The accuracy of the method was established by achieving reproducible results of 99.22–100.48% for the trisulphapyrimidine tablets and 99.18–101.1% for the Polysulpha tablets, Table 3.

The authors thank Nabil M. Omar, Faculty of Pharmacy, Assiut University, Assiut, Egypt, for helpful discussions and support of this work.

References

1. "US Pharmacopeia XXI, National Formulary XVI," US Pharmacopeial Convention, Rockville, MD, 1985, pp. 988–993.
2. Poet, R. B., and Pu, H. H., *J. Pharm. Sci.*, 1973, **62**, 809.
3. Su, S. C., Hartkopf, A. V., and Karger, B. L., *J. Chromatogr.*, 1976, **119**, 523.
4. Cobb, P. H., and Hill, G. T., *J. Chromatogr.*, 1976, **123**, 444.
5. Pryde, A., and Gilbert, M. T., "Applications of High Performance Liquid Chromatography," Chapman and Hall, London and New York, 1979, p. 73.
6. Farmi, A. A., Tylor, D., and Mashi, S. Z., *Drug Develop. Ind. Pharm.*, 1984, **10**, 31.
7. Parasrampuria, J., and Das Gupta, V., *Drug Develop. Ind. Pharm.*, 1986, **12**, 251.
8. Hinze, W. L., *Sep. Purif. Methods*, 1981, **10**, 195.
9. Armstrong, D. W., and Demond, W., *J. Chromatogr. Sci.*, 1984, **22**, 411.
10. Kujimura, K., Ueda, T., and Ando, T., *Anal. Chem.*, 1983, **55**, 446.
11. Kawaguchi, Y., Tanaka, M., Nakae, M., Funazo, R., and Shono, T., *Anal. Chem.*, 1983, **55**, 1852.
12. Armstrong, D. W., Demond, W., Alak, A., Hinze, W. L., Riehl, T. E., and Bui, K. H., *Anal. Chem.*, 1985, **57**, 234.
13. Hinze, W. L., Riehl, T. E., Armstrong, D. W., Demond, W., Alak, A., and Ward, T., *Anal. Chem.*, 1985, **57**, 237.
14. Armstrong, D. W., Demond, W., and Czech, B. P., *Anal. Chem.*, 1985, **57**, 481.
15. Bender, M. L., and Komiyama, M., "Cyclodextrin Chemistry," Springer-Verlag, New York, 1978.
16. Uekama, R., Hirayama, F., Otagiri, M., Otagiri, Y., and Ikeda, R., *Chem. Pharm. Bull.*, 1978, **26**, 1162.
17. Uekama, R., Hirayama, F., Nasu, S., Matsuo, N., and Irie, T., *Chem. Pharm. Bull.*, 1978, **26**, 3477.

Paper 8/01367E
Received April 6th, 1988
Accepted December 14th, 1988

Thin-layer Chromatographic Scanner, Spectrophotometric and High-performance Liquid Chromatographic Methods for the Determination of Colchicine

Taha M. Sarg, Maher M. El-Domiaty and Mokhtar M. Bishr
Faculty of Pharmacy, Zagazig University, Zagazig, Egypt
Osama M. Salama and Ahmed R. El-Gindy
Islamic Centre for Medical Sciences, Kuwait

One high-performance liquid chromatographic (HPLC) and two thin-layer chromatographic (TLC) methods are proposed for the determination of colchicine in crude drugs and pharmaceutical preparations. The TLC scanner method is based on measurement of the absorbance of the separated colchicine spot; alternatively, after scraping the spot from the plate and elution the absorbance can be measured spectrophotometrically. The HPLC assay was carried out isocratically on a reversed-phase column using MeOH - H_2O (60 + 40). The recoveries were 99.2 ± 1.23, 99.1 ± 1.12 and 99.1 ± 2.01% for the TLC scanner, spectrophotometric and HPLC methods, respectively. The methods were shown to be sensitive and specific and can be used as an alternative to the pharmacopoeial methods having been applied to the determination of colchicine in corms of *Merendera persica* and in three pharmaceutical preparations.

Keywords: *Thin-layer chromatographic scanner method; spectrophotometry; high-performance liquid chromatography; colchicine determination; pharmaceutical preparations*

The plant alkaloid colchicine is known to provide effective pain relief in acute gouty arthritis.[1,2] It is the predominant alkaloid in plants of the family Liliaceae, especially of the genera *Colchicum* and *Merendera*.[3–5]

Typically, the official methods for the determination of colchicine in crude drugs and pharmaceutical preparations are gravimetric[6–9] or colorimetric.[8,10,11] Other methods, *viz.*, colorimetric and spectrophotometric,[2,12–16] fluorimetric,[17,19] volumetric[16] and chromatographic[20–23] assays have also been described. Most of these methods are designed to measure the total alkaloid content and hence are not specific. They involve multiple extraction and purification procedures, often followed by a derivatisation step or by chemical reaction prior to the actual determination. Reactions with hydroxylamine hydrochloride,[24] iron(III) chloride,[25] nitric acid,[26] iodine[27] and aluminium lithium hydride[15] have been exploited. Polarographic investigations[28] have not been widely undertaken and have been electrochemically oriented.[29] Therefore, the reported methods lack either simplicity, precision or specificity and have various other disadvantages.[22] More recently, an HPLC method has been described[30] that is concerned more with the separation of colchicine derivatives than with quantification, which requires a complicated gradient elution technique.

The work described in this paper was undertaken to demonstrate explicitly the exploitation of both a simple HPLC method and a TLC scanner method for the rapid and precise determination of colchicine. Also discussed is a low-cost method that involves TLC followed by elution and the spectrophotometric determination of colchicine. The three proposed methods were applied successfully to the determination of colchicine in corms of *Merendera persica*, in which colchicine is the major alkaloid,[5] and in a number of pharmaceutical preparations.

Experimental and Results

Materials

In this work, one crude drug and several commercial pharmaceutical dosage forms containing colchicine were used. A pure colchicine sample was used to confirm the accuracy and efficiency of the proposed methods. The following samples were employed: (1) corms of *Merendera persica* L., family Liliaceae (Hamdard Foundation, Pakistan, Waqf); (2) colchicine tablets (Evans Medical, Greenford, Middlesex, UK) containing 500 μg of colchicine per tablet; (3) ColBenemid tablets (Merck, Sharp and Dohme, St. Louis, MO, USA) containing 500 μg of colchicine and 500 mg of probenecid per tablet; and (4) Urosolvine effervescent granules (Nile, Cairo, Egypt) each 5 g containing colchicine (300 μg), piperazine hydrate (0.128 g), atropine sulphate (0.128 mg) and sodium citrate (the difference).

Apparatus

The TLC scanner method employed a Shimadzu C5-930 TLC scanner. Spectrophotometric determinations were carried out using a Shimadzu UV-260 spectrophotometer and silica gel G pre-coated plates (Merck). Chromatographic assays were conducted on a Shimadzu LC-4 HPLC instrument equipped with a UV detector.

Determination of Colchicine in Corms of *M. persica* L.

Sample preparation

Coarsely powdered corms (5.0 g) were transferred into an apparatus for the continuous extraction of drugs and extracted exhaustively with 70% *V/V* ethanol. The alcohol was removed by evaporation under reduced pressure and the remaining aqueous residue was extracted with chloroform (4 × 30 ml). The combined extracts were evaporated to dryness and the resulting residue was then either dissolved in 5 ml of methanol (stock solution for the TLC scanner and HPLC determinations) or in 1 ml of methanol (stock solution for spectrophotometric assays).

TLC scanner assay

Procedure. The prepared stock extract of *M. persica* corms (10 μl) was spotted on silica gel G pre-coated plates, which were developed using chloroform - methanol (95 + 5) as the solvent system. The air-dried plates were subjected to UV measurement using a TLC scanner operating at 243 nm. This procedure was repeated six times.

Quantification. The peak areas for six colchicine determina-

tions were measured and the mean was calculated. The amount of colchicine in the prepared sample (Table 1) was then obtained using a calibration graph of average peak area *versus* known concentration of pure colchicine. The calibration graph was linear in the range 1.0–6.0 μg (spotted amount) of colchicine and had a zero intercept.

Precision and recovery. The precision and recovery were determined by repeated analysis of a single sample (5 g) of powdered corms of *M. persica* L. to which 1 mg of pure colchicine had been added (*i.e.*, each 10-μl spotted volume should contain 2 μg of the added colchicine). The results given in Table 2 indicate good repeatability with a coefficient of variation (CV) of 1.24% and a standard deviation (SD) of 1.23%.

Spectrophotometric assay

Procedure. The stock solution (10 μl) was spotted (together with pure colchicine as a marker) on a pre-coated silica gel G plate. The plate was developed using $CHCl_3$ - MeOH (95 + 5) and then air-dried. The colchicine spots (R_F, 5.5) were detected under UV light (366 nm) and checked against the colchicine marker. These spots were then scraped from the plate and the colchicine was eluted using methanol. The methanolic extract was filtered quantitatively, the volume adjusted to 5 ml and the UV absorbance measured at 350 nm. Each sample was analysed six times.

Quantification. The mean absorbance for six determinations was calculated and the concentration of colchicine determined with the aid of a calibration graph of known concentration of pure colchicine *versus* absorbance. The calibration graph was linear in the range 1.76–8.8 μg with a zero intercept. The results are shown in Table 1.

Precision and recovery. The precision and recovery of this method were determined by the procedure described for the TLC scanner method but using 0.3 mg of pure colchicine (*i.e.*, each spotted volume should contain 3 μg of added colchicine). The results, with an SD of 1.12% and a CV of 1.13%, are given in Table 2.

HPLC assay

Chromatographic system. A Shimadzu LC-4 chromatograph, fitted with a UV detector operating at a wavelength of 243 nm, was employed. A reversed-phase Zorbax-ODS C_{18} column (15 cm × 4 mm i.d.) was used at 40 °C. The mobile phase was MeOH - H_2O (60 + 40) in the isocratic mode with a flow-rate of 0.5 ml min^{-1}. The injection volume was 1 μl.

Quantification. The mean peak area for six determinations of colchicine (R_t, 9.5 min) was calculated and the concentration of colchicine in the sample (Table 1) was obtained from a calibration graph, which was constructed by plotting the peak areas against the known concentrations of the pure compound. The calibration graph was linear over the range 0.2–1.5 μg of pure colchicine and passed through the origin.

Precision and recovery. The efficiency of this method was verified by the good reproducibility obtained for repeated injections of the same sample, prepared after the addition of 2.5 mg of pure colchicine to 5 g of powdered corms (*i.e.*, 0.5 μg of pure colchicine in each injection) (Table 2). The CV was 2.03% and the SD 2.01%.

Table 1. Determination of colchicine in corms of *M. persica* by three different methods

Method	Colchicine*/ μg per gram of powder	Colchicine, % *m/m*
TLC scanner	571.6	0.057
Spectrophotometric	580	0.058
HPLC	570	0.057

* Mean of six determinations

Table 2. Precision achieved by three different methods

Run No.	Recovery, % TLC scanner	Spectrophotometric	HPLC
1	98.0	99.8	96.8
2	99.4	97.2	98.2
3	99.8	100.5	101.5
4	101.9	99.4	99.9
5	99.1	98.3	99.5
6	98.9	98.5	98.1
7	97.9	99.6	100.2
8	100.3	97.9	97.6
9	98.5	99.1	100.1
10	98.2	100.7	99.1
Average	99.2	99.1	99.1
SD	1.23	1.12	2.01
CV	1.24	1.13	2.03

Determination of Colchicine in Pharmaceutical Preparations

The three proposed methods were applied to the determination of colchicine in three commercial pharmaceutical preparations (see under Materials).

Sample preparation

Tablets. Twenty tablets (colchicine or ColBenemid) were weighed accurately and pulverised. An amount of finely powdered tablets equivalent to 5 mg of colchicine was extracted with methanol, the combined methanol extracts were filtered and the volume was adjusted to give a stock solution containing 0.5 mg ml^{-1} of colchicine.

Effervescent granules. An accurately weighed amount of finely powdered effervescent granules (5 g) equivalent to 0.3 mg of colchicine was dissolved in water. After the effervescence had ceased, the resulting solution was extracted with chloroform. The chloroform was dried using anhydrous sodium sulphate and removed by distillation and the residue was dissolved in methanol to give a stock solution containing 0.5 mg ml^{-1} of colchicine.

Table 3. Determination of colchicine (μg) in three dosage forms using the proposed methods

Dosage form	TLC scanner method Mean* ± SD†	CV, %†	Recovery, %	Spectrophotometric method Mean* ± SD†	CV, %†	Recovery, %	HPLC method Mean* ± SD†	CV, %†	Recovery, %
I‡	500.5 ± 1.7	0.21	100.1	499.0 ± 2.7	0.54	99.8	499.1 ± 3.2	0.64	99.8
II§	499.8 ± 3.0	0.60	99.9	498.0 ± 3.7	0.74	99.6	498.6 ± 3.3	0.66	99.7
III¶	298.6 ± 2.3	0.79	99.5	298.4 ± 1.6	0.53	99.4	297.6 ± 4.6	1.54	99.2

* Results are the mean of six determinations.
† SD = standard deviation; CV = coefficient of variation.
‡ Colchicine tablets (500 μg per tablet).
§ ColBenemid tablets (500 μg of colchicine and 500 mg of probenecid per tablet).
¶ Colchicine effervescent granules. Each 5 g contains 300 μg of colchicine, 0.128 g of piperazine hydrate, 0.128 mg of atropine sulphate and sodium citrate making up the difference.

Procedure

The prepared samples were assayed using the TLC scanner, spectrophotometric and HPLC methods as described for the determination of colchicine in corms of *M. persica*. The results are given in Table 3.

Discussion and Conclusion

The work described in this paper was prompted by interest in the corms of *M. persica*, which have been used successfully for the treatment of rheumatoid arthritis and other diseases[31,32] in some Asian and Arabian countries. The main purpose of the investigation was to develop simple, sensitive and rapid methods having a high degree of specificity for the determination of colchicine in crude drugs and pharmaceutical preparations.

In order to determine the efficiency of the proposed methods, pure colchicine was added in known amounts to the samples prior to the assay procedures. The recoveries were quantitative. The results indicated that high recovery was achieved: 99.2, 99.1 and 99.1% for the TLC scanner, spectrophotometric and HPLC methods, respectively. The CVs were 1.24, 1.13 and 2.03%, respectively.

The HPLC method provided satisfactory resolution of colchicine (R_t, 9.5 min) from related compounds such as colchicoside (R_t, 6.7 min) and allowed the determination of as little as 0.2 μg of colchicine in less than 10 min employing a simple isocratic technique. Hence this method is useful for rapid, routine work, requiring no reconditioning of the HPLC column. In terms of simplicity and sensitivity, the results showed that this method has advantages over the reported HPLC assay.[30]

In the TLC scanner method the absorbance was found to be proportional to the concentration of colchicine up to 6 μg and as little as 1 μg could be determined easily. Similar results (Tables 1–3) were obtained with the spectrophotometric assay. However, the scanning method has the advantage of measuring the absorbance due to colchicine directly on the plate, hence avoiding loss of material and giving savings in time and effort.

We believe that these results are sufficiently good to merit replacement of the tedious, non-specific and less sensitive pharmacopoeial methods with one of the proposed methods. The method chosen would depend on the laboratory facilities available, the nature of the sample and the scale and purpose of the determination.

The HPLC method is recommended for both the quantitative and qualitative determination of colchicine in crude drugs containing colchicine and its related compounds, owing to the good separation provided by the chromatographic system. In addition the method can be used to determine sub-microgram amounts of colchicine in pharmaceuticals.

The TLC scanner method is capable of determining colchicine in both crude drugs and pharmaceuticals with a high degree of accuracy. It also has the advantage of requiring only simple and relatively inexpensive apparatus.

The spectrophotometric method requires even less expensive apparatus that is probably available in most laboratories. Although this method gives satisfactory results, it involves additional steps for the scraping and elution of colchicine from the adsorbent, leading to a potential loss of colchicine.

The proposed methods provide a wide range from which the analyst can select the technique that best suits the laboratory equipment available and the purpose of the work. Comparisons of the time and equipment required and of the limits of determination of colchicine for each method are given in Table 4.

Table 4. Comparison of sensitivity and requirements of the proposed methods

Method	Apparatus	Time*/ min	Range of determination/ μg of colchicine
Spectrophotometric . .	UV spectrophotometer TLC plates (silica gel)	60	1.7–8.8
TLC scanner	TLC scanner TLC plates (silica gel)	30	1.0–6.0
HPLC	Simple HPLC instrument fitted with a UV detector	10	0.2–1.5

* For the determination of colchicine in the crude drug an extra 40 min are required for extraction.

The authors are indebted to Dr. A. A. Al-Awadi, Minister of Public Health and President of the Islamic Organization of Medical Sciences, Kuwait, and to all members of the Islamic Centre for Medical Sciences for their encouragement and assistance throughout this work.

References

1. Laurance, D. R., and Benaeth, P. N., "Clinical Pharmacology," Fifth Edition, Churchill Livingstone, London, 1980.
2. Smith, G., Bullivant, J. M., and Cox, P. H., *J. Pharm. Pharmacol.*, 1963, **15**, 92T.
3. Reynolds, J. E. F., and Prasad, A. B., *Editors*, "Martindale, The Extra Pharmacopoeia," Twenty-eighth Edition, Pharmaceutical Press, London, 1982, p. 416.
4. Potesilova, H., Alcara, C., and Santavy, F., *Collect. Czech. Chem. Commun.*, 1969, **34**, 2128.
5. Kaul, J. K., Moza, B. K., Santavy, F., and Vrublovsky, P., *Collect. Czech. Chem. Commun.*, 1964, **29**, 1689.
6. "Egyptian Pharmacopoeia 1953," Fouad I University Press, Cairo, 1953, p. 698.
7. "The Pharmacopeia of the United States of America, 1970," Board of Trustees, Bethesda, MD, 1970, p. 142.
8. "British Pharmacopoeia 1973," HM Stationery Office, London, 1973, p. 121.
9. "Pharmacopeé Francaise," Volume 1, Ordre National des Pharmaciens, Paris, 1974, p. 181.
10. "British Pharmacopoeia 1968," Pharmaceutical Press, London, 1968, p. 238.
11. "The Pharmaceutical Codex," Eleventh Edition, Pharmaceutical Press, London, 1979, p. 218.
12. Wood, D. R., *Pharm. J.*, 1957, **178**, 188.
13. Pesez, M., *Ann. Pharm. Fr.*, 1957, **15**, 630.
14. Schmit, J. M., *Bull. Trav. Soc. Pharm. Lyon*, 1968, **12**, 31.
15. Dusinsky, G., Machovicova, F., and Tyllova, M., *Fam. Obz.*, 1967, 397.
16. Karawya, M. S., and Diab, A. M., *J. Assoc. Off. Anal. Chem.*, 1975, **58**, 1171.
17. Arai, T., and Okuyama, T., *Anal. Biochem.*, 1975, **69**, 443.
18. Croteau, R., and Leblanc, R. M., *Photochem. Photobiol.*, 1978, **28**, 33.
19. Arai, T., and Okuyama, T., *Seikagaku*, 1973, **45**, 19.
20. Bonati, A., and Bacchini, M., *Fitoterapia*, 1966, **37**, 24.
21. Berurier, M. H., and Mathis, M. C., *Ann. Pharm. Fr.*, 1973, **31**, 457.
22. Hussein, F. T., and Nasra, M. A., *Plant. Med.*, 1974, **25**, 396.
23. Zweig, G., "Handbook of Chromatography," CRC Press, Cleveland, OH, 1972.
24. Mack, H., and Finn, E. J., *J. Am. Pharm. Assoc.*, 1950, **39**, 532.
25. Pearce, E. M., *J. Chromatogr.*, 1959, **2**, 108.
26. Smolenski, S. J., Grane, F. A., and Voight, R. F., *J. Am. Pharm. Assoc.*, 1958, **47**, 359.
27. Gardner, J. E., and Dean, S. J., *Drug Stand.*, 1960, **28**, 50.
28. Santavy, F., *Pharm. Acta Helv.*, 1948, **23**, 380.

29. Woodson, A. L., and Smith, D. E., *Anal. Chem.*, 1970, **42**, 242.
30. Forni, G., and Massarani, G., *J. Chromatogr.*, 1977, **131**, 444.
31. El-Gindy, A. R., Sabir, M., Nazimuddin, S. K., Zahoor, M., and Shehab, J., "Islamic Medicine Conference," Volume IV, Karachi, Pakistan, 1986.
32. Sarg, T. M., El-Domiaty, M., Salama, O. M., Bishr, M., and El-Gindy, A. R., "Conference of Pharmaceutical Sciences XX," Cairo, Egypt, 1988, p. 62.

Paper 8/00987B
Received March 11th, 1988
Accepted August 23rd, 1988

Assessment of On-line Nitration Reactions as a Means of Determining Nitrate by Reverse Flow Injection With Reductive Amperometric Detection at a Glassy Carbon Electrode

Arnold G. Fogg, S. Paul Scullion and Tony E. Edmonds
Chemistry Department, Loughborough University of Technology, Loughborough, Leicestershire LE11 3TU, UK

Five compounds were investigated for use as on-line reagents in concentrated sulphuric acid for the reductive reverse flow injection amperometric determination of nitrate as a nitro derivative at a glassy carbon electrode. The sulphuric acid was diluted rapidly on injecting the reagent solution into a sample carrier stream and therefore the nitration reaction, which generally only takes place at sulphuric acid concentrations of greater than about 70% , had to be rapid. Thiophene-2-carboxylic acid was found to be the most suitable reagent of those studied. The nitration reaction was sufficiently rapid and the first of two reduction steps was at −0.19 V *versus* SCE (as indicated by linear sweep voltammetry); hence the determination was free from interference by dissolved oxygen. Problems associated with contamination of the electrode surface with reduction product, which caused loss of signal after making repeated injections over an extended period, remained.

Keywords: *Nitrate determination; on-line nitration; reverse flow injection; amperometric detection; thiophene-2-carboxylic acid*

The over-all aim of this work was the development of an amperometric detector for the determination of nitrate in hydroponic fluids based on a flow injection system in which a suitable organic compound is nitrated in sulphuric acid medium and the resulting nitro derivative is determined reductively at a glassy carbon electrode. A sensitive method was not required as the nitrate content of hydroponic fluids is relatively high. However, a particular requirement was that the nitro derivative should be reducible at a low negative potential (more positive than about −0.3 V *versus* SCE) so that dissolved molecular oxygen would not interfere. For satisfactory use in a flow injection system the compound would have to nitrate rapidly and, ideally, the nitration should occur at as low a sulphuric acid concentration as possible: only a single derivative should be formed, or, if two derivatives were formed, ideally they should be reduced at the same potential.

In a search for a suitable reagent, the nitration of 15 compounds was studied by differential-pulse polarography.[1] Polarography was used in these initial screening studies because electrode contamination problems, with the need for frequent repolishing, make the development of methods utilising glassy carbon electrodes very time consuming. Generally, reductions occur at more negative potentials on glassy carbon electrodes than at mercury electrodes, but a good indication of the usefulness of the reagent can still be obtained. Benzoic acid proved to be the best reagent for use with polarography.[1] Formation of 3-nitrobenzoic acid was complete in 30 s by vortex mixing in the determination of 1×10^{-5}–5×10^{-3} M nitrate with good precision (coefficient of variation <2% at the higher levels), and a single reduction wave at −0.13 V *versus* Ag - AgCl was obtained. Salicylic acid and resorcinol, with peaks at −0.14 and −0.15 V, respectively, were shown to be satisfactory reagents in many respects, but the response in each instance was no longer rectilinear above 1×10^{-3} M. Thiophene-2- and thiophene-3-carboxylic acids were nitrated rapidly but gave more than one peak.

In the work described here, first the responses at a glassy carbon electrode of the nitro derivatives of five of the reagents were studied using linear sweep voltammetry. Then the feasibility of carrying out nitration reactions on-line by injection of reagent solutions in concentrated sulphuric acid into a nitrate carrier stream was studied using a glassy carbon electrode to detect the nitro derivatives formed.

Experimental

Linear sweep voltammetry was carried out using a PAR 174A polarographic analyser (Princeton Applied Research). The three-electrode system consisted of a glassy carbon working electrode, a platinum foil counter electrode and a saturated calomel reference electrode (SCE). Solutions were deoxygenated with nitrogen except where indicated otherwise. A scan speed of 10 mV s^{-1} was adopted.

Solutions of the nitro derivatives for linear sweep voltammetry were prepared as follows. The organic compounds were dissolved in concentrated sulphuric acid to give a 1×10^{-2} M reagent solution. The nitrate sample solution (1 ml) was pipetted into 3 ml of the reagent solution contained in a test-tube and the combined solution was vortex mixed for 30–60 s. The solution was then made up to 25 ml in a calibrated flask with suitable cooling.

For the reverse flow injection experiments a 1×10^{-1} M solution of the reagents in concentrated sulphuric acid was used. The glassy carbon electrode was incorporated in a laboratory-built detector cell of wall-jet configuration.[2] A single-line flow injection manifold was used with a Gilson Micropuls peristaltic pump and a Rheodyne 5020 low-pressure injection valve. The sample loop was filled by means of an all-glass or all-plastic syringe: the sulphuric acid medium is very viscous and care must be taken while doing this. Transmission tubing (0.58 mm i.d.) made of PTFE was used. The potential of the glassy carbon electrode was maintained at the required value by means of a Metrohm E611 VA-Detector which also monitored the current flowing.

The glassy carbon electrode was used newly-polished in both linear sweep and flow injection studies. Studies were made to investigate the effect of electrochemical pre-treatment on the signals obtained. Previously, for other determinands, high positive potential pre-treatment had proved advantageous when using oxidation processes[3] and high negative pre-treatment was used to inhibit reduction of oxygen, albeit with slight inhibition of determinand reduction processes.[4] Here, for the nitro derivatives of thiophene-2-carboxylic acid, treatment of the electrode at +1.5 V for 45 s

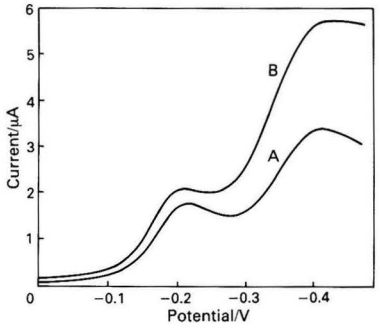

Fig. 1. Linear sweep voltammograms of nitrated thiophene-2-carboxylic acid. Equivalent nitrate concentration in measured solution = 4×10^{-4} M. Sweep rate = 0.01 V s^{-1}. Carrier stream and reagent solution: A, deoxygenated and B, not deoxygenated

followed by 10 s at −1.0 V gave slightly sharper linear sweep voltammograms. Results from the flow system were improved for the first six injections, but then the signal became erratic. A major problem was the increase in background current with positive potential pre-treatment. Negative potential pre-treatment (−1.5 V) reduced the linear sweep peak height for salicylic acid and did not separate the peak from that of oxygen. Further, the electrode tended to become pitted with the negative pre-treatment. For all these reasons the glassy carbon electrode was used subsequently newly-polished.

The blank signal obtained on injecting concentrated sulphuric acid into neutral inert eluent with limited to medium dispersion was found to be high. In order to minimise the size of the blank signal in the procedure that was finally adopted for use, the sample carrier stream was made 1.5 M in sulphuric acid, and single-channel flow injection manifolds, which gave extensive dilution of the concentrated sulphuric acid before presentation to the glassy carbon electrode, were chosen. A system using a small injection volume (25 μl), a long transmission tube (4.2 m) and a relatively slow flow-rate (3.3 ml min^{-1}) was suitable.

The use of normal flow injection, in which a sample solution is injected into a reagent carrier stream, is impracticable here owing to the degradative effect of concentrated sulphuric acid on the pump tubing, the safety problems associated with pumping sulphuric acid and the high background currents obtained in solutions of high sulphuric acid concentration. However, the use of reverse flow injection, in which reagent solution is injected into a sample stream, would normally be more appropriate as nitrate sample solutions, such as hydroponic fluid, are inexpensive and in plentiful supply.

Results

Of the reagents that had proved most suitable for use with polarography, benzoic acid and salicylic acid were studied here. Linear sweep voltammetry of the 3-nitrobenzoic acid solution gave a single peak at −0.45 V *versus* SCE at the glassy carbon electrode. At this potential there would be interference from dissolved oxygen. Further, although 3-nitrobenzoic acid is formed fully within 30 s by vortex mixing when the reagent is applied to static solution methods, no signal was obtained when nitration was attempted on-line by injecting 75 μl of 1×10^{-1} M benzoic acid in concentrated sulphuric acid into a 1×10^{-3} M nitrate carrier stream. Clearly the acidity of the injected reagent solution decreases rapidly by dispersion, and the rate of nitration of benzoic acid is not sufficiently fast for any appreciable amount of the nitro derivative to be formed.

Salicylic acid behaved similarly. The potential of the reduction peak obtained with linear sweep voltammetry was erratic and seemed to depend slightly on the nitrate concentration: −0.5 and −0.44 V at 1×10^{-4} and 5×10^{-3} M nitrate, respectively. In contrast to polarographic calibration graphs obtained for salicylic acid, which were not rectilinear above 1×10^{-3} M nitrate, the calibration graphs obtained here were rectilinear in the range 1×10^{-4}–5×10^{-3} M.

Table 1. Effect of transmission tube length on blank and signal size. Flow-rate = 5 ml min^{-1}; measurement potential = −0.3 V; and injection volume = 50 μl

Length of transmission tube/m	Peak current /μA: Blank	Peak current /μA: 1×10^{-3} M nitrate	Signal to blank ratio
0.5	0.90	1.75	1.9
1.0	0.40	1.40	3.5
3.0	0.10	0.77	7.7
4.2	0.07	0.62	8.9

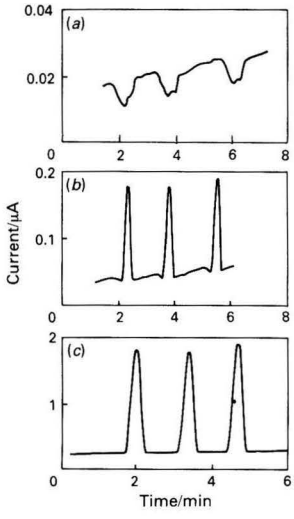

Fig. 2. Typical flow injection signals obtained using the recommended procedure and manifold. Nitrate concentration in carrier stream: (*a*) 0, (*b*) 5×10^{-4} and (*c*) 5×10^{-3} M

As with benzoic acid no difference in signal size was observed when salicylic acid in concentrated sulphuric acid was injected into a carrier stream containing zero and 1×10^{-3} M nitrate.

Isoquinoline gave peaks at −0.07 and −0.18 V at the glassy carbon electrode using linear sweep voltammetry but gave no signal in the flow injection system.

Linear sweep voltammetry of thiophene-2-carboxylic acid at the glassy carbon electrode gave two peaks of approximately equal height at −0.19 and −0.39 V (Fig. 1). The peaks were shifted to more negative potentials on successive scans (not shown) indicating that contamination of the electrode surface was occurring. Washing the electrode with ethanol and wiping the surface dry caused the peaks to shift back to the original potentials. Nitration of thiophene-2-carboxylic acid has been shown to give 55% of the 4-nitro isomer and 41% of the 5-nitro isomer.[5] Tirouflet and Fournari[6] studied the reduction of nitrated thiophene-2-carboxylic acid and showed that the more positive reduction peak is due to 5-nitrothiophene-2-carboxylic acid.

The linear sweep voltammograms shown in Fig. 1 were obtained for both deoxygenated and non-deoxygenated solutions. Clearly, dissolved oxygen increases the height of the first peak only slightly, but has a marked effect on the height of the second peak. The possibility of using high salt concentrations to reduce the solubility of oxygen was investigated.

Saturated solutions of anhydrous sodium sulphate and potassium chloride in 0.1 M sulphuric acid eluent reduced the oxygen signals to 20 and 30% of their original values, respectively. At such high concentrations crystallisation within the flow injection system was a problem, however, and this possibility was abandoned.

Using the flow injection system with a flow-rate of 5 ml min^{-1}, a transmission tube length of 3 m and a 75-μl injection volume the following peak heights were obtained for 1×10^{-3} M nitrate in the carrier stream (values in parentheses are the corresponding blanks): 0.94 (0.05), 1.86 (0.15), 2.49 (0.25), 2.70 (0.30), 3.08 (0.35), 4.28 (0.45), 5.20 (0.55), 6.34 (0.97) and 6.40 (1.97) μA at −0.20, −0.25, −0.30, −0.35, −0.40, −0.50, −0.60, −0.70 and −0.80 V, respectively. The two reduction processes are more drawn out than in the linear sweep voltammograms. The following background currents were obtained with the flow injection system with a blank eluent: <0.01, <0.01, 0.01, 0.03, 0.05, 0.15, 0.70, 1.50, 2.50 and 3.00 μA (deoxygenated carrier stream) and <0.01, 0.01, 0.02, 0.05, 0.15, 0.40, 1.40, 2.50, 3.20 and 4.50 μA (non-deoxygenated) at 0, −0.1, −0.2, −0.3, −0.4, −0.5, −0.6, −0.7, −0.8 and −0.9 V, respectively. The influence of dissolved oxygen above −0.3 V is clearly seen, in that a slightly lower signal was obtained when eluent and reagent were deoxygenated with nitrogen. Oxygen would not have been completely removed as it would have diffused back through the flow injection tubing. In all further experiments a measurement potential of −0.3 V was adopted.

The injection of reagent in concentrated sulphuric acid, even into a 1.5 M sulphuric acid carrier stream, using a short transmission tube length before the amperometric detector resulted in a high blank signal. A comparison of the signal obtained for 1×10^{-3} M nitrate with the blank signal at different lengths of transmission tube is given in Table 1. Clearly an appreciable dilution of the sulphuric acid is required in order to obtain a low blank signal. Despite the decrease in signal size with increasing transmission tube length the signal to blank ratio is increased up to at least a length of 4.2 m.

The effect of flow-rate was not marked; the highest nitrate signal to blank signal ratio (10.8) was obtained for the slowest flow-rate used here (3.4 ml min^{-1}) and this was used in subsequent work.

The effect of injection volume was also studied, the smallest volume of reagent in sulphuric acid injected being 25 μl. This volume gave a very small negative blank, albeit with a loss of signal size, and was subsequently adopted particularly as absorption problems at the electrode were minimised.

Throughout this work a 0.1 M solution of the reagent in concentrated sulphuric acid was used, this being the highest concentration of reagent that did not lead to precipitation problems within the injection valve. Reducing the concentration of sulphuric acid excessively resulted in a complete loss of signal. This might be expected as the nitronium ion is only formed at sulphuric acid concentrations greater than 80%.[7] Fortunately, the rate of nitration of thiophene-2-carboxylic acid is very rapid and extensive nitration occurs in the very short time interval after injection when dilution of the sulphuric acid is very limited.

With a 4.2-m transmission tube (0.58 mm i.d.), a flow-rate of 3.3 ml min^{-1} and a 25-μl injection volume, the signal was shown to be rectilinear in the range 5×10^{-4}–5×10^{-3} M. Coefficients of variation were between 4.8 and 2.6% (six injections) over this range (the loss of signal due to electrode contamination was not noticeable over six injections). The electrode was cleaned [as for linear sweep voltammetry (LSV)] when the concentration of nitrate in the eluent was changed. The detection limit was calculated to be about 1×10^{-4} M but was difficult to assess directly owing to the negative blank signal. Typical signals are shown in Fig. 2.

Thiophene-3-carboxylic acid gave three peaks by LSV, at −0.175, −0.34 and −0.53 V, but the peak at −0.34 V was the largest. As dissolved oxygen interfered no further work was performed with this system.

Discussion

An attempt has been made to find a satisfactory flow injection amperometric method for the determination of nitrate based on the on-line nitration of an organic reagent. In the most successful method developed to date a 0.1 M solution of thiophene-2-carboxylic acid in concentrated sulphuric acid (25 μl) was injected into the nitrate sample carrier stream (previously made 1.5 M in sulphuric acid) flowing at 3.4 ml min^{-1} in a single-channel manifold fitted with a transmission tube 4.2 m × 0.58 mm i.d. The nitro derivative formed was detected, and nitrate therefore determined by reduction at a glassy carbon wall-jet electrode without interference from dissolved molecular oxygen.

Loss of signal over six successive injections at the 5×10^{-3} M nitrate level was not noticeable, but contamination of the electrode did occur and became observable after about 10–15 injections (loss of signal about 10–15%). The injection of concentrated sulphuric acid solutions of the reagent posed some problems. The solution was very viscous and some pressure had to be applied in filling the sample loop by means of an all-glass or all-plastic syringe. Clearly this had to be done with great care.

The procedure is described here as a basis for further work. Improvements in valve design, in injection techniques and in electrode technology may result eventually in the method becoming viable and advantageous in selected application areas.

The authors thank the Agricultural and Food Research Council for financial support.

References

1. Fogg, A. G., Scullion, S. P., and Edmonds, T. E., *Analyst*, 1988, **113**, 979.
2. Fogg, A. G., and Summan, A. M., *Analyst*, 1984, **109**, 1029.
3. Chamsi, A. Y., and Fogg, A. G., *Analyst*, 1988, **113**, 1723.
4. Ghawji, A. B., and Fogg, A. G., *Analyst*, 1986, **111**, 157.
5. Marino, G., *Adv. Heterocycl. Chem.*, 1971, **13**, 235.
6. Tirouflet, J., and Fournari, P., *Bull. Chim. Soc. Fr.*, 1963, 1651.
7. Hoggett, J. G., Moodie, R. B., Penton, J. R., and Schofield, K., "Nitration and Aromatic Reactivity," Cambridge University Press, Cambridge, 1971, p.21.

Paper 8/04009E
Received October 10th, 1988
Accepted December 5th, 1988

Iodimetric Determination of Iodate, Bromate, Hypochlorite, Ascorbic Acid and Thiourea Using Flow Injection Amperometry

Mohamed A. Abdalla and Hassan M. Al-Swaidan
Department of Chemistry, College of Science, King Saad University, P.O. Box 2455, Riyadh 11451, Saudi Arabia

Iodate, bromate and hypochlorite were determined as iodine by flow injection amperometry at a platinum or glassy carbon electrode by injecting them into an eluent 0.20 M in hydrochloric acid and 0.024 M in potassium iodide or an eluent 2 M in sulphuric acid and 0.12 M in potassium iodide. The rectilinearity range is from 10^{-3} to 10^{-7} M. Organic compounds that can be oxidised or iodinated by iodine were determined on-line by injecting them in acidic solution into an iodate - iodide eluent and observing the decrease in the iodine signal. The determination was also performed by injecting a pre-reacted solution of iodine and the organic compound and monitoring the excess of iodine.

Keywords: *Flow injection; amperometry; iodimetry; ascorbic acid and thiourea determination*

Iodine exists in a number of oxidation states, the most commonly used in analytical chemistry being iodide and triiodide. The triiodide ion is a sufficiently good oxidising agent and reacts quantitatively with a number of reductants. On the other hand, strong oxidising agents react quantitatively with the easily oxidised iodide ion.

Iodination reactions have been used extensively to determine numerous organic compounds that are either iodinated or oxidised by iodine. Both direct and indirect titrimetric methods have been used. In the direct method, standard triiodide ion or iodine dissolved in potassium iodide solution is utilised for direct titration of the substance to be determined. In the indirect method, the triiodide ion is formed by reaction of the excess of iodide ion with an oxidising agent and the liberated triiodide ion is titrated with a standard sodium thiosulphate solution using starch as indicator, or the end-point of the titration can be determined mono- or bi-amperometrically.[1,2]

Iodine is reduced at potentials less positive than *ca.* +0.50 V *versus* SCE.[2] Recently, several methods for the determination of iodate, iodide, hypochlorite, ascorbic acid and sulphite by flow injection using voltammetric and spectrometric detection have been reported.[3–6] This paper describes the use of an acidic solution of potassium iodide for the determination of iodate, bromate and hypochlorite in solution using flow injection amperometry. The flow injection system was used to study the production of iodine on-line and its subsequent reaction with ascorbic acid and thiourea. The proposed method is more sensitive and easier to apply than the flow injection method based on the formation of a starch - iodine complex, and is simpler than the flow injection method based on electrochemical detection because deoxygenation of the reaction solutions is unnecessary.

Experimental

A flow of eluent was produced with a Minipuls 2 peristaltic pump and injections (25 μl) were made with a Rheodyne 5020 injection valve. The injection valve was connected to a laboratory-built cell fitted with a Metrohm EA 286 glassy carbon electrode by means of a suitable length of 0.58-mm bore Teflon tubing. The use of the laboratory-built detector has been described previously.[7–10] Details of the construction of the wall-jet detector cell have been reported elsewhere.[11] The detector cell was used as described previously, partially immersed in 0.01 M sulphuric acid with the Metrohm counter and reference electrodes. It was found not to be necessary to de-gas the eluent. The potential of the working electrode was held at a +0.10 V *versus* SCE, unless indicated otherwise, using a Metrohm E 506 polarographic analyser with a built-in recorder. The coefficient of variation (ten measurements) was generally less than 1%.

Preliminary Studies

For the presentation of the pre-formed iodine sample, minimum dispersion is required and a 1-m delay coil was found to be convenient and to give good reproducibility. When iodine was formed in a solution that was 1×10^{-5} M in iodate, 0.0048–0.024 M in iodide and 0.2 M in hydrochloric acid, the iodine signal remained constant; however, when sulphuric acid was used, the addition of an excess of iodide was found to be necessary. For this reason, in subsequent experiments involving the pre-formation of iodine and its pre-reaction with organic compounds, sample solutions for injection were made 0.2 M in hydrochloric acid and 0.2 M hydrochloric acid was used as the eluent.

Standard solutions 10^{-6}–10^{-4} M in potassium iodate were prepared in 0.024 M potassium iodide and 0.2 M hydrochloric acid, thus liberating iodine. Two minutes after preparation, 25-μl aliquots of each solution were injected into the eluent (0.2 M hydrochloric acid) and carried to the glassy carbon electrode. The iodine signal was found to be rectilinear up to the 10^{-4} M level in a solution initially 1×10^{-4} M in iodate and 0.024 M in iodide. The recommended method is as follows.

Reagents

Standard solutions of potassium iodate (1×10^{-2} M), potassium bromate (1×10^{-2} M), potassium iodide (6×10^{-2} M), ascorbic acid (1×10^{-2} M) and thiourea (1×10^{-2} M) were prepared from analytical-reagent grade chemicals unless indicated otherwise.

Hydrochloric acid (0.2 M). A stock solution of 0.2 M was prepared in the usual way.

Sodium hypochlorite solution (*ca.* 2×10^{-2} M). Obtained from a commercial sodium hypochlorite reagent. This solution was standardised iodimetrically using potassium dichromate and sodium thiosulphate.

Hydrochloric acid - potassium iodide eluent, 0.024 M *in potassium iodide and* 0.2 M *in hydrochloric acid*. Dissolve 2 g of potassium iodide in 50 ml of water, add 8.9 ml of concentrated hydrochloric acid, cool the solution, dilute to 500 ml in a calibrated flask and mix.

Sulphuric acid - potassium iodide eluent, 0.12 M *in potassium iodide and* 2 M *in sulphuric acid*. Dissolve 10 g of potassium

iodide in 100 ml of water, add 115.8 ml of concentrated sulphuric acid, cool the solution, dilute to 500 ml in a calibrated flask and mix.

Procedures

Determination of iodate, bromate and hypochlorite

Inject 25 µl of the iodate, bromate or hypochlorite sample or standard solution, containing 10^{-3}–10^{-7} M iodate or bromate or 1×10^{-4}–100×10^{-4} M hypochlorite, into the eluent and record the decrease in the current signal. Use a 2-m delay coil. Hold the working electrode at +0.1 V *versus* SCE.

On-line iodimetric determination of ascorbic acid and thiourea

Injection of pre-reacted solution. Pipette 0.5 ml of 1×10^{-2} M potassium iodate solution, 2 ml of 6×10^{-2} M potassium iodide solution and 1–4 ml of a 1×10^{-3} M solution of the organic compound into a 50-ml calibrated flask and dilute to volume with hydrochloric acid so that the final solution is 0.2 M in hydrochloric acid. Mix and allow the solution to stand for 2 min. Inject 25 µl of this solution into an eluent consisting of 0.2 M hydrochloric acid. Use a 1-m delay coil.

Direct injection into potassium iodate - potassium iodide eluent. Inject 25 µl of a standard solution of the organic compound (1×10^{-6}–1×10^{-4} M) prepared in 0.2 M hydrochloric acid into an eluent consisting of 1×10^{-4} M potassium iodate and 0.024 M potassium iodide and record the decrease in the current signal. Use a 6-m delay coil.

Results

The effects of the hydrochloric acid concentration of the eluent containing 0.024 M potassium iodide and of the potassium iodide concentration of the eluent 0.2 M in hydrochloric acid on the signal obtained for the injection of iodate or hypochlorite are shown in Tables 1 and 2, respectively.

The effects of the sulphuric acid concentration of the eluent containing 6×10^{-2} M potassium iodide and of the potassium iodide concentration of the eluent 2 M in sulphuric acid on the signal obtained for potassium iodate are shown in Tables 3 and 4, respectively. An eluent 2 M in sulphuric acid and 0.036 M in potassium iodide is required to remove the double peak, otherwise there is no change in the peak height at acid concentrations of between 1 and 2 M.

Table 1. Effect of hydrochloric acid concentration of the eluent on the signal obtained for the reduction of iodine formed from potassium iodide solution. Potassium iodide concentration, 0.024 M; iodate concentration, 3×10^{-5} M

Hydrochloric acid concentration/M	Peak current/µA
0.2	3.7
0.4	3.8
0.6	3.9
0.8	3.9

Table 2. Effect of potassium iodide concentration on the signal obtained for the reduction of iodine formed from various potassium iodide solutions. Hydrochloric acid concentration, 0.2 M; iodate concentration, 3×10^{-5} M

Potassium iodide concentration/M	Peak current/µA
0.0048	3.6
0.0096	3.7
0.0144	3.9
0.0192	3.9
0.024	3.9

Typical calibration graphs for the determination of iodate and bromate obtained using the recommended hydrochloric acid - potassium iodide procedure are straight lines that pass through the origin. The linearity range is 0–1.5×10^{-4} M for both iodate and bromate. The signals used to construct the calibration graph for hypochlorite using the hydrochloric acid - potassium iodide system are shown in Fig. 1. Similar results were obtained when sulphuric acid was used.

Iodine was formed on-line by injecting 25 µl of 0.2 M hydrochloric acid into a neutral or slightly alkaline potassium iodate - iodide eluent. The height of the iodine signal observed

Table 3. Effect of sulphuric acid concentration of the eluent on the signal obtained for the reduction of iodine formed from potassium iodide solution. Iodide concentration, 0.06 M; iodate concentration, 1.0×10^{-5} M

Sulphuric acid concentration/M	Peak current/µA
0.2	6*
0.4	12*
0.6	15.6*
0.8	17.6
1.0	18
2.0	18

* Double peak.

Table 4. Effect of potassium iodide concentration on the signal obtained for the reduction of iodine formed from various potassium iodide solutions. Sulphuric acid concentration, 2 M; iodate concentration, 1×10^{-5} M

Potassium iodide concentration/M	Peak current/µA
0	0
0.012	9.2*
0.024	11.6*
0.036	16.4
0.048	17.2
0.06	18
0.12	18

* Double peak.

Table 5. Rectilinearity of response on injection of iodine. Injected solution: various concentrations of iodate solution, 0.024 M in potassium iodide and 0.2 M in hydrochloric acid. Eluent, 0.2 M hydrochloric acid

Equivalent potassium iodate concentration in injected solution/M	Current signal/µA
1×10^{-6}	0.144
1×10^{-5}	1.45
1×10^{-4}	14.6
1×10^{-3}	148

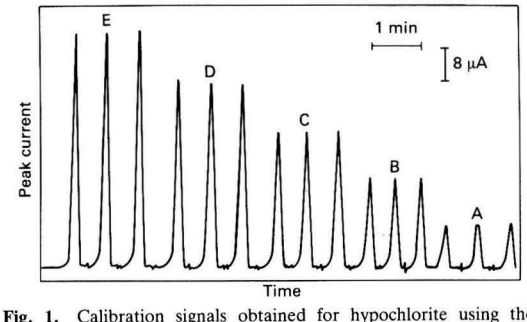

Fig. 1. Calibration signals obtained for hypochlorite using the hydrochloric acid - potassium iodide system. Equivalent hypochlorite concentration in injected solution: A, 2×10^{-4} M; B, 4×10^{-4} M; C, 6×10^{-4} M; D, 8×10^{-4} M; and E, 10×10^{-4} M

at the working electrode increased with increasing potassium iodate concentration.

Table 5 shows the signal obtained for the injection of pre-formed iodine at various equivalent concentrations of iodate. Typical data for calibration graphs for the determination of ascorbic acid and thiourea are given in Table 6. The calibration graphs are rectilinear and the stoicheiometry of the reaction between iodine and the organic compound is 1 : 1 for both ascorbic acid and thiourea. The signals used to obtain the data from ascorbic acid are shown in Fig. 2.

The effect of the hydrochloric acid concentration on the direct injection of both hydrochloric acid and a hydrochloric acid solution of the organic analyte into the potassium iodate - potassium iodide eluent, using a 6-m delay coil, is shown in Table 7. Typical calibration graphs obtained for ascorbic acid and thiourea using the recommended procedure are given in Fig. 3. For both methods, varying the length of the delay coil between 1 and 4 m has relatively little effect on the peak height although the peaks became broader.

Discussion

The solution conditions employed in the iodimetric titration for the determination of bromate, iodate and hypochlorite were shown to be directly applicable to flow injection amperometry.

Two simple methods for the determination of iodate, bromate and hypochlorite can be used by injecting a sample solution within the concentration range 0.01–2 × 10^{-3} M into an eluent 0.2 M in hydrochloric acid and 0.024 M in potassium iodide and observing the reduction of the iodine formed at a glassy carbon electrode, held at 0.10 V *versus* SCE. Alternatively, an eluent 2 M in sulphuric acid and containing an excess of potassium iodide (6 × 10^{-2} M) can be used. The signals obtained are due to the reduction of iodine produced by reaction of iodate, bromate and hypochlorite with an acidic iodide solution. The concentration of potassium iodide in the eluent required to give a 100% signal at the 10^{-5} M level of iodate, bromate and hypochlorite was found to be 0.0144 M; however, a concentration of 0.024 M in the eleuent was used in

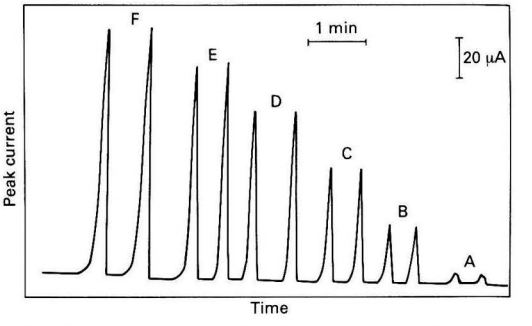

Fig. 2. Pre-reaction method: calibration signals obtained for ascorbic acid. Equivalent concentration: A, 1 × 10^{-4}; B, 0.8 × 10^{-4}; C, 0.6 × 10^{-4}; D, 0.4 × 10^{-4}; E, 0.2 × 10^{-4}; and F, 0 M

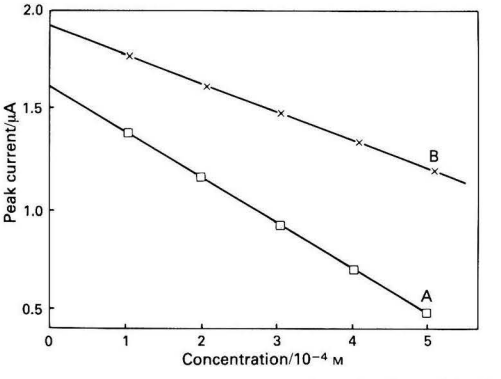

Fig. 3. Calibration graphs obtained using the direct injection method. A, Thiourea; and B, ascorbic acid

Table 6. Typical current data for calibration graphs for the determination of ascorbic acid and thiourea after reaction with iodine using the recommended procedure. Initial iodate concentration, 1 × 10^{-4} M

Equivalent determinand concentration in injected solution/10^{-4} M	Current/μA	
	Ascorbic acid	Thiourea
1	<0.1	<0.1
0.8	0.6	0.9
0.6	4.1	4.3
0.4	7.5	7.7
0.2	11.1	11.2
0	14.7	14.6

Table 7. On-line formation of iodine and iodination. Effect of hydrochloric acid concentration in injected solution on the signal. Delay coil, 6 m

Hydrochloric acid concentration/M	Signal without added ascorbic acid/μA	Signal with 1 × 10^{-5} M ascorbic acid in injected solution/μA	Difference in signal/μA
0.1	0.70	0.40	0.3
0.2	1.30	0.90	0.4
0.3	1.79	1.33	0.46
0.4	2.30	1.81	0.49

Table 8. Comparison of results obtained for the determination of iodate, bromate, hypochlorite, ascorbic acid and thiourea using the proposed flow injection amperometric and titrimetric methods

Compound	Concentration/ 10^{-5} M	Recovery, %*		*t* (calculated)†
		Proposed method	Titrimetric method	
Iodate	1	101.3 + 0.1	102.1 + 0.6	0.71
	0.1	100.8 + 0.4	—	—
Bromate	1	100.4 + 0.3	99.9 + 0.9	0.81
	0.1	101.2 + 0.5	—	—
Hypochlorite	1	100.3 + 0.2	99.8 + 0.7	0.91
	0.1	102.3 + 0.4	—	—
Ascorbic acid	1	100.2 + 0.4	99.4 + 0.8	0.91
	0.1	101.3 + 0.3	—	—
Thiourea	1	101.2 + 0.3	99.6 + 0.9	1.1
	0.1	102.1 + 0.4	—	—

* Mean + standard deviation for ten determinations.
† Theoretical value = 2.26 at the 95% confidence limit.

this work to ensure an excess of iodide at all levels of iodate, bromate and hypochlorite studied. From the values of the current obtained at different acid concentrations, it is apparent that a reasonably high acidity is required for complete formation of iodine.

The flow injection amperometric method for the determination of bromate, iodate and hypochlorite is rapid and can be considered to be more convenient and sufficiently precise for use in certain applications. The procedure becomes more competitive than, and compares favourably with, the titrimetric method using starch as indicator,[1,2] particularly when sample solutions of lower concentration are to be analysed. A statistical comparison of the proposed method with the titrimetric method is shown in Table 8. The *t*-test values obtained indicate that there is no significant difference between the two methods; however, the proposed method is superior when sample solutions of lower concentration are to be analysed.

Conclusions

Preliminary experiments have indicated that the proposed procedure can be used for the determination of organic compounds that are either iodinated or oxidised by iodine, and a simple flow injection procedure has been described for the iodimetric determination of ascorbic acid and thiourea. Ascorbic acid and thiourea can be determined down to the 10^{-6} M level very conveniently by flow injection amperometry at a glassy carbon electrode. In this procedure an excess of iodine is determined by injecting the organic compound prepared in 0.2 M hydrochloric acid into an eluent consisting of potassium iodate - potassium iodide and monitoring the iodine at a glassy carbon electrode held at +0.1 V *versus* SCE.

In the second procedure, organic compounds are determined iodimetrically on-line. Iodine is produced and the determinands are iodinated or oxidised by iodine. The sample solution must be acidic so that the iodine is liberated in the iodate - iodide eluent on injection. This procedure is very rapid and the calibration graphs are rectilinear. The procedure could readily be adapted for the routine intermittent analysis of an acidic solution of a determinand in a control situation by injecting sample aliquots at the required time intervals.

References

1. Ashmore, M. R. F., "Titrimetric Organic Analysis," Interscience, New York, 1964.
2. Serjeant, E. P., "Potentiometry and Potentiometric Titrations," Wiley, New York, 1984.
3. Kamson, O. F., *Anal. Chim. Acta*, 1986, **179**, 475.
4. Hernandez-Mendez, J., Alonso Mateos, A., Almendral Parra, M. J., and Garcia de Maria, C., *Anal. Chim. Acta*, 1986, **184**, 243.
5. Fogg, A. G., Guta, C. W., and Chamsi, A. Y., *Analyst*, 1987, **112**, 253.
6. Chamsi, A. Y., and Fogg, A. G., *Analyst*, 1986, **111**, 879.
7. Fogg, A. G., Ali, Md. A., and Abdalla, M. A., *Analyst*, 1983, **108**, 840.
8. Fogg, A. G., Chamsi, A. Y., and Abdalla, M. A., *Analyst*, 1983, **108**, 464.
9. Fogg, A. G., Bsebsu, N. K., and Abdalla, M. A., *Analyst*, 1982, **107**, 1040.
10. Fogg, A. G., Bsebsu, N. K., and Abdalla, M. A., *Analyst*, 1982, **107**, 1462.
11. Fogg, A. G., and Summan, A. M., *Analyst*, 1984, **109**, 1029.

Paper 8/00303C
Received January 28th, 1988
Accepted January 3rd, 1989

Effects of Temperature, Filtration and Container Material on Storage of an Acid Stream Water

William Davison, Colin Woof and Edward Tipping
Freshwater Biological Association, The Ferry House, Ambleside, Cumbria LA22 0LP, UK

Precise measurements of the pH of an acid stream water (pH 4.8, 4 °C) have been made on filtered and unfiltered samples stored at three different temperatures over 15 d. Sub-samples stored in glass bottles had a significantly lower pH, by 0.02, than those stored in polythene bottles, presumably due to outgassing of CO_2. Filtration did not affect the pH, but storage in glass bottles for 15 d introduced a variation of ±0.1 pH. Whereas the pH of samples stored at 10 and 20 °C did not change over a 2-week period, storage at 4 °C caused the pH to increase by 0.1. The temperature dependence of the pH could be predicted by assuming that it was controlled by the hydrolysis of aluminium, for which enthalpy data are available.

Keywords: *pH; storage; acid stream; freshwater; aluminium*

Research into the phenomenon of acid rain has highlighted the lack of information concerning the storage of samples of natural water prior to determining their pH. Most workers engaged in intensive field studies have used polythene bottles because they are inexpensive, light, unbreakable and easily cleaned. However, consideration of the pH changes in more neutral water (pH > 5), associated with re-equilibration with atmospheric CO_2, has led to recommendations that well sealed, gas-tight bottles of borosilicate glass should be used.[1] In this work we have compared the pH of samples of a natural acid stream water stored in polythene and borosilicate glass bottles. As there is an option of storage at stream temperature or ambient air temperature, the experiment was performed at three different temperatures. Further, pH measurements are often performed on samples collected for a variety of analytical determinations, some of which require filtration. There is some debate as to whether it is appropriate to filter "in the field" or prior to analysis and whether such filtration will affect the pH of the sample. Therefore, measurements were made on both filtered and unfiltered samples.

Experimental

Materials and Equipment

A Radiometer PHM 64 pH meter was used in conjunction with a Corning 003 11 101J glass electrode and a Beckman 39416 calomel reference electrode equipped with a quartz fibre junction (electrode D in reference 3). These electrodes have been found to perform very well.[2,3] The pH was measured after stirring the solution for 4 min and then allowing the solution to remain quiescent for 4 min. Electrodes were calibrated with two buffers: 0.05 mol kg^{-1} potassium hydrogen phthalate, and 0.025 mol kg^{-1} disodium hydrogen phosphate - 0.025 mol kg^{-1} potassium dihydrogen phosphate. The pH of these buffers at 4, 10 and 20 °C was taken to be 3.998 and 6.957, 3.997 and 6.912, and 4.000 and 6.873, respectively.[4] All containers were acid-washed with 1 mol kg^{-1} of nitric acid and then rinsed thoroughly with distilled water prior to use. The meter and electrodes were allowed to equilibrate for at least 2 h in the constant temperature rooms prior to measurement. A sub-sample of the same buffer solution was stored in the appropriate constant temperature room overnight, prior to measurement.

Procedure

The pH of sub-samples of water that had been treated in various ways (Fig. 1) was measured. A 10-l water sample was collected in a polythene bottle, fitted with a screw top, from Gaitscale Gill (NY 258021) in the English Lake District on 5th March 1986 (day 0), when the water temperature was 2.1 °C. After 2 h it was stored in a laboratory cold room at a constant temperature of 4 ± 1 °C. A portion of the sample was filtered (designated F0) by suction through a 0.45-μm membrane filter (Millipore) and transferred into three 1-l polythene bottles. Unfiltered water was used to fill three further 1-l polythene bottles. The pH of portions of the filtered and unfiltered samples was measured in a cold room (4 °C). One polythene bottle containing filtered water, and one containing unfiltered water, were transferred into a room thermostated at 10 ± 1 °C. Two other similar bottles were transferred into a room thermostated at 20 ± 1 °C. The next day (day 1) the pH of each of these solutions was measured. A sample of each solution from the 1-l bottles was then transferred into a 100-ml borosilicate glass bottle and another into a 100-ml polythene bottle, both of which were filled to overflowing before replacing the cap. There was a small air space in each of the polythene bottles, but all the air was excluded from the borosilicate glass bottles. The sub-samples were stored in the same cold room as their mother 1-l bottle. The two bottles containing unfiltered water, stored at 10 and 20 °C, were treated differently from the others. Half of the solution from each of these bottles was filtered in the appropriate constant temperature room (F1) and the resulting filtered and unfiltered water samples were stored in both borosilicate and polythene bottles, as for the other sub-samples. Fourteen days later (day 14) the pH of all the sub-samples was determined.

When the original 10-l sample was collected from the stream, eight samples were also collected in borosilicate glass bottles that were filled to overflowing and stoppered, so as to avoid entrainment of air. These eight bottles were stored in the cold room (4 °C). The pH of four of the samples was measured on day 1 and that of the remaining four on day 14.

Three water samples were collected from the same stream on three other sampling days in early 1986: 25th February, 11th March and 8th April. They were analysed for all major components according to previously described methods,[5] the pH being measured on quiescent solutions with a Radiometer GK2401C combination electrode (Table 1).

Results and Discussion

The electrodes responded quickly, giving readings stable to at least ±0.02 pH min^{-1} within 4 min under both quiescent and stirred conditions at all temperatures. The pH values for the stirred solutions were generally lower than for the quiescent

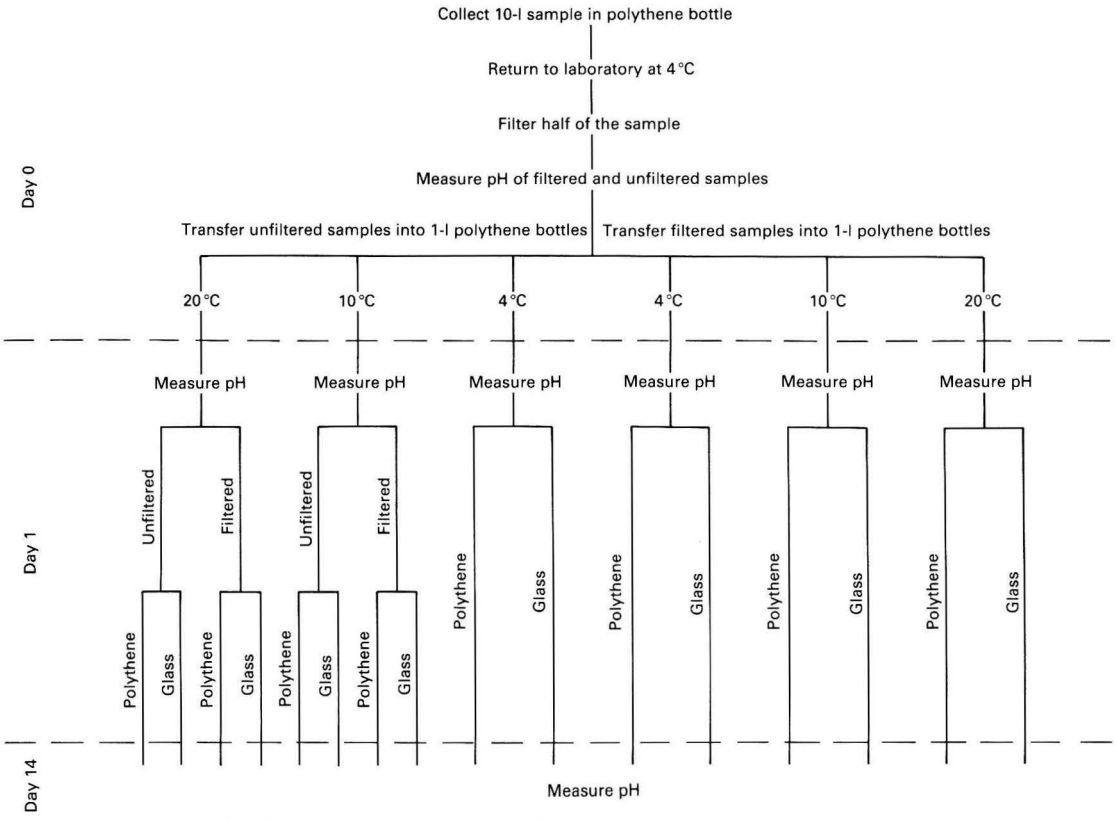

Fig. 1. Schematic outline of the measuring and sub-sampling procedures for a 10-l sample of water from Gaitscale Gill

solutions, by *ca.* 0.05 pH. The latter were used in evaluating the data (Table 2), because they had an effectively longer equilibration time, and are considered to be less prone to errors associated with liquid junctions.[2,6]

From Table 2 it is clear that there was no significant difference between the paired results for the filtered and unfiltered samples. Paired *t*-tests confirmed this observation. The filtered sample stored at 20 °C had a pH of 4.31, which was markedly different from the pH of its unfiltered counterpart (4.70). The consistency of all the other results indicates that this must be due to contamination, from either an inadequately rinsed filter or polythene bottle, and so these very low values were omitted from the data analysis.

A paired *t*-test between the results for polythene and glass bottles revealed that after 13 d the samples stored in glass bottles had a significantly ($p < 0.02$) lower pH. If the completely sealed glass bottle prevents outgassing of CO_2 more efficiently than polythene, then the pH would be expected to be lower. However, the mean difference of 0.021 (standard deviation, 0.017 at six degrees of freedom) is small and is within the errors of most routine pH measurements on freshwater samples. A similar good agreement for storage in glass and polythene containers has been observed for rainwater[7] and neutral tap water[8] samples.

Although there is some variation in the data, there is no evidence for any change in pH from day 1 to day 14 for samples stored at 10 or 20 °C. For samples stored at 4 °C the pH increased from 4.78 at day 0 and day 1 to 4.90 at day 14 in polythene containers. The two samples, filtered and unfiltered, which had been stored in glass bottles also had a higher pH after storage. It is difficult to see why the pH of samples stored at 4 °C should increase, while those at 10 and 20 °C remained the same. Support for this finding should have been available from the individual samples collected in glass bottles, but by day 14 these gave a highly variable pH, mean 4.85 ± 0.12. This variability must have been associated with storage because the four similarly collected samples measured on day 1 gave a consistent pH that agreed with the values for the bulk sample. All these changes in pH are much less than those found for more neutral samples stored at room temperature in polypropylene syringes,[9] where CO_2 exchanging through the walls of the syringe has a marked effect on pH.

The other variable, temperature, affected the pH systematically. On day 1 it was 4.78 at 4 °C, 4.75 at 10 °C and 4.70 at 20 °C. The pH of most solutions change with temperature, mostly as a result of changes in the equilibrium constants of the various species in solution, but partly as a result of changes in activity coefficients.[10] For near-neutral soft waters, which are buffered by the carbonate system, but not influenced by precipitation of calcium carbonate, the pH decreases by 0.08 when the temperature increases from 10 to 20 °C,[11,12] provided that the system is closed to the atmosphere, preventing exchange of CO_2. Similar, simple temperature corrections are not generally available for acid waters, so we have examined the possible controlling reactions.

In acid waters, such as those from Gaitscale Gill, aluminium is the only hydrolysable cation (Table 1), and so its speciation, together with that of humic material, must control the pH.

The carboxyl groups of humic material could influence the pH of such solutions, either by complexation with aluminium or by their direct protonation. However, Perdue[13] has shown that the enthalpy of ionisation of carboxyl groups is generally

Table 1. Analyses of water samples collected from Gaitscale Gill

	Date		
	25.2.86	11.3.86	8.4.86
pH	4.93	4.87	4.93
Conductivity/μS cm^{-1}	41.5	51.0	50
Calcium/μmol l^{-1}	25	25	25
Magnesium/μmol l^{-1}	27	30	27
Sodium/μmol l^{-1}	157	173	173
Potassium/μmol l^{-1}	6	11	9
Chloride/μmol l^{-1}	191	211	196
Sulphate/μmol l^{-1}	25	30	33
Nitrate/μmol l^{-1}	38	85	73
Fluoride/μmol l^{-1}	1.6	1.7	1.6
Total monomeric aluminium/μmol l^{-1}	10.1	19.4	18.2
Organic complexed aluminium/μmol l^{-1}	0.5	0.6	—
Dissolved organic carbon/mg l^{-1}	1.42	1.04	0.92

Table 2. The pH of acid stream samples measured on quiescent solutions, the same day as the sample collection (day 0), and 1 and 14 d later (days 1 and 14). Measurements designated as (B) were made on sub-samples of one 10-l bulk stream sample. Measurements designated as (I) were made on stream samples which were collected independently into different bottles. UF indicates unfiltered, F0 indicates filtered on day 0 and F1 indicates filtered on day 1

		Day 0	Day 1		Day 14	
Temperature/ °C	Sample	Poly-thene	Poly-thene	Glass	Poly-thene	Glass
4	UF (I)	—	—	4.80	—	4.69
	UF (I)	—	—	4.80	—	4.81
	UF (I)	—	—	4.81	—	4.99
	UF (I)	—	—	4.80	—	4.90
	UF (B)	4.80	4.79	—	4.88	4.88
	F0 (B)	4.77	4.77	—	4.93	4.89
10	UF (B)	—	4.75	—	4.76	4.74
	F0 (B)	—	4.75	—	4.76	4.74
	F1 (B)	—	—	—	4.80	4.76
20	UF (B)	—	4.70	—	4.71	4.68
	F0 (B)	—	4.31	—	4.32	4.25
	F1 (B)	—	—	—	4.70	4.70

close to zero and so their interactions should not influence the temperature dependence of pH. Moreover, even if the enthalpy of humic interactions were not zero the concentration of dissolved organic matter in this and similar surrounding streams is so low, usually <2 mg l^{-1}, that its effect on pH will be negligible.[14] That leaves only the speciation of aluminium. Aluminium in water from Gaitscale Gill is undersaturated with respect to the formation of solid phases, such as gibbsite, and so only solution equilibria need be considered.

To calculate the effect of aluminium hydrolysis on the temperature dependence of pH three simple solutions were considered consisting of 5 mmol l^{-1} of Na^+ and 0, 10 and 20 μmol l^{-1} of total soluble aluminium. The concentration of chloride required to give each solution a pH of 4.78 at 4 °C was calculated and then, with [Cl^-] constant for each solution, the pH was calculated accurately at 10 and 20 °C. The equilibria considered, together with the required thermodynamic data, are given in Table 3. In performing the calculations, pCO_2 = 0.0003 atm was assumed. Computations were carried out iteratively, the correct pH being that which simultaneously satisfied the mass-balance requirements of the solution.

The calculated change in pH with temperature (Table 4) for an aluminium concentration of 20 μmol l^{-1} agrees well with the measured change for water from Gaitscale Gill. There is no temperature effect when the water is free from aluminium because only the enthalpies of aluminium hydrolysis have been considered and not surprisingly the temperature effect

Table 3. Equilibria used to calculate the temperature dependence of the pH of acid waters

Equilibrium	$-\log_{10} K$	ΔH/ kJ mol^{-1}	Reference
$Al^{3+} + H_2O \rightleftharpoons Al(OH)^{2+} + H^+$	−4.99	49.4	15, 16
$Al^{3+} + 2H_2O \rightleftharpoons Al(OH)_2^+ + 2H^+$	−10.13	96.2*	15
$Al^{3+} + 4H_2O \rightleftharpoons Al(OH)_4^- + 4H^+$	−22.16	177.8	15, 16

* Interpolated value of ΔH.

Table 4. Effect of the temperature dependence of aluminium hydrolysis on the pH of a simple acidic solution (pH 4.8). [Na^+] = 0.5 mmol l^{-1}, pCO_2 = 0.0003 atm, I = 0.5 mmol l^{-1} and [Cl^-] was varied to adjust to an appropriate pH. The pH of water from Gaitscale Gill (day 1) measured at the same temperatures is also given

[Al]/ μmol l^{-1}	[Cl^-]/ μmol l^{-1}	pH		
		4 °C	10 °C	20 °C
0	516.5	4.78	4.78	4.78
10	545.5	4.78	4.76	4.73
20	574	4.78	4.75	4.69
Gaitscale Gill		4.78	4.75	4.70

increases with the concentration of aluminium. In most natural acid waters the concentration of monomeric aluminium is less than 20 μmol l^{-1},[5] and so the change in pH with temperature for water from Gaitscale Gill is probably an extreme example.

There is a clear need for measurements of the temperature dependence of pH for a range of waters of various composition. For waters with pH > 5.5, where the pH is determined largely by carbonate equilibria, the temperature dependence can be calculated readily. Precise measurements of the pH of neutral soft waters over a range of pH have confirmed the validity of such calculations.[17] This work has shown that if the concentration of inorganic monomeric aluminium is known it should be possible to predict the temperature dependence of the pH of acid waters. Although the zero enthalpy of carboxyl groups[13] indicates that the humic component of waters will not affect the temperature dependence of pH, this hypothesis has still to be tested.

Conclusions

The pH of the particular acid water studied here was not affected appreciably by filtration, storage temperature or container material. Measurements made within 2 d of sampling were highly reproducible and after 15 d there were only small changes, associated with storage at 4 °C and irreproducibility in borosilicate glass bottles. The changes that were observed were generally smaller than the errors associated with measuring the pH of dilute solutions.[2,3,6] Although results for other waters may vary, the constancy of the various measurements made in this work indicate that the pH measured in the laboratory should truly reflect the *in situ* pH, accurate measurements of which are difficult to obtain.[18] Moreover, it appears that a knowledge of the concentration of inorganic monomeric aluminium may be sufficient to allow an accurate prediction of the change in pH of a sample of natural acid water with temperature.

References

1. Covington, A. K., Whalley, P. D., and Davison, W., *Pure Appl. Chem.*, 1985, **57**, 877.
2. Davison, W., and Woof, C., *Anal. Chem.*, 1985, **57**, 2567.
3. Davison, W., and Harbinson, T. R., *Analyst*, 1988, **113**, 709.
4. Covington, A. K., Bates, R. G., and Durst, R. A., *Pure Appl. Chem.*, 1985, **57**, 531.

5. Tippping, E., Woof, C., Backes, C. A., and Ohnstad, M., *Water Res.*, 1988, **22**, 321.
6. Midgley, D., *Atmos. Environ.*, 1987, **21**, 173.
7. Nguyen, V. D., and Valenta, P., *Fresenius Z. Anal. Chem.*, 1987, **253**, 260.
8. Schock, M. R., and Schock, S. C., *Water Res.*, 1982, **16**, 1455.
9. Burke, E. M., and Hillman, D. C. J., *in* Knapp, C. M., Mayer, C. L., Peck, D. V., Baker, J. R., and Filbin, G. J., US Environmental Protection Agency Publication, 1987, EPA/600/8-87/019, Environmental Protection Agency, Las Vegas, NV, pp. 59–75.
10. Mattock, G., "pH Measurement and Titration," Heywood, London, 1961.
11. Langelier, W. F., *J. Am. Water Works Assoc.*, 1946, **38**, 179.
12. Davison, W., and Heaney, S. I., *Limnol. Oceanogr.*, 1978, **23**, 1194.
13. Perdue, E. M., *in* Jenne, E. A., *Editor*, "Chemical Modelling in Aqueous Systems," American Chemical Society, Washington, DC, 1979.
14. Tipping, E., Hilton, J., and James, B., *Freshwater Biol.*, 1988, **19**, 371.
15. May, H. M., Helmke, P. A., and Jackson, M. L., *Geochim. Cosmochim. Acta*, 1979, **43**, 861.
16. Couterier, Y., Michard, G., and Sarazin, G., *Geochim. Cosmochim. Acta*, 1984, **48**, 649.
17. Burn, M. C., *PhD Thesis*, University of Newcastle upon Tyne, 1987.
18. Davison, W., and Gardner, M. J., *Anal. Chim. Acta*, 1986, **182**, 17.

Paper 8/04083D
Received October 13th, 1988
Accepted January 13th, 1989

Semi-automated Kinetic Determination of Phenolic Compounds Using a Fluoride-selective Electrode and Based on Their Micellar-catalysed Reaction With 1-Fluoro-2,4-dinitrobenzene

Helen A. Archontaki, Michael A. Koupparis* and Constantinos E. Efstathiou
Laboratory of Analytical Chemistry, Department of Chemistry, University of Athens, 104 Solonos Street, Athens 10680, Greece

A kinetic - potentiometric method is described for the determination of phenol and phenolic drugs based on monitoring their reaction with 1-fluoro-2,4-dinitrobenzene, catalysed by cetyltrimethylammonium bromide micelles, using a fluoride-selective electrode. The measurement step was automated by interfacing a digital electrometer to a microcomputer. By measuring the initial slopes ($\Delta E/\Delta t$), kinetic parameters (reaction order and rate constants) were obtained and kinetic determinations in the range 6×10^{-6}–7×10^{-4} M were performed for phenol, acetaminophen, isoxsuprine, nylidrin, isoproterenol and metaraminol. Micellar catalysis was found to enhance the reaction rate of the various phenolic compounds tested by between 37 and 290 times. The proposed method did not suffer any interference from excipients or from cloudy and coloured solutions and was evaluated by assaying acetaminophen in commercial formulations. The results showed good agreement with those obtained using established methods.

Keywords: *Kinetic determination of phenols; fluoride-selective electrode; 1-fluoro-2,4-dinitrobenzene; acetaminophen; cetyltrimethylammonium bromide; micellar catalysis*

Kinetic (reaction rate) methods of analysis exhibit some advantages over the conventional equilibrium methods, which make them very attractive in the development of analytical methodology. Ion-selective electrodes (ISEs) have been shown to be very useful for monitoring analytical reactions for kinetic analysis. These electrodes can monitor either one of the reactants or products of a reaction without any serious interference from the co-existing substances. Therefore, the combination of kinetic methods of analysis with ion-selective potentiometry provides an excellent and versatile technique with increased selectivity and freedom from optical interferences.

The theoretical aspects (capabilities and limitations) of ISEs and details of their application to kinetic analysis and kinetic studies have been reported previously.[1]

Potentiometric recorders connected to analogue or digital electrometers provide continuous recordings of potential *versus* time curves (E - t curves), which can be treated manually to derive the "reaction rate" measurement using the three common kinetic approaches (slope, variable-time and fixed-time). Various analogue and digital ratemeters have been described for kinetic - spectrophotometric analysis; these ratemeters can also be used in kinetic - potentiometric analysis with slight modification. Hybrid circuits of a window comparator have been designed and employed in kinetic - potentiometric analysis using the variable-time approach.[2–4]

In this paper the construction of an interface suitable for connecting a digital electrometer to a low-cost microcomputer is described. This system was used to study kinetically the reaction of phenolic compounds with 1-fluoro-2,4-dinitrobenzene (FDNB) in the presence of micelles of cetyltrimethylammonium bromide (CTAB) and to develop a semi-automated kinetic method for the determination of these compounds.

1-Fluoro-2,4-dinitrobenzene undergoes nucleophilic aromatic substitution by primary and secondary amines, phenolic compounds,[5] thiols and hydrazino compounds. The dinitrophenyl derivatives obtained are useful for equilibrium spectrophotometric,[6–13] gas chromatographic[14,15] and high-performance liquid chromatographic[16,17] determinations. The reactions of FDNB were found to be catalysed by cationic and non-ionic micelles.[18–21] Connors and Wong[22,23] studied the kinetics of the reaction of FDNB with amines catalysed by CTAB micelles and used this micellar catalysis to improve the spectrophotometric determination of amines. The micellar catalysis of the reaction of FDNB with phenoxide and thiophenoxide has also been studied kinetically using spectrophotometry.[20]

The ability of a fluoride-selective electrode to monitor fluoride ions liberated by organic reactions has been employed successfully in kinetic methods for the determination of amino acids,[24] amines[25] and hydrazino compounds.[26] These methods are based on monitoring the reaction of these substances with FDNB.

The reaction of phenolic compounds with FDNB is similar to that of amino compounds and is an example of a nucleophilic aromatic substitution reaction, with the formation of an intermediate complex. A dinitrophenyl ether derivative is then formed with the liberation of fluoride ion, as shown below:

$$\mathrm{R\text{–}C_6H_4\text{–}OH + (NO_2)_2C_6H_3F} \underset{k_{-1}}{\overset{k_1}{\rightleftharpoons}}$$

$$\mathrm{(NO_2)_2\overset{(-)}{C}_6H_3(F)\overset{(+)}{O}H\text{–}C_6H_4\text{–}R} \xrightarrow{k_2}$$

$$\mathrm{(NO_2)_2C_6H_3\text{–}O\text{–}C_6H_4\text{–}R + H^+ + F^-} \quad \ldots (1)$$

Experimental

Apparatus

The system for potentiometric rate measurements consists of a combination fluoride electrode (Orion Model 96-09) and a digital electrometer (Orion 801 pH - pIon meter) interfaced to a microcomputer (Amstrad CPC 6128). The timing-control circuit of the digital electrometer was modified (by substitution of components of smaller values for a resistor and a capacitor) to make the range of display time 0.09–0.6 s instead of the original 0.6–5 s. All measurements were performed in a thermostated (±0.2 °C) double-walled reaction cell with continuous magnetic stirring. The electrode was stored in 1×10^{-3} M fluoride solution when not in use.

* To whom correspondence should be addressed.

Brief description of the interface. A schematic diagram of the interface circuits between the electrometer and the microcomputer is shown in Fig. 1. The interface consists of two units. The first unit (A) is plugged into the socket located in the rear panel of the 801 digital electrometer. This socket is normally used for connecting the electrometer to a digital printer. The digital readout of the electrometer is encoded in BCD (Binary Coded Decimal). Sixteen lines (four lines for each of the four decimal digits of the potential reading) are available from the socket for general interface applications. The second unit (B) is plugged into the expansion socket of the CPC 6128 microcomputer, where the lines of the address, data and control buses are available to the user. The interface units A and B are interconnected to a multi-line cable of the ribbon type.

The interface unit A contains two buffer/latch integrated circuits (ICs) (Intel 8212) and one quad buffer IC (74125). The eight input lines of each 8212 IC are connected to the BCD output lines of two decimal digits of the displayed potential. The four input lines of the 74125 IC are connected to the flags of the electrometer. Two flags only are required for potential readings, the "sign (+/−)" flag and the "data valid" flag.

Interface unit B contains an address decoder and a 5-V power supply (not shown in Fig. 1). The address decoder consists of a 74154 4- to 16-line decoder and a combination of gates. The input of the decoder is connected directly to the 16-line address bus (lines A_{15}-A_0) and the IORQ (Input - Output Request) line of the microcomputer control bus. The address decoder issues "device select pulses" to the interface unit A when the microcomputer is executing properly addressed input commands. Three different "device select pulses" are required to allow each of the three buffer ICs located in the interface unit A to be connected in sequence, thus making their respective inputs available to the data bus of the microcomputer.

Brief description of the software. The control program, named KINMOD (KINetic MODule), was written in BASIC. KINMOD is a menu-driven, interactive program that turns the microcomputer monitor into a potential - time (E - t) recorder with capabilities far exceeding those of conventional y - t recorders. The main advantage of using the KINMOD program over directly recording the E - t curves is the possibility of direct calculation of the slope of the recorded curves. Also, no measurement has to be repeated in order to re-adjust the recorder span and the chart speed such as for too short or off-scale recordings. Linear parts of the E - t curves are located visually and their slopes ($\Delta E/\Delta t$) are calculated automatically.

From the main menu, the operator can (*i*) fix the measurement settings; (*ii*) make a measurement; (*iii*) save current (E - t) data on a disk; (*iv*) display current data; (*v*) define queue (of)/copy/erase files; (*vi*) display old files; (*vii*) set new default values; and (*viii*) exit to BASIC.

The following settings can be fixed (the available range of the adjustable parameter and the corresponding default values are given in parentheses): (*i*) the relative starting point of the E-axis (0–100, 90); (*ii*) the E-axis full scale (5–100 mV, 20 mV); (*iii*) the t-axis full scale (10–300 s, 100 s); (*iv*) the sampling time interval (0.5–10 s, 1 s); (*v*) the potential change margin (0–5 mV, 2 mV); (*vi*) the stirring time margin (0–10 s, 5 s); and (*vii*) the margin mode (AND/OR, OR). The last three adjustments allow the sampling of E - t data to start automatically after a fixed potential change and/or after a fixed stirring time. These adjustments exclude from the data files the initial E - t points, which are sometimes useless for the characterisation of the reaction owing to the initial dilution of the reacting mixture and incomplete stirring after the addition of the reagent, which initiates the reaction under study.

After the E - t points have appeared on the screen, the operator can select (using cursors) the data area in which the slope, $\Delta E/\Delta t$, should be calculated by linear regression. Regression data (slope, correlation coefficient and coefficient of variation) appear in screen windows. The E - t curve or swarms of E - t curves from old files can be displayed over various potential or time scales and a hard copy of the actual display can be obtained by a carrying out a screen-dump routine at any time.

The performance of the hardware and software was tested using highly reproducible voltage ramps from an analogue integrator. The slope of these ramps was varied over a wide range (0.01–7 mV s^{-1}). The reproducibility of the measured slopes was in the range 0.04–1.4%, the small slopes being less reproducible, owing to the finite resolution (0.1 mV) of the potential readings.

Reagents

All reagents were of analytical-reagent grade unless stated otherwise and de-ionised, distilled water was used throughout.

Phenolic compound solutions, 0.1000 M. Standard stock solutions were prepared from phenol or USP grade acetaminophen, metaraminol hydrogen tartrate, nylidrin hydrochloride, isoproterenol hydrochloride and isoxsuprine hydrochloride. The purity of the drugs used was calculated using the official USP methods.[27] Working standard solutions in the range $1 \times 10^{-5} - 1 \times 10^{-3}$ M were prepared daily from the stock solutions by diluting with water or, for very acidic solutions (metaraminol hydrogen tartrate), with 0.0100 M borate buffer of pH 9.0.

1-Fluoro-2,4-dinitrobenzene working solution, 4.0% *m/V* (0.215 M) *in acetone*. A 1.00-g mass of FDNB (Sigma) was dissolved in 25.0 ml of acetone. The solution was stored in a sealed, amber-coloured glass vial in a refrigerator when not in use. Under these conditions, the solution was stable for at least 1 month. This reagent is vesicatory and should be handled carefully.

Buffer solutions, 0.100 M. Stock solutions of pH 5.5, 8.0 and 9.0 were prepared from succinic acid, tris(hydroxymethyl)-aminomethane (Tris) and boric acid, respectively. Mixed working 0.0300 M buffer solutions were prepared from the stock solutions and also contained 3.00×10^{-5} M NaF and 5.00×10^{-3} M *trans*-1,2-diaminocyclohexane-*N,N,N',N'*-tetraacetic acid (DCTA). When micellar catalysis was to be employed, these mixed buffer solutions also contained 1.5 or 3.0 mM CTAB (Merck).

Standard fluoride solutions. Working standard solutions were prepared from 0.1000 M NaF solution with appropriate dilution. All fluoride solutions were stored in polyethylene bottles.

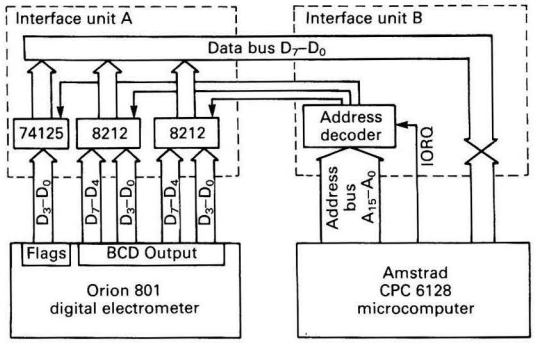

Fig. 1. Schematic diagram of the interface circuits between the Orion 801 digital electrometer and the Amstrad CPC 6128 microcomputer

Measurement Procedure

A 10.00-ml volume of a working standard or sample solution of the analyte and 5.00 ml of the mixed borate buffer of pH 9.0 or Tris buffer of pH 8.0 were pipetted manually into the thermostated (25.0 °C) reaction cell. The stirrer was started and, after the potential had been stabilised (about 30 s as shown by the electrometer readings), the reaction was initiated by the rapid injection of 100 μl of FDNB working solution and, at the same time, the microcomputer was commanded to collect the data. The reaction was followed for about 2–3 min and its course was shown on the monitor of the microcomputer, the data (potential *versus* time) being stored on a disk. The cell was then evacuated and washed twice with mixed borate buffer solution, ready to proceed to the next sample. A blank (water) was included for each calibration graph.

The data were recalled and the initial slope $\Delta E/\Delta t$ (mV s^{-1}) was measured by visually selecting the linear part of the reaction curve as displayed on the monitor (correlation coefficient being an indication). Calibration graphs of $\Delta E/\Delta t$ *versus* concentration were constructed using standard solutions of the analyte.

The slope (S) of the electrode response required for the kinetic study was determined periodically by successive additions of micro-amounts of 0.1000 M NaF stock solution in 10.00 ml of water mixed with 5.00 ml of mixed borate buffer solution (free of fluoride).

Sample Preparation

For the assay of drugs in tablets, not less than 20 tablets were weighed and finely powdered. An accurately weighed portion of the powder containing about 2.5 mmol of the drug was transferred into a 500-ml calibrated flask, dissolved in water using a vortex mixer and diluted. Filtered or centrifuged portions of these solutions were diluted further so that the drug concentration lay within the range of the calibration graph (Table 2) and were then treated as described under Measurement Procedure.

For assay of drugs in liquid preparations (*i.e.*, syrups), 5.00-ml aliquots were suitably diluted so that the drug concentration of the solutions obtained lay within the range of the calibration graph. Care should be taken to drain all of the usually viscous liquid from the pipette.

Results and Discussion

Kinetic Study of the Reaction of Phenolic Compounds with FDNB

The kinetic parameters of the over-all reaction can easily be calculated from the initial slopes $(\Delta E/\Delta t)_0$ of the E - t curves[24]

$$(\Delta E/\Delta t)_0 = S(1/[F^-]_0)k^{st}_{exp}\, c_{0,phenol}[FDNB]_0 \quad .. \quad (2)$$

where S is the slope of the E *versus* ln c response curve of the fluoride electrode [being equal to −24.8 mV $(\ln c)^{-1}$ and not affected by the presence of micelles], $[F^-]_0$ is the initial fluoride concentration (1×10^{-5} M, added to the mixed buffer for reproducible initial potential readings) and k^{st}_{exp} is the experimental stoicheiometric over-all rate constant of the second-order reaction, varying with pH. No correction for the possible catalytic effect of the phenoxide ion on the second step of the over-all reaction [equation (1)] and on the hydrolysis of FDNB was attempted.

If the phenolic hydroxyl group is the only group that reacts with FDNB, the value of k for phenoxide can be calculated using the equation $k = k^{st}_{exp}/a_1$, where a_1 is the amount of phenoxide present, which can be calculated from the pK_a.

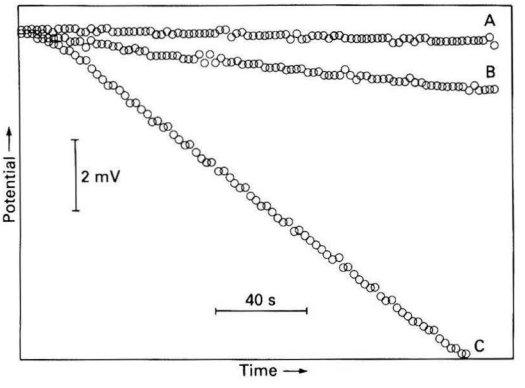

Fig. 2. Effect of pH on the phenol - FDNB reaction at 25 °C. Phenol, 6.67×10^{-4} M; and FDNB, 1.43×10^{-3} M. pH: A, 5.0; B, 8.0; and C, 8.7

Table 1. Kinetic parameters of the reaction of phenolic compounds with FDNB. Conditions: $[FDNB]_0$, 1.43×10^{-3} M; temperature, 25 °C; pH, 9.0 (unless stated otherwise); and [CTAB], 1.0×10^{-3} M (unless stated otherwise)

Compound	k^{st}_{exp} (±SD)/l mol^{-1} s^{-1}		Reaction order (±SD)	
	Uncatalysed	Micellar-catalysed	Uncatalysed	Micellar-catalysed
Phenol* (C_6H_5OH) (pK_a = 10.0)	0.0213 ± 0.0004 (k = 0.444 ± 0.008)	6.2 ± 0.3 (290)†	0.92 ± 0.02	0.91 ± 0.05
Acetaminophen ($CH_3CONHC_6H_4OH$-4) (pK_a = 9.5)	0.068 ± 0.001 (k = 0.283 ± 0.004)	9.4 ± 0.4 (137)†	0.86 ± 0.01	0.85 ± 0.02
Nylidrin hydrochloride $[C_6H_5CH_2CH_2CH_2CH(CH_3)\overset{+}{N}H_2CH(CH_3)CH(OH)C_6H_4OH$-4]	0.078 ± 0.003	11.6 ± 0.7‡ (148)† 6.2 ± 0.3§	0.86 ± 0.01	0.94 ± 0.09 0.80 ± 0.09
Isoproterenol hydrochloride $[(CH_3)_2CH\overset{+}{N}H_2CH_2CH(OH)C_6H_3(OH)_2$-3,4]	0.0088 ± 0.0002	0.53 ± 0.01 (59)†	0.92 ± 0.02	0.77 ± 0.02
Isoxsuprine hydrochloride§ $[C_6H_5OCH_2CH(CH_3)\overset{+}{N}H_2CH(CH_3)CH(OH)C_6H_4OH$-4] ..	0.054 ± 0.002	14.3 ± 0.6 (264)†	0.92 ± 0.02	0.80 ± 0.01
Metaraminol hydrogen tartrate $[H_3\overset{+}{N}CH(CH_3)CH(OH)C_6H_4OH$-3]	0.101 ± 0.005	3.8 ± 0.2 (37)†	0.90 ± 0.03	0.77 ± 0.02

* pH = 8.7.
† Values in parentheses are the number of times the reaction rate has been increased using micellar catalysis.
‡ [CTAB] = 0.5×10^{-3} M.
§ pH = 8.0.

Table 2. Analytical characteristics of the determination of phenolic compounds in aqueous solutions using the kinetic - potentiometric micellar-catalysed method. Conditions: temperature, 25 °C; [FDNB], 1.43×10^{-3} M; and [CTAB], 1×10^{-3} M

Compound	Final linear range tested/μM	Sensitivity (±SD)/ mV s^{-1} l μmol^{-1}	r
Phenol*	6–70	-0.0218 ± 0.0009	0.993
Acetaminophen*	6–70	-0.0336 ± 0.0013	0.997
Isoxsuprine† . .	6–40	-0.0506 ± 0.0019	0.998
Nylidrin†	6–70	-0.0218 ± 0.0011	0.994
Isoproterenol* . .	60–700	-0.00188 ± 0.00005	0.998
Metaraminol* . .	10–700	-0.0135 ± 0.00008	0.995

* pH 9.0 (borate buffer).
† pH 8.0 (Tris buffer).

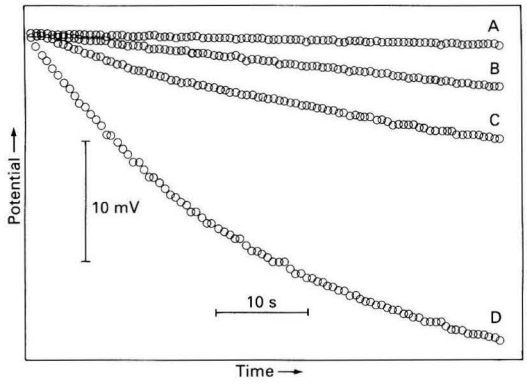

Fig. 3. Effect of pH on the phenol - FDNB reaction at 25 °C with micellar catalysis. Phenol, 6.67×10^{-5} M; FDNB, 1.43×10^{-3} M; and CTAB, 1×10^{-3} M. A, Blank at pH 8.0; B, blank at pH 9.0; C, reaction at pH 8.0; and D, reaction at pH 9.0

This is possible only for the uncatalysed reaction as micellar catalysis increases the ionisation.

From experiments carried out with various concentrations of the phenolic compound and at a constant concentration of FDNB, the reaction order with respect to the phenolic compound can be obtained.

Fig. 2 shows typical reaction curves for the uncatalysed phenol - FDNB reaction at various pH. As can be seen, the pH has a marked effect on the reaction rate; this can be explained either by the high reactivity of phenoxide compared with phenol (the amount of phenoxide present at pH 8.7 is only 4.8%) and/or by the catalytic effect of hydroxide ions on the second step of the reaction. Higher pH values were not tested as high concentrations of hydroxide ions interfere with the fluoride electrode.[24]

The effect of pH on the micellar catalysis by CTAB of the phenol - FDNB reaction (blank) was also studied (Fig. 3). As can be seen, cationic micelles are very good catalysts for anionic (phenoxide) nucleophilic attack. In addition to the net micellar catalysis of the reaction, the change in the acid dissociation of phenol must be taken into account when measuring this effect. Various other surfactants were also tested (*e.g.*, trimethyloctadecylammonium bromide, sodium lauryl sulphate and Triton X-405). Anionic micelles had no effect on the reaction rate, whereas non-ionic micelles produced a slight increase. From these results it was decided to use only CTAB at pH 9.0 for the kinetic study and method development.

The kinetic data (experimental reaction rate and order for the uncatalysed and catalysed reactions) for the phenolic compounds studied are summarised in Table 1. Phenol and acetaminophen only have a reactive phenolic group, whereas the other compounds tested also have an amino group. Hence the value of k for the phenoxide reaction was calculated only for these two compounds. The only kinetic data reported in the literature are for phenol[20] and were obtained from spectrophotometric experiments. A value for k of 0.681 l mol^{-1} s^{-1} for the uncatalysed phenoxide reaction and a 230-fold increase in this value using micellar catalysis (6.67×10^{-3} M CTAB) have been reported, which are very close to the values obtained in this work. The agreement between the spectrophotometric and kinetic - potentiometric data demonstrates the utility of the fluoride electrode for accurate kinetic studies.

The effect of temperature on the micellar-catalysed phenol - FDNB reaction was studied in the range 20–30 °C. From the calculated values of k^{st}_{exp} [the experimental slope of the electrode at each temperature was used in equation (2)], an activation energy of 44 ± 2 kJ mol^{-1} was found using an Arrhenius plot. As an approximately 1.7-fold increase in the value of k^{st}_{exp} occurs for a 10-°C temperature change, the temperature of the reaction mixture must be controlled.

In contrast to classical homogeneous solution catalysis, which involves a reaction mechanism with a lower activation energy, the so-called "micellar catalysis" is due to hydrophobic and electrostatic interactions of reactants with micellar aggregates. Several publications have been devoted to the effect of micellar and other aggregates on chemical reaction rates and equilibria.[28–32]

In the present work, the hydrophobic adsorption of the neutral FDNB molecules and the electrostatic attraction between the negatively charged phenoxide ion and the cationic micelles of CTAB may explain the acceleration of the reaction.

Kinetic Determination of Phenolic Compounds and Analytical Applications

As can be concluded from equation (1), the initial slope of the reaction curve is linearly related to the phenol concentration because the reaction is first-order with respect to phenols (Table 1).

A pH of 9.0 (borate buffer) or 8.0 (Tris buffer) and a temperature of 25 °C were selected as the optimum conditions for routine determinations. These conditions were a compromise between the effect of pH and temperature on both the rate of the micellar-catalysed reaction and the hydrolysis of FDNB, and their effect on the operational characteristics of the fluoride-selective electrode. For those phenolic compounds having a high reaction rate (isoxsuprine and nylidrin), a pH of 8.0 (Tris buffer) is preferable for the determination, as the initial linear part of the E - t curves is extended by reducing the rate of the reaction.

Fig. 4 shows typical reaction curves used for the calibration graph of acetaminophen. The data obtained for the phenolic compounds tested are shown in Table 2, which summarises the useful analytical ranges, the slopes of the calibration graphs (sensitivities) and their standard deviations (SDs) and the correlation coefficients (r). The precision (relative standard deviation) of the measurements was 1–3% ($n = 3$).

In order to examine the applicability of the proposed method to the determination of phenol drugs in commercial formulations, a recovery study was performed on synthetic mixtures of acetaminophen (5×10^{-5} M) containing various common excipients (10 mg ml^{-1}). No interference was found from sodium chloride, carboxypolymethylene, magnesium stearate, talc, lactose, mannitol, galactose, sorbitol, sugar and glycerine. From these results it can be seen that in the absence of amines, hydrazino compounds and thiols, which also react with FDNB, the determination is highly selective.

The proposed method was applied to the determination of

Table 3. Comparison of results obtained for the determination of acetaminophen in commercial formulations using the proposed kinetic - potentiometric and established methods

Formulation	Nominal content	Amount found: Proposed method (KP) (±SD*)	Amount found: Reference method (Ref.)*	Relative difference (KP − Ref.), %
Tablets (mg)—				
Norgesic (Riker Laboratories)	450	438 ± 15	453†	−3.3
Medamol (Greek National Pharmaceutical Industry)	500	483 ± 18	506†	−4.5
Neo Dalmin (Norma Hellas)	500	518 ± 16	515†	+0.6
Syrups (mg ml^{-1})—				
Dolal (Famar)	25	26.4 ± 0.8	26.0†	+1.5
Panadol (Sterling Winthrop Group)	24	24.6 ± 0.6	24.3†	+1.2
Depon (Squibb)	24	22.4 ± 0.6	23.0†	−2.6
Tempra (Mead Johnson)	24	24.2 ± 0.5	24.1‡	+0.4
Drops (mg ml^{-1})—				
Tempra (Mead Johnson)	100	101.7 ± 2.2	102‡	−0.3

* $n = 3$.
† Belal *et al.*[33]
‡ Bristol Myers spectrophotometric method.

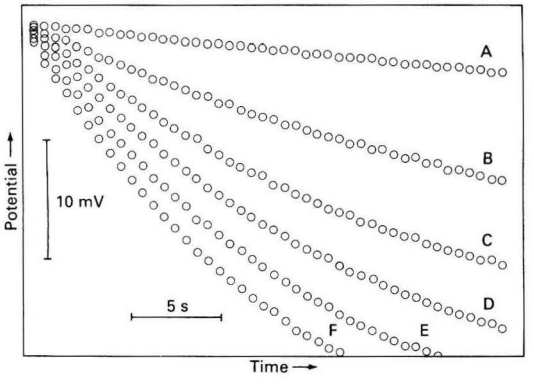

Fig. 4. Typical reaction curves for the acetaminophen - FDNB reaction with micellar catalysis, for a calibration graph at pH 9.0 and 25 °C. Acetaminophen: A, blank; B, 1.33×10^{-5}; C, 2.67×10^{-5}; D, 4.00×10^{-5}; E, 5.33×10^{-5}; and F, 6.67×10^{-5} M. FDNB, 1.43×10^{-3} M; and CTAB, 1×10^{-3} M

acetaminophen in commercial pharmaceutical formulations. The results of these assays and a comparison with established methods are given in Table 3.

Conclusions

The proposed method is a simple, selective and rapid means of determining phenolic compounds, even in turbid and coloured samples. This work has also demonstrated the usefulness of ion-selective electrodes for kinetic studies of organic reactions and for kinetic analysis together with the potential of micellar catalysis. The modified electrometer can be used for the automation of measurements in any potentiometric method employing glass or ion-selective electrodes.

References

1. Efstathiou, C. E., Koupparis, M. A., and Hadjiioannou, T. P., *Ion-Sel. Electrode Rev.*, 1985, **7**, 203.
2. Efstathiou, C. E., and Hadjiioannou, T. P., *Anal. Chem.*, 1975, **47**, 864.
3. Efstathiou, C. E., and Hadjiioannou, T. P., *Anal. Chim. Acta*, 1977, **89**, 55.
4. Efstathiou, C. E., Koupparis, M. A., and Hadjiioannou, T. P., *Chem. Biomed. Environ. Instrum.*, 1983, **12**, 215.
5. Pedro, A., and Lehmann, F., *Anal. Chim. Acta*, 1971, **54**, 321.
6. Sanger, F., *Biochem. J.*, 1945, **39**, 507.
7. McIntire, F. C., Clements, L. M., and Sprouli, M., *Anal. Chem.*, 1953, **25**, 1757.
8. Dubin, D. T., *J. Biol. Chem.*, 1960, **235**, 783.
9. Kolbenzen, M. J., Eckert, J. N. E., and Brefshneider, B. F., *Anal. Chem.*, 1962, **34**, 583.
10. Couch, R., *J. Assoc. Off. Anal. Chem.*, 1975, **58**, 599.
11. Weber, J. D., *J. Pharm. Sci.*, 1976, **65**, 105.
12. Goodwin, J. F., *Clin. Chem.*, 1968, **14**, 1080.
13. Ryan, J. A., *J. Pharm. Sci.*, 1984, **73**, 1301.
14. Timbrell, J. A., Wright, J. M., and Smith, C. M., *J. Chromatogr.*, 1977, **138**, 165.
15. Cohen, I. C., Norcup, J., Růžička, J. H. A., and Wheals, B. B., *J. Chromatogr.*, 1969, **44**, 251.
16. Lawrence, J. F., and Frei, R. W., "Chemical Derivatization in Liquid Chromatography," Elsevier, Amsterdam, 1976.
17. Barends, D. M., Blauw, J. S., Mijnsbergen, C. W., Govers, C. J. L. R., and Hulshoff, A., *J. Chromatogr.*, 1985, **322**, 321.
18. Bunton, C. A., and Robinson, L., *J. Org. Chem.*, 1969, **34**, 780.
19. Bunton, C. A., and Robinson, L., *J. Am. Chem. Soc.*, 1970, **92**, 356.
20. Chaimovich, H., Blanco, A., Chayet, L., Costa, L. M., Monteiro, P. M., Bunton, C. A., and Paik, C., *Tetrahedron*, 1975, **31**, 1139.
21. Bunton, C. A., Cerichelli, G., Ihara, V., and Sepulvera, L., *J. Am. Chem. Soc.*, 1979, **101**, 2429.
22. Connors, K. A., and Wong, M. P., *J. Pharm. Sci.*, 1979, **68**, 1470.
23. Wong, M. P., and Connors, K. A., *J. Pharm. Sci.*, 1983, **72**, 146.

24. Athanasiou-Malaki, E., and Koupparis, M. A., *Analyst*, 1987, **112**, 757.
25. Athanasiou-Malaki, E., Koupparis, M. A., and Hadjiioannou, T. P., *Anal. Chem.*, in the press.
26. Athanasiou-Malaki, E., and Koupparis, M. A., *Talanta*, in the press.
27. "The United States Pharmacopeia XXI," United States Pharmacopeial Convention, Rockville, MD, 1985, pp. 11, 647, 751, 569 and 576.
28. Fendler, J. H., "Membrane Mimetic Chemistry," Wiley, New York, 1982.
29. Fendler, J. H., and Fendler, E. J., "Catalysis in Micellar and Macromolecular Systems," Academic Press, New York, 1975.
30. Bunton, C. A., *Catal. Rev. Sci. Eng.*, 1979, **20**, 1.
31. Love, L. J. C., Habarta, J. G., and Dorsey, J. G., *Anal. Chem.*, 1984, **56**, 1132A.
32. Pelizzetti, E., and Pramauro, E., *Anal. Chim. Acta*, 1985, **169**, 1.
33. Belal, S. F., Elsayed, M. A. H., Elwalily, A., and Abdine, H., *Analyst*, 1979, **104**, 919.

Paper 8/04599B
Received November 18th, 1988
Accepted January 4th, 1989

Kinetic and Chemometric Studies of the Determination of Creatinine Using the Jaffé Reaction

Part I. Kinetics of the Reaction: Analytical Conclusions

María Llobat-Estellés, Adela Sevillano-Cabeza and Pilar Campíns-Falcó
Departamento de Química Analítica, Facultad de Química, Universidad de Valencia, Burjassot, Valencia, Spain

A kinetic - spectrophotometric study of the Jaffé reaction was carried out and the kinetic behaviour, calibration step and interfering effect of albumin on creatinine standard solutions were studied. It was concluded that there is a variation in the kinetic behaviour of the system when higher concentrations of creatinine, picrate or sodium hydroxide are tested. The experimental conditions for quantifying creatinine must be chosen so that the kinetic behaviour is the same in the dynamic concentration range. Changes in the absorbance (ΔA) *versus* concentration equations were chosen as the most suitable for calibration graphs. It was also shown that creatinine results will have a proportional bias error if the interfering effect of albumin is not taken into consideration.

Keywords: *Jaffé reaction; kinetic - spectrophotometric study; creatinine; calibration step; albumin interfering effect*

The creatinine level in human serum samples is generally accepted as an indication of the presence or absence of renal failure. Although several methods have been proposed for the determination of creatinine, the classical Jaffé reaction has continued to be the method of choice. Several studies have emphasised the use of the kinetic phase of the reaction in order to reduce the effects of interferences.

Since Lustgarten and Wenk[1] confirmed that there was a linear relationship between the change in absorbance (ΔA) and creatinine concentration (c) using the Jaffé reaction, several studies of this reaction have been carried out.

Vasiliades[2] studied the kinetics and mechanism of the alkaline picrate - creatinine reaction and demonstrated that the forward reaction is first order with respect to the picric acid, hydroxide and creatinine concentrations up to a hydroxide concentration of 0.7 mol l^{-1} and that the reverse reaction (the dissociation of the complex) shows a complex dependence on the hydroxide concentration. The conditions used in the study were selected so as to obtain the maximum amount of kinetic - mechanistic information rather than to investigate practical applications of the reaction.

Shoucri and Pouliot[3] have shown that the Jaffé reaction for the assay of creatinine appears to follow pseudo-first-order kinetics but that the first-order rate constants are different for different serum samples, ranging from 4.0×10^{-3} to 8.4×10^{-3} s^{-1}. In order to take account of this variation these workers indicated that it was necessary to use a mathematical treatment for the reliable kinetic determination of creatinine. This equation uses the different rate constants for standard creatinine and serum samples tested in the ΔA method.

Recently, Kroll and co-workers also examined the dependence of the reaction rate on the concentration of picrate[4] and sodium hydroxide[5] and expressed the rate of the Jaffé reaction as a function of the concentration of creatinine, picrate and hydroxide. These workers, using the linear relationship between rate constants and the concentration of hydroxide, concluded that the model proposed by Vasiliades[2] holds only when the hydroxide concentration is higher than 0.5 mol l^{-1} but not when it is less than 0.2 mol l^{-1}. They therefore proposed another model and developed a non-dilution method for urinary creatinine based on the dependence of the Jaffé reaction on the sodium hydroxide concentration.

On the other hand, the review by Spencer[6] on the determination of creatinine showed that over the last decade a large variety of reaction conditions has been used in the kinetic modification of the Jaffé reaction. This is particularly so with variations in the picrate and sodium hydroxide concentrations and in the measurement interval. Spencer concluded that this has resulted in conflicting data both for the precision of the assay and for the extent of interferences.

As there is some confusion in the literature, it was decided to confirm the kinetics of the reaction in order to establish its analytical possibilities before testing the method chemometrically by applying it to serum samples. The main aim of this work was, therefore, to examine the kinetic data and evaluate their analytical application.

Spencer[6] showed that there is disagreement in the literature concerning the effect of interferents such as proteins, ketones and keto acids and bilirubin and glucose on the kinetic determination of creatinine. Moreover, the most recently published paper[7] on this kinetic method demonstrated that the effect of albumin is the easiest to study because the interferent - picrate reaction for the other interferents is almost complete by the time the first absorbance reading is taken. These workers showed that the reaction of alkaline picrate with human serum albumin is very complex and that the effect of the latter can be compensated for by a curve-fitting method and by preparing standards containing 50 g l^{-1} of albumin.

With this in mind, our objectives were to determine the optimum conditions for the reaction and to study the effect of albumin interference on the determination of creatinine using the simple and rapid ΔA method. This is the method normally used in routine clinical work, and it has the advantages that knowledge of the blank analytical signal is not required and that any constant bias error can be corrected.

Experimental

Instrumentation

All spectrophotometric measurements were made on a Shimadzu UV-240 spectrophotometer coupled with an optional programme unit (OPI-2).

A Frigedor Selecta-396 refrigerator unit for use with a water-bath and a Thermotronic Selecta-389 immersion thermostat, capable of maintaining the temperature to within ±0.05 °C, were also used. All the solutions were previously

heated to a working temperature of 25.00 ± 0.05 °C in a thermostat and this temperature was maintained in the reaction cell during the experiment.

Reagents

All solutions were prepared in distilled water and all reagents were of analytical-reagent grade unless stated otherwise.

Sodium hydroxide (Probus) stock solution, 5.0 mol l^{-1}.

Picric acid (Merck) stock solution, 2.08×10^{-2} mol l^{-1}.

Alkaline picrate. Working alkaline picrate reagent was prepared by mixing 90 ml of picric acid and 10 ml of sodium hydroxide stock solutions. This reagent was prepared fresh daily.

Creatinine (Fluka) stock solution, 1.0 g l^{-1}. Working standards were prepared by diluting this stock solution.

Albumin solution, 50 g l^{-1}. Prepared from Bovine Albumin (Fluka, Fraction V).

Procedures

Kinetic and calibration studies

Appropriate volumes of sodium hydroxide, picric acid and creatinine stock solutions were added to 25-ml calibrated flasks to obtain solutions of the required concentrations. The final volume was 25 ml. Zero time was taken as the moment at which the last drop of creatinine solution was added. The absorbance was measured at 485 nm and at a temperature of 25 °C against a reagent blank prepared in the same way, but without creatinine, and was recorded as a function of time.

Interference study

Appropriate volumes of creatinine or albumin and creatinine working solutions were transferred into test-tubes and diluted with distilled water to a volume of 3 ml. Then, 2 ml of working alkaline picrate reagent were added. In this instance zero time was taken as the moment at which the last drop of this reagent was added. The subsequent steps were as described above.

Results and Discussion

Kinetic Data

In order to test the determination of creatinine chemometrically using the kinetic Jaffé reaction, it is first necessary to validate the published kinetic data in order to assess their analytical utility as this has not been demonstrated conclusively in the literature.

Effect of Creatinine Concentration

The effect of the creatinine concentration on the reaction rate has been widely studied[1–4] and a pseudo-first-order kinetics with respect to creatinine concentration was obtained.

Response curves were obtained for two series of solutions containing various creatinine concentrations, a fixed concentration of 0.2 mol l^{-1} of sodium hydroxide and 3.3×10^{-3} and 6.6×10^{-9} mol l^{-1} of picrate, respectively. The graphs for the first series are linear up to 105 s, whereas the graphs for the second are linear only up to 75 s in the concentration ranges 3.6×10^{-5}–72.8×10^{-5} and 3.6×10^{-5}–47.6×10^{-5} mol l^{-1} of creatinine, respectively. The slopes of these graphs can be used as a measure of the initial reaction rate.

For a pseudo-first-order dependence, straight lines must be obtained when the initial reaction rate (mol l^{-1} s^{-1}) is plotted against the initial concentration. In this way and by using the molar absorptivity of the complex formed (7.8×10^3 l mol^{-1} cm^{-1}), apparent rate constants (k_c) of 2.85×10^{-3} and $(5.5 \pm 0.2) \times 10^{-3}$ s^{-1} (from five replicates) were calculated for 3.3×10^{-3} and 6.6×10^{-3} mol l^{-1} of picrate, respectively. The values of k_c can also be obtained by the integral method. Fig. 1 shows graphs of ln ΔA *versus* time (s) for the two series of solutions just mentioned and shows that the kinetic behaviour varies when the creatinine concentration increases. For the two series of solutions, straight lines were obtained up to a creatinine concentration of 14.6×10^{-5} mol l^{-1} in the ranges 45–305 and 45–180 s, respectively. These lines have the same slope for both series and are equal to the slope obtained for creatinine concentrations higher than 14.6×10^{-5} mol l^{-1} when small intervals of time are considered (Fig. 1).

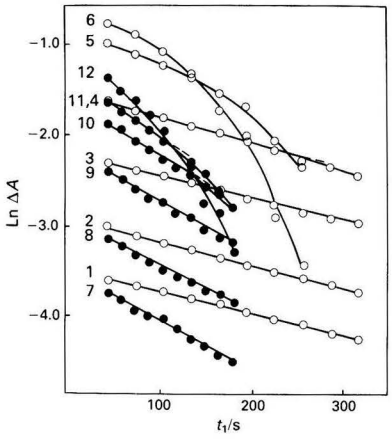

Fig. 1. Variation of ln ΔA with time for different creatinine concentrations. Conditions: sodium hydroxide, 0.2 mol l^{-1}; temperature, 25 °C; picrate, (○) 3.3×10^{-3} and (●) 6.6×10^{-3} mol l^{-1}; and creatinine for (○): 1, 3.6×10^{-5}; 2, 7.3×10^{-5}; 3, 14.6×10^{-5}; 4, 29.3×10^{-5}; 5, 58.3×10^{-5}; and 6, 72.8×10^{-5} mol l^{-1} and for (●): 7, 3.6×10^{-5}; 8, 7.3×10^{-5}; 9, 14.7×10^{-5}; 10, 29.3×10^{-5}; 11, 36.6×10^{-5}; and 12, 47.6×10^{-5} mol l^{-1}

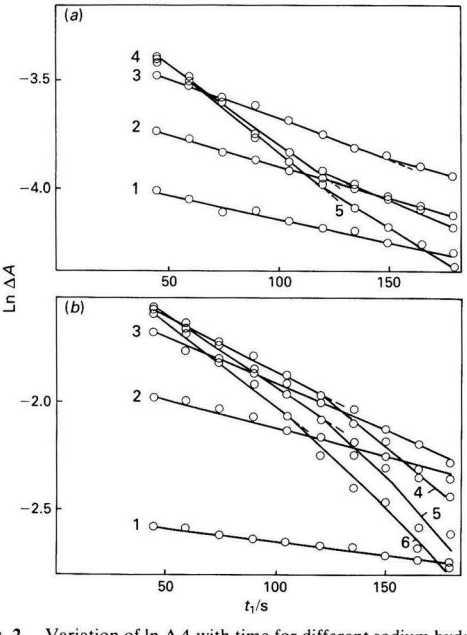

Fig. 2. Variation of ln ΔA with time for different sodium hydroxide concentrations. Conditions: picrate, 3.3×10^{-3} mol l^{-1}; temperature, 25 °C; creatinine, (*a*) 7.2×10^{-5} mol l^{-1} and (*b*) 58.3×10^{-5} mol l^{-1}; and sodium hydroxide: (*a*) 1, 0.12; 2, 0.18; 3, 0.24; 4, 0.30; and 5, 0.40 mol l^{-1} and (*b*) 1, 0.06; 2, 0.12; 3, 0.18; 4, 0.24; 5, 0.30; and 6, 0.40 mol l^{-1}

This could explain the variation in the values of k_c described in the literature,[3] whereas this variation is not consistent if the same kinetic behaviour is examined over a creatinine concentration range. Shoucri and Pouliot[3] showed the necessity of using a rigorous equation for the reliable kinetic determination of creatinine. However, this procedure is not necessary if the study of the creatinine concentration is carried out under experimental conditions where the value of k_c can be determined.

The values of k_c obtained are $(2.7 \pm 0.1) \times 10^{-3}$ s^{-1} (for three concentrations) and $(5.6 \pm 0.3) \times 10^{-3}$ s^{-1} (from five replicates for each of three concentrations) for 3.3×10^{-3} and 6.6×10^{-3} mol l^{-1} of picrate, respectively. These results agree with those obtained using the differential method.

Effect of Reaction Parameters

In order to study the effect of the concentration of each reagent on the initial reaction rate, two series of experiments with creatinine concentrations of 7.2×10^{-5} and 58.3×10^{-5} mol l^{-1} and with 0.2 M sodium hyroxide solution and various picrate concentrations were carried out. The initial reaction rate increases steadily with the picrate concentration. The absorbance (A) - time (t) graphs are linear for the first series up to 90 s in the picrate concentration range 1.0×10^{-3}–6.6×10^{-3} mol l^{-1}, whereas for the second series these plots are linear only up to 75 s and in the picrate concentration range 1.0×10^{-3}–4.0×10^{-3} mol l^{-1}. These results are in agreement with those obtained in the previous section. Application of the differential method under suitable experimental conditions gave a pseudo-first-order dependence on the picrate concentration. Apparent rate constants (k_p) of 0.91 and 0.97 s^{-1} were obtained for creatinine concentrations of 7.2×10^{-5} and 58.3×10^{-5} mol l^{-1}, respectively.

From the ln ΔA - t graphs it was found that there was a variation in the kinetic behaviour for the high creatinine concentrations when the picrate concentration was also high. Values for k_p of 0.8 and 1.0 s^{-1}, respectively, were obtained for the two series using the integral method.

The influence of the sodium hydroxide concentration in the range 0.06–0.4 mol l^{-1} on the initial reaction rate was studied for 3.3×10^{-3} mol l^{-1} of picrate. For both creatinine concentrations the initial rate increases proportionally with the sodium hydroxide concentration. The A - t graphs indicate that the linearity range decreases when the sodium hydroxide concentration increases and that the decrease is much greater with the high creatinine concentrations tested. The apparent rate constants (k_s) obtained with the differential method were 1.9×10^{-2} and 1.7×10^{-2} s^{-1} for creatinine concentrations of 7.2×10^{-5} and 58.3×10^{-5} mol l^{-1}, repectively, and a pseudo-first-order kinetics was obtained.

Fig. 2 shows the ln ΔA - t graphs for the two series of solutions described above. For the lower creatinine concentration (7.2×10^{-5} mol l^{-1}) straight lines are obtained up to 0.24 mol l^{-1} of sodium hydroxide, whereas for higher concentrations of sodium hydroxide two different straight lines are observed. This variation in the slope could be attributed to the influence of the reverse reaction, *i.e.*, dissociation of the complex formed, as described by Vasiliades.[2]

As can be seen from Fig. 2, this effect is even more pronounced for the higher creatinine concentration (58.3×10^{-5} mol l^{-1}). From this study a sodium hydroxide concentration of 0.2 mol l^{-1} was chosen as the working concentration.

By using time intervals over which the dissociation of the complex was negligible, a value for k_s of 2.0×10^{-2} s^{-1} was obtained for both creatinine concentrations.

A study of the influence of the temperature on the reaction was performed in the range 20–35 °C. The initial reaction rate increases as the temperature and creatinine concentration increase. The log - log plot shows a reaction order of one with respect to the creatinine concentration over the temperature range 20–35 °C. In order to calculate the activation energy (E) and the frequency factor (F), the Arrhenius equation was applied to creatinine concentrations in the range 0–58.3×10^{-5} mol l^{-1} for sodium hydroxide and picrate concentrations of 0.2 and 2.6×10^{-3} mol l^{-1}, respectively. The graph of ln k *versus* $1/T$ is a straight line ($\ln k = 12.05 - 2730.6 \times 1/T$) with a correlation coefficient (r) of −0.99 for $E = 22.68$ kJ mol^{-1} and $F = 1.7 \times 10^5$ s^{-1}.

Table 1. Values of k_{total} calculated from equation (1)

Creatinine concentration /10^{-5} mol l^{-1}	Picrate concentration /10^{-3} mol l^{-1}	Sodium hydroxide concentration /mol l^{-1}	v/10^{-7} mol l^{-1} s^{-1}	k_{total}/ l^2 mol^{-2} s^{-1}
7.3	3.30	0.20	2.10	4.36
29.2	3.30	0.20	8.40	4.36
72.8	3.30	0.20	21.04	4.38
3.7	6.60	0.20	2.48	5.08
14.6	6.60	0.20	9.35	4.85
29.3	6.60	0.20	17.50	4.52
36.6	6.60	0.20	21.70	4.49
7.2	0.99	0.20	0.78	5.47
7.2	1.98	0.20	1.60	5.61
7.2	3.30	0.20	2.10	4.42
7.2	3.96	0.20	2.67	4.68
7.2	6.60	0.20	4.47	4.70
58.0	0.99	0.20	6.27	5.46
58.0	1.98	0.20	13.00	5.66
58.0	2.97	0.20	17.50	5.08
58.0	3.96	0.20	22.40	4.88
7.2	3.30	0.12	1.65	5.79
7.2	3.30	0.18	2.21	5.17
7.2	3.30	0.24	3.39	5.95
58.0	3.30	0.18	17.40	5.05
58.0	3.30	0.24	20.80	4.53

Kinetic Model

From these results, the rate equation for the reaction is as follows:

$$v = k_{total}\,[\text{picrate}][\text{creatinine}][\text{OH}^-] \quad \ldots \quad (1)$$

Using this equation, the mean value found for k_{total} was 5.0 l^2 mol^{-2} s^{-1}, with a standard deviation of 0.5 l^2 mol^{-2} s^{-1} (calculated for 21 experiments) (Table 1), which is in agreement with that obtained by Vasiliades.[2]

Alternatively, the value of k_{total} can be calculated by means of the following equations:

$$k_{total} = \frac{k_c}{[\text{picrate}][\text{OH}^-]} \quad \ldots \quad (2)$$

$$k_{total} = \frac{k_p}{[\text{OH}^-]} \quad \ldots \quad (3)$$

$$k_{total} = \frac{k_s}{[\text{picrate}]} \quad \ldots \quad (4)$$

The values of k_c, k_p and k_s were calculated as described previously. From equations (2)–(4) the mean value of k_{total} was found to be 4.9 ± 0.8 l^2 mol^{-2} s^{-1}, which is in good agreement with that obtained from equation (1).

Calibration Study

As shown previously, the possible working conditions for the kinetic determination of creatinine using the Jaffé reaction are numerous. These working conditions were therefore studied by reference to the calibration step. The methods used to obtain the calibration graphs were the initial-rate (v - c), ΔA

Table 2. Study of the calibration step

Calibration graph	Picrate concentration/ 10^{-3} mol l^{-1}	Time/ s	David's test	Cochran's test	Creatine concentration range/ 10^{-5} mol l^{-1}	Equation*	s_{yx}	*F*- or *t*-Test	Detection limit/ 10^{-5} mol l^{-1}	Quantification limit/ 10^{-5} mol l^{-1}
v - *c* . .	3.3	0–105	—	—	3.6–72.8	$a = (-5 \pm 8) \times 10^{-3}$ $b = 22.1 \pm 0.2$	1.2×10^{-4}	Linear	0.2	0.6
	6.6†	0–75	Normal	Homoscedasticity	3.6–47.6	$a = (7 \pm 2) \times 10^{-4}$ $b = 43.0 \pm 0.8$	3.3×10^{-4}	Linear	0.05	0.2
ΔA - *c*	3.3	45–105	—	—	3.6–72.8	$a = (8 \pm 8) \times 10^{-3}$ $b = 1270 \pm 20$	1.6×10^{-2}	Linear	0.2	0.6
	3.3	45–135	—	—	3.6–58.3	$a = (3 \pm 1) \times 10^{-2}$ $b = 1740 \pm 40$	1.9×10^{-2}	Linear	0.1	0.4
	3.3	45–165	—	—	3.6–29.3	$a = (11 \pm 7) \times 10^{-3}$ $b = 2400 \pm 40$	8.2×10^{-3}	Linear	0.1	0.4
	3.3	45–195	—	—	3.6–14.6	$a = (1 \pm 2) \times 10^{-2}$ $b = 3000 \pm 200$	1.4×10^{-2}	Linear	0.1	0.4
	6.6†	45–75	Normal	Homoscedasticity	3.6–47.6	$a = (1.8 \pm 0.8) \times 10^{-}$ $b = 1000 \pm 30$	1.2×10^{-2}	Linear	0.07	0.2
	6.6†	45–105	Normal	Homoscedasticity	3.6–36.6	$a = (3 \pm 1) \times 10^{-2}$ $b = 1870 \pm 60$	1.8×10^{-2}	Linear	0.03	0.1
	6.6†	45–120	Normal	Homoscedasticity	3.6–29.3	$a = (2 \pm 1) \times 10^{-2}$ $b = 2350 \pm 70$	1.4×10^{-2}	Linear	0.05	0.15
	6.6†	45–180	Normal	Homoscedasticity	3.6–14.6	$a = (100 + 8) \times 10^{-4}$ $b = 3970 \pm 10$	9.9×10^{-4}	Linear	0.03	0.1
A - *c* . .	6.6†	45	Normal	Homoscedasticity	3.6–73.2	$a = (0.1 \pm 2) \times 10^{-2}$ $b = 2360 \pm 50$	3.1×10^{-2}	Linear	0.3	0.9
	6.6†	90	Normal	Homoscedasticity	3.6–58.5	$a = (7 \pm 2) \times 10^{-2}$ $b = 3550 \pm 50$	2.7×10^{-2}	Linear	0.2	0.6
	6.6†	180	Normal	Homoscedasticity	3.6–36.6	$a = (1 \pm 0.5) \times 10^{-1}$ $b = 5500 \pm 200$	4.9×10^{-2}	Linear	0.1	0.3

* a = intercept; b = slope.
† Results obtained for five replicates.

(ΔA - *c*) and fixed-time (*A* - *c*) methods. Only the linear range of the calibration graphs was studied.

Table 2 shows the different results obtained with these three methods. In all instances the distributions were normal as indicated by David's test[8] and the corresponding variances were homoscedastic when Cochran's test[8] was applied.

When using the initial-rate method for the higher picrate concentration, the dynamic range of the creatinine concentration and the time interval are smaller than for the lower picrate concentration. However, the slope of the calibration graph is higher and the detection and quantification limits are lower.

Using the ΔA method it was found that, for the two picrate concentrations tested, there is a decrease in the linear range and an increase in the slopes of the calibration graphs when the time increment increases. The detection and quantification limits are similar for both series (Table 2).

With the fixed-time method the dynamic range of creatinine concentrations decreases as the time increases. The slope of the corresponding calibration graphs varies from 2360 ± 50 to 5500 ± 200 and the detection and quantification limits decrease.

The standard error of estimates (s_{yx}) increases in the order initial-rate, ΔA and fixed-time methods (Table 2). From the results obtained, it can be inferred that for the same dynamic range of creatinine concentrations, the initial-rate method is to be preferred because the value of s_{yx} is smaller than that given by the other methods. The ΔA and fixed-time methods have an additional disadvantage: the dynamic range is decreased when the time increment (ΔA method) or time (fixed-time method) is increased. However, an increase in the slope of the calibration graphs is obtained. Nevertheless, the ΔA method has the advantage that knowledge of the blank analytical signal is not required and that any constant systematic error can be corrected.

Interference Study

The determination of creatinine using the Jaffé reaction suffers from a lack of specificity due to the interfering effect of a number of substances present in serum. A number of techniques have been proposed to isolate creatinine from the interfering non-creatinine chromogens, the kinetic modification being the most widely used.

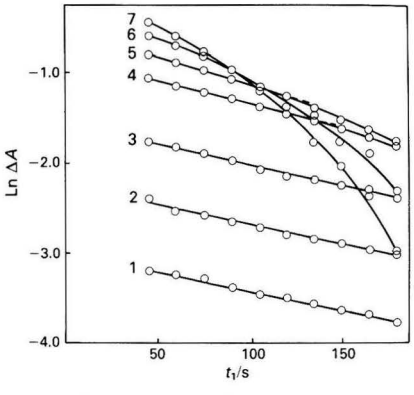

Fig. 3. Variation of ln ΔA with time for different creatinine concentrations. Conditions: picrate, 6.6 × 10^{-3} mol l^{-1}; sodium hydroxide, 0.2 mol l^{-1}; temperature, 25 °C; and creatinine: 1, 3.6 × 10^{-5}; 2, 7.3 × 10^{-5}; 3, 14.7 × 10^{-5}; 4, 29.3 × 10^{-5}; 5, 36.6 × 10^{-5}; 6, 47.60 × 10^{-5}; and 7, 58.5 × 10^{-5} mol l^{-1}

For this method the potential interfering effects of substances such as bilirubin, glucose, acetoacetate and albumin have been studied.[4–7] Results in the literature suggest that albumin is the most serious interferent. Pardue *et al.*[7] showed that the reaction of alkaline picrate with human serum albumin is very complex and that the interfering effect of the latter can be compensated for by using a curve-fitting method.

The aim of this work was to study the effect of albumin interference on the calibration step with respect to practical applications of the Jaffé reaction. Because the usual method for the determination of creatinine used in clinical laboratories

is the ΔA method, we attempted to evaluate the possibility of minimising the effect of albumin on this method so as to obtain more reliable results.

The effect of five albumin concentrations from 51.2 to 7.7 g l^{-1} on the calibration step was evaluated. The order of addition of the reagents was modified so that the experimental conditions were similar to those used for quantifying creatinine in serum. This modification leads to a decrease in the value of k_c from $(5.6 \pm 0.3) \times 10^{-3}$ to $(4.7 \pm 0.2) \times 10^{-3}$ s^{-1} (from three concentration values). However, the kinetic behaviour is unchanged (Fig. 3) as straight lines with the same slopes were obtained for creatinine standard concentrations of up to 14.6 mol l^{-1} in the range 45–180 s. To obtain the same value of k_c for higher creatinine concentrations, a smaller time interval is required (Table 3).

The effect of albumin on the kinetic behaviour of the Jaffé reaction for three different creatinine concentrations ($\geq 3.7 \times 10^{-5}$ mol l^{-1}) is shown in Fig. 4.

For low creatinine concentrations the ln ΔA - t graphs show that albumin has a marked effect on the early part of the reaction. This effect is less for albumin concentrations below 15.4 g l^{-1}. Other creatinine concentrations tested show a similar pattern. For example, for a 14.7×10^{-5} mol l^{-1} creatinine concentration the interfering effect of 25.4 g l^{-1} of albumin is smaller, and for a 36.6×10^{-5} mol l^{-1} creatinine concentration this effect is not significant for all albumin concentrations tested.

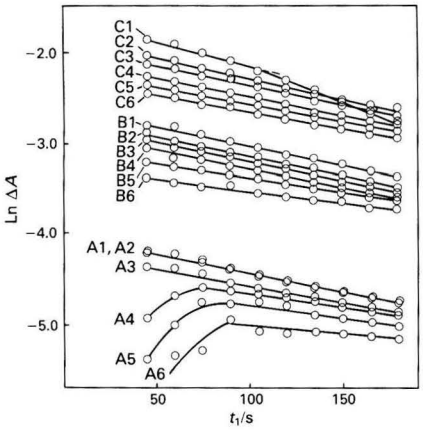

Fig. 4. Variation of ln ΔA with time for different creatinine and albumin concentrations. Creatinine: (A) 3.7×10^{-5}; (B) 14.6×10^{-5}; and (C) 36.6×10^{-5} mol l^{-1}. Albumin: 1, 0; 2, 7.7; 3, 15.4; 4, 25.4; 5, 38.4; and 6, 51.2 g l^{-1}. Conditions: picrate, 6.6×10^{-3} mol l^{-1}; sodium hydroxide, 0.2 mol l^{-1}; and temperature, 25 °C

Fig. 4 also shows that for higher creatinine concentrations, in the presence of albumin, the linear range of the ln ΔA - t graphs is greater than that obtained with creatinine alone. The dynamic range of creatinine concentrations is therefore increased in the presence of albumin with no decrease in the measurement time interval.

For five series of solutions containing different albumin concentrations and creatinine concentrations in the range 3.7×10^{-5}–36.6×10^{-5} mol l^{-1}, the ln ΔA - t graphs show a modification of the kinetic behaviour for albumin concentrations of 38.4 and 51.2 g l^{-1} and creatinine concentrations of less than 29.3×10^{-5} and 36.6×10^{-5} mol l^{-1}, respectively. For the other series of solutions, which contain 7.7, 15.4 and 25.4 g l^{-1} of albumin, respectively, the values of k_c obtained for the different creatinine concentrations tested (n) are 4.8 ± 0.3 ($n = 5$), 4.6 ± 0.4 ($n = 5$) and 4.2 ± 0.1 s^{-1} ($n = 8$), respectively. The first two values are similar to those obtained in the absence of albumin; however, the last value is lower, possibly due to the greater inhibiting effect of the albumin. The slope of the calibration graph is smaller for this albumin concentration (25.4 g l^{-1}) than that obtained with creatinine alone and with 7.7 and 15.4 g l^{-1} of albumin (Table 3). The values of s_{yx} and of the detection and quantification limits are also shown in Table 3. The values obtained are similar in all instances.

Conclusions

The kinetic study described here has shown that there is a variation in the kinetic behaviour of the system for the highest creatinine and picrate concentrations tested. Further, sodium hydroxide favours the dissociation of the complex formed, this effect being evidently greater for higher sodium hydroxide concentrations.

Experimental conditions for the determination of creatinine must be chosen so that the kinetic behaviour is the same in the dynamic concentration range, with a constant value of k_c.

In spite of these effects, the calibration study has shown that there is a wide variety of conditions that will yield a linear relationship between the analytical signal and the creatinine concentration. From the calibration graphs tested, we chose the ΔA *versus* concentration (c) equations as knowledge of the blank analytical signal is not necessary and also any constant systematic error can be corrected. From the different ΔA values studied, the best sensitivity was obtained under the following conditions: 0.2 M sodium hydroxide; 6.6×10^{-3} M picric acid; and a 45–180-s time interval, although the dynamic range of creatinine concentrations is smaller. Bearing in mind

Table 3. Effect of albumin on the calibration step

Albumin present/ g l^{-1}	Time/s	Creatinine concentration range/ 10^{-5} mol l^{-1}	Equation	s_{yx}	t-Test	Detection limit/ 10^{-5} mol l^{-1}	Quantification limit/ 10^{-5} mol l^{-1}
—	45–75	3.7–47.6	$a = (3 \pm 6) \times 10^{-3}$ $b = 810 \pm 20$	8.3×10^{-3}	Linear	0.2	0.6
—	45–105	3.7–36.6	$a = (-0.4 \pm 4) \times 10^{-3}$ $b = 1550 \pm 20$	5.9×10^{-3}	Linear	0.1	0.3
—	45–120	3.7–29.3	$a = (40 \pm 4) \times 10^{-3}$ $b = 1820 \pm 30$	5.0×10^{-3}	Linear	0.05	0.1
—	45–180	3.7–14.6	$a = (0.4 \pm 9) \times 10^{-3}$ $b = 3000 \pm 100$	7.5×10^{-3}	Linear	0.1	0.3
25.4	45–180	5.3–36.6	$a = (6 \pm 3) \times 10^{-2}$ $b = 1850 \pm 60$	9.6×10^{-3}	Linear	1.2	4.0
15.4	45–180	3.7–36.6	$a = (15 \pm 1) \times 10^{-3}$ $b = 2300 \pm 40$	1.1×10^{-2}	Linear	0.2	0.5
7.7	45–180	3.7–36.6	$a = (3 \pm 1) \times 10^{-2}$ $b = 2390 \pm 50$	1.5×10^{-2}	Linear	0.4	1.2

the low concentration of creatinine present in normal serum, these are the most suitable conditions.

Data obtained from the study of albumin interference indicate that its effect is greatest during the early part of the reaction. This substance will also introduce proportional errors into the determination of creatinine in serum because a variation in the slope of the calibration graphs is produced with respect to that obtained with creatinine alone.

References

1. Lustgarten, J. A., and Wenk, R. E., *Clin. Chem.*, 1972, **18**, 1419.
2. Vasiliades, J., *Clin. Chem.*, 1976, **22**, 1664.
3. Shoucri, R. M., and Pouliot, M., *Clin. Chem.*, 1977, **23**, 1527.
4. Kroll, M. H. and Elin, R. J., *Clin. Chem.*, 1983, **29**, 2044.
5. Kroll, M. H., Chesler, R., Hagengruber, C., Blank, D. W., Hestner, J., and Rawe, M., *Clin. Chem.*, 1986, **32**, 446.
6. Spencer, K., *Ann. Clin. Biochem.*, 1986, **23**, 1.
7. Pardue, H. L., Bacon, B. L., Nevius, M. G., and Skoug, J. W., *Clin. Chem.*, 1987, **33**, 278.
8. Commissariat a l'Energie Atomique, "Statistique Appliquée a l'Exploitation des Mesures," Masson, Paris, 1978.

Paper 8/02048E
Received May 23rd, 1988
Accepted December 5th, 1988

Kinetic and Chemometric Studies of the Determination of Creatinine Using the Jaffé Reaction

Part 2.* Application to Human Serum Samples: Kinetic Behaviour and Chemometric Evaluation of the Determination

Pilar Campíns-Falcó, Adela Sevillano-Cabeza and María Llobat-Estellés
Departamento de Química Analítica, Facultad de Química, Universidad de Valenica, Burjassot, Valencia, Spain

The kinetic behaviour of the reaction of alkaline picrate with creatinine in human serum samples was found to be similar to that for standard creatinine solutions containing albumin. A chemometric evaluation of the kinetic determination of creatinine using the Jaffé reaction was carried out. The analysis of variance (ANOVA) method applied to the $\Delta A_{45,180}$ values, obtained from two replicates of three different serum samples over a period of 10 d, showed that the between-day and between-replicate variations added a component to the total variability, the residual error (σ_R^2) being 5×10^{-5}. A study of the accuracy of the determination was carried out by means of percentage recovery experiments, Youden's method and the standard additions method. Percentage recovery experiments showed that albumin has a marked effect on the results obtained. The application of Youden's method to four serum samples indicated that the method does not have a constant bias error, but, by applying the standard additions method it was concluded that the method has a proportional bias error. The recovery factor, defined as the ratio of the slope of the standard additions graph to that of the standard response graph, was also calculated for the four serum samples. The best values were obtained with different standard response graphs (7.7, 15.4 and 25.6 g l^{-1} of albumin) for each sample. A modification of the routine procedure used in clinical laboratories is proposed. This modification is based on the principles of the standard additions method and gives better results for creatinine content than those obtained with the routine procedure.

Keywords: *Jaffé reaction; creatinine kinetic determination; chemometric study; constant bias error; proportional bais error*

In Part 1[1] of this series the kinetic data for the determination of creatinine using the Jaffé reaction were studied from an analytical viewpoint. The calibration step and the effect of albumin interference on the reaction were also studied. The main aim of the present paper was to evaluate the kinetic behaviour of the serum samples. Shoucri and Pouliot[2] showed that the rate constant for ten different serum samples varied from $(4.0 \pm 0.3) \times 10^{-3}$ to $(8.4 \pm 0.8) \times 10^{-3}$ s^{-1}.

In Part 1 a constant kinetic behaviour was observed over a specific creatinine concentration range and in this paper we endeavour to establish whether this conclusion can be extended to serum samples. With regard to the precision and accuracy of the determination of creatinine, Pardue *et al.*,[3] evaluated a curve-fitting method and obtained excellent results. The present paper demonstrates the repeatability of standards with or without human serum albumin and of serum samples and describes the application of the standard additions method to testing for proportional bias error. The accuracy of the method was evaluated from percentage recovery experiments.

Another aim of this paper was to evaluate the determination of creatinine chemometrically using the simple and fast change in absorbance (ΔA) method generally used in routine clinical work.

The detection of errors and elimination of the identifiable sources of error is a continuous process in analytical chemistry. The sources of systematic errors present in analytical methodology may be classified into four categories[4]: (1) calibration - system; (2) direct interference; (3) constant; and (4) proportional errors. Sources (1) and (2) are incorrigible errors, whereas constant and proportional errors are corrigible because the data recorded during the analysis of an actual sample can be used to calculate their magnitude and appropriate corrections can be made.

A constant error, as defined by Cardone,[5] is due to a significant relative response, either positive or negative, that is not attributable to the analyte. This can be measured directly or is mathematically related to a zero sample size arising from interferents in the matrix or to a physico-chemical property of the measurement system, which is independent of the size of the sample. From this definition it is evident that the blank, as a measure of the constant error, must be determined when both analyte and matrix are present; the problem can be resolved by applying Youden's method.[6]

A proportional error results from a significant relative change in the analyte response per unit of analyte concentration, either positive or negative. This is attributable to a parameter of the measurement system, procedure or method and its magnitude is constant at all levels of the analyte concentration.[5] The standard additions method posseses an intrinsic property, namely, that the standard additions calibration graph is an *in situ* procedure for normalisation of the proportional error of the method from the point at which the analyte spike is introduced.

When the analytical result is corrected for the constant and proportional bias errors, the results obtained by the standard additions method will agree with those given by the conventional calibration graph technique on the same sample within the variance of the random error of the method.

In this paper the presence or absence of bias errors was studied by applying the Youden and standard additions methods to the kinetic determination of creatinine in serum samples using the ΔA method and working conditions described previously.[1] The calibration step and the precision of the measurements was also examined by means of the analysis of variance (ANOVA) method,[1] and the diagnostic test (ratio of repeatability to reproducibility) for an intra-

* For Part 1 of this series see reference 1.

laboratory procedure was evaluated. In addition, a modification of the routine procedure generally used in clinical laboratories for quantifying creatinine is proposed.

Experimental

Instrumentation

The instrumentation and apparatus used were as described in Part 1.[1]

Reagents

The chemicals used were as described in Part 1[1] and all solutions were prepared as described previously.[1]

Procedure

Distilled water was added to appropriate volumes of albumin and creatinine working solutions (or human serum samples) to obtain a volume of 3 ml. Then, 2 ml of working alkaline picrate reagent were added and zero time was taken as the moment at which the last drop of this reagent was added. The absorbance was measured at 485 nm against a reagent blank prepared in the same way, but without creatinine, and was recorded as a function of time.

Results and Discussion

Kinetic Behaviour of Serum Samples

In Part 1[1] the kinetic behaviour of creatinine alone and of creatinine with alkaline picrate in the presence of albumin was described. In the present paper the kinetic behaviour of the serum samples was studied in order to extend the conclusions obtained previously[1] to these samples.

Four serum samples were tested, three of which had a normal creatinine content and the fourth an abnormal creatinine content. Two series of experiments were carried out for all the samples: in the first the creatinine content was varied but the sample matrix was kept constant, whereas in the second both creatinine and matrix contents were varied. Fig. 1 shows the ln ΔA - time graphs corresponding to a normal or an abnormal serum when the creatinine content was varied. For samples containing 2 ml of normal serum and various concentrations of creatinine standard (up to 31.1 mg l^{-1} in a final volume of 5 ml), straight lines with the same slope in the range 45–180 s were obtained. For the same amount of serum and 41.1 mg l^{-1} of creatinine standard a variation in the kinetic behaviour with time can be seen. This agrees with the kinetic behaviour observed when albumin is present.[1]

The abnormal serum produces the same behaviour and the slope for the two first solutions (which exhibit a unique kinetic behaviour) coincide with those obtained for the normal serum.

Fig. 2 shows the ln ΔA - time graphs corresponding to the two samples mentioned above when both creatinine and matrix contents were varied. For normal serum, only the solution containing 0.5 ml of serum in a final volume of 5 ml exhibits a variation in kinetic behaviour similar to that observed when albumin is present and when the creatine concentration is low.[1] As expected the abnormal serum shows the same behaviour observed for high creatinine concentrations. Fig. 2 also indicates that the slopes are similar for solutions of normal and abnormal serum, which do not exhibit the above-mentioned modifications of the kinetic behaviour. The albumin concentration present does not appear to produce an appreciable change in the values of k_c obtained. As we have previously observed a small variation in the value of k_c with albumin concentration,[1] it was necessary to ascertain whether the precision of the determination of the values of k_c corresponding to serum prevents this variation from being observed. Hence the precision of this determination was evaluated by an accurate method such as the ANOVA method[1] using Wilson's model.[7] The following variance components were then calculated: between-day (reproducibility); between-replicate (repeatability); and sample - day interaction. For this purpose three different serum samples were analysed in duplicate over a period of 10 d. The average value of k_c obtained for each sample was $(4.5 \pm 0.3) \times 10^{-3}$, $(4.7 \pm 0.4) \times 10^{-3}$ and $(4.6 \pm 0.4) \times 10^{-3}$ s^{-1}, respectively.

The ANOVA data calculations are shown in Table 1. The total sum of the squares is the total of the squared deviations of the individual values from the over-all mean. The mean squares (MS) are the ratios of the sum of the squares to the number of degrees of freedom. The experimental ratio F is given by $(MS)_i/(MS)_x$, where i = A, B or AB and $x = (MS)_R = \sigma_R^2$ for AB and $(MS)_{AB}$ for A and B. The expected values of the mean squares are given in the last column of Table 1.

The values of F_i were compared with the critical values of F. If F_i is greater than the tabulated value of F, then the hypothesis of no added variance due to a specific factor is rejected with the designated confidence level.

The calculated value of F_{AB} lies between the two tabulated $F_{0.05,18}$ and $F_{0.005,18}$ values; by convention a double asterisk is

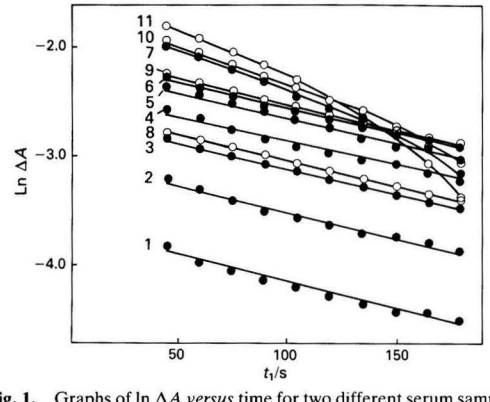

Fig. 1. Graphs of ln ΔA *versus* time for two different serum samples with a fixed matrix and various concentrations of creatinine added (●, normal matrix; and ○, abnormal matrix). Conditions: volume of serum samples taken: (●) 2 and (○) 1 ml. Picrate, 7.4×10^{-3} mol l^{-1}; sodium hydroxide, 0.2 mol l^{-1}; and creatinine concentration added for: (●) 1, 0; 2, 6.2; 3, 12.4; 4, 18.6; 5, 24.8; 6, 31.1; 7, 41.4; and for (○): 8, 0; 9, 12.4; 10, 24.8; and 11, 41.4 mg l^{-1}

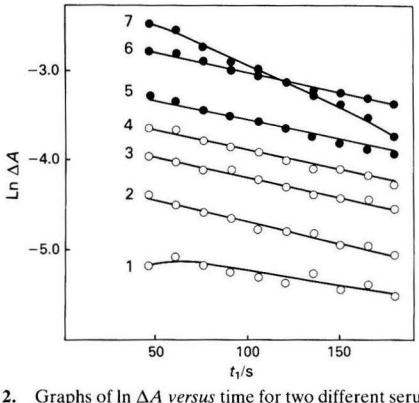

Fig. 2. Graphs of ln ΔA *versus* time for two different serum samples and various volumes of matrix taken; (○) normal matrix; and (●) abnormal matrix. Conditions: picrate, 7.4×10^{-3} mol l^{-1}; sodium hydroxide, 0.2 mol l^{-1}; and matrix volume: 1, 0.5; 2, 1.0; 3, 2.0; 4, 3.0; 5, 0.5; 6, 1.0; and 7, 2.0 ml

Table 1. ANOVA data calculations. If F_A and $F_B > F_{0.005}$ tabulated, then by convention a triple asterisk is placed next to the value. ns = not significant

Source of variation	Total sum of squares	Degrees of freedom	Mean squares	F	Error of mean squares
Between-day (reproducibility) (A)	1.30×10^{-6}	9	1.4×10^{-7}	0.84 ns	$\sigma_R^2 + 6\sigma_A^2 + 2\sigma_{AB}^2$
Between-replicate (repeatability) (B)	0.18×10^{-6}	2	0.9×10^{-7}	0.58 ns	$\sigma_R^2 + 20\sigma_B^2 + 2\sigma_{AB}^2$
Interaction (AB)	3.1×10^{-6}	18	1.7×10^{-7}	2.77***	$\sigma_R^2 + 2\sigma_{AB}^2$
Residual error	1.85×10^{-6}	30	0.6×10^{-7}	—	σ_R^2

Table 2. ANOVA method applied to the determination of creatinine in serum samples. The triple asterisk and ns are as in Table 1

Source of variation	Total sum of squares	Degrees of freedom	Mean squares	F	$F_{0.05}$	Error of mean squares
Between-day (A)	2.4×10^{-3}	9	2.7×10^{-4}	5.51***	2.21	$\sigma_R^2 + 6\sigma_A^2$
Between-replicate (B)	1.2×10^{-3}	2	6.0×10^{-4}	12.24***	3.32	$\sigma_R^2 + 20\sigma_B^2$
Interaction (AB)	1.0×10^{-3}	18	0.6×10^{-4}	1.16 ns	1.99–1.93	$\sigma_R^2 + 2\sigma_{AB}^2$
Residual error	1.5×10^{-3}	30	0.5×10^{-4}	—	—	σ_R^2

placed next to this value. When the value of F_{AB} is significant an interaction occurs, showing that the effect of a factor A is dependent on the level of factor B (and *vice versa*). This would mean that the variance of the value of k_c between samples is subject to day to day variation. The values of F_A and F_B obtained indicate that the between-day and between-replicate variance components are not significant, because F_A and F_B are less than the corresponding tabulated values.

The correctly estimated variance components are $\sigma_R^2 = 6.0 \times 10^{-8}$ and $\sigma_{AB}^2 = 5.5 \times 10^{-8}$; σ_A^2, σ_B^2 cannot be detected because of the small sizes of F_A and F_B. The average value of k_c is $(4.6 \pm 0.3) \times 10^{-3}$ s^{-1}. From these results it was not possible to confirm the existence of a clear variation in the values of k_c when the serum samples were varied; however, a small variation in the values of k_c was observed when working with albumin and creatinine standards.

Kinetic Determination of Creatinine in Serum Samples

In Part 1, from the calibrating graphs tested, the use of ΔA *versus* c equations was recommended, as with the ΔA method knowledge of the blank analytical signal was not necessary and any constant systematic error could be corrected. From the different ΔA values studied, the best sensitivity was obtained for the 45–180-s time interval, although the dynamic range of concentrations was smaller. Bearing in mind the low concentration of creatinine present in normal serum, it was considered that this time interval is the most suitable for quantifying creatinine in serum samples.

Initially, the repeatability of the ΔA values was tested for five replicates of three standards containing 4.1, 8.3 and 16.6 mg l^{-1} of creatinine. The relative standard deviations found were 4.3, 2.2 and 3.4%, respectively. The precision of the ΔA values obtained from serum samples was also tested using the ANOVA method by recording the analytical signals of two replicates of three different serum samples over a period of 10 d. The average value of ΔA obtained together with the standard deviation ($n = 20$) for the three samples were 0.17 ± 0.01, 0.156 ± 0.008 and 0.158 ± 0.007.

The ANOVA data are given in Table 2. The values of F_A and F_B obtained are significant, hence the between-day and between-replicate variations add a component to the total variability. The correctly estimated variance components are $\sigma_A^2 = 3.7 \times 10^{-5}$, $\sigma_B^2 = 2.8 \times 10^{-5}$ and $\sigma_R^2 = 5 \times 10^{-5}$. The repeatability is very close to the reproducibility, the ratio being greater than 0.7 (ratio = 0.9), which signifies that our laboratory is performing consistently.

After the precision of the analytical signal had been tested, the next step was to study the accuracy of the determination. To do this, known amounts of creatinine were added to aliquots of three serum samples with a normal creatinine content and the percentage recovery was calculated using the calibration graphs obtained for serum samples containing 0, 7.7, 15.4 and 25.6 g l^{-1} of albumin.[1] The graph of percentage recovery *versus* standard creatinine added is shown in Fig. 3. As can be seen the percentage recovery varies for the different calibration graphs used, which were obtained for creatinine alone or creatinine with different amounts of albumin. In all the samples tested the percentage recovery increased with an increase in the albumin content. It was also found that for each sample, a unique calibration graph with a specific albumin content exists giving the best results. Hence for the first, second and third samples (A, B and C) the appropriate albumin contents are 15.4, 25.6 and 15.4 g l^{-1}, respectively. In all instances the worst results are obtained when the calibration graph for creatinine alone is used. From these results it can be concluded that the albumin content present in the serum sample influences the determination of creatinine using the Jaffé reaction and that a different calibration graph is therefore required for each serum sample.

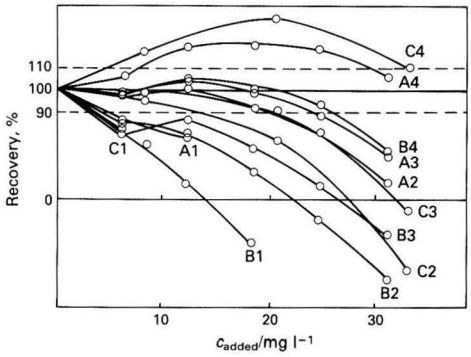

Fig. 3. Percentage recovery *versus* standard creatinine added showing the different calibration graphs obtained with various albumin concentrations: 1, 0; 2, 7.7; 3, 15.4; and 4, 25.6 g l^{-1} for serum samples A, B and C. Conditions: picrate, 7.4×10^{-3} mol l^{-1}; and sodium hydroxide, 0.2 mol l^{-1}

We shall now examine whether the determination of creatinine presents a constant and/or a proportional bias error and whether the results obtained from this study are concordant with those obtained in the percentage recovery experiments.

Constant and proportional bias errors are corrigible errors because the data recorded during the analysis of an actual sample can be used to calculate their magnitude and appropriate corrections can be made. From the definition of constant error it is evident that the blank, as a measure of the constant error, must be determined when both analyte and matrix are present. As discussed by Cardone,[4] the technique reported by

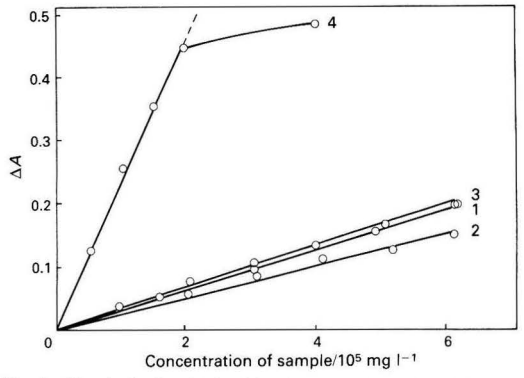

Fig. 4. Youden's plot obtained for three normal (1, 2 and 3) and one abnormal (4) serum sample. Conditions: picrate, 7.4×10^{-3} mol l^{-1}; and sodium hydroxide, 0.2 mol l^{-1}

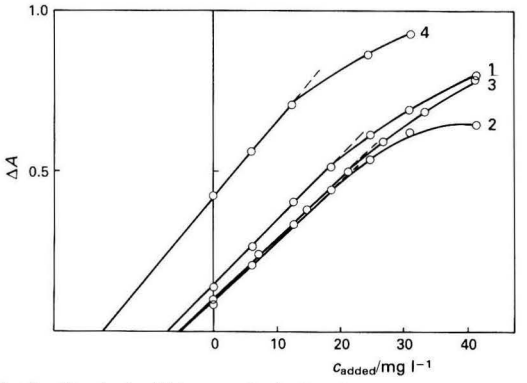

Fig. 5. Standard additions graphs for four (1, 2, 3 and 4) different serum samples. For details, see text. Conditions: picrate, 7.4×10^{-3} mol l^{-1}; and sodium hydroxide, 0.2 mol l^{-1}

Youden[6] in 1947 calculates the error in this way, because the constant error is determined in the presence of the sample matrix at zero sample concentration. This error is determined from the intercept of a straight line graph obtained by plotting analytical signal recorded *versus* sample content.

The Youden plots for four serum samples were obtained: three of the samples had a normal creatinine content and the fourth an abnormal creatinine content. Different aliquots of each serum sample were analysed and the corresponding analytical signals were recorded. The results obtained are illustrated in Fig. 4. The intercepts of the straight lines give the total Youden blank (TYB), which represents the constant error of the method extrapolated to the zero sample level as mentioned above. The TYB confidence intervals at the selected confidence level (95%) can be calculated to determine whether the expected zero value is included in the interval. In all instances tested it was found that the zero value is included in the corresponding interval and, therefore, it can be concluded that the method does not exhibit a constant bias error.

The standard additions method possesses an intrinsic property, namely, that the standard additions calibration graph is an *in situ* normalisation procedure from the point at which the analyte spike is introduced. Normalisation of the proportional error results in a change in the slope of the standard additions response graph from that of the standard response graph. Both the standard graph and the standard additions graph are the responses of the reference standard, the former in a solvent system and the latter in the same solvent system but with the sample matrix present. The recovery factor, defined as the ratio of the slope of the standard additions graph to that of the standard response graph, was proposed by Cardone[5] as a measure of the proportional error of the system.

To evaluate this bias error the standard additions method was applied to the four serum samples mentioned above and known amounts of creatinine (0–41.4 mg l^{-1}) were added to 2-ml aliquots of serum samples 1 and 2. For serum samples 3 and 4, 1.5- and 1.0-ml aliquots, respectively, were taken and the known amounts of standard creatinine added were 0–41.4 and 0–33.1 mg l^{-1}, respectively. The graphs of A *versus* c_{added} are shown in Fig. 5. Straight lines are obtained up to 18.6 mg l^{-1} of added creatinine for samples 1 and 2 and up to 20.7 and 12.4 mg l^{-1} of added creatinine for samples 3 and 4, respectively.

Table 3 gives the equations of the standard response graphs for different contents of albumin and those found by applying the standard additions method to the four serum samples tested. The percentage recovery factor is also given; the most suitable percentage recovery factor for each serum sample is obtained from different standard response graphs. For samples 1 and 3 this value is obtained from the standard response graph corresponding to 15.4 g l^{-1} of albumin present, whereas for samples 2 and 4 the percentage recovery factor is obtained from the standard response graphs corresponding to 25.6 and 7.7 g l^{-1} of albumin present, respectively. This means that the albumin present is an important factor in the kinetic determination of creatinine in serum samples.

To confirm this fact another experiment was performed by analysing different volumes of the four serum samples following the described procedure. The corresponding creati-

Table 3. Percentage recovery factors for different serum samples corresponding to different standard response graphs with varying albumin concentrations and to the standard additions graphs

Standard response graphs—

Albumin present/g l^{-1}	Equation*	s_{yx}	t-Test
0	$a = (6 \pm 8) \times 10^{-3}$ $b = (25.6 \pm 0.7) \times 10^{-3}$	7.6×10^{-3}	Linear
7.7	$a = (3 \pm 1) \times 10^{-2}$ $b = (21.2 \pm 0.4) \times 10^{-3}$	1.3×10^{-2}	Linear
15.4	$a = (13 \pm 9) \times 10^{-3}$ $b = (20.5 \pm 0.4) \times 10^{-3}$	1.1×10^{-2}	Linear
25.6	$a = (2 \pm 2) \times 10^{-2}$ $b = (17.4 \pm 0.7) \times 10^{-3}$	1.9×10^{-2}	Linear

Standard additions graphs—

Sample	Equation	s_{yx}	t-Test
1	$a = (14 \pm 1) \times 10^{-2}$ $b = (20.3 \pm 0.9) \times 10^{-3}$	1.2×10^{-2}	Linear
2	$a = (11.1 \pm 0.6) \times 10^{-2}$ $b = (17.9 \pm 0.5) \times 10^{-3}$	7.1×10^{-3}	Linear
3	$a = (9.2 \pm 0.5) \times 10^{-2}$ $b = (19.8 \pm 0.4) \times 10^{-3}$	6.2×10^{-3}	Linear
4	$a = (4.3 \pm 0.5) \times 10^{-2}$ $b = (22.6 \pm 0.6) \times 10^{-3}$	5.0×10^{-3}	Linear

Recovery factor, %—

	Albumin content of calibration solution/ g l^{-1}			
Sample	0	7.7	15.4	25.6
1	79.3	95.8	99.0	116.7
2	69.9	84.4	87.3	102.9
3	77.3	93.4	96.6	113.8
4	88.3	106.6	110.2	129.9

* a = intercept; b = slope.

Table 4. Creatinine concentration found using the conventional mathematical equation and standards containing various concentrations of albumin

		Concentration found/mg l^{-1}				
	Volume	Albumin content of standard/g l^{-1}				Standard additions
Sample	taken/ml	0	7.7	15.4	25.6	method
1	1	17.0*	18.5	20.5	23.1	17.0
		17.0†	19.7	20.8	23.3	
	2	13.0	14.4	15.9	17.9	
		13.2	15.3	16.1	18.2	
	3	11.2	12.3	13.7	15.4	
		11.3	13.1	13.8	15.6	
2	1.5	11.3	12.3	13.7	15.4	15.5
		11.3	13.1	13.8	15.6	
	2	10.3	11.3	12.5	14.1	
		10.4	12.0	12.7	14.3	
	2.5	9.0	9.8	10.9	12.3	
		9.1	10.5	11.1	12.5	
	3	8.7	9.6	10.6	12.0	15.7
		8.8	10.2	10.8	12.1	
3	1.5	11.3	12.3	13.7	15.4	
		11.3	13.1	13.8	15.6	
	3	9.3	10.3	11.4	12.8	
		9.4	10.9	11.5	13.0	
4	0.5	93.0	102.5	113.9	128.1	95.0
		94.3	109.2	115.3	129.7	

* Values obtained for standards containing 4.1 mg l^{-1} of creatinine.
† Values obtained for standards containing 8.3 mg l^{-1} of creatinine.

nine concentration was calculated from the equation generally used for quantifying creatinine in routine work

$$c_x = c_t \frac{\Delta A_x}{\Delta A_t} \quad \ldots \quad (1)$$

where c_x and c_t are the creatinine concentrations present in the sample and standard, respectively, and ΔA_x and ΔA_t are the corresponding analytical signals obtained. Table 4 shows the results obtained for the four serum samples using standards containing creatinine (4.1 and 8.3 mg l^{-1}) and different amounts of albumin (0, 7.7, 15.4 and 25.6 g l^{-1}). When the volume of serum sample taken is the same as that used in the standard additions method the results obtained agree with those found from the percentage recovery factor. In addition, when the volume taken is smaller or larger, the best values are found for an albumin content that depends on the corresponding dilution.

Therefore, it is not possible to use a unique standard for quantifying creatinine in any particular serum sample. From these results a modification is proposed which involves the analysis of a solution containing a known amount of creatinine standard and the same volume of serum sample, instead of the standard solution normally used as a reference.

Let us consider a serum sample solution with an unknown creatinine concentration (c_m) and a reference solution with a creatinine concentration $c_r = c_m + c_{added}$, where c_{added} is the concentration of standard creatinine added. As ΔA_m and ΔA_r ($= \Delta A_m + \Delta A_{added}$) are the analytical signals corresponding to c_m and c_r, respectively, then equation (1) becomes

$$c_m = (c_m + c_{added}) \frac{\Delta A_m}{\Delta A_m + \Delta A_{added}} \quad \ldots \quad (2)$$

The operational equation is easily obtained from equation (2) and has the form

$$c_m = \frac{\Delta A_m}{\Delta A_r - \Delta A_m} \cdot c_{added} \quad \ldots \quad (3)$$

Table 5. Results obtained by application of the proposed modification and by the standard additions method

			Concentration found/mg l^{-1}	
Sample	Volume taken/ml	Creatinine added/mg l^{-1}	Equation (3)	Standard additions method
1	2.0	6.2	18.1	17.0
	2.0	12.4	16.7	
2	2.0	6.2	15.5	15.5
	2.0	12.4	14.9	
3	1.5	8.3	14.7	15.7
4	1.0	12.4	95.2	95.0

Table 5 presents the results obtained for the four serum samples using equation (3) and it can be seen that they show good agreement with those found using the standard additions method.

The percentage recovery obtained when 6.2 mg l^{-1} of standard creatinine was added to the different serum samples was between 80 and 110% using the recommended procedure [equation (3)] and between 40 and 70% using equation (1) (the visual procedure). The recommended procedure is therefore more accurate than the conventional procedure. On the other hand, the reproducibility of the proposed method will be similar to that obtained with the conventional procedure, because the analytical signal employed is the same.

In conclusion, the kinetic behaviour of the serum samples tested corresponds to that observed previously with standards of creatinine and albumin.[1] With regard to the kinetic determination of creatinine in serum samples, the between-day and between-replicate variations add a component to the total variability, as demonstrated by application of the ANOVA method.

The application of Youden's method shows that the proposed method does not exhibit a constant systematic error. Use of the standard additions method shows that the determination exhibits a proportional systematic error. From these results, a modification of the routine procedure used in clinical laboratories for the determination of creatinine in serum samples is proposed. The modified procedure is more accurate than the conventional procedure.

Recommended Procedure

A 2.0-ml volume of human serum sample is placed in each of two test-tubes. Then, 1 ml of distilled water is added to the first tube and 1 ml of standard creatinine solution containing between 31.0 and 93.0 mg l^{-1} of creatinine to the second. A 2-ml aliquot of the working alkaline picrate reagent is then added to each tube and the change in absorbance between 45 and 180 s is measured at 485 nm and at a temperature of 25 °C. The corresponding creatinine concentration is calculated from equation (3). If the ΔA value is greater than 0.50, 1 ml of serum sample should be taken so that the results obtained are not affected by the variation in the matrix to analyte ratio.

References

1. Llobat-Estellés, M., Sevillano-Cabeza, A., and Campíns-Falcó, P., *Analyst*, 1989, **114**, 597.
2. Shoucri, R. M., and Pouliot, M., *Clin. Chem.*, 1977, **23**, 1527.
3. Pardue, H. L., Bacon, B. L., Nevius, M. G., and Skoug, J. W., *Clin. Chem.*, 1987, **33**, 278.
4. Cardone, M. J., *J. Assoc. Off. Anal. Chem.*, 1983, **66**, 1257.
5. Cardone, M. J., *J. Assoc. Off. Anal. Chem.*, 1983, **66**, 1283.
6. Youden, W. J., *Anal. Chem.*, 1947, **19**, 946.
7. Wilson, A. L., *Talanta*, 1970, **17**, 31.

Paper 8/02046I
Received May 23rd, 1988
Accepted December 5th, 1988

Analysis of Trifluralin and Other Dinitroaniline Herbicide Residues by Zero-order and Derivative Ultraviolet Spectrophotometry

Seydou Traore
Département de Chimie, Faculté des Sciences, Université C. A. Diop de Dakar, Dakar, Senegal
Jean-Jacques Aaron*
Institut de Topologie et de Dynamique des Systèmes de l'Université Paris 7, Associé au CNRS, 1 rue Guy de la Brosse, 75005 Paris, France

The utility of zero-order and first- and second-derivative ultraviolet (UV) spectrophotometry for the identification of benfluralin, trifluralin, isopropalin and oryzalin is discussed. These four herbicides were determined by zero-order and first-derivative UV spectrophotometry, with linear calibration graphs established between 50 and 100 concentration units and limits of detection ranging from 1 to 7 μg ml^{-1}. The application of these techniques to the residue analysis of fortified soils and niebe and peanut leaves is described. Trifluralin residues were found to be 6.7, 8 and 1.7 μg ml^{-1} in samples of fortified soils, niebe leaves and peanut leaves, respectively. Isopropalin residues were found to range from 62 to 154 μg ml^{-1} in samples of fortified niebe leaves.

Keywords: *Derivative ultraviolet spectrophotometry; dinitroanaline herbicides; trifluralin residues; isopropalin residues*

Trifluralin and other dinitro-*N,N*-dialkylaniline derivatives represent a class of powerful herbicides that are mainly used to control crops in tropical African countries because of their plant growth inhibiting properties.[1] However, they have the disadvantage of being relatively toxic and, therefore, a variety of analytical methods have been proposed to identify and/or quantify their residues in several types of media and substrates.[1–28] To date, dinitroaniline herbicides have been evaluated mainly by gas chromatography (GC),[1,3,6,7,10–19] gas chromatography - mass spectrometry (GC - MS),[20] high-performance liquid chromatography (HPLC),[21,22] thin-layer chromatography (TLC),[23,24] ^{19}F Fourier transform nuclear magnetic resonance (NMR) spectroscopy,[25] negative chemical ionisation MS,[26] ultraviolet (UV) spectrophotometry[1,2,6,7,9,27] and photochemical fluorimetry.[28] Several analytical studies have been concerned with the evaluation of trifluralin, benfluralin and isopropalin in formulations and technical-grade materials.[1,2,6–9,17,27,28] The analysis of benfluralin, trifluralin and isopropalin residues has been performed by GC, with detection limits varying between 0.1 ng g^{-1} and 1 μg ng^{-1}, according to the type of column and detection system used.[1,3–5,13–18] A TLC method has also been reported for the analysis of trifluralin residues in paprika, with a detection limit of 20 pg ml^{-1}.[23] For oryzalin residue analysis, derivatised GC and GC - MS techniques, with detection limits of 0.001–0.05 μg g^{-1}, and 0.05 ng, respectively, have been proposed by Bardalaye and Wheeler.[10,20] Also, HPLC methods have been described for oryzalin residue analysis in soil and wastewater, with detection limits of 0.02 μg g^{-1} and 0.5 ng ml^{-1}, respectively.[21,22]

Although UV spectrophotometry has been utilised to a much lesser extent than other techniques because of its lower sensitivity and selectivity, it has been claimed by several workers[6,9,27] that this is a very precise and reproducible method for the quantification of dinitroaniline herbicides.

The aim of this work was to investigate the suitability of zero-order and first- and second-derivative UV spectrophotometry for identifying and quantifying several dinitroaniline herbicides in technical-grade material. The usefulness of UV spectrophotometry for the analysis of herbicide residues in plants and soils was also examined.

* To whom correspondence should be addressed.

Experimental

Materials

The dinitroaniline derivatives used in this work were trifluralin (α,α,α-trifluoro-2,6-dinitro-*N,N*-dipropyl-4-toluidine), benfluralin (*N*-butyl-*N*-ethyl-α,α,α-trifluoro-2,6-dinitro-4-toluidine), isopropalin (2,6-dinitro-*N,N*-dipropylcumidine) and oryzalin [4-(dipropylamino)-3,5-dinitrobenzenesulphonamide]. They were commercial preparations (technical-grade, Lilly Research Centre, Windlesham, Surrey, UK)

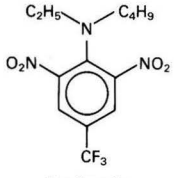

Benfluralin

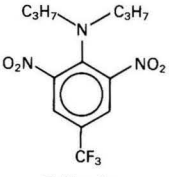

Trifluralin

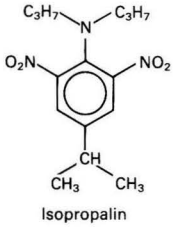

Isopropalin

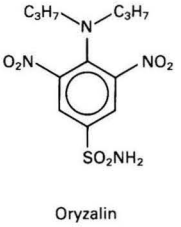

Oryzalin

donated by Rhone Poulenc-Phytosanitaire (Lyon, France). All the dinitroaniline derivatives were used as received. Their purity was checked by measuring their melting- or boiling-points, which were found to be in good agreement with literature values.

The solvents used were spectrophotometric-grade cyclohexane, ethanol and methanol (Aldrich, Strasbourg, France).

Apparatus

Zero-order and first- and second-derivative absorption spectra were recorded at room temperature (298 K), between 500 and 200 nm, using a Beckman Model 3600 UV - visible

spectrophotometer. A Beckman Series 30 derivative accessory unit was used to obtain the derivative spectra. The wavelength calibration was checked by using a holmium oxide filter supplied by Beckman. The accuracy of the absorbance measurements was about 5%.

Procedures

Fortification

Niebe (*Vigna sinensis*) and peanuts (*Arachis hypogaea*), which are widely used crops in western Africa, were fortified with standard solutions of trifluralin and isopropalin in methanol. Four different types of treatment were carried out.

Treatment 1. Two portions of soil were used: one acted as a blank, and the other was treated with 1.6×10^{-3} M trifluralin methanolic solution. Then, niebe seeds were placed and germinated in both portions of soil.

Treatment 2. Two portions of soil in which niebe seeds had previously been germinated were used. The first portion was treated with 2% trifluralin solution and the other was used as a blank.

Treatment 3. This was the same as Treatment 1, except that peanut seeds were used instead of niebe seeds.

Treatment 4. Two portions of soil were used: one acted as a blank, and the other was treated with 7.1% isopropalin solution. Then, niebe seeds were placed and germinated in both portions of soil.

Extraction

The procedure employed for extraction of the herbicide residues was adapted from that described by Johnson and co-workers.[29,30] A representative 25-g sample of soil, leaves or seeds was blended with 200 ml of methanol. Seeds were ground before use. The methanolic solution was stirred moderately for 10 min and then stored in a refrigerator (+5 °C) for 24 h in order to achieve complete dissolution of the chlorophyll pigments (for the extraction from leaves). The methanolic solution was filtered through Whatman No. 1 filter-paper and 40% sodium chloride solution was added to the filtrate.

Results and Discussion

Zero-order UV Absorption Spectra

The UV absorption spectra of benfluralin, trifluralin, isopropalin and oryzalin are characterised by two broad, moderately absorbing bands in the 240–285 and 375–385 nm regions, respectively (Table 1). The former band is attributed to a ^1L_a transition and the latter band to a ^1L_b transition, according to the spectral notation of Platt.[32] The $\lambda_{max.}$ values are in excellent agreement with previously published data.[6,7,30] However, the experimental $\lambda_{max.}$ values for the ^1L_b transition band are significantly smaller than those calculated using the strict additivity rule of substituent effects on the UV spectra of benzenic compounds.[31] The differences between the calculated and experimental $\lambda_{max.}$ values range from 31 nm for trifluralin to 70 nm for oryzalin (Table 1). This apparent non-additivity of substituent effects is probably due to the partial steric inhibition of resonance by the dialkylamino and nitro groups in the *ortho* position. It is also worth noting that the change in solvent polarity does not produce a significant shift in the $\lambda_{max.}$ values for any of the dinitroaniline derivatives studied.

As can be seen from Table 1, the $\lambda_{max.}$ values of the ^1L_a and ^1L_b bands are very close for benfluralin, trifluralin and oryzalin; hence it is not possible to identify these three compounds using their zero-order UV spectra. In contrast, isopropalin can be distinguished from the other dinitroanilines because of the lower $\lambda_{max.}$ value of its ^1L_a band.

Table 1. Zero-order UV spectral characteristics of benfluralin, trifluralin, isopropalin and oryzalin

Compound*	Solvent†	$\lambda_{max.}$‡/nm (log $\varepsilon_{max.}$)	$\lambda_{max.}$ (calculated)§/nm
Benfluralin	C	275 (3.96); 376 (3.43)¶	—
	M	275 (4.10); 376 (3.62)	417
Trifluralin	C	275 (3.80); 376 (3.34)‖	—
	M	276 (3.91); 386 (3.41)	417
Isopropalin	C	240 (3.04); 380 (2.92)**	—
	M	240 (3.15); 380 (3.11)	423
Oryzalin	C††	—	—
	M	285 (4.00); 385 (3.49)‡‡	455

* Herbicide concentrations were between 1×10^{-4} and 5×10^{-4} M.

† C = cyclohexane; M = methanol.

‡ The short- and long-wavelength bands correspond to ^1L_a and ^1L_b transitions, respectively. Precision: ±1 mm.

§ Values of $\lambda_{max.}$ calculated for the ^1L_b transition using the substituent increments ($\Delta\lambda$) strict additivity rule.[31] Values of $\Delta\lambda$ were as follows: $\Delta\lambda_{NO_2} = 65$; $\Delta\lambda_{NR_2} = 26$; $\Delta\lambda_{i\text{-}C_3H_7} = 13$; and $\Delta\lambda_{SO_2NH_2} = 45$ nm.[31] In the absence of a $\Delta\lambda_{CF_3}$ value, $\Delta\lambda_{CH_2F} = 7$ nm[31] was used. $\lambda_{max.}^{MeOH}$ (C_6H_6) = 254 nm.[31]

¶ Literature[7] values: 275 nm (—); 376 nm (3.38).

‖ Literature[7] values: 275 nm (—); 376 nm (3.38).

** Literature[6] values: 230 nm (4.15); 386 nm (3.23) in hexane.

†† Oryzalin was not soluble in cyclohexane.

‡‡ Literature[30] values: 285 nm (3.66); 385 nm (3.11).

Table 2. First- and second-derivative UV spectral characteristics of benfluralin, trifluralin, isopropalin and oryzalin in methanol at 298 K

Compound*	Wavelength†/nm: First-derivative spectrum	Wavelength†/nm: Second-derivative spectrum
Benfluralin . .	240, 262_m, 286, 342_m, 446	252, 270_m, 295, (304)
Trifluralin . .	240, 261_m, 285, 343_m, 444	250, (264_m), 267_m, 293
Isopropalin . .	244, 266, 455	225, 230, 240_m, 246, 258_m, (263_m), 272, 282
Oryzalin . .	244, 268_m, 292, 446	253, 282_m, (286_m), 302

* Herbicide concentrations were between 1×10^{-4} and 5×10^{-4} M.

† Wavelengths quoted are the maxima. Wavelengths denoted with a subscript m correspond to the minima. Shoulders are given in parentheses.

First- and Second-derivative UV Spectra

The first- and second-derivative UV spectra of benfluralin, trifluralin, isopropalin and oryzalin were recorded in methanol (Table 2). As expected, these spectra provide a greater number of components than the zero-order spectra and this should improve the analytical identification of these compounds. Nevertheless, the first-derivative spectra of benfluralin and trifluralin (Fig. 1) are almost identical, with maxima (peaks) at about 240, 285 and 445 nm and minima (troughs) at about 261 and 343 nm (Table 2). This similarity prevents the identification of both compounds. In contrast, their second-derivative spectra are characterised by maxima at 252 and 295 nm, a shoulder at 304 nm and a minimum at 270 nm for benfluralin, and by maxima at 250 and 293 nm, a shoulder at 264 nm and a minimum at 267 nm for trifluralin (Fig. 1), which makes it possible to distinguish between them. The first-derivative spectrum of isopropalin exhibits three peaks at 244, 266 and 455 nm, whereas that of oryzalin shows three peaks at 244, 292 and 446 nm and a trough at 268 nm, which allows their differentiation. The second-derivative spectra of isopropalin and oryzalin also exhibit very different wavelength values, with maxima at 225, 230, 246, 272 and 282 nm, minima at 240 and 258 nm and a shoulder at 263 nm for the former compound and maxima at 253 and 302 nm, a minimum at 282 nm and a shoulder at 286 nm for the latter herbicide (Table 2). Hence it is possible to determine both compounds qualitatively and also to distinguish them from

benfluralin and trifluralin. A similar finding has been reported recently for the second-derivative spectral identification of purines and pyrimidines.[33]

Analytical Figures of Merit

A statistical treatment of the analytical data for the determination of the four herbicides by zero-order and first-derivative UV spectrophotometry is presented in Table 3. As expected, the zero-order absorbance $A_{max.}$ (absorbance value at analytical wavelength $\lambda_{max.}$) correlates very well with the concentration of the herbicides. The correlation coefficient is greater than 0.97 for all four compounds. The zero-order linear dynamic ranges (LDR) are between 50 and 100 concentration units. For the first-derivative spectra, the peak to base line amplitudes, which were determined at selected wavelengths as described previously,[33] give satisfactory correlations with the concentrations of herbicides, yielding correlation coefficients very close to unity. The LDR values range from 10 to 50 concentration units (Table 3).

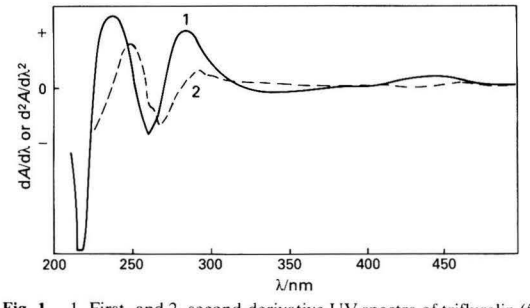

Fig. 1. 1, First- and 2, second-derivative UV spectra of trifluralin (5×10^{-4} M) in methanol

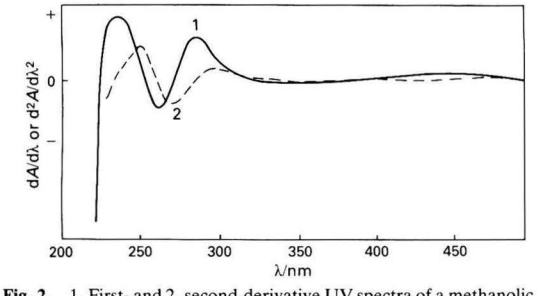

Fig. 2. 1, First- and 2, second-derivative UV spectra of a methanolic extract of soil fortified with 2% trifluralin solution

Limits of detection (LOD) were evaluated from zero-order and first-derivative spectral measurements and were obtained by determining the concentration of analyte (in $\mu g\ ml^{-1}$) giving an absorbance (A) or a $dA/d\lambda$ signal (at the analytical wavelength) equal to three times the fluctuation of the A_{sv} or $(dA/d\lambda)_{sv}$ value of the solvent (noise). The solvent signal values were calculated for 8–10 samples. Except for oryzalin, the zero-order LOD values (range, 1–7 $\mu g\ ml^{-1}$) are lower than the corresponding first-derivative values (range, 1.5–5.0 $\mu g\ ml^{-1}$) (Table 3). They are comparable to those reported in the literature for formulations and technical-grade materials using GC, zero-order UV spectrophotometry and photochemical fluorimetry,[1,2,6–9,28] which vary between 0.001 and 20 $\mu g\ ml^{-1}$ according to the analytical method and the particular herbicide.

Analysis of Trifluralin Residues in Soil

The zero-order and first- and second-derivative UV spectra of trifluralin residues in soil were recorded in methanol. The soil was fortified with 2% trifluralin solution. The zero-order UV spectrum exhibits two maxima at 275 and 382 nm, which are characteristic of trifluralin (Table 1). The first- and second-derivative spectra are virtually identical with those of trifluralin (Fig. 1), with maxima at 238, 284 and 444 nm and a

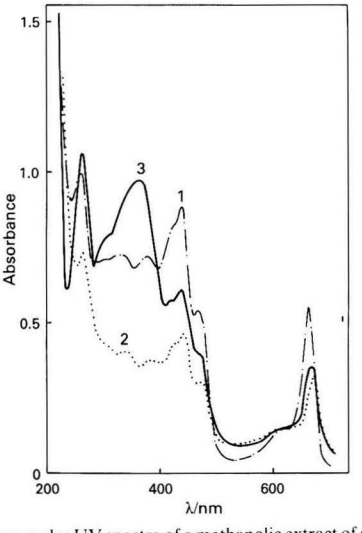

Fig. 3. Zero-order UV spectra of a methanolic extract of chlorophyll from niebe leaves: 1, untreated; and fortified with 2% trifluralin solution 2, before and 3, after germination of the seeds

Table 3. Data obtained from the zero-order and first-derivative spectral measurements of benfluralin, trifluralin, isopropalin and oryzalin

Compound	Spectral measurement*	λ_{AN}†/nm	LDR‡	Slope§	Correlation coefficient§	LOD¶/ $\mu g\ ml^{-1}$
Benfluralin	Zero order	376	100	1441	0.976	1.0
	First derivative	240	10	5.3	0.995	3.0
Trifluralin	Zero order	386	100	3217	0.998	1.0
	First derivative	285	50	5.6	0.968	1.5
Isopropalin	Zero order	380	50	1173	0.998	1.0
	First derivative	266	10	3.2	0.998	5.0
Oryzalin	Zero order	385	100	2304	0.998	7.0
	First derivative	244	20	8.2	0.999	2.5

* All first-derivative spectral measurements were performed using the peak to base line amplitudes of the first-derivative maxima (zero-crossing method).[33]

† λ_{AN} = analytical wavelength of the peak used for determining the calibration graph.

‡ LDR = linear dynamic range, corresponding to the ratio of the upper concentration of linearity (within 5%) to the limit of detection.

§ Values calculated by the statistical treatment of 4–6 measurements for each calibration graph.

¶ LOD = limit of detection, defined as the concentration of the solution giving a signal to noise ratio of 3.

minimum at 261 nm (first-derivative spectrum, Fig. 2) and maxima at 250 and 294 nm and a minimum at 268 nm (second-derivative spectrum, Fig. 2). By using the zero-order spectrophotometric calibration graph, the trifluralin residue was found to be about 6.7 μg ml^{-1} in fortified soil.

Analysis of Trifluralin Residues in Niebe and Peanut Leaves

Figs. 3 and 4 show the zero-order UV spectra of extracts of niebe and peanut leaves fortified in the field with 2% trifluralin solution. When the treatment was performed before germination of the seeds, no characteristic band for trifluralin was detected and only bands attributable to the chlorophyll pigments present in the methanolic extract were found, with maxima (or shoulders) at 225, 260, 440 (615) and 665 nm (Fig. 3, curves 1 and 2 and Fig. 4, curve 1). The same behaviour was observed for the first- and second-derivative spectra. This demonstrates the absence of trifluralin residues under these conditions. In contrast, when the treatment of niebe and peanuts was performed after germination of the seeds, two bands were obtained at 265 and 380 nm, very close to the characteristic maxima of trifluralin (Fig. 3, curve 3 and Fig. 4, curve 2). On the basis of the calibration graphs, the trifluralin residues were calculated to be about 8 and 1.7 μg ml^{-1} in fortified niebe and peanut leaves, respectively. The recoveries ranged from 80 to 90% at these fortification levels.

Analysis of Isopropalin Residues in Niebe Leaves

The zero-order UV spectra of extracts of niebe leaves fortified in the field with 7.1% isopropalin solution are shown in Fig. 5. When the plants were treated before germination of the seeds, the spectrum was identical with that of the untreated extract (Fig. 5, curves 1 and 2), which indicates the absence of isopropalin residues under these conditions. The same conclusion can be reached from examination of the first- and second-derivative spectra, which are similar for both isopropalin-treated and -untreated extracts (Figs. 6 and 7). The maxima and minima are ascribed to the chlorophyll pigments of the extracts. In contrast, the spectra of extracts of niebe leaves fortified with isopropalin after germination of the seeds show the presence of additional bands. The zero-order spectrum exhibits two maxima at about 250 and 380 nm (Fig. 5, curve 3), which can be attributed to isopropalin. The slight red-shift observed for the first maximum wavelength relative to that of the ^1L_a band of pure isopropalin is probably due to a certain degree of overlap with the spectrum of chlorophyll. The first-derivative spectrum exhibits a broad maximum between 266 and 280 nm, which can be ascribed to isopropalin. Similarly, the second-derivative spectrum shows maxima at 225, 243 and 280 nm and a broad minimum at about 260 nm, which can be attributed to isopropalin (Fig. 8). By using the zero-order and first-derivative spectrophotometric calibration graphs, the isopropalin residues were calculated to be between 62 and 154 μg ml^{-1} when the niebe leaves were fortified with 7.1% isopropalin solution after germination of the seeds. The recoveries ranged from 80 to 95% at these fortification levels.

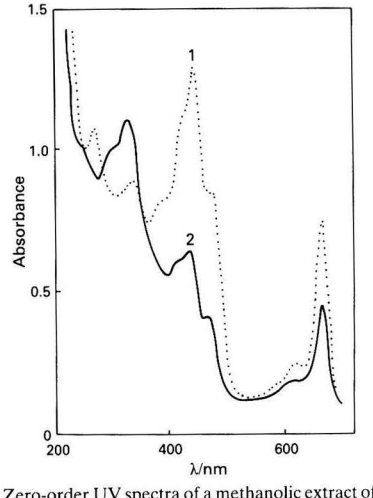

Fig. 4. Zero-order UV spectra of a methanolic extract of chlorophyll from peanut leaves: 1, untreated; and 2, fortified with 2% trifluralin solution after germination of the seeds

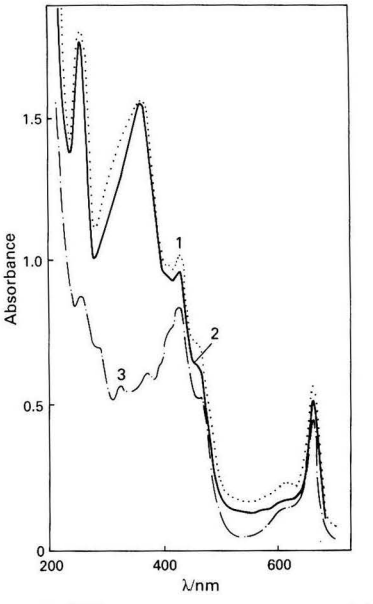

Fig. 5. Zero-order UV spectra of a methanolic extract of chlorophyll from niebe leaves: 1, untreated; and fortified with 7.1% isopropalin solution 2, before and 3, after germination of the seeds

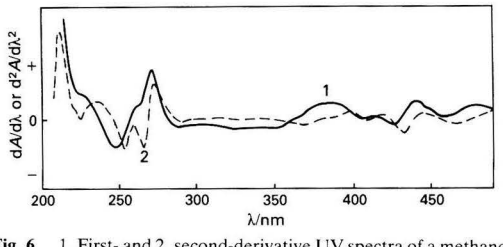

Fig. 6. 1, First- and 2, second-derivative UV spectra of a methanolic extract of chlorophyll from untreated niebe leaves

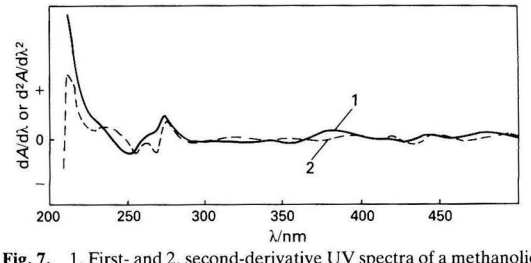

Fig. 7. 1, First- and 2, second-derivative UV spectra of a methanolic extract of chlorophyll from niebe leaves fortified with 7.1% isopropalin solution before germination of the seeds

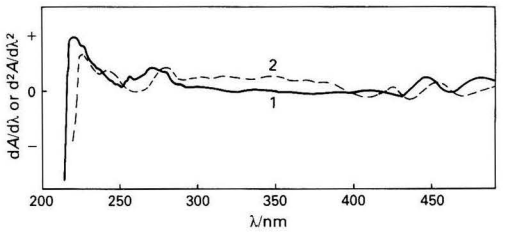

Fig. 8. 1, First- and 2, second-derivative UV spectra of a methanolic extract of chlorophyll from niebe leaves fortified with 7.1% isopropalin solution after germination of the seeds

Conclusion

It has been demonstrated that first- and second-derivative UV spectrophotometry is a useful and reliable technique for the identification of dinitroaniline herbicides. Also, zero-order and first-derivative spectral measurements can be used for the determination of benfluralin, trifluralin, isopropalin and oryzalin, with good precision, down to about 1.0 μg ml^{-1}. These techniques were applied to the analysis of trifluralin and isopropalin residues in soils and niebe and peanut leaves.

References

1. Johnson, W. S., and Franck, R., *in* Zweig, G., *Editor*, "Analytical methods for Pesticides and Plant Growth Regulators," Volume IV, Academic Press, New York, 1974, p. 335.
2. Cyr, T., Cyr, N., and Haque, R., *in* Zweig, G., *Editor*, "Analytical Method for Pesticides and Plant Growth Regulators," Volume IX, Academic Press, New York, 1977, p. 75.
3. Hall, M., and Mallew, D. N. B., *J. Chromatogr. Sci.*, 1976, **14**, 451.
4. Smith, A. E., *J. Agric. Food Chem.*, 1972, **20**, 829.
5. Lawrence, J. F., *J. Chromatogr.*, 1976, **121**, 85.
6. Decker, O. D., and Franck, R., *J. Assoc. Off. Anal. Chem.*, 1974, **57**, 645.
7. Hambleton, L. G., *J. Assoc. Off. Anal. Chem.*, 1973, **56**, 567.
8. Fuzesi, M., *J. Assoc. Off. Anal. Chem.*, 1971, **54**, 711.
9. Hambleton, L. G., *J. Assoc. Off. Anal. Chem.*, 1971, **54**, 125.
10. Bardalaye, P. C., and Wheeler, W. B., *Analyst*, 1984, **109**, 255.
11. Stan, H. J., and Mrowetz, D., *J. Chromatogr.*, 1983, **279**, 173.
12. Fehringer, N. V., and Walters, S. M., *J. Assoc. Off. Anal. Chem.*, 1984, **67**, 91.
13. Lee, M. B., and Chau, A. S. Y., *J. Assoc. Off. Anal. Chem.*, 1983, **66**, 1322.
14. Edgerton, T. R., Scott, W., and Linder, R. E., *J. Anal. Toxicol.*, 1985, **9**, 15.
15. Cessna, A. J., Grover, R., Kerr, L. A., and Aldred, M. L., *J. Agric. Food Chem.*, 1985, **33**, 504.
16. Fehringer, N. V., and Walters, S. M., *J. Assoc. Off. Anal. Chem.*, 1986, **69**, 90.
17. Gudehn, A., and Kolmodinhedman, B., *J. Chromatogr.*, 1987, **387**, 420.
18. Brodesser, J., and Schoeler, M. F., *Vom Wasser*, 1987, **69**, 61.
19. Miellet, A., *Ann. Falsif. Expert. Chim. Toxicol.*, 1987, **80**, 467.
20. Bardalaye, P. C., Wheeler, W. B., and Templeton, J. L., *J. Chromatogr.*, 1984, **314**, 450.
21. Mary, T. D., and Loh, A., *Anal. Chem.*, 1980, **52**, 1381.
22. Warner, J. S., Engel, J. M., and Mondron, P. J., Report (1985), EPA/600/4-85/024, Order No. PB85–188 985; *Gov. Rep. Announce. (U.S.)*, 1985, **85**, Abstr. No. 535 873.
23. Halasi, R., and Damon, I. A., *Hvana Ishrana*, 1984, **25**, 205.
24. Kofman, I. Sh., "Proceedings of the 3rd International Symposium on Instrumentation for High Performance TLC," Institute of Chromatography, Bad Dueikheim, FDR, 1985, p. 113.
25. Mazzola, E. P., Borsetti, A. P., Page, S. W., and Bristol, D. W., *J. Agric. Food. Chem.*, 1984, **32**, 1102.
26. Moyer, J. R., and Elder, J. L., *J. Agric. Food Chem.*, 1984, **32**, 866.
27. Dabrowska, A., Gwiadza, M., and Kotarski, A., *Zesg. Prob. Postepow Nauk. Roln.*, 1986, **319**, 255.
28. Traore, S., and Aaron, J. J., *Anal. Lett.*, 1987, **20**, 1995.
29. Johnson, W. S., and Franck, R., *J. Agric. Food Chem.*, 1972, **20**, 1222.
30. Decker, O. D., and Johnson, W. S., *in* Zweig, G., *Editor*, "Analytical Methods for Pesticides and Plant Growth Regulators," Volume VIII, 1976, p. 433.
31. Jaffe, H. H., and Orchin, M., "Theory and Applications of Ultraviolet Spectroscopy," Wiley, New York, 1962.
32. Platt, J. R., *J. Chem. Phys.*, 1949, **17**, 484.
33. Aaron, J. J., and Gaye, M. D., *Talanta*, 1988, **35**, 513.

Paper 8/04094J
Received October 17th, 1988
Accepted January 4th, 1989

Fluorimetric Determination of Thallium in Silicate Rocks With Rhodamine B After Separation by Adsorption on a Crown Ether Polymer*

Hideko Koshima and Hiroshi Onishi†
University of Tsukuba, Tsukuba-shi, Ibaraki-ken 305, Japan

A procedure was developed for the determination of thallium (≤0.05 p.p.m.) in silicate rocks and related materials. It is based on the separation of thallium by adsorption on a column of a crown ether polymer, poly(dibenzo-18-crown-6), and elution, followed by fluorimetric determination using an improved Rhodamine B method. Thallium was determined in a variety of rock reference samples with almost quantitative recovery and a relative standard deviation of about 10%. The results obtained were generally in good agreement with those obtained by other workers.

Keywords: *Thallium determination; rock reference samples; crown ether polymer adsorption; fluorimetry; Rhodamine B*

The purpose of the work described in this paper was to develop a fluorimetric method for the determination of thallium in rocks (chiefly silicate rocks) and to analyse rock reference samples for thallium. The thallium content of igneous rocks has been given as 0.05–1.7 p.p.m.[1] and the crustal average as 0.5 p.p.m.[2]

Various techniques for the determination of trace amounts of thallium have been reviewed by Sager,[3] while fluorimetric methods for its determination in silicate rocks with Rhodamine B have been described by Onishi,[4] Matthews and Riley[5] and Schnepfe.[6] In this work, the fluorimetric methods were compared and the method of Matthews and Riley was adopted with minor modifications. An alternative fluorimetric method in which thallium is separated by isobutyl methyl ketone extraction and cation exchange has also been used.[7]

In a previous paper,[8] we showed that microgram amounts of thallium(III) could be separated efficiently from large amounts of iron(III) on a column of the crown ether polymer poly(dibenzo-18-crown-6) [poly(DB18C6)]. It was thought that the application of this separation method to rock analysis would simplify the existing techniques.[5–7] In the proposed procedure thallium was isolated by adsorption on poly(DB18C6)[8] and then determined by an improved Rhodamine B method.

Experimental

Samples, Reagents and Apparatus

Thirty rock reference samples, including 22 Geological Survey of Japan (GSJ) samples, were analysed.

A standard thallium(I) solution was prepared by dissolving thallium(I) nitrate in 0.05 M sulphuric acid.

A glass-wool plug was placed in a glass column (80 × 10 mm i.d.) with a PTFE stopcock at the bottom and the column was then filled with 0.5 g of poly(DB18C6) (Fluka, Buchs, Switzerland; screened to <20 mesh) in a water slurry. The polymer column was conditioned by passing 1 M hydrochloric acid through it and could be used repeatedly after washing with water, 0.2 M hydrochloric acid containing 85% *V/V* acetone and finally 1 M hydrochloric acid.

A Kotaki UM-2S fluorimeter with 1-cm Pyrex cells was used; the excitation source was a Toshiba SHL-100UV mercury lamp with a UV-01 filter (>420 nm). The fluorescence intensity was measured using a 580-nm interference filter.

Procedure

Weigh 0.3–1 g of (igneous) silicate rock powder in a 50-ml PTFE beaker. Run a blank with each set of determinations. Add 5 ml of concentrated nitric acid and 10 ml of 46% *m/m* hydrofluoric acid to the powder, heat the covered beaker on a hot-plate for about 3 h and evaporate the solution to dryness. Treat the residue with 5 ml of concentrated nitric acid and again evaporate to dryness. Add 5 ml of hydrochloric acid (1 + 1), evaporate to dryness and dissolve the residue in 10 ml of 4 M hydrochloric acid and 30 ml of water. If insoluble matter is present, filter through a No. 5B (medium texture) filter-paper (Toyo Roshi). Add 1 ml of bromine water to the filtrate and remove the excess of bromine by heating. Use a starch - potassium iodide test paper to check that removal of bromine is complete.

Pass the solution through the poly(DB18C6) column at a flow-rate of 1 ml min^{-1} and wash the column with 20 ml of 1 M hydrochloric acid. Elute thallium with 15 ml of 0.2 M hydrochloric acid containing 85% *V/V* acetone at a flow-rate of 0.5 ml min^{-1} and evaporate the effluent with 0.5 ml of sulphuric acid (1 + 5) until the residue becomes brown. Destroy the organic matter by treating with three 20-mg portions of ammonium peroxodisulphate and dissolve the residue in 5.0 ml of hydrochloric acid (1 + 4). Add 0.5 ml of bromine water to ensure the oxidation of thallium(I) and remove the excess of bromine by heating.

Transfer the solution into a separating funnel with 5.0 ml of hydrochloric acid (1 + 4), add 1.0 ml of 0.2% *m/V* Rhodamine B in water and 5.00 ml of benzene,* shake the mixture for 2 min, separate the benzene extract and centrifuge it for 1 min. Transfer the clear extract into a glass cell, allow it to stand for 20 min and then measure the fluorescence intensity. Use dilute aqueous solutions of Rhodamine B (*e.g.*, 0.5 mg l^{-1} for 0.5 μg of thallium) to adjust the fluorimeter to a suitable sensitivity.

The calibration graph is constructed by taking 0–1.5 μg of thallium through the procedure beginning with the addition of 0.5 ml of sulphuric acid (1 + 5).

For the decomposition of lake and river sediments and slate, use fuming rather than concentrated nitric acid.

For the decomposition of limestone and dolomite, add 5 ml of hydrochloric acid (1 + 1) and filter off the insoluble matter

* Presented at the 37th Annual Meeting of the Japan Society for Analytical Chemistry, Sapporo, October, 1988.

† To whom correspondence should be addressed.

* **Caution**—Benzene is highly toxic and appropriate precautions should be taken.

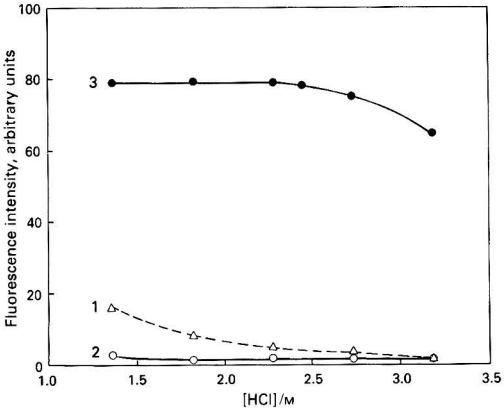

Fig. 1. Effect of hydrochloric acid concentration on the fluorescence intensity. Fluorescence intensity of 1, the blank measured immediately; 2, the blank; and 3, 0.5 μg of thallium *versus* the blank measured 20 min after transferring the extract into the cell

Table 1. Effect of hydrochloric acid concentration on the separation of thallium. Hydrochloric acid (40 ml) containing 0.5 μg of thallium(III) and 200 mg of iron(III) was used

[HCl]/M	Recovery, %
0.5	98, 101, 105
1.0	95, 99, 100
1.5	95, 96, 101

Table 2. Recovery of thallium from rock samples

Sample	Mass/g	Thallium added/μg	Recovery, %*
JG-1a	0.5	1.0	97
JB-1a	1.0	0.5	100
JLk-1	0.3	1.0	95
JLs-1	1.0	0.5	100
JDo-1	1.0	0.5	102
JSl-1	0.4	1.0	96

* Average of two or three determinations.

Table 3. Effect of fluoride, nitrate and gold added to rock samples

Sample	Mass/g	Addition	Thallium, p.p.m.*
JG-1a	0.5	NaF 0.2 g + $NaNO_3$ 0.4 g	0.97†
JB-1a	1.0	NaF 0.2 g + $NaNO_3$ 0.4 g	0.098†
JG-1a	0.5	Au 0.1 μg	1.0‡

* Average of three or four determinations. For results without the additives, see Table 4.

† Additions were made to a 1 M hydrochloric acid solution of the decomposed sample.

‡ Gold was added before sample decomposition.

using a nitrocellulose membrane filter (0.45-μm pore size). Decompose the residue and filter with fuming nitric and hydrofluoric acids. Finally, convert to the hydrochloric acid solution, combine with the filtrate and adjust to 1 M in hydrochloric acid.

Results and Discussion

In the fluorimetric method of Schnepfe[6] the sample solution must be allowed to stand overnight or for a minimum of 8 h before extraction with Rhodamine B - benzene. The benzene extract must then stand for 1–2 h before measurement of the fluorescence intensity. Therefore, this method was not adopted in the work described here.

Table 4. Results obtained for the determination of thallium in rock reference samples

	Sample	Thallium, p.p.m. This work*	Thallium, p.p.m. Other work
GSJ—			
JG-1	Granodiorite	1.0	1.03,[9] 0.98,[10] 1.03,[11] 1.13[12]
JG-1a	Granodiorite	1.0†	1.16[12]
JG-2	Granite	1.6	1.5[12]
JG-3	Granodiorite	0.41	0.4[12]
JR-1	Rhyolite	1.6	1.73[12]
JR-2	Rhyolite	1.8	1.9[12]
JA-1	Andesite	0.13	<0.2[12]
JA-2	Andesite	0.35	0.3[12]
JA-3	Andesite	0.21	0.25[12]
JB-1	Basalt	0.11	0.102,[9] 0.090,[10] 0.103,[11] <0.2[12]
JB-1a	Basalt	0.11‡	<0.2[12]
JB-2	Basalt	<0.05	0.049,[11] <0.2[12]
JB-3	Basalt	0.05	0.052,[11] <0.2[12]
JGb-1	Gabbro	0.06	<0.2[12]
JP-1	Peridotite	<0.05	—
JF-1	Feldspar	1.3	1.1[12]
JF-2	Feldspar	1.1	1.4[12]
JLk-1	Lake sediment	1.7	—
JLs-1	Limestone	<0.05	—
JDo-1	Dolomite	<0.05	—
JSl-1	Slate	0.80	—
JSd-1	River sediment	0.43	—
USGS§—			
G-2	Granite	0.90	1.02,[5] 0.96,[7] 0.87,[10] 1.20,[13] 0.84,[14] 1.04[15]
GSP-1	Granodiorite	1.4	1.87,[5] 1.78,[7] 1.28,[10] 1.22,[13] 1.73,[14] 1.55[15]
AGV-1	Andesite	0.34	0.39,[5] 0.43,[7] 0.33,[10] 0.40 and 0.96,[11] 1.63,[13] 0.40,[14] 0.39[15]
BCR-1	Basalt	0.30	0.59,[5] 0.48,[7] 0.26,[10] 0.35,[13] 0.34[15]
PCC-1	Peridotite	<0.05	0.35,[5] 0.28,[7] 0.002,[10] 0.0020,[11] 0.0008,[13] 0.0032[15]
DTS-1	Dunite	<0.05	0.13,[5] 0.74,[7] 0.006,[10] 0.0021[11]
NIM¶—			
NIM-G	Granite	0.90	0.94[10]
NIM-L	Lujavrite	0.34	0.30[10]

* Average of two or three determinations.

† Average of eight determinations; relative standard deviation, 7.4%.

‡ Average of six determinations; relative standard deviation, 13%.

§ USGS = United States Geological Survey.

¶ NIM = National Institute for Metallurgy (South Africa).

One difference between the methods of Onishi[4] and Matthews and Riley[5] is the hydrochloric acid concentration during the Rhodamine B - benzene extraction, *i.e.*, 1.6 and 2.7 M, respectively. The effect of the hydrochloric acid concentration on the fluorescence intensity was re-examined (Fig. 1). As a result, a final concentration of about 2.2 M was chosen and the fluorescence intensity was measured after allowing the extract to stand in the cell for 20 min. The fluorescence intensities of both the blank and 0.5 μg of thallium remained constant for a further 40 min. The calibration graph was almost linear for 0–1.0 μg of thallium but deviated slightly from linearity at 1.5 μg. The relative standard deviation for the determination of 0.5 μg of thallium was 1.1%

(n = 5). The average blank value was 0.015 μg of thallium (n = 25) and the standard deviation was 0.006 μg. Up to 100 μg of iron(III), 0.1 μg of gold(III) and 10 μg of gallium(III) did not interfere with the determination of 0.5 μg of thallium. The fluorescence intensity of thallium decreased by 40% in the presence of 5 μg of gold(III), however.

The effect of the hydrochloric acid concentration on the separation of thallium was examined (Table 1), with satisfactory recoveries of thallium being obtained from an approximately 1 M hydrochloric acid solution.

Decomposition of granodiorite JG-1a with nitric acid - hydrofluoric acid and sulphuric acid - hydrofluoric acid gave the same result, *i.e.*, 1.0 p.p.m. of thallium. The reported loss of thallium using sulphuric acid - hydrofluoric acid[5] was not observed; this is in agreement with earlier work.[4] When basalt JB-1a was decomposed with sulphuric acid - hydrofluoric acid, however, it was difficult to dissolve the residue in 1 M hydrochloric acid. Therefore decomposition with nitric acid - hydrofluoric acid was adopted.

Several GSJ reference samples, to which known amounts of thallium had been added, were analysed as described under Procedure (Table 2). Recoveries were found to be satisfactory.

Because fluoride and nitrate are not completely removed by the decomposition procedure, their effect on the determination was studied (Table 3). These species were tolerated at the amounts examined. Also, although gold is not separated from thallium by the proposed procedure, as much as 0.1 μg of gold does not interfere (Table 3).

In order to assess the accuracy of the proposed method, thallium was determined in the National Bureau of Standards Standard Reference Material (NBS SRM) 1633a, Coal Fly Ash. The sample (0.5 g) was decomposed with fuming nitric acid and hydrofluoric acid and the final solution was made 1 M in hydrochloric acid. Insoluble matter was filtered off and thallium was separated from an aliquot of the filtrate (1/5 of the total filtrate) and determined. The average result was 5.5 p.p.m. of thallium (n = 4, two separate samples) with a relative standard deviation of 2.6% (certified value, 5.7 ± 0.2 p.p.m. of thallium).

Table 4 shows the thallium content of 30 rock reference samples. The relative standard deviations for JG-1a and JB-1a are relatively large but may be judged to be acceptable. The average blank value (with the calibration graph blank subtracted) was 0.008 μg of thallium (n = 16) and the standard deviation was 0.007 μg of thallium. On the basis of these data and the data for the calibration graph blank, the limit of determination was calculated to be about 0.05 p.p.m. of thallium for a 1-g sample. As regards Table 4, isotope dilution mass spectrometry was the technique used in references 9 and 11 and flameless atomic absorption spectrometry in references 10 and 12. The values obtained by Matthews and Riley[5] and Böhmer and Pille[7] for PCC-1 and DTS-1 are extremely high; the reasons for this are not known. In general, the results obtained in this work are in good agreement with those reported elsewhere.

We thank A. Ando of the Geological Survey of Japan for providing the rock samples and for valuable discussions.

References

1. de Albuquerque, C. A. R., and Shaw, D. M., *in* Wedepohl, K. H., *Editor*, "Handbook of Geochemistry," Volume II/5, Springer-Verlag, Berlin, 1972, p. 81-E-10.
2. Mason, B., and Moore, C. B., "Principles of Geochemistry," Fourth Edition, Wiley, New York, 1982, p. 47.
3. Sager, M., "Spurenanalytik des Thalliums," Georg Thieme, Stuttgart, 1986.
4. Onishi, H., *Bull. Chem. Soc. Jpn.*, 1957, **30**, 827.
5. Matthews, A. D., and Riley, J. P., *Anal. Chim. Acta*, 1969, **48**, 25.
6. Schnepfe, M. M., *Anal. Chim. Acta*, 1975, **79**, 101.
7. Böhmer, R. G., and Pille, P., *Talanta*, 1977, **24**, 521.
8. Koshima, H., and Onishi, H., *Anal. Sci.*, 1987, **3**, 417.
9. Murozumi, M., Nakamura, S., and Igarashi, T., *Nippon Kagaku Kaishi*, 1978, 1515.
10. Heinrichs, H., *Fresenius Z. Anal. Chem.*, 1979, **294**, 345.
11. Saito, T., Shimizu, H., and Masuda, A., *Geochem. J.*, 1987, **21**, 237.
12. de Castro, M. A., Bugagao, R., Ebarvia, B., Roque, N., and Rubeska, I., *Geostand. Newsl.*, 1988, **12**, 47.
13. Marowsky, G., and Wedepohl, K. H., *Geochim. Cosmochim. Acta*, 1971, **35**, 1255.
14. Sager, M., and Tölg, G., *Mikrochim. Acta*, 1982, **II**, 231.
15. Ikramuddin, M., *At. Spectrosc.*, 1983, **4**, 101.

Paper 8/04561E
Received November 16th, 1988
Accepted January 4th, 1989

Extraction and Spectrophotometric Determination of Zirconium(IV) With *N*-Phenylbenzohydroxamic Acid and Phenylfluorone

H. Dasaratha Gunawardhana and Priyantha M. Sugathapala
Centre for Analytical Research and Development, Department of Chemistry, University of Colombo, P.O. Box 1490, Colombo-3, Sri Lanka

N-Phenylbenzohydroxamic acid reacted with zirconium(IV) in 3.5 M hydrochloric acid to give a colourless complex that could be extracted into chloroform. The chloroform extract of the zirconium(IV) complex, on a second extraction from a dilute hydrochloric acid medium (0.5 M) in the presence of phenylfluorone and acetone, formed an intensely coloured complex with an absorption maximum at 534 nm. The molar absorptivity under optimum conditions was 1.125×10^4 dm^3 mol^{-1} cm^{-1}. The system obeyed Beer's law up to 7 p.p.m. of zirconium(IV) in the extract. Large amounts of many cations and anions, including a ten-fold molar excess of vanadium(IV), iron(III) and molybdenum(VI), were tolerated. Equimolar amounts of aluminium(III), fluoride, phosphate and vanadium(V) were also tolerated. A slight interference from titanium(IV) and niobium(V) was observed when the mole ratio of zirconium(IV) to foreign ion exceeded 1.0 : 0.3. The method was applied successfully to the determination of zirconium(IV) in zircon sand.

Keywords: *Zirconium(IV) determination; spectrophotometry; N-phenylbenzohydroxamic acid; phenylfluorone; liquid - liquid extraction*

The determination of zirconium(IV) using atomic absorption spectrometry is difficult if high sensitivity is required, due to its low oscillator strength and the formation of stable oxides in the flame and, sometimes, stable carbides in non-flame atomisers. The development of a sensitive and selective spectrophotometric method for the determination of zirconium(IV) is, therefore, of interest.

Pilipenko *et al.*[1,2] reported the use of phenylfluorone (2,6,7-trihydroxy-9-phenyl-3*H*-xanthen-3-one) (PF) and an alcohol in conjunction with *N*-phenylbenzohydroxamic acid (NPBHA) to achieve an enhancement of the intensity of the colour in the determination of titanium(IV). *N*-Phenylfurohydroxamic acid[3] and *N*-phenyllaurohydroxamic acid[4] have also been used in place of NPBHA. A sensitive and selective method adopting a similar procedure has been developed[5] recently using NPBHA. The method consists of a first extraction of the metal from a strong mineral acid medium into a solution of NPBHA in chloroform, followed by reaction of the resulting chloroform extract with a solution of PF in acetone and dilute hydrochloric acid. This paper describes the extraction of zirconium(IV) with a solution of NPBHA in chloroform[6] and its subsequent reaction with a solution of PF in acetone and hydrochloric acid, which produces a coloured organic layer with a maximum absorption at 534 nm.

Experimental

Apparatus

A Cecil Model 373 visible spectrophotometer was used for absorbance measurements. A Varian DMS 90 UV - visible spectrophotometer was used for recording the spectra.

Reagents

Analytical-reagent grade chemicals were used wherever possible. All solvents were purified and distilled prior to use. *N*-Phenylbenzohydroxamic acid was prepared using the procedure described by Majumdar[6] and the purity of the recrystallised product was checked by its melting-point. Analytical-reagent grade PF (Eastman) was used without further purification. It is thought that 1,1,1-trichloroethane could be used in place of chloroform, but this was not verified.

A stock solution of zirconium(IV) was prepared by dissolving zirconium(IV) nitrate in concentrated hydrochloric acid and diluting the solution appropriately.

Recommended Procedure for the Spectrophotometric Determination of Zirconium(IV)

First extraction

Transfer an aliquot of a sample solution containing up to 70 μg of zirconium(IV) into a separating funnel and dilute to 10.0 cm^3 with 7 M hydrochloric acid so that the final concentration of hydrochloric acid is 3.5 M. Add 10.0 cm^3 of 0.3% *m/V* NPBHA in chloroform and equilibrate for 3 min.

Second extraction

Withdraw 5.0 cm^3 of the organic phase from the first extraction and transfer it into a dry separating funnel. Add 2.0 cm^3 of 0.02% *m/V* PF in acetone, then add 5.0 cm^3 of 0.5 M hydrochloric acid and equilibrate for 1 min. Separate the organic phase and measure the absorbance of this phase at 534 nm against a reagent blank.

The solution of PF in acetone was prepared by mixing 1.0 cm^3 of 0.3% *m/V* PF in *N,N*-dimethylformamide with 15.0 cm^3 of acetone. This method of preparation was found to be a convenient means of producing a suitable solution of PF in acetone; the solution should be prepared fresh each day.

Results and Discussion

Absorption Spectrum of the Extracted Zirconium(IV) - NPBHA - PF Complex

Zirconium(IV) forms a colourless complex with NPBHA. This complex, on a second extraction with PF in acetone, forms a red complex with a prominent absorption maximum at 534 nm measured against a reagent blank (Fig. 1). If an alcoholic solution of PF is used, as for titanium(IV)[2] and molybdenum(VI),[5] a red solid separates out between the two layers, resulting in a yellowish organic phase. A solution of PF in acetone was found to give a red organic phase without the undesirable separation of a red solid. The red complex remained stable for up to 3 h after the second extraction provided that the organic phase was separated from the aqueous phase soon after the extraction.

Effect of Concentrations of Hydrochloric Acid and Chloride Ion

The concentration of hydrochloric acid in the first extraction was varied from 0.3 to 4.3 M and the concentration was

determined by titration with a standard solution of potassium hydroxide (0.12 M), which was standardised against a standard solution of potassium hydrogen phthalate (0.100 M) with phenolphthalein as the indicator (Fig. 2). The optimum concentration of hydrochloric acid for the first extraction of zirconium(IV) was found to be 3.5 M. The protonation of NPBHA and the hydrolysis of the zirconium(IV) ion can be attributed to the observed lower extraction and consequent lower absorbance values at 534 nm at higher and lower acidities (Fig. 2).

In the second extraction, the concentration of hydrochloric acid was varied from 0.10 to 2.0 M while maintaining the total chloride ion concentration at 0.5 M. The results indicate that the optimum concentration of hydrochloric acid is 0.5 M (Fig. 3, A). The highest absorbance was obtained when the hydrogen ion concentration was equal to that of the chloride ion. At low acidities the zirconium(IV) - NPBHA - PF complex broke down due to hydrolysis of zirconium(IV). With increasing concentrations of hydrochloric acid beyond 0.5 M, the organic phase became more yellow in appearance, and this was accompanied by a decrease in absorbance at 534 nm when measured against a reagent blank. The protonation of PF at high acidities may lead to the breakdown of the zirconium(IV) - NPBHA - PF complex.

Variation of the chloride ion concentration also produced a similar effect (Fig. 3, B, C and D), indicating that chloride ions are involved in the formation of the complex. At high hydrogen ion concentrations (0.5 M and above), there is a decrease in absorbance with increasing chloride ion concentration. The formation of the protonated species $[H_2PF]Cl_2$ is enhanced under these conditions, hence leading to the breakdown of the zirconium(IV) - NPBHA - PF complex. However, at low hydrogen ion concentrations, the complex is stabilised to a certain extent by chloride ions.

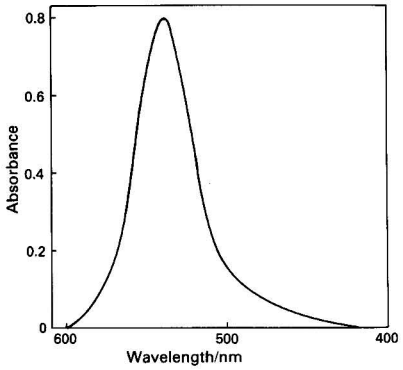

Fig. 1. Absorption spectrum of the zirconium(IV) - NPBHA - PF complex extracted into chloroform - acetone against a reagent blank. Zirconium(IV), 10 p.p.m.; NPBHA, 0.2% *m/V* in chloroform; and PF, 0.02% *m/V* in acetone

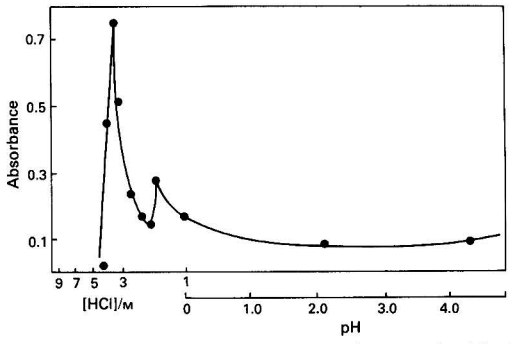

Fig. 2. Effect of HCl concentration on the first extraction (absorbance at 534 nm). Zirconium(IV), 10.0 p.p.m.; NPBHA, 0.20% *m/V* in chloroform; and PF, 0.025% *m/V* in acetone. [HCl] (second extraction), 0.5 M

Effect of Concentrations of NPBHA and PF

The absorbance of the zirconium(IV) - NPBHA - PF complex at 534 nm increases with increasing concentration of NPBHA and reaches a maximum when the concentration of NPBHA in chloroform is maintained at about 0.3% *m/V* (Fig. 4). This corresponds to a 257-fold molar excess of NPBHA, which is almost four times greater than the amount of ligand required for the extraction of molybdenum(VI).[5] Higher or lower concentrations of NPBHA lead to a decrease in absorbance and this could be explained on the same basis as for the extraction of molybdenum(VI).[5]

The absorbance at 534 nm remains unaltered on changing the concentration of PF from a 12- to a 17-fold molar excess. Although higher concentrations of PF give higher absorbances against reagent blanks, an instability of the organic phase producing cloudiness is observed unless the volume of acetone is increased. Although the molar excess of NPBHA required is higher than in the extractions of titanium(IV)[4] and molybdenum(VI),[5] the molar excess of PF needed is smaller than in the other two instances. This may be due to changing the solvent from ethanol to acetone.

Verification of Beer's Law

The verification of Beer's law was carried out under the following optimum conditions: NPBHA, 0.3% *m/V* in chloroform; HCl, 3.5 M (first extraction); PF, 0.02% *m/V* in acetone;

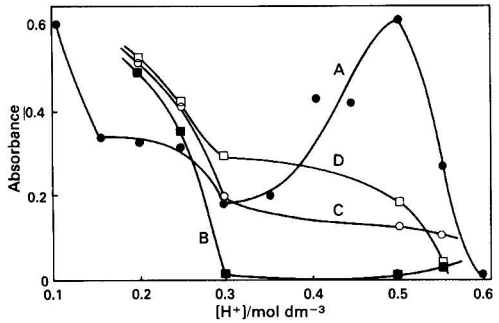

Fig. 3. Effect of hydrogen and chloride ion concentrations on absorbance at 534 nm. Zirconium(IV), 10.0 p.p.m.; NPBHA, 0.30% *m/V* in chloroform; and PF, 0.0167% *m/V* in acetone. [HCl] (first extraction), 3.5 M. Chloride ion concentration in the second extraction: A, 0.50; B, 0.75; C, 1.00; and D, 2.00 M

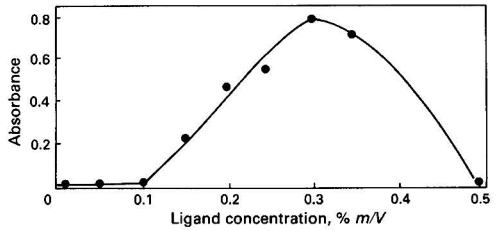

Fig. 4. Effect of NPBHA concentration on absorbance at 534 nm. Zirconium(IV), 10.0 p.p.m.; [HCl] (first extraction), 3.5 M; PF, 0.025% *m/V* in acetone; and [HCl] (second extraction), 0.5 M

Table 1. Tolerance limits for foreign ions in the determination of zirconium(IV) using the proposed method. Zirconium(IV), 3.0 p.p.m.; NPBHA, 0.3% *m/V* in chloroform; [HCl] (first extraction), 3.5 M; PF, 0.02% *m/V* in acetone; [HCl] (second extraction), 0.5 M

Foreign ion	Tolerance limit, p.p.m.	Molar ratio, zirconium(IV) : ion
Vanadium(V)	5.0	0.59
Vanadium(IV)	85.6	10.18
Titanium(IV)	28.0	0.36
Iron(III)	100.0	10.89
Molybdenum(VI)	10.0	6.39
Niobium(V)	5.0	0.32
Fluoride	5.0	1.58
Phosphate	10.0	0.63

HCl, 0.5 M (second extraction); and shaking time, 3 min. The system obeys Beer's law (at 534 nm) up to 7 p.p.m. of zirconium(IV) in the extract. A negative deviation was observed at higher concentrations. The molar absorptivity at 534 nm was 1.125×10^4 dm^3 mol^{-1} cm^{-1}. A Beer's law plot gave a reproducible, rectilinear calibration graph.

Effect of Foreign Ions

The proposed method can tolerate a ten-fold molar excess of iron(III) and vanadium(IV) (Table 1), a six-fold excess of molybdenum(VI) and a 1.5-fold excess of fluoride. The tolerance limit was defined as the amount of foreign ion causing a deviation of more than 0.02 A. The tolerance limit for vanadium(V) is a 0.6-fold molar excess. The reduction of vanadium(V) to vanadium(IV) using a mild reducing agent such as sulphur dioxide or iodide would increase the tolerance limit of the method towards vanadium.

The tolerance limit for both niobium(V) and titanium(IV) is a 0.3-fold molar excess. Therefore, the method cannot be applied to the determination of zirconium(IV) in titanium-containing minerals. As a large excess of anions such as fluoride and phosphate is not tolerated, it is difficult to overcome the interference from titanium(IV) by the addition of masking agents such as those used in the determination of molybdenum(VI).[5] It is thought that hafnium(IV) would also cause positive interference.

Application

The proposed spectrophotometric method was applied to the determination of zirconium(IV) in zircon sand. A solution of the zircon sand was prepared by fusion with potassium hydrogen sulphate. It was not possible to achieve complete dissolution of the zircon by fusion. The concentration of zirconium(IV) in the fused zircon solution was determined using the EDTA back-titration method.[7] The concentration of zirconium(IV) found by titrating a large volume of this solution was 3.5 p.p.m. The proposed spectrophotometric method gave a value of 3.1 p.p.m.

References

1. Pilipenko, A. T., Shpak, E. A., and Zul'figarov, O. S., *Zh. Anal. Khim.*, 1974, **29**, 1074.
2. Pilipenko, A. T., Shpak, E. A., and Zul'figarov, O. S., *Zh. Anal. Khim.*, 1975, **30**, 1009.
3. Pilipenko, A. T., Shpak, E. A., and Gremenko, M. V., *Zh. Anal. Khim.*, 1975, **30**, 1535.
4. Gunawardhana, H. D., *Analyst*, 1983, **108**, 952.
5. Gunawardhana, H. D., and Fernando, S. A., *Can. J. Chem.*, 1987, **65**, 1124.
6. Majumdar, A. K., "*N*-Benzoylphenylhydroxylamine and its Analogues," Pergamon Press, Oxford, 1972.
7. Schwarzenbach, G., "Complexometric Titrations," Interscience, New York, 1960, p. 71.

Paper 8/02227E
Received June 3rd 1988
Accepted December 16th, 1988

Separation of Trace Amounts of Aluminium on a Strong Anion-exchange Resin Loaded With a Sulphonated Azo Dye

Maria Pesavento, Antonella Profumo, Carla Riolo and Teresa Soldi
Dipartimento di Chimica Generale, Universita' di Pavia, Viale Taramelli 12, 27100 Pavia, Italy

The sulphonated azo dye Chromotrope 2B is sorbed quantitatively by the strong anion exchanger AG 1-X8. A chelating resin is obtained, which is able to sorb aluminium from aqueous solutions selectively. The distribution equilibria were investigated under different conditions and interpreted on the basis of a Donnan equilibrium based model for the resin. A separation and pre-concentration method for aluminium in natural waters is proposed, based on the use of the modified resin in a column at ambient pressure. The selectivity with respect to other metal ions was good; this was to be expected because Chromotrope 2B in solution is also selective for aluminium. Recoveries of 100 ± 1% were obtained, with a pre-concentration factor of 50, at a total aluminium concentration of 2×10^{-6} mol kg^{-1}.

Keywords: *Aluminium; modified anion-exchange resin; separation; Chromotrope 2B; spectrophotometry*

It was demonstrated in a previous paper[1] that strong anion exchangers loaded with sulphonated azo dyes could act as chelating resins, which were able to sorb copper and nickel ions from aqueous solution. The conditions for sorption or elution could be calculated *a priori* if some independently determinable quantities were known. The importance of this point is demonstrated by the fact that almost all the reports dealing with this subject describe attempts to correlate the sorption and elution behaviour of the system under study with the complexation characteristics in aqueous solution. The agreement was only seldom satisfactory, probably because in many instances the existence of the important Donnan equilibrium,[2,3] was neglected. The aim of this work was to develop a system similar to those studied previously for copper and nickel,[1] but which could be used for the separation and pre-concentration of trace levels of aluminium from aqueous solutions.

It has been shown[4] that aluminium is strongly complexed by those sulphonated azo dyes that possess a *peri*-dihydroxylic structure. In particular, 1,8-dihydroxy-2-(*p*-nitrophenylazo)-naphthalene-3,6-disulphonic acid (Chromotrope 2B) appeared to be the most suitable because it is readily available and is very stable both as a solid and when dissolved in aqueous solution.

Experimental

Equipment and Materials

A Carlo Erba Spectracomp 601 spectrophotometer with 1-cm quartz cells was used throughout.

An Orion 901 potentiometer with a combined Ross glass electrode (Orion) was employed for measurement of the pH. The potentiometric cell was standardised using Gran's method, as described previously.[4]

All reagents were of analytical-reagent grade unless stated otherwise and doubly distilled water was used throughout.

An aluminium standard solution (1000 p.p.m.) was prepared by dissolving aluminium chloride hexahydrate (99.999%, Aldrich) in 0.02 M hydrochloric acid and was standardised complexometrically.[5]

The anion-exchange resin, AG 1-X8, 100–200 mesh, was obtained from Bio-Rad; it was used after washing for 10 h with 0.1 M sodium hydroxide solution, then with 0.1 M hydrochloric acid and finally three times with water, as described by Gregor *et al.*[6]

Chromotrope 2B was obtained from Aldrich and used without further purification. It was sorbed on the resin by adding a small volume of an aqueous solution containing the required amount of dye to an appropriate amount of washed resin and stirring the suspension vigorously until the aqueous phase became colourless (about 30 min).

A solution of Chrome Azurol S (CAS) was prepared by dissolving 20 mg of the solid substance (Aldrich, dye content 65%) in 50 ml of water - ethanol (1 + 1).

Acetate buffer of pH 4.8 was obtained by dissolving 82.05 g of sodium acetate and 0.26 mol of hydrochloric acid in 1 l of water.

Spectrophotometric Determination of Aluminium with CAS

The method used was that originally proposed by Pakalns[7] and developed by Kennedy and Powell.[8]

A 1-ml volume of CAS solution, 1 ml of acetate buffer and 20 µl of thioglycollic acid (80%; RPE, Carlo Erba) were transferred into a 25-ml calibrated flask. An aliquot of the sample solution containing 0.5–4.0 µg of aluminium was added to the flask and the mixture was diluted to volume. (The sample solution had previously been treated with 0.01 M hydrochloric acid for 30 min on a steam-bath.[8]) The absorbance was recorded at 567.5 nm.

Investigation of Aluminium Distribution Between an Aqueous Solution and the Resin: Batch Procedure

A volume (20–200 ml) of an aqueous solution with a fixed ionic composition (0.01–1.00 mol kg^{-1} of sodium chloride), containing a fixed concentration of aluminium (8×10^{-4}–2×10^{-5} mol kg^{-1}), and of the resin loaded with Chromotrope 2B (0.1–0.3 mmol of reagent) were used in each experiment. The acidity was varied by adding standard hydrochloric acid or sodium hydroxide solution and was measured potentiometrically. At each titration point, the mixture was allowed to reach equilibrium (about 1 h was required) and the two phases were separated by centrifuging for 5 min at 3000 rev min^{-1}. An aliquot of the aqueous phase was analysed for its total aluminium content using the CAS spectrophotometric method described above. All the experiments were carried out in thermostated cells at 25 °C.

Pre-concentration of Aluminium Using the Column Procedure

A 20 × 0.8 cm i.d. borosilicate glass column was filled with 3 g of resin loaded with a total of 0.2 mmol of Chromotrope 2B. Flow-rates of 0.5–1 ml min^{-1} could be obtained at ambient pressure by suitable adjustment of the stop-cock position. The sample solutions were passed through the column imme-

diately after 1% of 1 M acetate buffer of pH 6 had been added to the solutions. The sorbed aluminium was eluted with 20 ml of 0.01 M hydrochloric acid. After elution and reconditioning with doubly distilled water, the column could be employed at least 100 times without further loading of Chromotrope 2B, due to the fact that the reagent is strongly held on the resin.

Results and Discussion

Sorption of Chromotrope 2B on AG 1-X8

The maximum capacity of AG 1-X8 for Chromotrope 2B is 1.60 mmol of reagent per gram of dry resin and each sorbed Chromotrope 2B molecule releases two chloride ions. In this work, the resin was only partly loaded with the reagent, *i.e.*, with not more than 30% of the fixed charged groups. In this way, other anions present in solution do not compete with Chromotrope 2B for sorption on the resin. This interference becomes more important the more hydrophobic the ions involved; the order is as follows: perchlorate > nitrate > bromide > chloride > acetate.[1] It was found that chloride does not cause any release of Chromotrope 2B from the resin up to a concentration of 1 M and perchlorate up to 10^{-3} M. Di- and tri-valent ions such as sulphate or phosphate do not compete at all.

Sorption of Trace Amounts of Aluminium on AG 1-X8 Loaded With Chromotrope 2B: Batch Procedure

The sorption was studied in sodium chloride solutions, because chloride ion competes weakly with Chromotrope 2B for sorption on the resin; it also appears not to be able to complex aluminium.[9] In all the experiments, a large molar excess of Chromotrope 2B with respect to metal ion was used in order to obtain reproducible analytical conditions.

Fig. 1 shows the sorption curves of aluminium on AG 1-X8 loaded with Chromotrope 2B; the ratio of sorbed to total aluminium (f) is plotted against the pH of the solution. The sorption reaction can be written as follows (charges omitted for simplicity):

$$\mathrm{Al} + n\overline{\mathrm{H_2L}} \rightleftharpoons \overline{\mathrm{AlH_xL}_n} + q\mathrm{H}$$

$$K_{ex} = \frac{[\overline{\mathrm{AlH_xL}_n}][\mathrm{H}]^q}{[\mathrm{Al}][\overline{\mathrm{H_2L}}]^n} \quad \ldots \quad (1)$$

The fraction of sorbed aluminium is given by

$$f = \frac{[\overline{\mathrm{AlH_xL}_n}]g}{[\overline{\mathrm{AlH_xL}_n}]g + [\mathrm{Al}]Z_{\mathrm{Al}}V} = \frac{1}{1+\left(\frac{[\mathrm{H}]^q Z_{\mathrm{Al}} V}{K_{ex}[\overline{\mathrm{H_2L}}]^n g}\right)} \quad (2)$$

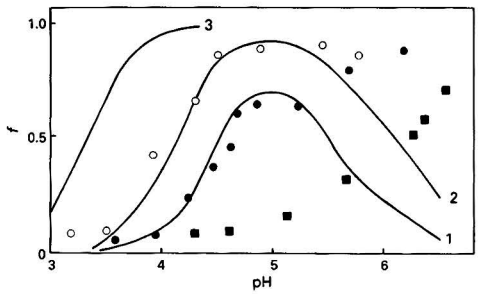

Fig. 1. Sorption of aluminium on AG 1-X8 loaded with Chromotrope 2B from 0.1 mol kg^{-1} NaCl solution; T = 25 °C. Ordinates: fraction of sorbed ion. (○) Aluminium, 0.00111 mmol; Chromotrope 2B, 0.506 mmol; resin, 3.10 g; and V = 50 ml. Continuous curve 2, calculated. (●) Aluminium, 0.01112 mmol; Chromotrope 2B, 0.107 mmol; resin, 1.91 g; and V = 50 ml. Continuous curve 1, calculated. (■) Aluminium, 0.01112 mmol; resin, 1.40 g; and V = 50 ml. Curve 3, complex formation in aqueous solution

where the square brackets indicate the concentration both in solution and in the resin phase (in molality) and the bars the species in the resin phase; g is the number of grams of water in the resin phase, V the volume (in millilitres) of the aqueous solution, K_{ex} the extraction coefficient and Z_{Al} the ratio of the total concentration of aluminium in solution (c_{Al}) to the aluminium present as the aqua-ion ([Al]).

In this work, the following aluminium hydroxo species were found to be formed in 0.1 mol kg^{-1} sodium chloride solution: $Al(OH)_3$, $[Al(OH)_4]^-$ and $[Al_{13}(OH)_{32}]^{7+}$ (see below).

Owing to the presence of polynuclear species, Z_{Al} depends on the aluminium aqua-ion concentration, which can be determined by solving the following mass balance equation for [Al]:

$$c_{Al} = [Al] + [Al]\left(\frac{K_{1,3}}{[H]^3}\right) + [Al]\left(\frac{K_{1,4}}{[H]^4}\right) + 13\left(\frac{K_{13,32}[Al]^{13}}{[H]^{32}}\right) \quad \ldots \quad (3)$$

The values of n and q [equation (1)] were established by means of the following relationship:

$$\log\left(\frac{1-f}{Z_{Al}f}\right) = -\log K_{ex}\left(\frac{g}{V}\right) - n\log[\overline{\mathrm{H_2L}}] - q\mathrm{pH} \quad \ldots \quad (4)$$

$\mathrm{Log}[(1-f)/Z_{Al}f]$ was plotted against pH to obtain the value of q (at constant $[\overline{\mathrm{H_2L}}]$) and against $\log[\overline{\mathrm{H_2L}}]$ (at constant pH) to obtain the value of n. Under the conditions employed, n is equal to 1 and q to 2. Hence the sorption reaction is similar to the complexation reaction in aqueous solution.[4]

Log K_{ex} can be obtained from equation (4), and some of the values obtained under different conditions are given in Table 1. Owing to the existence of the Donnan potential at the interface of the resin - aqueous solution,[2,3] it can be demonstrated that the extraction coefficient K_{ex} is related to the formation constant of the complex in 0.1 mol kg^{-1} sodium chloride solution (K_F) by the relationship

$$K_{ex} = K_F\left(\frac{a_{Cl}}{\bar{a}_{Cl}}\right)\left(\frac{y_{Al}y_{H,0.1}{}^2y_{AlL,0.1}\bar{y}_{H_2L}}{y_H{}^2y_{Al,0.1}y_{H_2L,0.1}\bar{y}_{AlL}}\right) \quad \ldots \quad (5)$$

The activity of the species Y is indicated by a_Y and its activity coefficient by y_Y. The activity coefficients in 0.1 mol kg^{-1} sodium chloride solution are indicated by $y_{Y,0.1}$.

As reported previously for copper and nickel,[1] the activity coefficients of metal ions and protons in aqueous solution were calculated by means of the specific interaction theory.[10] Also, the activity of chloride in the resin phase was equal to that calculated previously (1.6 mol kg^{-1}).[1] Some values of $\log K_F' = \log K_F(\bar{y}_{H_2L}y_{AlL,0.1}/\bar{y}_{AlL}y_{H_2L,0.1})$ calculated by means of equation (5) are shown in Table 1.

Table 1. Extraction coefficients (K_{ex}) for the extraction of aluminium from sodium chloride solutions on to AG 1-X8 loaded with Chromotrope 2B

Sodium chloride concentration/ mol kg^{-1}	Log K_{ex}*	$\mathrm{Log}\, a_{Cl}\left(\frac{y_{H,0.1}{}^2y_{Al}}{y_{Al,0.1}y_H{}^2}\right)$	Log K_F'† (calculated)
0.01	−6.68	−1.605	−4.89
0.1‡	−6.30	−1.000	−5.01
0.1	−6.26	−1.000	−4.97
1.0	−5.70	−0.593	−4.92

* Mean value of three independent determinations (standard deviation, 0.04). V = 50 ml; c_{Al} = 2.226 × 10^{-5} mol kg^{-1}; Chromotrope 2B = 0.506 mmol.

† Log K_F' = log $K_F(\bar{y}_{H_2L}y_{AlL,0.1}/\bar{y}_{AlL}y_{H_2L,0.1})$.

‡ V = 25 ml; c_{Al} = 2.226 × 10^{-4} mol kg^{-1}; Chromotrope 2B = 0.050 mmol.

Table 2. Separation of aluminium from tap water on AG 1-X8 loaded with Chromotrope 2B

Sample*	Al found after sorption and elution/ mg l^{-1}	Spike recovery, %
Tap water	0.0225	—
Tap water†	0.0220	—
Tap water + 0.0200 mg l^{-1} of Al	0.0421	98.0
Tap water + 0.0400 mg l^{-1} of Al	0.0629	101.0

* A 300-ml volume of tap water was analysed.

† Sample treated with 0.01 M HCl on a steam-bath for 30 min before passing it through the column.

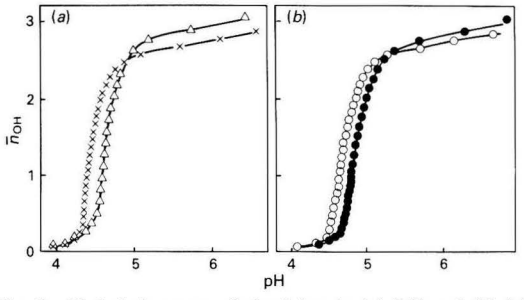

Fig. 2. Hydrolysis curves of aluminium in (*a*) 0.01 and (*b*) 1.0 mol kg^{-1} NaCl solutions; T = 25 °C. c_{Al}: (×) 6.01 × 10^{-4}; (△) 2.09 × 10^{-4}; (○) 1.099 × 10^{-3}; and (●) 4.90 × 10^{-4} mol kg^{-1}

The mean value of log K_F' is −4.98, which is in fairly good agreement with the complex formation constants in 0.1 mol kg^{-1} aqueous solution; the values for log K_F were −4.70 in sodium perchlorate[4] and −5.15 in sodium chloride. This last value was obtained from this work. A similar result was obtained during a study of the sorption of copper(II) and nickel(II).[1] The fact that K_F' is very near to the formation constant in 0.1 mol kg^{-1} aqueous solution implies that the activity coefficients ratio, $(y_{AlL,0.1}\bar{y}_{H_2L}/y_{H_2L,0.1}\bar{y}_{AlL})$, has a value of about one, which is not unreasonable.

The sorption curves calculated from equation (2) are shown in Fig. 1; a value for log K_{ex} of −6.44 obtained from equation (5), with log K_F equal to −5.15, was used for the calculations. Curve 3 in Fig. 1 is the formation curve of the aluminium - Chromotrope 2B complex in aqueous solution under the same conditions as for the sorption curve 2. It is evident that the use of a correctly calculated value of K_{ex} produces a good agreement with the experimental results, whereas calculation of the sorption based only on the formation constants in solution does not give the correct result.

Fig. 1 also shows the curve obtained by plotting the fraction of sorbed metal ion (f) against the pH of the solution, in the presence of pure AG 1-X8 resin not loaded with Chromotrope 2B. It can be seen that the sorption of aluminium on the resin at a pH lower than 5 requires the presence of the chelating agent, and hence that the sorption occurs according to equation (1). At lower acidities, however, the mechanism must be different and probably involves the sorption of neutral or anionic species such as $Al(OH)_3$ and $[Al(OH)_4]^-$. This would explain why the calculated sorption curves (1 and 2) fit the experimental points only up to pH 5.

Sorption and Elution of Trace Amounts of Aluminium on AG 1-X8 Loaded With Chromotrope 2B: Column Operations

On the basis of the results obtained above, it is possible to state that the retention of aluminium on the column should be quantitative at pH 5.8–6.0 and the elution quantitative at pH 2. This was tested by passing some synthetic solutions containing known amounts of aluminium through the column and eluting the sorbed metal as described in the procedure. Recoveries of 100 ± 1% (mean of four different determinations) were obtained, with an achievable pre-concentration factor of 50.

Aluminium is completely separated from lead, zinc, nickel, cadmium, calcium and magnesium, as expected from the fact that Chromotrope 2B complexes these metal ions weakly.[11] The sorption conditions were c_{Al}, 2 × 10^{-6} mol kg^{-1}; c_M, 1 × 10^{-4} mol kg^{-1}; V, 300 ml; I, 0.1 mol kg^{-1} of acetate buffer; and pH, 6.

Copper is completely retained on the resin together with aluminium, and iron only partially. Both can then be eluted quantitatively with 0.01 mol kg^{-1} hydrochloric acid.

Some possible interfering anions commonly present in natural waters were tested, including fulvic and humic acids. The recovery of aluminium was unaffected up to an anion concentration of 10 mg l^{-1}. The method was applied to the determination of aluminium in tap water from Pavia. The results are presented in Table 2.

Table 3. Hydrolysis constants for aluminium in sodium chloride solutions:

$$K_{m,i} = \frac{[Al_m(OH)_i][H]^i}{[Al]^m}$$

Sodium chloride concentration/ mol kg^{-1}	Log $K_{1,3}$*	Log $K_{1,4}$*	Log $K_{13,32}$*
0.01	−14.0	−22.6	−100.4
0.10	−14.4	−21.4	−105.2
1.00	−15.0	−20.7	−111.8

* Standard deviation = 0.1.

Hydrolysis of Aluminium in Sodium Chloride Solutions

The correct measurement of Z_{Al} requires knowledge of the conditional constants for the hydrolysis of aluminium. These were determined in sodium chloride solutions at the concentrations used in this work, *viz.*, 0.01, 0.10 and 1.00 mol kg^{-1}. The reaction was studied by titrating several solutions with a fixed aluminium concentration and ionic composition with standard hydrochloric acid or sodium hydroxide as described previously.[12] The pH of the solution at each titration point was measured potentiometrically with a glass electrode. The pH was examined in the range 2–7.

Typical hydrolysis curves, obtained by plotting the average number of hydroxyl groups bound to each aluminium ion ($\bar{n}_{OH}$)[13] against the pH of the solution, are shown in Fig. 2. The formation of polynuclear hydroxo derivatives is demonstrated by the fact that different aluminium concentrations produce different hydrolysis curves. In order to obtain the hydrolysis constants for aluminium from the potentiometric data, the SUPERQUAD program was used.[14]

Some results obtained at different sodium chloride concentrations are presented in Table 3. Only the presence of the mononuclear species $Al(OH)_3$ and $[Al(OH)_4]^-$ and the polynuclear species $[Al_{13}(OH)_{32}]^{7+}$ could be proved from the data obtained here.

This work was supported financially by the National Research Council of Italy (CNR, Rome).

References

1. Pesavento, M., Profumo, A., and Biesuz, R., *Talanta*, 1988, **35**, 431.
2. Boyd, G. E., and Bunrl, K., *J. Am. Chem. Soc.*, 1967, **89**, 1776.
3. Merle, V., and Marinsky, J. A., *Talanta*, 1984, **31**, 199.
4. Pesavento, M., Riolo, C., Soldi, T., and Garcia, R., *Ann. Chim. (Rome)*, 1982, **72**, 217.

5. Cheng, K. L., and Warmuth, F. J., *Chemist-Analyst*, 1959, **48**, 74.
6. Gregor, H. P., Belle, J., and Marcus, R. A., *J. Am. Chem. Soc.*, 1954, **76**, 1884.
7. Pakalns, P., *Anal. Chim. Acta*, 1965, **32**, 57.
8. Kennedy, J. A., and Powell, K. J., *Anal. Chim. Acta*, 1986, **184**, 329.
9. Sillen, L. G., and Martell, A. E., "Stability Constants of Metal-ion Complexes," Special Publ. No. 25, Suppl. No. 1, The Chemical Society, London, 1964.
10. Ciavatta, L., *Ann. Chim. (Rome)*, 1980, **70**, 551.
11. Pesavento, M., and Soldi, T., *Analyst*, 1983, **108**, 1128.
12. Pesavento, M., *Ann. Chim. (Rome)*, 1983, **73**, 173.
13. Sillen, L. G., *Acta Chem. Scand.*, 1956, **10**, 186.
14. Gans, P., Sabatini, A., and Vacca, A., *J. Chem. Soc., Dalton Trans.*, 1985, 95.

Paper 8/03177K
Received August 3rd, 1988
Accepted January 4th, 1989

Spectrophotometric Determination of Trace Amounts of Iron(III) With Norfloxacin as Complexing Reagent

Prodromos B. Issopoulos
Laboratory of Analytical Chemistry, Department of Inorganic and Analytical Chemistry, University of Ioannina, Ioannina, Greece

The complexation of iron(III) with norfloxacin in acidic solution at 25 °C, at an ionic strength of about 0.3 M and a pH of 3.0 has been studied. The water-soluble complex formed, which exhibits an absorption maximum at 377 nm, was used for the spectrophotometric determination of trace amounts of iron(III). The molar absorptivity was 9.05×10^3 l mol^{-1} cm^{-1} and the Sandell sensitivity 6.2 ng cm^{-2} of iron(III) per 0.001 A. The formation constant (K_f) was determined spectrophotometrically and was found to be 4.0×10^8 at 25 °C. The calibration graph was rectilinear over the range 0.25–12.0 p.p.m. of iron(III) and the regression line equation was $A = 0.163c - 0.00042$ with a correlation coefficient of 0.9998 ($n = 9$). Common cations, except cerium(IV), did not interfere with the determination. The results obtained for the determination of iron(III) using the described procedure and the thiocyanate method were compared statistically by means of the Student *t*-test and no significant difference was found.

Keywords: *Norfloxacin reagent; iron(III) - norfloxacin complex; spectrophotometry; iron(III) determination*

Norfloxacin (NRF) [1-ethyl-6-fluoro-1,4-dihydro-4-oxo-7-(1-piperazinyl)quinoline-3-carboxylic acid] is a synthetic, broad-spectrum fluoroquinolone antibacterial agent for oral administration, which has *in vitro* activity against Gram-positive and Gram-negative aerobic bacteria.

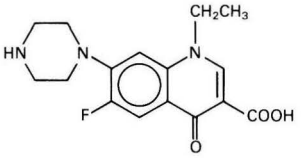

As the structural formula shows, NRF is related to other quinolones including cinoxacin, ciprofloxacin, enoxacin, ofloxacin and nalidixic acid. The fluorine atom provides increased potency against Gram-negative organisms and its piperazine moiety is responsible for the antipseudomonal activity. Norfloxacin also inhibits desoxyribonucleic acid (DNA) synthesis and is bactericidal.[1,2]

Recently, numerous compounds that are widely used in pharmacology as therapeutic agents have been proposed as ligands for the complexation of iron(III) for the spectrophotometric determination of this element. Hence, the use of salicylic acid (a substance with cicatrising, keratolytic and dermatological action) and some of its derivatives, such as acetylsalicylic acid and salicylamide (compounds with well known analgesic, antipyretic and anti-inflammatory action), for the formation of the mixed-ligand iron(III) - salicylate - purpurin complex has been described.[3] In addition, the formation of an iron(III) - 2-thiobarbituric acid complex[4] (2-thiobarbituric acid and its derivatives act on the cardiovascular system[5] and possess psychopharmacological[6] and anticonvulsant[7] properties) and the complexation of iron(III) with hydroxyurea has been reported[8] (hydroxyurea is a drug with proven antitumour activity and is now used in cancer therapy[8–11]).

In this paper, the formation of a water-soluble 1 : 2 complex between iron(III) and NRF and the study of some structural and spectral characteristics are described. The complexation reaction was applied to the spectrophotometric determination of trace amounts of iron(III).

Experimental

Reagents

De-ionised, freshly doubly distilled water was used throughout. All reagents used were of analytical-reagent grade unless indicated otherwise.

Standard iron(III) solution, 10^{-2} M. A 4.825-g amount of ammonium iron(III) sulphate dodecahydrate (pro analysi, Merck, Article No. 3776) was dissolved in water, acidified with a few millilitres of concentrated sulphuric acid (pro analysi) to prevent hydrolysis and then diluted to 1000 ml with 0.1 M ammonium sulphate solution. The concentration of the resulting solution was determined colorimetrically.[12] Solutions of lower concentration were obtained by accurate dilution of this solution with 0.1 M ammonium sulphate.

Standard NRF solution, 10^{-2} M. A 3.22-g amount of NRF (Naka, Batch No. N-00715/8-87) was dissolved in the minimum volume of 0.05 M sulphuric acid and the solution was diluted to 1000 ml with 0.1 M ammonium sulphate solution. The exact concentration of NRF in the resulting solution was determined spectrophotometrically by comparison with a standard solution of NRF obtained from Naka. More dilute solutions were prepared by appropriate dilution with 0.1 M ammonium sulphate.

Ammonium sulphate solution, 0.1 M. Prepared by dissolving 13.3 g of ammonium sulphate (Fluka, puriss., pro analysi, No. 09980) in water and diluting to 1000 ml with water. The concentration of iron(III) in the solution was determined to be 1.2×10^{-2} μg ml^{-1}.

Apparatus

A Perkin-Elmer Model 124 double-beam recording spectrophotometer and a Hitachi Perkin-Elmer Model 139 single-beam spectrophotometer, both with thermostated cell holders and matched 10.0-mm quartz cells were used for absorbance measurements. A Beckman Model H2 pH meter with a glass electrode was used for all pH measurements. A Model NBS ultrathermostat (Gebrüder Haake) was also used.

Recommended Procedure for the Formation of the Iron(III) - NRF Complex

A volume (V = 1–5 ml) of the standard iron(III) solution was transferred quantitatively into a 25-ml calibrated flask thermostated at 25 ± 0.5 °C. Then, twice this volume, *i.e.*, $2V$ ml,

of the standard NRF solution, measured accurately, was added and the mixture was diluted to volume with 0.1 M ammonium sulphate solution, while simultaneously adjusting the pH to 3.0. The resulting solution was mixed by shaking. The yellow complex was formed instantaneously and was stable for at least 20 d.

Recommended Procedure for the Spectrophotometric Determination of Trace Amounts of Iron(III)

An appropriate volume of the standard iron(III) solution [or of another iron(III) solution of lower concentration] equivalent to 6.25–300 μg of iron(III) was transferred into a 25-ml calibrated flask. A 10.0-ml aliquot of the NRF standard solution was added and, after mixing well, the pH was adjusted to 3.0 with a few drops of 0.1 M ammonia solution. The calibrated flask was placed in a water-bath thermostated at 25 ± 0.5 °C and after 10 min the contents were diluted to volume with 0.1 M ammonium sulphate solution and mixed thoroughly.

The flask, which contained 0.25–12.0 p.p.m. of iron(III), was again placed in the water-bath until measurements were performed. The absorbance was measured at 377 nm using 10.0-mm quartz cells thermostated at 25 ± 0.5 °C against an iron(III) blank solution, which had been treated similarly. The concentration of iron(III) was calculated from a calibration graph, which had been prepared previously (see below).

Calibration Graph

A calibration graph for the determination of iron(III) was obtained using the optimum conditions given in the recommended procedure. Beer's law was obeyed between 0.25 and 12.0 p.p.m. of iron(III). The linearity of the concentration (c) *versus* absorbance (A) graph was checked by a linear least-squares treatment using an Apple IIc computer. The regression line equation, obtained from nine determinations, was calculated to be $A = 0.163c - 0.00042$. The slope and intercept were obtained with a correlation coefficient of 0.9998 ($n = 9$).

Results and Discussion

The formation of the iron(III) - NRF complex was examined at different pH values in equimolar or non-equimolar solutions. All the measurements were carried out under constant conditions [temperature, 25 ± 0.5 °C; ionic strength, *ca.* 0.3 M (maintained with 0.1 M ammonium sulphate solution); and pH, 3.0]. At lower pH values, *i.e.*, between 0.5 and 2.0, the complex is yellowish orange but becomes yellow at pH 3.0 and above. The order of addition of the standard solutions has no effect on the formation of the complex.

Absorption Spectra

The absorption spectrum of the complex was scanned in the double mode at a scan rate of 120 nm min^{-1}, at pH 3.0 and with a volume ratio of 1:2 for a 10^{-3} M concentration of iron(III) and a 10^{-2} M concentration of NRF against an iron(III) blank. The iron(III) - NRF complex has an absorption maximum at 377 nm. The absorption spectrum of an NRF solution (10.0 μg ml^{-1}) was recorded under the same operating conditions against a reagent blank. The absorption of the NRF solution at 377 nm is negligible, hence NRF has no effect on the determination of iron(III) at this wavelength. In fact, the spectrum of NRF shows a maximum absorption at 276 nm (Fig. 1).

The molar absorptivity of the iron(III) - NRF complex at 377 nm was 9.05×10^3 l mol^{-1} cm^{-1} (average of six determinations) and the Sandell sensitivity 6.2 ng cm^{-2} of iron(III) per 0.001A.

The yellow colour of the complex remained unchanged (maximum wavelength, intensity) for at least 20 d; in contrast, the colour of the iron(III) - thiocyanate complex faded rapidly, particularly when the solution was exposed to light, because of reduction of iron(III) by thiocyanate or its decomposition products.

Composition of the Iron(III) - NRF Complex

A study of the composition of the iron(III) - NRF complex using the continuous variation[13] and mole ratio methods[14] indicated that the complex has a 1:2 composition, while the formation constant (K_f) under the experimental conditions described above was calculated to be 4.0×10^8 (average of six determinations). The results of this study indicate that the most likely structural formula for the complex is that shown in Fig. 2.

Effect of pH

The effect of pH on the formation of the iron(III) - NRF complex in aqueous solution was investigated. In each instance, the desired pH was obtained by adding the appropriate volume of 0.1 M sulphuric acid or 0.1 M ammonia solution. The use of a suitable buffer solution was avoided, because the presence of any foreign ion could interfere with formation of the complex and with its absorption spectrum.

The optimum pH for a constant maximum absorbance at 377 nm was found to be 3.0. In more acidic or more alkaline solutions, the absorbance decreased and $\lambda_{max.}$ was shifted

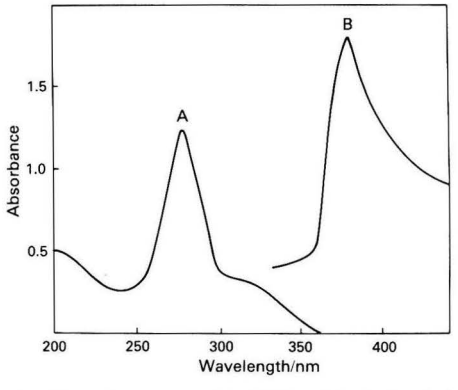

Fig. 1. Absorption spectra of A, NRF, and B, the iron(III) - NRF complex [iron(III) concentration, 11.2 μg ml^{-1}]. Conditions: temperature, 25 ± 0.5 °C; ionic strength, 0.3 M; pH, 3.0; and scan rate, 120 nm min^{-1}

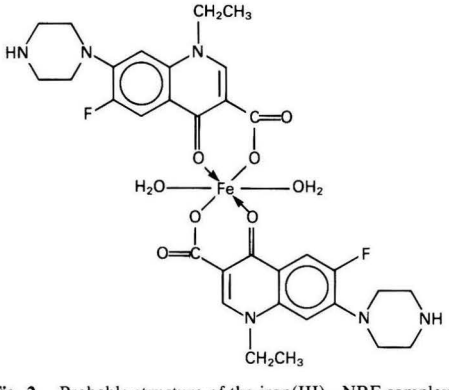

Fig. 2. Probable structure of the iron(III) - NRF complex

from 375 to 384 nm, probably because of incomplete formation of the complex or because of a change in the structure of the complex itself. Above pH 8.0 the solution became turbid due to the precipitation of iron(III) hydroxide.

Table 1. Assessment of the precision and accuracy of the proposed method

Solution No.	Iron(III), p.p.m. Added	Found	SD, p.p.m.	RSD, %*	Standard analytical error†
1	0.5	0.494			
2	0.5	0.478			
3	0.5	0.509			
4	0.5	0.524			
5	0.5	0.524			
	Mean:	0.5058	0.020	3.93	0.009
6	4.0	3.95			
7	4.0	4.01			
8	4.0	4.07			
9	4.0	4.10			
10	4.0	3.86			
	Mean:	3.998	0.096	2.41	0.043
11	8.0	8.02			
12	8.0	8.34			
13	8.0	8.20			
14	8.0	8.09			
15	8.0	7.90			
	Mean:	8.11	0.168	2.08	0.075
16	11.2	11.17			
17	11.2	11.42			
18	11.2	11.57			
19	11.2	11.11			
20	11.2	10.80			
	Mean:	11.214	0.297	2.65	0.133

* Mean RSD = 2.77%.

† Mean standard analytical error ($SD/\sqrt{n}$) = 0.065.

Table 2. Tolerance limits for the determination of iron(III). Iron(III) concentration, 8.0 p.p.m.

Foreign ion	Added as	Amount tolerated, p.p.m.
Li^{I}	Cl^-	1000
Na^{I}	Cl^-	1000
K^{I}	NO_3^-	1000
Cs^{I}	Cl^-	1000
Mn^{II}	SO_4^{2-}	1000
Zn^{II}	Cl^-	1000
Al^{III}	NO_3^-	750
Sn^{II}	Cl^-	750
Cu^{II}	NO_3^-	50
Co^{II}	NO_3^-	50
Ni^{II}	Cl^-	50
Cr^{III}	Cl^-	50
Ce^{IV}	SO_4^{2-}	Interfered at all levels
PO_4^{3-}	Na^+	
F^-	Na^+	
Citrate	Na^+	
Oxalate	Na^+	
Tartrate	Na^+	

Stability of the NRF Reagent

No difference was observed between the calibration graphs obained using the freshly prepared standard NRF solution and those obtained with NRF solutions that had been stored in a refrigerator (4 °C) for 8 d or at room temperature (25 °C) for at least 48 h.

Sensitivity, Precision and Accuracy

The apparent molar absorptivity and Sandell sensitivity of the complex are 9.05×10^3 l mol^{-1} cm^{-1} and 6.2 ng cm^{-2} of iron(III) per 0.001 A, respectively (average of six determinations).

In order to study the precision and accuracy of the proposed method, standard solutions containing four different concentrations of iron(III) were prepared and five absorbance measurements were made on each standard iron(III) solution. The over-all relative standard deviation (RSD) for 20 determinations was 2.77%, while the standard analytical error ($SD/\sqrt{n}$) did not exceed 0.065. The results of this study are given in Table 1.

Effect of Foreign Ions

The effect of foreign ions on the determination of iron(III) was investigated by adding known amounts of each foreign ion to a solution containing 8.0 p.p.m. of iron(III) and then determining the latter using the recommended procedure. The results are presented in Table 2 and indicate that almost all the common cations that are normally associated with iron in various types of sample, *e.g.*, mineral, industrial and biological samples, do not interfere with the determination of iron(III), with the exception of cerium(IV) which interferes seriously.

Comparison With an Established Method

Solutions of iron(III) of four different concentrations, *viz.*, 4.0, 6.0, 8.0 and 10.0 p.p.m., were each analysed five times using the proposed procedure and simultaneously by the thiocyanate method.[12,15] The results are presented in Table 3. The thiocyanate method was chosen for this comparison because its determination limit for iron(III) is at the p.p.m. level, which is comparable to that of the proposed method.

According to Woods and Mellon,[12] for the thiocyanate method, Beer's law is obeyed up to 10.0 p.p.m. of iron(III) in the pH range 1.5–1.65. In order to increase the sensitivity of the method [by increasing the intensity of the colour of the iron(III) - thiocyanate complex and the stability of the colour], acetone was added. Acetone has a low dielectric constant and it has been found that the intensity of the colour of the iron(III) - thiocyanate complex in 50–60% aqueous acetone is about twice as high as in water and that the rate at which the colour fades is slower in aqueous acetone than in water. It has also been shown that there is less interference from ions such as fluoride and oxalate in an aqueous acetone solution than in water alone. For all of these reasons the procedure with aqueous acetone[16] was preferred and was used as the method of comparison.

Table 3. Determination of iron(III) at different concentrations using the proposed procedure and comparison with the thiocyanate method

Concentration of iron(III), p.p.m.	Proposed procedure Found, p.p.m. ± SD*	RSD, %	Thiocyanate method Found, p.p.m. ± SD*	RSD, %	*t*-Value†
4.0	3.998 ± 0.096	2.41	4.010 ± 0.034	0.84	0.74
6.0	6.02 ± 0.046	0.77	6.010 ± 0.065	1.08	1.68
8.0	8.11 ± 0.168	2.08	8.140 ± 0.089	1.10	0.60
10.0	10.20 ± 0.291	2.86	10.180 ± 0.349	3.43	0.49

* Average of five determinations.

† *t*-Value (calculated) = 0.88 for eight degrees of freedom and $p = 0.05$; *t*-value (tabulated) = 1.86.

All the sets of results were compared statistically by calculating t-values using the equation $t = (\bar{x}_1 - \bar{x}_2)/S[(n_1 + n_2)/n_1n_2]^{\frac{1}{2}}$, where $\bar{x}_1$ is the mean of the first sample of n_1 observations, $\bar{x}_2$ the mean of the second sample of n_2 observations, S^2 the pooled variance of the two samples and n_1 and n_2 are the number of determinations for samples 1 and 2, respectively. For eight degrees of freedom and at the 95% confidence level none of the calculated t-values exceeded the tabulated t-value. This indicates that there is no significant difference between the proposed procedure and the extensively used iron(III) - thiocyanate method for the determination of iron(III) at the p.p.m. level.

The author thanks Kleon Tsetis for the use of the Quality Control Laboratory of UNI-PHARMA during a large part of this work and Anastassios Tsetis for providing the norfloxacin used and for his valuable discussions during the course of the quinolones research project.

References

1. "Drug Information 88," Published by Authority of the Board of Directors of the American Society of Hospital Pharmacists, Bethesda, MD, 1988, pp. 415–420.
2. "Drug Facts and Comparisons," J. B. Lippincott, Philadelphia and Toronto, 1988, pp. 1610 and 1611.
3. Capitán, F., Arrebola Ramirez, A., and Jimenez Linares, C., *Analyst*, 1986, **111**, 739.
4. Morelli, B., *Analyst*, 1983, **108**, 870.
5. Agarwal, J., Gupta, Y. K., Bhargava, K. P., and Shanker, K., *Indian J. Chem., Sect. B*, 1981, **20**, 714.
6. Srivastava, V. K., Satsangi, R. K., Shankar, K., and Kishor, K., *Pharmazie*, 1981, **36**, 252.
7. Dhasmana, A., Barthwal, J. P., Pandey, B. R., Ali, B., Bhargava, K. P., and Parmar, S. S., *J. Heterocycl. Chem.*, 1981, **18**, 635.
8. Stearns, B., Losee, K. A., and Bernstein, J., *Med. Pharm. Chem.*, 1963, **6**, 201.
9. "Martindale, The Extra Pharmacopoeia," Twenty-eighth Edition, Pharmaceutical Press, London, 1982, p. 212.
10. "British Pharmacopoeia 1980," HM Stationery Office, London, 1980, p. 231.
11. "US Pharmacopeia, XXI Revision," US Pharmacopeial Convention, Rockville, MD, 1985, p. 518.
12. Woods, J. T., and Mellon, M. G., *Ind. Eng. Chem. Anal. Ed.*, 1941, **13**, 551.
13. Job, P., *Ann. Chim. (Paris)*, 1928, **9**, 113.
14. Yoe, J. H., and Jones, A. L., *Ind. Eng. Chem. Anal. Ed.*, 1944, **16**, 111.
15. Vogel, A. I., "A Textbook of Quantitative Inorganic Analysis," Third Edition, Longman, London, 1961, pp. 785–787.
16. Sandell, E. B., "Colorimetric Determination of Traces of Metals," Third Edition, Interscience, New York, 1959, pp. 524–535.

Paper 8/03312I
Received August 15th, 1988
Accepted December 14th, 1988